



Santo Tomás Project

NI 43-101 Technical Report Mineral Resource Estimate

Sinaloa/Chihuahua/Sierra Madre Occidental Region, México

Effective Date: April 21, 2023

Prepared for: Oroco Resource Corp.

1201-1166 Alberni Street

Vancouver, British Columbia V6E 3Z3

Prepared by: Ausenco Engineering USA South Inc.

595 S. Meyer Ave

Tucson, Arizona 85701

List of Qualified Persons:

James Arthur Norine, P.E., Ausenco Engineering USA South Inc.

Peter Mehrfert, P. Eng., Ausenco Engineering Canada Inc.

Scott Burkett, SME-RM B.Sc. Geo., SRK Consulting (US) Inc.

Ron Uken, Ph.D. Geo., Pr. Sci. Nat., SRK Consulting (Canada) Inc.



CERTIFICATE OF QUALIFIED PERSON

James Arthur Norine, P.E.

I, James Arthur Norine, P.E., certify that:

1. I am employed as Vice President, Southwest USA with Ausenco Engineering USA South ("Ausenco"), with an office address of 595 S. Meyer Avenue, Tucson, Az, USA.
2. This certificate applies to the technical report titled Santo Tomás Project, NI 43-101 Technical Report Mineral Resource Estimate (the "Technical Report"), prepared for Oroco Resources (the "Company") with an effective date of April 21, 2023 (the "Effective Date").
3. I graduated from Northern Arizona University, Flagstaff, Arizona with a B.S. in Mechanical Engineering.
4. I am a registered professional engineer in the state of Arizona, USA, license #42008.
5. I have practiced my profession for 23 years. My relevant experience includes Mechanical Engineering and Project Management as they relate to the Delivery of Base and Precious Metals Processing plants in North America. I have practiced Mechanical Engineering and Project Management for 23 years. I have worked for previous engineering consulting and construction management companies for over 18 1/2 years and 3 ½ years for Ausenco Engineering. I have been working in my profession continuously since 2000.
6. I have read the definition of "Qualified Person" set out in the National Instrument 43-101 Standards of Disclosure for Mineral Projects ("NI 43-101") and certify that by virtue of my education, affiliation to a professional association and past relevant work experience, I fulfill the requirements to be a "Qualified Person" for those sections of the Technical Report that I am responsible for preparing.
7. I visited the Santo Tomás site between September 21, 2023 – September 23, 2023.
8. I am responsible for Sections 1.1, 1.2, 1.11.5, 1.12.1, 2.1, 2.2, 2.3, 2.4, 2.7, 3, 5, 15 – 22, 24, 25.1, 25.7 and 27 of the Technical Report of the Technical Report.
9. I am independent of the Company as independence is defined in Section 1.5 of NI 43-101.
10. I have been involved with the Santo Tomás Project during the preparation of this technical report.
11. I have read NI 43-101 and the sections of the Technical Report for which I am responsible have been prepared in compliance with that Instrument. As of the effective date of the Technical Report, to the best of my knowledge, information and belief, the sections of the Technical Report for which I am responsible contain all scientific and technical information that is required to be disclosed to make those sections of the Technical Report not misleading.

Dated: June 15, 2023

"Signed and Sealed"

James Arthur Norine, P.E.

CERTIFICATE OF QUALIFIED PERSON

Peter Mehrfert, P.Eng.

I, Peter Mehrfert, P. Eng., certify that:

1. I am employed as a Process Engineer with Ausenco Engineering Canada, with an office at 1050 W Pender St, Vancouver, BC V6E 3S7.
2. This certificate applies to the technical report titled *Santo Tomás Project, NI 43-101 Technical Report Mineral Resource Estimate* (the "Technical Report"), prepared for Oroco Resources (the "Company") with an effective date of April 21, 2023 (the "Effective Date").
3. I graduated from the University of British Columbia in 1996 where I obtained a Bachelor of Applied Science in Mining and Mineral Process Engineering.
4. I am a Professional Engineer, registered with Engineers and Geosciences of British Columbia, member number 100283.
5. I have practiced my profession continuously for 28 years and have been involved in the design, evaluation and operation of mineral processing facilities during that time. Approximately half of my professional practice has been the supervision and management of metallurgical test work related to feasibility and prefeasibility studies of projects involving flotation technologies. Previous copper projects that I have worked on that have similar features to Santo Tomás are: Gibraltar, Lomas Bayas, Mt Milligan, Jose Maria and Highland Valley Copper.
6. I have read the definition of "Qualified Person" set out in the National Instrument 43-101 Standards of Disclosure for Mineral Projects ("NI 43-101") and certify that by virtue of my education, affiliation to a professional association and past relevant work experience, I fulfill the requirements to be a "Qualified Person" for those sections of the Technical Report that I am responsible for preparing.
7. I have not visited the Santo Tomás property.
8. I am responsible for sections 1.1, 1.9, 1.11.4, 1.11.5, 1.12.1, 1.12.4, 2.1, 2.2, 2.3, 2.7, 3, 13, 25.1, 25.5, 25.7, 26.1, 26.3 and 27 of the Technical Report.
9. I am independent of the Company as independence is defined in Section 1.5 of NI 43-101.
10. I have had no previous involvement with the Santo Tomás Project.
11. I have read NI 43-101 and the sections of the Technical Report for which I am responsible have been prepared in compliance with that Instrument. As of the effective date of the Technical Report, to the best of my knowledge, information and belief, the sections of the Technical Report for which I am responsible contain all scientific and technical information that is required to be disclosed to make those sections of the Technical Report not misleading.

Dated: June 15, 2023

"Signed and Sealed"

Peter Mehrfert, P. Eng.

CERTIFICATE OF QUALIFIED PERSON
Scott Burkett, B.Sc. Geology, SME-RM

I, Scott Burkett, B.Sc., Geology SME-RM, do hereby certify that:

1. I am Principal Consultant of SRK Consulting (U.S.), Inc., 999 Seventeenth Street, Suite 400, Denver, CO, USA, 80202.
2. This certificate applies to the technical report titled Santo Tomás Project, NI 43-101 Technical Report Mineral Resource Estimate (the "Technical Report"), prepared for Oroco Resources (the "Company") with an effective date of April 21, 2023 (the "Effective Date").
3. I graduated with a degree in B.S Geology from University of Idaho in 2007. I am a Registered Member of the Society for Mining, Metallurgy & Exploration. I have worked as a Geologist for a total of 16 years since my graduation from university. My relevant experience includes mineral exploration, QA/QC and mineral resource estimates.
4. I have read the definition of "qualified person" set out in National Instrument 43-101 (NI 43-101) and certify that by reason of my education, affiliation with a professional association (as defined in NI 43-101) and past relevant work experience, I fulfill the requirements to be a "qualified person" for the purposes of NI 43-101.
5. I visited the Santo Tomás property on March 30 for three days.
6. I am responsible for sections 1.1, 1.3, 1.5 - 1.8, 1.10, 1.11.2, 1.11.3, 1.11.5, 1.12.1- 1.12.3, 2.1 - 2.7, 3, 4, 6, 10, 11, 12, 14, 25.1, 25.2, 25.4, 25.6, 25.7, 26.1, 26.2 and 27 of the Technical Report.
7. I am independent of the issuer applying all of the tests in section 1.5 of NI 43-101.
8. I have not had prior involvement with the property that is the subject of the Technical Report.
9. I have read NI 43-101 and Form 43-101F1 and the sections of the Technical Report I am responsible for have been prepared in compliance with that instrument and form.
10. As of the aforementioned Effective Date, to the best of my knowledge, information and belief, the sections of the Technical Report I am responsible for contains all scientific and technical information that is required to be disclosed to make the Technical Report not misleading.

Dated: June 15, 2023

"Signed and Sealed"

Scott Burkett, B.Sc., Geology SME-RM
Principal Consultant (Exploration Geologist)

CERTIFICATE OF QUALIFIED PERSON

Ronald Uken, Pr.Sci.Nat, Principal Consultant

I, Ronald Uken, Pr.Sci.Nat, Principal Consultant, certify that:

1. I am employed as a Structural Geologist with SRK Consulting (Canada) Inc. (SRK), with an office address of 2600–320 Granville St., Vancouver, BC V6C 1S9.
2. This certificate applies to the technical report titled Santo Tomás Project, NI 43-101 Technical Report Mineral Resource Estimate (the “Technical Report”), prepared for Oroco Resources (the “Company”) with an effective date of April 21, 2023 (the “Effective Date”).
3. I am a graduate of the University of Natal (KwaZulu-Natal), South Africa in 1999 with a Ph.D. in the Faculty of Science, (Structural and Metamorphic Geology).
4. I am a professional Scientist registered with the South African Council for Natural Scientific Professions, for Geological Science (Reg. no 400322/11)
5. I have practiced my profession for 24 years since graduating with a PhD. My relevant experience includes employment in academia and as a consultant to the mining industry. My specialization is in structural mapping and 3-D structural modelling of ore deposits. This includes the application of structural geology to exploration, mineral resource estimation, geotech and hydrogeology. As a consultant I have worked on a range of precious and base metal projects throughout Africa, the Middle East and the Americas, offering structural geology support as well as working with site geologists assisting with mapping, data collection, logging and structural interpretation.
6. I have read the definition of “Qualified Person” set out in the National Instrument 43-101 Standards of Disclosure for Mineral Projects (“NI 43-101”) and certify that by virtue of my education, affiliation to a professional association and past relevant work experience, I fulfill the requirements to be a “Qualified Person” for those sections of the Technical Report that I am responsible for preparing.
7. I visited the Santo Tomás project site between Jan 19 to Jan 24, 2022; March 29 to April 11, 2022; March 28 to April 3, 2023, a total duration of 26 days. I was directly involved with assisting the Company with surface geological and structural mapping, drill core investigation and interpretation. I undertook structural modelling and assisted with interpreting the structural controls on mineralisation as inputs into the resource estimation.
8. I am responsible for 1.1, 1.4, 1.6, 1.11.1, 1.11.2, 1.11.5, 1.12.1, 2.1, 2.2, 2.3, 2.4, 2.7, 3, 6, 7, 8, 9, 23, 25.1, 25.3, 25.4, 25.7, 26.1, 26.3 and 27 of the Technical Report.
9. I am independent of the Company as independence is defined in Section 1.5 of NI 43-101.
10. I have no current or previous financial involvement with the Santo Tomás Project.
11. I have read NI 43-101 and the sections of the Technical Report for which I am responsible have been prepared in compliance with that Instrument. As of the effective date of the Technical Report, to the best of my knowledge, information and belief, the sections of the Technical Report for which I am responsible contain all scientific and technical information that is required to be disclosed to make those sections of the Technical Report not misleading.

Dated: June 15, 2023

“Signed and Sealed”

Ronald Uken, Pr.Sci.Nat, Principal Consultant

Important Notice

This report was prepared as National Instrument 43-101 Technical Report for Oroco Resource Corp. (Oroco) by Ausenco Engineering USA South Inc. (Ausenco), and SRK Consulting (Canada) Inc., collectively the Report Authors. The quality of information, conclusions, and estimates contained herein is consistent with the level of effort involved in the Report Authors' services, based on i) information available at the time of preparation, ii) data supplied by outside sources, and iii) the assumptions, conditions, and qualifications set forth in this report. This report is intended for use by Oroco subject to terms and conditions of its contracts with each of the Report Authors. Except for the purposes legislated under Canadian provincial and territorial securities law, any other uses of this report by any third-party are at that party's sole risk.

Table of Contents

1	SUMMARY.....	1
1.1	Introduction.....	1
1.2	Property Description and Location.....	1
1.3	Mineral Tenure & Ownership.....	1
1.4	Geology and Mineralization.....	2
1.5	History – Exploration Programs.....	2
1.5.1	Exploration Programs.....	2
1.6	Exploration and Drilling.....	4
1.6.1	Exploration by Oroco.....	4
1.6.2	Drilling History.....	5
1.6.3	Oroco Drilling.....	5
1.7	Sample Preparation, Analysis, Security and QA/QC.....	6
1.8	Data Verification.....	7
1.9	Mineral Processing and Metallurgical Testing.....	7
1.10	Mineral Resource Estimation.....	8
1.11	Interpretation and Conclusions.....	9
1.11.1	Geology and Mineralization.....	9
1.11.2	Exploration, Drilling and Analytical Data Collection Support of Mineral Resource Estimation.....	10
1.11.3	Mineral Resource Estimates.....	10
1.11.4	Metallurgy.....	10
1.11.5	Risks and Opportunities.....	10
1.12	Recommendations.....	11
1.12.1	Overall.....	11
1.12.2	Preliminary Economic Assessment Future Study.....	11
1.12.3	Exploration, Geology and Mineral Resources.....	11
1.12.4	Mineral Processing.....	12
2	INTRODUCTION.....	13
2.1	Introduction.....	13
2.2	Scope of Work.....	13
2.3	Qualified Persons.....	14
2.4	Site Visits and Scope of Personal Inspection.....	15
2.5	Effective Dates.....	15
2.6	Previous Technical Reports.....	15
2.7	Units and Abbreviations.....	16
3	RELIANCE ON OTHER EXPERTS.....	23
4	PROPERTY DESCRIPTION AND LOCATION.....	24
4.1	Property Location.....	24

4.2	Mexican Mineral Tenure System.....	25
4.2.1	Governing Law and Regulations.....	25
4.2.2	Mexican Public Registry of Mining.....	25
4.2.3	Assessment Work, Reporting and Mining Duties	25
4.2.4	Valid Concession Holders & Surface Rights	26
4.2.5	Location Surveys.....	26
4.3	Mineral Tenures of The Project Property and the Resource Property	26
4.3.1	Legal Survey of the Property	28
4.3.2	Obligations to Maintain the Property	30
4.3.3	Surface Rights.....	30
4.4	Permits and Liabilities.....	31
4.5	Risks	31
5	ACCESSIBILITY, CLIMATE, LOCAL RESOURCES, INFRASTRUCTURE AND PHYSIOGRAPHY	32
5.1	Physiography	32
5.2	Local Resources.....	34
5.3	Accessibility	35
5.4	Climate	35
5.5	Infrastructure	35
5.5.1	Regional Infrastructure.....	35
5.5.2	Local Infrastructure	36
5.5.3	Infrastructure for Exploration	38
6	HISTORY	40
6.1	Exploration History.....	40
6.2	Historical Mineral Resource Estimates.....	43
7	GEOLOGICAL SETTING AND MINERALIZATION	45
7.1	Regional Geology	45
7.1.1	Stratified Rocks.....	45
7.1.2	Intrusive Rocks.....	46
7.1.3	Structural Geology & Mineralization.....	48
7.2	Property Geology	48
7.2.1	Introduction.....	48
7.2.2	Stratified Rocks.....	52
7.2.3	Intrusions	53
7.2.4	Alteration.....	58
7.2.5	Structure.....	64
7.2.6	Mineralization.....	77
7.2.7	Geological Chronology and Controls to Mineralization.....	79
7.2.8	Guerrero Terrane – Jurassic – Cretaceous Arc Volcanics, Intrusions, and Sediments.....	79
7.2.9	Laramide Orogeny – Late Cretaceous to Paleocene (80 to 55 Ma)	79
7.2.10	Pre-Basin and Range – SMO Volcanic Province Faulting	80
8	DEPOSIT TYPES.....	81

8.1	Porphyry Deposits.....	81
8.2	Laramide-Age Porphyry Deposits of NW México	83
9	EXPLORATION.....	87
9.1	Remote Sensing.....	87
9.1.1	2021 LiDAR Survey	87
9.1.2	Satellite Multispectral Review	89
9.2	Geophysical Surveys.....	89
9.2.1	Airborne Magnetism Survey	89
9.2.2	Surface 3D DCIP Survey	93
9.3	Geological Mapping, and Mineral Sampling	99
9.4	Site Access for Exploration.....	99
10	DRILLING.....	100
10.1	Drilling on the Property	100
10.2	Downhole Surveys	109
10.2.1	Downhole Geophysical Survey	111
10.2.2	Downhole Televiwer Survey.....	111
10.3	Summary and Interpretation of Relevant Results.....	111
10.4	Drill Methods	112
10.5	North Zone Drilling	118
10.6	South Zone Drilling.....	122
10.7	Geological Logging	125
10.8	Recovery.....	125
10.9	Geological and Hydrological Drilling	126
11	SAMPLE PREPARATION, ANALYSES AND SECURITY	127
11.1	Sampling Methods.....	127
11.1.1	Historical Sampling Methods	127
11.1.2	Oroco Sampling Methods.....	127
11.2	Density (Specific Gravity) Determinations	129
11.2.1	Historical Density	129
11.2.2	Oroco Density Program	129
11.3	Analytical and Test Laboratories.....	130
11.3.1	Historical samples	130
11.3.2	Phase 1 Drilling by Oroco.....	130
11.3.3	Metallurgical Laboratory.....	131
11.3.4	Laboratory Independence.....	131
11.4	Sample Preparation and Analysis	131
11.5	Sample Security	132
11.5.1	Historical Sample Security	132
11.5.2	Phase 1 Core Program Sample Security.....	132
11.5.3	Commercial Reference Material Security	133
11.6	Sample Storage.....	133

11.6.1	Historic Pulp and Coarse Reject Storage	133
11.6.2	Phase 1 Oroco Pulp and Coarse Reject Storage	133
11.7	Quality Control and Quality Assurance.....	134
11.7.1	Historical QA/QC.....	134
11.7.2	Oroco Phase 1 Program QA/QC.....	134
11.8	Check and Re-Assay Programs.....	138
11.8.1	Historical Check and Re-Assay	138
11.8.2	Phase 1 Oroco Drilling Check Assay	138
11.8.3	Oroco Re-Assays.....	138
11.9	Databases	138
11.9.1	Santo Tomás Phase I Drilling – QA/QC Detailed Analysis	139
11.9.2	Standards.....	141
11.9.3	Field Duplicates.....	145
11.9.4	Coarse Duplicates.....	147
11.9.5	Pulp Check Assays	159
11.10	Comments on Sample Preparation, Analyses and Security.....	160
12	DATA VERIFICATION.....	161
12.1	Oroco Verification	161
12.2	Assay Data and QA/QC Results Verification.....	162
12.3	Down Hole Survey Data Verification	162
12.4	Point Load Testing and Specific Data Verification	162
12.5	Core Orientation Verification of Continuity	162
12.5.1	Geological Data Verification	163
12.6	Field Surveying Data Verification.....	163
12.7	Verification Performed by the QP.....	164
12.8	Site Inspection.....	165
12.9	Limitations on Data Verification	165
12.10	Opinion on Data Adequacy	166
13	MINERAL PROCESSING AND METALLURGICAL TESTING	167
13.1	Introduction.....	167
13.2	Metallurgical Test Work.....	167
13.2.1	Sample Preparation	167
13.2.2	Chemical and Mineralogical Characterization.....	168
13.2.3	Comminution	170
13.2.4	Flotation Test work	170
13.2.5	Concentrate Quality	177
13.2.6	Tailings Acid-Base Measurements	178
13.3	Recovery Estimates	178
13.3.1	Copper (Cu).....	178
13.3.2	Molybdenum (Mo)	179
13.3.3	Gold (Au)	179

13.4	Conclusions.....	181
14	MINERAL RESOURCE ESTIMATES.....	183
14.1	Introduction.....	183
14.2	Drillhole Database	183
14.2.1	Assay.....	185
14.2.2	Survey.....	186
14.2.3	Specific Gravity	186
14.3	Geological Model	186
14.3.1	Structural Geologic Model.....	186
14.3.2	Oxidation Model.....	190
14.3.3	Mineralization Grade Shells.....	191
14.4	Exploratory Data Analysis.....	195
14.4.1	Statistical Analyses.....	195
14.4.2	Composite Length Analysis.....	202
14.4.3	Capping Analysis	204
14.5	Spatial Continuity	213
14.6	Block Model.....	219
14.7	Estimation Methodology.....	221
14.8	Block Model Validation	223
14.8.1	Visual Comparison.....	223
14.8.2	Comparative Statistics	231
14.9	Resource Classification	239
14.10	Reasonable Prospects for Eventual Economic Extraction	241
14.11	Copper Equivalent Calculation	245
14.12	Mineral Resource Statement.....	245
14.13	Mineral Resource Sensitivity	246
14.14	Relevant Factors	248
14.15	Opinion on Mineral Resource Estimates.....	248
15	MINERAL RESERVE ESTIMATES	249
16	MINING METHODS	250
17	RECOVERY METHODS	251
18	PROJECT INFRASTRUCTURE.....	252
19	MARKET STUDIES AND CONTRACTS.....	253
20	ENVIRONMENTAL STUDIES, PERMITTING AND SOCIAL AND COMMUNITY IMPACT.....	254
21	CAPITAL AND OPERATING COST	255
22	ECONOMIC ANALYSIS	256
23	ADJACENT PROPERTIES	257
23.1	La Reforma Mine.....	257
23.2	El Tempisque Deposit.....	257

23.3	Bahuerachi	257
23.4	El Sauzal Mine.....	257
24	OTHER RELEVANT DATA AND INFORMATION.....	258
25	INTERPRETATION AND CONCLUSIONS.....	259
25.1	Introduction.....	259
25.2	Mineral Tenure, Surface Rights, Water Rights, Royalties and Agreements	259
25.3	Geology and Mineralization	259
25.4	Exploration, Drilling and Analytical Data Collection in Support of Mineral Resource Estimation.....	259
25.5	Metallurgical Test Work.....	259
25.6	Mineral Resources Estimates.....	260
25.7	Risks and Opportunities.....	260
26	RECOMMENDATIONS.....	262
26.1	Overview.....	262
26.2	Exploration and Drilling and Recommended PEA Study	262
26.3	Metallurgical Test Work.....	263
27	REFERENCES.....	265

List of Tables

Table 1-1:	Project Historical Technical Work and Studies.....	3
Table 1-2:	Historical and Oroco Drilling Campaigns, Total Assays, Holes and Meters Drilled.....	5
Table 1-3:	Oroco Drill Hole Inclusion/Exclusion Table.....	5
Table 1-4:	2022-2023 Core Drilling Program Undertaken by the Oroco Program	6
Table 1-5:	Mineral Resource Statement, Effective April 21, 2023 - SRK Consulting (US), Inc.	9
Table 1-6:	Proposed Budget Summary	11
Table 2-1:	Report Contributors	14
Table 2-2:	List of Other Units and Abbreviations.....	17
Table 4-1:	List of Xochipala Gold, S.A. de C.V.'s Santo Tomás Core Concessions	27
Table 4-2:	List of Minera Xochipala, S.A. de C.V.'S Santo Tomás Peripheral Concessions (80% interest)	28
Table 6-1:	Historical Exploration Programs.....	40
Table 7-1:	List of Samples from the Santo Tomás Porphyry Deposit Selected for Geochronological Analysis	49
Table 7-2:	Oroco Vein Type Classification at Santo Tomás	59
Table 10-1:	Oroco Drill hole Inclusion / Exclusion Table.....	100
Table 10-2:	Oroco and Historical Drilling and Assaying as used in this MRE.....	101
Table 10-3:	Project Drill Collars – Coordinates in WGS84 UTM Zone 12N.....	106
Table 10-4:	Brasiles Prospect Exploration Drill Hole Collar Information (WGS84 UTM Zone 12N)	108
Table 10-5:	In-hole Attitude and Geophysical Surveys by Drill Hole, including Set-out method and number of Samples Taken	109

Table 10-6:	Listing of Significant Cu Composite Intervals from the North Zone and South Zone	112
Table 10-7:	Listing of Significant Cu Composite Intervals from the Braziles Prospect Exploration Drilling	117
Table 11-1:	QA/QC Duplicate and Standard Insertion Scheme	135
Table 11-2:	QA/QC Standard CRM Insertion Criteria.....	136
Table 11-3:	Santo Tomás Phase I Drilling (MRE) QA/QC Sample Insertion Rate	139
Table 11-4:	ALS Methods and Analytical Detection Limits.....	140
Table 11-5:	Determined Lower Practical Detection Limits	141
Table 11-6:	CRM Best Values (BV), Based on 4-Acid Digest/ICP Finish (Cu, Ag, Mo) or Fire-Assay/ICP Finish (Au) ..	142
Table 11-7:	Standard Failure Count and Calculated Bias for Cu and Au.....	143
Table 11-8:	Standard Failure Count and Calculated Bias for Ag and Mo.....	143
Table 11-9:	Relative Error and Calculated Slope for Different Duplicate Types	145
Table 11-10:	Summary of Min/Max Plot Analysis for FDUP Pairs	146
Table 11-11:	Summary Table of AVRD Analysis for FDUP Pairs	147
Table 11-12:	Summary of Min/Max Plot Analysis for CDUP Pairs	148
Table 11-13:	Summary Table of AVRD Analysis for CDUP Pairs.....	149
Table 11-14:	Summary of Min/Max Plot Analysis for PDUP Pairs	150
Table 11-15:	Summary Table of AVRD Analysis for PDUP Pairs.....	151
Table 11-16:	Summary Table of Pulp Blank Performance.....	152
Table 11-17:	Pulp Blank Calculated Potential Carry-Over	152
Table 11-18:	Summary Table of Coarse Blank Performance.....	155
Table 11-19:	Pulp Blank Calculated Potential Carry-Over	156
Table 12-1:	Oroco Core facility Standard Operating Procedure List	161
Table 12-2:	Data Collection Summary on Oroco and Historical Drilling	163
Table 13-1:	Selected Metallurgical Variability Samples	167
Table 13-2:	Head Assay Data.....	168
Table 13-3:	Mineral Composition Data.....	168
Table 13-4:	Sulphide Mineral Liberation Data.....	169
Table 13-5:	Comminution Test Data Summary	170
Table 13-6:	Rougher Flotation Results – Effect of Grind and Chemistry – Master Composite.....	172
Table 13-7:	Rougher Flotation Results – Variability Samples	172
Table 13-8:	Metallurgical Balance – Master Composite Locked Cycle Test.....	175
Table 13-9:	Variability Cleaner Flotation Test Results	176
Table 13-10:	Master Composite Concentrate – Minor Elements	177
Table 14-1:	Drilling Summary on the Santo Tomás Property.....	183
Table 14-2:	Modification of Missing Data.....	185
Table 14-3:	Indicator Grade Shell Summary - Cu in North Zone	193
Table 14-4:	Indicator Grade Shell Summary - Cu in South Zone.....	194
Table 14-5:	Summary Descriptive Statistics for Raw Sample Intervals (2m Composites).....	196
Table 14-6:	Summary Descriptive Statistics for Specific Gravity (SG) Measurements by Lithology	200
Table 14-7:	Correlation Coefficients of Primary Elements – All Domains.....	201
Table 14-8:	Summary Descriptive Statistics for 2m Composite Samples	204
Table 14-9:	Summary Upper Capping Applied for Santo Tomás.....	205

Table 14-10:	Tabulated Capping Options for North Zone Copper	206
Table 14-11:	Tabulated Capping Options for Molybdenum (Both Zones)	208
Table 14-12:	Tabulated Capping Options for Gold (Both Zones)	210
Table 14-13:	Tabulated Capping Options for Silver (Both Zones)	212
Table 14-14:	Variography Parameters for Key Economic Variables	214
Table 14-15:	Santo Tomás 2023 MRE Block Model Parameters	219
Table 14-16:	Summary Estimation Parameters for Grade Variables	222
Table 14-17:	Summary Estimation Parameters for Geological Domains	222
Table 14-18:	Input Parameters for Economic Cut-Off Grade	242
Table 14-19:	Revenue Factors of Whittle Economic Pit Shell Scenarios	244
Table 14-20:	Mineral Resource Statement, Effective April 21, 2023 - SRK Consulting (US), Inc.	246
Table 14-21:	Grade-Tonnage Sensitivity to Cut-Off Grade	247
Table 26-1:	Proposed Budget Summary	262

List of Figures

Figure 4-1:	Property Location Map	24
Figure 4-2:	Oroco Controlled Concessions: the “Property”	29
Figure 4-3:	Access Road Stability Retaining Walls Built by Community Members with Oroco Financial Support	30
Figure 5-1:	Local Physiography with Mineralized Zones.....	33
Figure 5-2:	View of the Santo Tomás Deposit Area indicating North Zone, South Zone, and Brasiles towards the Northeast.....	34
Figure 5-3:	Local Infrastructure	37
Figure 5-4:	South Camp Aerial View (left), and El Ranchito Core Processing Facility Inside View (right)	38
Figure 5-5:	The El Ranchito Secure Core and Sample Pulp Storage Facility.....	39
Figure 7-1:	Regional Geology	47
Figure 7-2:	Project Geology, mapped by Oroco Project and SRK Geology Personnel.....	51
Figure 7-3:	Core Sample of Quartz Monzonite from STD-42 Note Core sample of the quartz monzonite (the yellow is a stain for K-feldspar) (A), host to the mineralization at Santo Tomás. A magnified photograph of the sample showing the porphyritic texture of the rock (B), the scale is in millimetres.....	55
Figure 7-4:	A) MZ/QM intruding LS northwestward to the B003-B004 drill holes; B) QM/QM sills emplaced along the bedding planes of LS next to El Río Fuerte southwestward to the B005 drill hole. The direction of the contacts is represented in the stereonet	56
Figure 7-5:	Outcrop of Phyllic Altered Quartz Monzonite Porphyry.....	62
Figure 7-6:	Outcrop of Contact between Hornfelsed Andesite (left) and a Quartz Monzonite Dike (right)	63
Figure 7-7:	Oblique View of Geology and Faulting Looking to the South	65
Figure 7-8:	Orientation data plots from the geological mapping campaign. Histogram and stereonet poles to faults measured in the area: stereonet showing the main orientation of the lithological contacts including faulted and non-faulted contacts: stereonet showing the main trends	67

Figure 7-9:	System of ID intruding the GD next to the El Río Fuerte and west of the N032-41 drill holes. The orientation of the dikes is represented in the stereonet. View looking South.....	68
Figure 7-10:	Stereonet showing the main fault systems of the Santo Tomás area in terms of orientation and kinematics; note the paleo-stresses calculated for every stereogram.....	69
Figure 7-11:	Compressional structures identified in the Brasiles area: a) drag fold related to the reverse fault showed on “b”, b): reverse fault plane, c): view looking north of duplex type structure cropping out next to El Río Fuerte: view looking N. Felsic dikes emplaced on the fault zone	70
Figure 7-12:	a) Plan view of dextral fault cutting and displacing vein mineralized with calcite-pyrite-chalcopyrite. b) Section view looking NNE of normal fault cutting and displacing intermediate-mafic dike and andesitic rocks. ID: intermediate-mafic dike; A: andesite. The structures measured on the faults, contact and vein are plotted in the stereonet. The color of the lines in the stereonet represents the color of the structure on the image	72
Figure 7-13:	Stereonet Calculated or the Oriented Structural Data Collected on Drill holes from North Zone	73
Figure 7-14:	Stereonet Calculated or the Oriented Structural Data Collected on Drill holes from South Zone.....	74
Figure 7-15:	Stereonet Calculated or the Oriented Structural Data Collected on Drill holes from Brasiles Prospect ...	75
Figure 7-16:	Core of major structures intercepted in different drill holes: all the structures correspond to shearing structures with development of cataclases-mylonites under brittle-ductile deformation regime. SC-Type structures, rotated clasts, enlarged clasts and offsets are observed in the deformation zones. The code in the corner of every photograph indicates the drill hole number and the depth of intersection.....	77
Figure 8-1:	Schematic Diagram of a Porphyry Cu System from Sinclair (2007).....	82
Figure 8-2:	Late Cretaceous to Early Tertiary “Laramide” intrusion-related deposits of Northwestern México	85
Figure 9-1:	Location outlines for the project LiDAR, airborne magnetics (plus radiometrics and VLF-EM), ground 3D DCIP survey, geological mapping and vegetation survey coverage.....	88
Figure 9-2:	The Microlevelled TMI Grid	91
Figure 9-3:	VOXI Susceptibility Inversion Model.....	92
Figure 9-4:	Iso-surfaces Generated from VOXI Magnetic Susceptibility Inversion Model	93
Figure 9-5:	DCIP Survey coverage on the Santo Tomás Project, showing the locations of the transmitter/Injection station sites and the receiver station locations (2D and 3D)	96
Figure 9-6:	Plan view of the Santo Tomás chargeability inversion model (left, in mV/V) and the resistivity inversion model (right, in Ohm-m) where the inversion model in each case is sub-horizontally plan sectioned by a plane dipping north at 10°. The section trace is demarcated by the gray ‘inclined contour’ line intersecting with the LiDAR-derived shaded topography.....	97
Figure 10-1:	Santo Tomás Project drill collar and hole trace locations for North and South Zones resource drilling, and exploration drilling at Brasiles	102
Figure 10-2:	North Zone drill hole collar locations and drill hole traces showing composite intervals > 0.1% Cu	103
Figure 10-3:	South Zone drill hole collar locations and drill hole traces showing composite intervals > 0.1% Cu	104
Figure 10-4:	Brasiles exploration drill hole collar locations and drill hole traces showing composite intervals > 0.1% Cu.....	105
Figure 10-5:	View of North Zone historical and contemporary drilling through topography showing thematic assay sample results. Data for GT001 and N045 through N047 are excluded.....	119
Figure 10-6:	View of North Zone historical and contemporary drilling through topography showing the disposition of the Significant Cu Composite Intervals from the North Zone as Listed in Table 10-5.....	120
Figure 10-7:	View of North Zone historical and contemporary drilling absent topography and displaying key logged lithologies used to constrain geological modeling in the North Zone	121

Figure 10-8:	View of South Zone Historical and Contemporary Drilling through Topography showing Thematic Assay Sample Results Data	122
Figure 10-9:	View of South Zone (left) and North Zone (right) chargeability shells from the unconstrained 3D DCIP inversion, showing the apparent of orientation of each zone	123
Figure 10-10:	View of South Zone historical and contemporary drilling absent topography and displaying key logged lithologies used to constrain geological modeling in the South Zone	125
Figure 11-1:	Photos of Oriented Core Logging, CRM Storage and Samples for Shipping.....	128
Figure 11-2:	A: Core Photo Capture Station at El Ranchito; B: Core Photo Preparation and QA in IMAGO@.....	129
Figure 11-3:	A: Specific Gravity Displacement Weight Equipment and Paraffin Wax Pot; B: UCS Point Load Tester...	130
Figure 11-4:	Sample Pulp Lockbox Secure Racking Storage (left); Coarse Reject Sample Offloading, (center); Cut Core Racking and Storage with Engraved Metal Box Tags (right) at the El Ranchito Secure Storage Facility.	133
Figure 11-5:	Oroco sample tag stickers	137
Figure 11-6:	Standard Envelope with Oroco Sample Number Added and Bagged (left) and empty PDUP (pulp duplicate marker) bag (right).	137
Figure 11-7:	PDL Determination, Mean Grade vs. Relative Difference, Cu (ppm).....	141
Figure 11-8:	Standard Control Chart for OREAS 151a Cu (ppm)	142
Figure 11-9:	FDUP Min Cu vs. Max Cu Plot	146
Figure 11-10:	FDUP Cumulative Frequency vs. AVRDR Plot for Cu, Au, Ag, and Mo.....	147
Figure 11-11:	Course Duplicate Min Au vs. Max Cu Plot.....	148
Figure 11-12:	CD Cumulative Frequency vs. AVRDR Plot	149
Figure 11-13:	Pulp Duplicate Min Au vs. Max Au Plot	150
Figure 11-14:	CD Cumulative Frequency vs. AVRDR Plot	151
Figure 11-15:	Pulp Blank Performance Chart Cu PPM	153
Figure 11-16:	Standard Performance Chart for OREAS 23b, Cu PPM	154
Figure 11-17:	Pulp Blank Potential Carry-Over or Smear, Cu PPM.....	155
Figure 11-18:	Coarse Blank Performance Chart for Cu	157
Figure 11-19:	Coarse Blank Performance Smear Chart for Cu	158
Figure 11-20:	Standard-Type Chart for CBLK2, Cu PPM.....	159
Figure 13-1:	Copper Rougher Kinetic Results – Master Composite.....	173
Figure 13-2:	Molybdenum Rougher Kinetic Results – Master Composite	173
Figure 13-3:	Copper Cleaner Performance – Master Composite	174
Figure 13-4:	Copper Recovery vs. Head Grade	178
Figure 13-5:	Molybdenum Recovery vs. Head Grade.....	179
Figure 13-6:	Predicted vs Actual Gold Recoveries.....	180
Figure 13-7:	Predicted vs Actual Silver Recoveries	181
Figure 14-1:	Drill Hole Locations on the Santo Tomás Property (scale in meters)	184
Figure 14-2:	Plan View of the Modeled Horst Block	187
Figure 14-3:	Geologic Mapping (Left) and Geology Model (Right) Comparison.....	189
Figure 14-4:	Comparison of Cross-Sectional Interpretation and Geologic Model (Looking Northeast)	190
Figure 14-5:	Cross-section of Oxidation Model (Looking Northeast).....	191
Figure 14-6:	Plan View of Mineralized Domains	192
Figure 14-7:	Log Histograms of Cu (ppm) Distribution in the North Zone (left) and South Zone (right)	197

Figure 14-8: Raw Sample Log Histograms for Mo, Ag, Au, and S in the North Zone	198
Figure 14-9: Raw Sample Log Histograms for Mo, Ag, Au, and S in the South Zone	199
Figure 14-10: Raw Sample Interval Histogram (left) and Log-Probability (right)	202
Figure 14-11: Distribution of Cu Grade in Raw and 2 m Composites	203
Figure 14-12: Log-Probability Chart on North Zone Cu for Capping Analysis	205
Figure 14-13: Log-Probability Chart on Mo (Both Zones) for Capping Analysis	207
Figure 14-14: Log-Probability Chart on Au (Both Zones) for Capping Analysis	209
Figure 14-15: Log-Probability Chart on Ag (Both Zones) for Capping Analysis	211
Figure 14-16: Normal Score Transformed Modelled Semi-Variogram for Cu in North Zone	215
Figure 14-17: Normal Score Transformed Modelled Semi-Variogram for Mo in North Zone	215
Figure 14-18: Normal Score Transformed Modelled Semi-Variogram for Au in North Zone	216
Figure 14-19: Normal Score Transformed Modelled Semi-Variogram for Ag in North Zone	216
Figure 14-20: Modelled Semi-Variogram for S in North Zone	217
Figure 14-21: Normal Score Transformed Modelled Semi-Variogram for Cu in South Zone	217
Figure 14-22: Normal Score Transformed Modelled Semi-Variogram for Mo in South Zone	218
Figure 14-23: Normal Score Transformed Modelled Semi-Variogram for Au in South Zone	218
Figure 14-24: Normal Score Transformed Modelled Semi-Variogram for Ag in South Zone	219
Figure 14-25: Aerial Extents of the Santo Tomás 2023 MRE Block Model	220
Figure 14-26: Cross-Section Used in Visual Comparison - North Zone Cu Values	224
Figure 14-27: Cross-Section Used in Visual Comparison - North Zone Mo Values	225
Figure 14-28: Cross-Section Used in Visual Comparison - North Zone Au Values	226
Figure 14-29: Cross-Section Used in Visual Comparison - North Zone Ag Values	227
Figure 14-30: Cross-Section Used in Visual Comparison - South Zone Cu	228
Figure 14-31: Cross-Section Used in Visual Comparison - South Zone Mo	229
Figure 14-32: Cross-Section Used in Visual Comparison - South Zone Au	230
Figure 14-33: Cross-Section Used in Visual Comparison - South Zone Ag	231
Figure 14-34: Swath plot in X direction - North Zone Cu	232
Figure 14-35: Swath plot in X direction - North Zone Mo	233
Figure 14-36: Swath plot in X direction - North Zone Au	234
Figure 14-37: Swath plot in X direction - North Zone Ag	235
Figure 14-38: Swath plot in X direction - South Zone Cu	236
Figure 14-39: Swath plot in Y direction - South Zone Mo	237
Figure 14-40: Swath plot in Y direction - South Zone Au	238
Figure 14-41: Swath plot in Y direction - South Zone Ag	239
Figure 14-42: Oblique View of Block Model Colored by Resource Classification	241
Figure 14-43: East Looking Section of Economic Pit Shell	243
Figure 14-44: Graph of Resource and Rock Tonnage by Economic Pit Shell Scenario	243

1 SUMMARY

1.1 Introduction

This report was prepared as a Canadian National Instrument 43-101 (NI 43-101) technical report on a Mineral Resource Estimate (MRE) for Oroco Resource Corporation (Oroco or the Company) by Ausenco Engineering USA South Inc. and Ausenco Engineering Canada, Inc. (collectively Ausenco) and SRK Consulting (US), Inc., SRK Consulting (Canada) (collectively SRK), on the Santo Tomás Project (the Project).

The responsibilities of the engineering companies who were contracted by Oroco to prepare this report are as follows:

- Ausenco managed and coordinated the work related to the report itself, reviewed the metallurgical test results and reviewed historical and present reports regarding site regional and local infrastructure.
- SRK (Denver) completed the data verification work and developed the mineral resource estimate and statement for the Project.
- SRK (Vancouver) completed the work related to geological setting, deposit type, exploration work, drilling, exploration works, sample preparation and analysis

1.2 Property Description and Location

The Santo Tomás property (the "Property") is in the municipality of Choix, in northern Sinaloa State, Mexico. The Property is centered at latitude 26°53'00" North (N) and longitude 108°11'30" West (W). The Property comprises a total of 1,172.9 hectares (ha) of concessions, covering the initial area of exploration and the area of the Santo Tomás North and South porphyry copper mineralization.

Access to the Property is by way of a 160 kilometer (km) paved highway and a two-lane road from the Pacific Ocean Port of Topolobampo, through the city of Los Mochis to the northern town of Choix. The southern end of the Property is reached either by an access road, part of which was originally built to service the El Sauzal Mine of Goldcorp in Chihuahua State or by using the current access road that passes through Cajón de Cancio and Rancho La Soledad. Total distance from El Ranchito to the project site is 38 km along most unimproved but maintained dirt roads.

The Property area is mountainous and is part of the southwestern Sierra Madre Occidental (SMO). The topography of the area is deeply incised. Steep-walled valleys rise in elevation from Río Fuerte, at 220 meters (m) elevation above sea level, to approximately 1,340 m at the El Bienestar Ranch.

1.3 Mineral Tenure & Ownership

One hundred percent of the legal title of the Core Concessions: Santo Tomás, Bob, Roberto Verde, Esme, Karisu, Karisu Fracc 1 and Tona, have been registered to Xochipala Gold (XG), an Oroco subsidiary, since December, 2019 (1,172.9 ha). Oroco indirectly (via subsidiaries) holds 95% of the issued shares of XG (5% are held by a Mexican individual). XG's 100% legal title is subject to a 10% contractual (not registered) interest in favor of third parties. Oroco holds a net 85.5% interest in the Core Concessions (95% in XG x 90% net interest in the concessions).

1.4 Geology and Mineralization

Porphyry Cu (Mo-Au-Ag) mineralization on the Property is closely associated with intrusives linked to the Late Cretaceous to Paleocene (90 to 40 Ma) Laramide Orogeny. Santo Tomás and most of the known porphyry copper deposits in México lie along a 1,500 km-long, NW trending belt sub-parallel to the western coast of México extending from the southwestern United States through to the state of Guerrero in México. The tectonomagmatic evolution of this belt is linked to the accretion of allochthonous terranes, onto the continental margin of North America in the Mesozoic and earliest Cenozoic, the largest represented by the Guerrero Composite Terrane. More specifically the Santo Tomás Property lies within the Tahue Terrane, a subterrane of the Guerrero Composite Terrane. This comprises a basement of Paleozoic accreted sedimentary rocks and Triassic rift-related, meta-igneous rocks. These basement strata are unconformably overlain by Middle Jurassic and Early Cretaceous age arc-related rocks of the Guerrero Arc. (Ortega-Gutiérrez et al., 1979; Henry and Fredrikson, 1987; Roldán-Quintana et al., 1993; Freydier et al., 1995). Island arc-related strata, comprising volcanic and volcanoclastic sequences of oceanic affinity and associated intrusive plutonic suites were accreted onto North America in the Late Cretaceous during the Laramide orogeny (Campa and Coney, 1983; Centeno-García et al., 1993). Exposed batholiths and associated stock and dikes, form an extensive NW-SE trending belt, the most extensive represented by the Sinaloa-Sonora Laramide batholith complex (Anderson and Silver, 1969; Gastil and Krummenacher, 1977; Valencia Moreno et al., 2003; Ramos-Velázquez et al., 2008). Laramide contraction was followed by Basin and Range Province extension. This was associated with the eruption and deposition of an extensive middle Cenozoic (Tertiary) volcano-sedimentary sequence, the SMO volcanic province, comprising andesitic volcanoclastics and flows, rhyolite ignimbrites, and intercalated sediments.

In the Santo Tomás area, Mesozoic-aged country rocks, comprising carbonate-rich sediments including limestone, marble bodies, sandstones, and large volumes of andesitic volcanic rocks were intruded by a range of Laramide intrusions related to the Late Cretaceous Sinaloa-Sonora Batholith. Multiple phases are recognized ranging from dioritic to monzonitic in composition. At Santo Tomás, the dominant intrusive lithology, closely associated with mineralization, is a Paleocene age (57.2 ± 1.2 Ma) quartz-monzonite. Mineralization is strongly structurally controlled by the Laramide-age deformation which controlled both the emplacement of the quartz-monzonite dike system and related hydrothermal alteration, hydrothermal breccias, and sulphide mineralization. Sulphides are dominated by pyrite-chalcopyrite-(molybdenite) with minor bornite, covellite, and chalcocite that are distributed in quartz monzonite and altered andesite country rock. Alteration comprises extensive zones of potassic, phyllic, propylitic, silica-albite and argillic hydrothermal alteration. Mineralization forms a tabular, southeast (SE) striking, northwest (NW) dipping zone primarily defined by finely disseminated sulphides and fracture-fillings with subordinate sulphides hosted in stockwork quartz veinlets. Minor mineralization is associated with skarn and replacement-style mineralization in the hanging wall limestone. Minor copper oxides occur near the surface.

Oroco, together with SRK, undertook a detailed mapping campaign on the Property. All mapping data were compiled into an Arc GIS project, comprising lithology and structural orientation data, and included active links to field photographs. All data were imported into 3D software (Leapfrog Geo™) and integrated with high-resolution drone data, lineament analysis data, geophysics data and drill hole data to further constrain lithology domains, contacts and structures and inform the lithostructural modeling and resource modeling process.

1.5 History – Exploration Programs

1.5.1 Exploration Programs

Santo Tomás has attracted the attention of mining companies since the late 1960's, though artisanal mining is evident in the main zone of mineralization. These workings are believed to date back to the early 1900's. Workings observed,

typically exploited high-grade oxide copper mineralization hosted in what appear to be breccias associated with mass wasting and collapse of large sections of limestone. Extensive zones of oxide copper at surface were likely the original attraction to the area.

Numerous companies carried out significant drilling programs and evaluation efforts. These drilling programs, resource estimates and mining engineering studies initially formed the basis for the re-evaluation of the deposit by Oroco. Approximately 60% of historic core was available. Historical engineering work culminated in a series of metallurgical, resource estimation based on an additional 4000 m of drilling in 40 holes in 1993/94, 33 reverse circulation drill holes + 7 diamond drill holes.

In 2010, John Thornton (Thor Resources LLC) compiled all the historical documentation and issued a resource estimate. This resource is classified as an historical estimate. The qualified person has not done sufficient work to classify the historical estimate as current mineral resources or mineral reserves; and the issuer is not treating the historical estimate as current mineral resources or mineral reserves. The exploration history is summarized in Table 1-1.

Table 1-1: Project Historical Technical Work and Studies

Year	Company	Work	Results
Early 1900's	Artisanal Miners	High grade Ox Cu Mining	No information on tonnes of material removed
1968 to 71	ASARCO	Road Building and drilling, 43 vertical diamond core holes and 16 vertical rotary percussion holes, 15,088 m total drilling	Property relinquished in 1973 after spending 1 million dollars
1973 to 77	Tormex - Peñoles	26 ASARCO holes re-logged. 5,336 m of 1/2 core split and assayed. 2,401 m of new drilling in 7 holes	New resource estimation undertaken. No information available. Property relinquished
1973	Government supported mapping by Davidge and Clark	Preliminary Geology and Mineralization of the Choix Area	Presumably data collected was capture by the governmental mapping program
1990	Esmeralda Group	Review and updating geological sections and plans	No information available
1991	Minera Real De Ángeles	Re-logged 12 ASARCO holes and re-assayed 2 holes	Good correlation between assay results reported
1992	Exall Resources Limited	Acquired property	--
1993	Exall Resources Limited	4,000m of 33 reverse circulation drill holes and 7 diamond drill holes	MRE completed
1993	Exall Resources Limited	Bateman Engineering Inc. retained to undertake a PFS	Metallurgy and Mine plan produced
1994	Exall Resources Limited	Metallurgical test work performed by Minetek S.A. de C.V. and Mountain States Research and Development	Test work indicates a 90% copper recovery rate using standard concentration methods, resulting in a 28% copper concentrate.

Year	Company	Work	Results
1994	Exall Resources Limited	Preliminary pit constrained Mineral Resource developed on previous Tormex and ASARCO drilling	Deposit evaluated as two pits: North and South. An estimate of the mineral resources was reported.
2011	Thor Resources LLC	Technical Report and mineral resource estimation (historical)	MRE completed.

1.6 Exploration and Drilling

1.6.1 Exploration by Oroco

Exploration work undertaken by Oroco in the period from 2017 to 2019 is described in Bridge (2020). Since 2019, Oroco has conducted an exploration program of remote sensing and airborne and ground geophysical surveys in preparation for a resource drilling campaign at North and South Zones. Since the commencement of resource drilling, surface exploration work has mostly comprised of selective geological mapping and a seven (7) drill hole exploration drilling initiative was campaigned at Brasiles. The location of each major contracted remote sensing and geophysical survey is displayed in Section 9 of this report.

Remote sensing work includes an airborne LiDAR survey to update and improve the resolution, accuracy and precision of the project digital elevation model and orthophotography record. The 342 km² LiDAR survey over the project was flown during the April dry season of 2021. Oroco has used the products of the LiDAR survey to comprise the master digital elevation model / digital terrain model (DEM / DTM) for the Project, where it has been used in the Project GIS and three-dimensional (3D) modeling platforms.

Geophysical surveys focused on an airborne survey for project magnetometry (with surface radiometric emission sensors and very low frequency-electromagnetic (VLF-EM) transmissions receivers), and a targeted (area-constrained) ground-based 3D direct current (DC) electrical resistivity and induced polarization (DCIP) survey. The selection of methods targets geophysical products that can specifically assist with broad geological definition of lithologies (passive magnetics and radiometric measurements, especially of potassium ('K')), major geological structures (VLF and resistivity contrasts) and targeting of metal-sulphide mineralized units (chargeability). Secondary alteration may also be evidenced in electrical data sets (resistivity) and in alteration forming secondary magnetic iron oxides (magnetics, magnetic remanence effects).

The heli-borne magnetics survey comprised of approximately 2,022 line km of traverse line flying at a line spacing of 50 m by 500 m tie-line flying totaling approximately 252 line km. A magnetic susceptibility inversion model was developed from the airborne magnetics dataset to assist with exploration and targeting of porphyry Cu mineralization.

A 3D DCIP ground survey of the Project, ultimately covering some 22 km² was undertaken between September 2020 and March 2021. The survey final dataset with approximately 715,000 pole-dipole data points over the grid enabled the generation of an unconstrained inversion model that defined areas of chargeability and resistivity (conductivity) that comprised a critical targeting tool for the resource and exploration drilling. A constrained model was subsequently developed and has been used to assist with the definition of major structural features.

Geological mapping and surface channel sampling, as well as the location of historical artisanal mining adits has been undertaken in support Project exploration. This work is detailed in other sections of this report.

1.6.2 Drilling History

Drilling campaigns were conducted by ASARCO, Tormex and Exall Resources Limited (Exall) between 1968 and 1993, with the most recent pre-Oroco drilling completed by Exall in 1993. A total of 106 drill holes (reverse circulation, percussion and diamond drill holes, collectively the 'historical' or 'legacy' drill holes) were completed on the Property (Thornton, 1994). ASARCO completed sixteen percussion holes in the late 1960s to early 1970s, but the logs and results for these holes have not been identified (Spring, 1992). The historical Santo Tomás drill hole database contains information on 90 drill holes (reverse circulation and diamond drill holes), totaling 21,075 m of lithological data, including 7,244 Cu assays.

Reverse circulation holes drilled to 1991 are designated herein as the "STD series" drill holes. Exall Resources Limited drilled an additional 40 holes to 1993, designated herein as the "STE series" drill holes (Table 1-2).

Table 1-2: Historical and Oroco Drilling Campaigns, Total Assays, Holes and Meters Drilled

Historical Drilling	No. of Assays	No. Drill holes	Total Length (m)	Average Length (m)
STD series to 1991	4,707	50	16,003	320
STE series, to 1994	2,537	40	5,071	127
Total Drilling	7,244	90	21,075	234

1.6.3 Oroco Drilling

Commencing on 28th July, 2021 and continuing through March 28th, 2023, Oroco completed 76 diamond drill holes for 48,480.88 m of diamond core drilling. This campaign represents the entirety of Phase 1 drilling by Oroco. Seven (7) of these holes were drilled for exploration purposes at the Brasiles prospect (5,116.36 m) and have been excluded from consideration in the MRE presented in this report (Section 14). Table 1-3 displays the drill holes and the total meters that were included and excluded in the present MRE. At the time the determination of the MRE was undertaken (effective date - April 21, 2023), assays for one (1) drill hole (N047) and Quality Assurance/Quality Control (QA/QC) check assay data for two (2) drill holes (N045 and N046) at North Zone had not been received. The MRE was therefore made using assay data from 65 (40,978.92 m) of the Phase 1 Oroco drill holes combined with available legacy results (Table 1-2). A single geotechnical hole drilled by Oroco, GT001, was also excluded.

Table 1-3: Oroco Drill Hole Inclusion/Exclusion Table

Inclusion status	Drill holes	Meters
Included	ST21-N001 to ST21-N010 N11 to N044 S001 to S021	40,978.92
Excluded	N045 to N047 GT001 B001 to B007	7,501.96
Total	76	48,480.88

Drill holes ST21-N001 through ST21-N010 and N011 through N047 are located in the Project’s North Zone. Holes S001 through S021 are located in the South Zone. Holes B001 through B007 are exploration holes drilled at the Brasiles Prospect (a.k.a Brasiles Zone). Hole GT001 is the first (and so far, the only) geotechnical drill hole on the project, and is located in southern North Zone.

The now complete Phase 1 drilling undertaken by Oroco (2021 – 2023) has confirmed and extended the distribution of known mineralization at North and South Zones, allowing for the calculation of the MRE being presented in this report (albeit the MRE excludes holes GT001, N044 through N047 for which assays and QA results were not available at the MRE effective date). B003 is the first significantly mineralized hole for which Oroco has copper assays in the Brasiles Prospect area, and so represents the discovery hole at Brasiles.

The latest drilling program statistics (Table 1-4) reflect longer drill holes in general. The change in drill hole orientation to angled vs vertical in previous historical campaigns, increased hole lengths. In general, the new holes were drilled to terminate in the footwall andesites, and not left terminating in mineralization. The Oroco drill holes were drilled approximately orthogonal to the mineralization strike and dip based on new geological models developed using the historical drilling.

Table 1-4: 2022-2023 Core Drilling Program Undertaken by the Oroco Program

Oroco 2022/23 Drilling	No. of Assays	No. Drill holes	Total Length (m)	Average Length (m)
North Zone	13,632	44	28,824	655
South Zone	5,503	21	12,154	578
Total Drilling	19,135	65	40,978	630

1.7 Sample Preparation, Analysis, Security and QA/QC

Sample preparation, analysis, security and quality assurance/quality control (QA/QC) at Santo Tomás follow industry standards. There is full chain-of-custody (COC) documentation from the drill rig to the assay laboratory. Drill core cutting, sampling and insertion of standards is fully documented and follows on-site Standard Operating Procedures (SOP). Drill core and standards are held in limited access, locked facilities.

All pulps and coarse rejects from the Oroco drilling program are returned to Choix, cataloged and stored in a built-for-purpose locked facility. Sample pulps are stored in locked containers. Coarse rejects are stored in large plastic, metal reinforced containers. Drill core samples are fully cataloged, and labeled drill core boxes are stored by hole number under cover in a locked facility.

The submission rate of blanks, Commercial Reference Materials (CRMs) and pulp/core/coarse reject duplicates is to industry standard. Lab failures are resolved with a re-assay (or re-assays) as required according to the Santo Tomás SOP. Results are not publicly released until QA/QC is completed.

Specific gravity (SG), point load, magnetic susceptibility, and Uniaxial Compressive Strength (UCS) data are collected under sampling programs defined in the Santo Tomás standard operating procedures manuals. Required calibrations and calibration frequencies for the sampling equipment are defined in the SOP’s.

Drill core logging, cutting, sampling a submission occurs under a well-designed and controlled program.

1.8 Data Verification

Oroco employs industry standard controls on data collection and subsequent data verification. There is significant focus on confidently identifying lithologies and alteration assemblages through the vetting of drill holes logs and employing spot and systematic spectral scanner measurements. This allows validation of the original data collected by the logging team.

Geotechnical data validation is undertaken using a system of comparative re-logging on selected sections of the core by members of the geotechnical logging team. This ensures a more closely aligned set of observations and results. Rock Quality Designation (RQD) logged data are compared against whole core photos to identify obvious outliers in the data. Where appropriate the core is re-logged prior to cutting.

Other data collection efforts including, SG, point load, magnetic susceptibility, spectral scanner data and UCS have equipment calibration requirements to ensure database results are comparable.

1.9 Mineral Processing and Metallurgical Testing

Metallurgical testing of Santo Tomás mineralized materials and host rocks began in 1975 with a limited amount of metallurgical flotation and acid leaching test work conducted between 1991 and 1994 to support the Prefeasibility Study Bateman prepared for Exall published in 1994. Ausenco's review of the previous test work found much of it to be conceptual in nature and not suitable to support a modern technical study. As such, a recent test work program was employed to represent an open pit operation proposed for Santo Tomás that would utilize current froth flotation methodology and reagents to produce saleable copper and molybdenum concentrates. Nine spatially representative variability samples were selected from the 2022 drilling campaign and shipped to ALS Metallurgy in Kamloops, BC for subsequent testing in Q3 2022. A Master Composite was then assembled from portions of selected samples to achieve a target feed grade of 0.34 percent copper.

The results of the Q2 2022 test work program are summarized below:

Mineral composition was measured for all samples using QEMSCAN techniques. Chalcopyrite accounted for approximately 98% of the copper observed in the samples. Molybdenite and sphalerite accounted for less than 0.1% of and pyrite accounted for 1.5% of the total mass. A detailed QEMSCAN Particle Mineral Analysis (PMA) conducted on the Master Composite sample indicated that chalcopyrite was 40% liberated at a primary grind size of 150 µm and pyrite showed increased liberation levels averaging 61% at this grind size.

Each of the variability samples was tested for comminution properties and a Rod Mill Work Index test was conducted on the Master Composite that returned a value of 18.4 kWhr/tonne. The 75th percentile values of Axb & ball mill work index from the variability samples were 30 and 18.3 kWh/tonne, respectively. These data suggests that High Pressure Grinding Roll (HPGR) crushing should be considered over semi-autogenous grinding (SAG) milling for this project since several of the samples are characterized as hard with respect to impact breakage. A locked cycle test was conducted on the Master Composite achieved a bulk concentrate grading of 24.7% Cu and 0.68% Mo and recoveries of 82.6% and 61.8% for copper and moly, respectively. The bulk concentrate from the lock cycle test contained 1.1 ppm gold and 114 ppm silver. The current test program did not include copper-molybdenum separation test work. Final concentrate produced from the Master Composite locked cycle test was analyzed for deleterious elements with zinc (Zn) and mercury (Hg) being elevated to levels which may trigger penalties at smelter. These elements have been identified as associated with the

skarn materials which have been flagged for exclusion from the mine plan moving forward. Penalty limits for these elements should be confirmed with a concentrate marketing specialist.

From the recent variability flotation test work results, Ausenco forecasts the following recoveries which are employed by SRK to develop the mineral resources presented in this report:

- Cu Recovery – 84.3%
- Mo Recovery – 66%
- Au Recovery – 57%
- Ag Recovery – 54%

1.10 Mineral Resource Estimation

The MRE has been prepared with an effective date of April 21, 2023 is shown in Table 1-5. The MRE is supported by a robust geologic model and constraining mineralized grade shells. The geologic model, resource estimation and classification were performed by SRK. A full description of the resource estimation methodology is provided in Section 14.

In order to meet the “reasonable prospects for eventual economic extraction” (RPEEE) requirement, the Project has been deemed amenable to open pit mining, with cut-off grades (CoG) established using benchmarked costs from similar deposits in Mexico and recoveries based on metallurgical test work to date. The Mineral Resources have been reported based on an in-situ CoG of 0.15% copper.

Mineral resources are not mineral reserves and do not have demonstrated economic viability. There is no certainty that all or any part of the mineral resources will be converted into mineral reserves in the future. The estimate of mineral resources may be materially affected by environmental permitting, legal, title, taxation, socio-political, marketing, or other relevant issues.

Table 1-5: Mineral Resource Statement, Effective April 21, 2023 - SRK Consulting (US), Inc.

Category	Zone	Tonnes Mt	Average Grade					Contained Metal ⁹				
			CuEq ¹⁰	Cu	Mo	Au	Ag	CuEq ¹⁰	Cu ¹¹	Mo ¹¹	Au ¹¹	Ag ¹¹
			%	%	%	ppm	ppm	Mlb	Mlb	Mlb	Koz	Koz
Indicated	North Zone	487.3	0.36	0.32	0.009	0.03	2.1	3,864	3,400	91.9	392.8	32,719
	Total Indicated	487.3	0.36	0.32	0.009	0.03	2.1	3,864	3,400	91.9	392.8	32,719
Inferred	North Zone	197.1	0.36	0.32	0.005	0.03	2.1	1,570	1,400	23.6	214.4	13,375
	South Zone	402.8	0.35	0.31	0.008	0.02	1.9	3,127	2,772	72.0	286.2	25,083
	Total Inferred	599.9	0.36	0.32	0.007	0.03	2.0	4,697	4,171	95.6	500.6	38,458

Notes:

1. Mineral resources are not mineral reserves and do not have demonstrated economic viability.
2. The Mineral Resources are reported at an in-situ cut-off grade of 0.15% Cu.
3. All figures are rounded to reflect the relative accuracy of the estimates. Totals in Table 1 may not sum or recalculate from related values in the table due to rounding of values in the table, reflecting fewer significant digits than were carried in the original calculations.
4. The MRE excludes identified oxide material due to a lack of confidence in recovery assumptions of oxidized tonnages at this stage of the project.
5. Metal assays are capped where appropriate. At this stage of the project, it is SRK’s opinion that all the elements included in the metal equivalents calculation have a reasonable potential to be recovered and sold.
6. All dollar amounts are presented in US dollars (US\$).
7. Bulk density is estimated on a block basis using specific gravity data collected on diamond drill core.
8. Economic pit constrained resource with reasonable prospects of eventual economic extraction (“RPEEE”) were based on a copper price of \$3.80/lb, molybdenum price of \$12.00/lb a gold price of \$1,650/oz, and a silver price of \$22.00/oz. Metal recovery factors of 84.3% for copper, 66% for molybdenum, 57% for gold and 54% for silver have been applied. Average slope angles of 50 degrees are applied (45 degrees for over 360 m elevation and 50 degrees below 360 m elevation) and is based on geotechnical data collected to date.
9. The in-situ economic copper (Cog) was calculated resulting in a 0.13% Cu CoG. To align with previously published mineral resources, Oroco has selected to use an effective CoG at 0.15% Cu. CoG assumptions include: a copper price of \$3.80/lb, molybdenum price of \$12.00/lb, gold price of \$1,650/oz, and silver price of \$22.00/oz. Suitable benchmarked technical and economic parameters for open pit mining, including a 99% mining recovery and costs of mining at \$2.25/t, processing at \$5.00/t, General & Administrative at \$1.00/t, and selling costs at \$1.00/t, with Private Royalties at 1.5%, have been applied in consideration of the RPEEE. Recoveries are applied as listed in Note 8.
10. Equivalent Copper (CuEQ) percent is calculated with the formula $CuEq\% = ((Cu\ grade * Cu\ recovery\ [84.3\%] * Cu\ price) + (Mo\ grade * Mo\ recovery\ [66\%] * Mo\ price) + (Au\ grade * Au\ recovery\ [57\%] * Au\ price) + (Ag\ grade * Ag\ recovery\ [54\%] * Ag\ price)) / (Cu\ price * Cu\ recovery\ [84.3\%])$. It assumed that the Santo Tomás Project will produce a conventional (flotation) copper concentrate product based on metal recoveries at 84.3% Cu, 66% Mo, 57% Au, and 54% Ag based on initial preliminary metallurgical test work.
11. Reported contained individual metals in Table 1 represent in-situ metal, calculated on a 100% recovery basis, except for CuEq% (see Note 10).

1.11 Interpretation and Conclusions

1.11.1 Geology and Mineralization

The geology of the deposit is well understood and the controls on mineralization are better defined with the completion of the Phase I drilling program. A much better understanding of structural controls and structure bounding limits on mineralization has been captured in the updated 3D geology, alteration and structural model and applied to the MRE

presented in this report. Additional drilling will be required in the southwest sector of the South Zone to better understand the limits on the mineralization and alteration observed and mapped at surface.

1.11.2 Exploration, Drilling and Analytical Data Collection Support of Mineral Resource Estimation

Additional surface mapping and exploration has been incorporated with the drilling-supported 3D models. Surface mapping and exploration should be continued to more precisely define the western footwall fault and resource internal faulting defined through drilling. Analytical data collection in support of the Mineral Resource Estimation should continue with a focus on historical drill re-logging and check sampling for comparison of historical results. This will confirm some of the historical reporting on the repeatability of target economic elements. Additional drilling in resource defined as Inferred will increase confidence in the resource estimate, especially in the South Zone that is currently all classified as Inferred.

An on-going review of the sulphide bearing veins and their orientations will help better refine additional drilling program design with regards to the dips and azimuth of drill holes.

1.11.3 Mineral Resource Estimates

In the opinion of the QP, Oroco has completed detailed and thorough geologic work programs to support the construction of a robust geologic model and fundamentally sound structural domain model. The models adequately reflect the geologic setting that both controls and limits mineralization in the North and South Zones. The oxidation model is rudimentary, however, it delineates oxidized material from reduced material that can be isolated in the block model properly. Oxide mineralization has been excluded from the MRE. A better constrained oxide resource may represent an opportunity in future resource estimates. Mineralization domains are utilized to constrain the MRE and limiting geologic features are used when tabulating the mineral resource statement. The MRE and statement for the Santo Tomás project conforms to satisfactory industry practices and satisfies the requirements of the CIM Definition Standards required for disclosure under NI 43-101.

1.11.4 Metallurgy

Porphyry-copper type mineralization is the primary focus for exploration on the Santo Tomás property. Exploration and drilling of the copper-porphyry mineralization at Santo Tomás has been conducted since October 1968. The porphyry copper mineralization is sulphide-dominant with chalcopyrite being the main Cu-bearing sulphide mineral (Borovic, 2006; Spring, 1992). The skarn and oxide copper potential of the Property is very much subordinate to the hypogene base metal-sulphide potential but offer an opportunity for additional mineral resources. Skarn mineralization is often elevated in zinc. Metallurgical test work undertaken in 2023 indicates active management of mill feed source should be employed in areas of limestone skarn contacts.

1.11.5 Risks and Opportunities

Additional drilling is required to upgrade mineral resource classifications. Currently, the South Zone is classified as inferred resources but with additional drilling there is potential to upgrade the classification and delineate more mineralized material.

Further logging and (re)sampling of historical drill core should be undertaken to increase confidence in the geologic interpretation and resource estimation.

Additional metallurgical test work should focus on expanding the grade range and add confidence to the metallurgical recovery estimates. A more detailed oxide copper resource evaluation is required as additional tonnes are currently excluded from the resource estimate. Separate and additional Cu-Mo separation metallurgical recovery work is also required.

Oroco needs to remain up to date on changes to the Mining Regulations.

1.12 Recommendations

1.12.1 Overall

The following subsections summarize the key recommendations identified for future stages of study for the Santo Tomás Project. Table 1-6 presents a budget for each recommended item described in the subsections that follow:

Table 1-6: Proposed Budget Summary

Description	Cost in US Dollars
PEA Report	700,000
Exploration Geology and Mineral Resources	1, 250,000
Mineral Processing	200,000
Total	2,150,000

1.12.2 Preliminary Economic Assessment Future Study

Santo Tomás represents an advanced stage exploration project targeting two zones of near surface porphyry-style mineralization. Further drilling and additional sampling of historical drillholes has the potential to develop additional mineral resources and increase confidence in existing mineral resources. Additional step-out and regional exploration drilling at Santo Tomás has the potential delineate additional mineralization, specifically in the South Zone where mineralization is observed on surface but has not been drilled.

In SRK’s opinion, the results of the exploration work completed on the Project to date are of substantial technical merit to recommend additional exploration expenditures. The next exploration campaign should include a combination of infill drilling to improve known mineralization continuity and geological understanding and exploration drilling in the South Zone to test for new economic mineralization. Additionally, the QP recommends a preliminary economic assessment (PEA) be conducted on the Project. SRK has estimated a PEA to cost approximately US\$700,000.

1.12.3 Exploration, Geology and Mineral Resources

SRK recommends the following work programs for the Project to further improve the deposit understanding to reduce uncertainty and risk associated with geology and mineral resources:

- Perform validation checks on historical drilling collars and downhole survey

- Re-assay retained drill core and/or sample pulps for all historical data.
- Perform re-logging or check logging of drilling data with an emphasis on zones of oxidation, transition, and reduction mineralogy.
- Expand the existing knowledge of the various alteration zones related to the porphyry mineralization at Santo Tomás. This may include collecting of additional mineralogical, geochemical or other data with 3D modeling of grouped alteration zonation to align with metallurgical recovery, deleterious materials, and understanding of deposit genesis.
- Additional resource definition drilling targeting zones of inferred mineralization along with expanding the known mineralization envelop to the north and south. Additionally drilling across the South Zone and in areas of inferred mineral resources in the North Zone will aid in reducing uncertainties in these areas as part of future studies.
- Continued advancement of the Project toward delivery of a Preliminary Economic Assessment (PEA)

The proposed budget to cover the drilling and sampling is approximately US\$1,250,000.

1.12.4 Mineral Processing

The following additional metallurgical tests are recommended for the next phase of study at an estimated cost of \$200K:

- Mineralogy

All future variability testing should include QEMSCAN, chemical and mineralogical characterization. A relationship between these measurements and field hyperspectral results should be developed.

- Comminution

Due to the variance demonstrated for the samples hardness measurements, it is recommended additional comminution test work (including regrind and piston press tests) be conducted on a larger number of samples.

- Flotation

Additional variability samples should be tested to optimize the flotation protocol developed during this test work program. Coarse Particle Flotation (CPF) should also be investigated in a scavenging application as is Cu-Mo flotation separation testing.

- Solid-liquid Separation

Concentrate dewatering requirements also need to be confirmed as should tailings thickening tests be conducted.

- Oxide Leaching

A full evaluation of the oxide materials is recommended including bottle roll tests and column leach studies.

2 INTRODUCTION

2.1 Introduction

The Santo Tomás Property, in Sinaloa State, México is a copper exploration project, located in northeastern Sinaloa State, near the border with Chihuahua, México. This MRE was prepared as a Technical Report for Oroco Resource Corp. ("Oroco") by SRK Consulting (US), Inc., SRK Consulting (Canada) and Ausenco.

This technical report documents a Mineral Resource Estimation for the Santo Tomás project prepared by SRK and Ausenco. It was prepared following the Canadian Securities Administrators' National Instrument (NI 43-101) and Form 43-101F1 Technical Report. Recommendations presented herein conform to the generally accepted Canadian Institute of Mining, Metallurgy and Petroleum's ("CIM") Mineral Exploration Best Practice Guidelines.

The quality of information, conclusions, and recommendations contained herein are consistent with the level of effort involved the review and two site visits by and is based on:

1. The information available at the time of preparation, through to April 21st, 2023;
2. Data supplied by outside sources; and,
3. The assumptions, conditions, and qualifications outlined in this report.

2.2 Scope of Work

The scope of work, as defined in a letter of engagement executed on the effective date of, between Oroco, SRK and Ausenco includes the review of historical technical information that was assembled by Oroco and its supporting consultants and the preparation of an Independent Technical Report. This work involves the assessment of the following aspects of this project:

- Access, topography, climate and local infrastructure;
- Regional and local geology;
- Exploration history;
- A review of historical and 2022/23 drilling data and exploration work carried out on the Property;
- Metallurgical Processing review
- Surface mapping and drill hole Geological (alteration, lithology, and structure) model preparation suitable for an MRE estimation;
- Review of any relevant previously publicly released mineral resource estimations made; and,
- Recommendations for additional work.

The exploration database was compiled and maintained by Oroco and third-party consultants. The contained information was reviewed by SRK where needed. The geological cross-sections and outlines for the copper mineralization were constructed by from the geological database provided by Oroco and its supporting consultants. In the opinion of SRK, the

geological model and drill hole data base developed on the Property is a reasonable representation of the distribution of the targeted mineralization at the current level of sampling.

SRK has no reason to doubt the reliability of the information provided by Oroco. This technical report is based on the following sources of information:

- Discussions with Oroco and its consulting personnel;
- Field geological and structural mapping on the Property by Oroco employees and consultants, including visiting rock outcroppings, and examining sample collections and drill core during and after the 2021-23 drilling program;
- Review of exploration data collected by Oroco and digital assemblies of historical exploration and drilling data dating from 1968; and
- Review of additional information from public domain sources.

Oroco’s collection of the available drill logs and re-logs available were reviewed. Detailed geological cross-sections (50 m spacing) containing current and historical drilling were reviewed and aided in the development of the 3D geological and structural model that was used to constrain grade distribution and develop the MRE.

2.3 Qualified Persons

The Qualified Persons for the report are listed in Table 2-1. By virtue of their education, experience, and professional association membership, they are considered a Qualified Person as defined by NI 43-101.

Table 2-1: Report Contributors

Qualified Person	Professional Designation	Position	Employer	Independent of Issuer Name(s)	Report Section
James Arthur Norine	P.E., Mech. Eng.	VP, Southwest USA	Ausenco	Yes	1.1, 1.2, 1.11.5, 1.12.1, 2.1, 2.2, 2.3, 2.4, 2.7, 3, 5, 15 – 22, 24, 25.1, 25.7 and 27.
Peter Mehrfert	P. Eng., Process	Process Engineer	Ausenco	Yes	1.1, 1.9, 1.11.4, 1.11.5, 1.12.1, 1.12.4, 2.1, 2.2, 2.3, 2.7, 3, 13, 25.1, 25.5, 25.7, 26.1, 26.3 and 27.

Qualified Person	Professional Designation	Position	Employer	Independent of Issuer Name(s)	Report Section
Scott Burkett	B.Sc., Geology SME-RM	Principal Consultant	SRK Consulting (US) Inc.	Yes	1.1, 1.3, 1.5 - 1.8, 1.10, 1.11.2, 1.11.3, 1.11.5, 1.12.1-1.12.3, 2.1 - 2.7, 3, 4, 6, 10, 11, 12, 14, 25.1, 25.2, 25.4, 25.6, 25.7, 26.1, 26.2 and 27.
Ron Uken	Ph.D., Geology Pr. Sci. Nat.	Principal Consultant	SRK Consulting (Canada) Inc.	Yes	1.1, 1.4, 1.6, 1.11.1, 1.11.2, 1.11.5, 1.12.1, 2.1, 2.2, 2.3, 2.4, 2.7, 3, 6, 7, 8, 9, 23, 25.1, 25.3, 25.4, 25.7, 26.1, 26.3 and 27.

2.4 Site Visits and Scope of Personal Inspection

Mr. Scott Burkett conducted a site visit on behalf of SRK on March 28, 2023 for three days reviewing Oroco’s core facility and evaluation of logging, sampling and geological, alteration and structural data collection. Mr. Burkett worked with Oroco consultants in the development of the geological and structural models specifically as applied to the resource estimation efforts.

Mr. Ron Uken visited the project site between Jan 19 to Jan 24, 2022; March 29 to April 11, 2022; March 28 to April 3, 2023, a total duration of 26 days. Mr. Uken was involved in field geological and structural mapping and verification of geological model for the resource estimation effort.

Mr. James Arthur Norine conducted a site on September 21st through to the 23rd to review existing infrastructure at the site and surrounding area.

2.5 Effective Dates

The effective date of the Mineral Resource estimation is April 21st 2023.

2.6 Previous Technical Reports

The Santo Tomás Project has been the subject of the following previous technical reports:

- Bridge, D., (2019). Geology, Mineralization, and Exploration of the Santos Tomás Cu-(Mo-Au-Ag) Porphyry Deposit, Sinaloa, Mexico: NI 43-101 Technical Report prepared by Dane A. Bridge Consulting Inc., for Oroco Resource Corp. and Altamura Copper Corp. Effective date: August 22, 2019, Filing date: September 10, 2019
- Bridge, D., (2020). Revised – Geology, Mineralization, and Exploration of the Santos Tomás Cu-(Mo-Au-Ag) Porphyry Deposit, Sinaloa, Mexico: NI 43-101 Technical Report prepared by Dane A. Bridge Consulting Inc., for Oroco Resource Corp. and Altamura Copper Corp. Effective date: August 22, 2019 and Revised April 21, 2020; Filing date: April 22, 2020

The QP's opinion contained herein is based on information provided to the Consultants by Oroco throughout the course of the investigations. SRK has relied upon the work of other consultants for metallurgy project areas in support of this technical report, as noted in Section 2.2. SRK has relied on internal experts and legal counsel for details on Project history, regional geology, geological interpretations, and information related to ownership. SRK has relied on Oroco for forward-looking commodity pricing assumptions. SRK has not performed an independent verification of land title and tenure information as summarized in Section 4 of this report, which was verified separately by Oroco legal counsel. SRK did not verify the legality of any underlying agreement(s) that may exist concerning the permits or other agreement(s) between Oroco and third parties. As such, SRK expresses no opinion as to the ownership status of the Project. This report has been prepared using the documents noted in the References section (Section 27). The Consultants used their experience to determine if the information from previous reports was suitable for inclusion in this technical report and adjusted information that required amending. This report includes technical information that required subsequent calculations to derive subtotals, totals, and weighted averages. Such calculations inherently involve a degree of rounding and consequently introduce a margin of error. Where these occur, the Consultants do not consider them to be material.

The sources of information include historical data and reports compiled by previous consultants and researchers of the Project and supplied by Oroco personnel, as well as other documents cited throughout the report and referenced in Section 27.

The QP has not independently reviewed ownership of the Project area and any underlying property agreements, mineral tenure, surface rights, or royalties. The QPs have fully relied upon, and disclaim responsibility for, information derived from Oroco Resource Corp. and legal experts retained by Oroco Resource Corp. for this information through the following documents:

SRK and Ausenco are relying upon mineral title verification surveys conducted by professional (registered) land surveyor (a "Perito Minero") Barney Green Lee Portillo ("Green"). Sr. Green's concession boundaries are used in this report.

2.7 Units and Abbreviations

All map locations and drill hole positions are in meters, and Universal Transverse Mercator (UTM) coordinates are in World Geodetic System (WGS) 84 Zone 12. All units and measurements presented in this report are in metric, except for the price weight of copper and molybdenum, which are presented in dollars per pound (lb.). Dollar values presented are in the United States of America dollars unless otherwise stated. The most common units and abbreviations presented in this document are listed below in Table 2-2.

Table 2-2: List of Other Units and Abbreviations

Abbreviation	Unit or Term
%	Percent
°	Degree
°C	degrees Centigrade
µm	Micron
2P	Proven and Probable
2SD	2 Standard Deviations
3D	Three-dimensional
3D DCIP	3D DC resistivity induced polarization
3P	Proven, Probable, and Possible
3SD	3 Standard Deviations
5PDL	5x the Practical Detection Limit
A	Ampere
A/m ²	amperes per square meter
AA	atomic absorption
ABA	Acid-base Accounting
ADL	Analytical Detection Limit
Ag	Silver
AGL	above ground level
ANFO	ammonium nitrate fuel oil
ASCII	American Standard Code for Information Interchange
ATV	Acoustic Televiewer
Au	Gold
AuEq	gold equivalent grade
AVRD	Absolute Value of the Relative Difference
AWG	American Wire Gauge
BV	Best Value
CCD	counter-current decantation
CDCI	Cerro de Cobre Inc.
cfm	cubic feet per minute
CIL	carbon-in-leach
CIM	Canadian Institute of Mining, Metallurgy and Petroleum
CLA	Composite Length Analysis
cm	centimeter
cm ²	square centimeter
cm ³	cubic centimeter
CMR	Compañía Minera Ruero, S.A. de C.V.

Abbreviation	Unit or Term
CoG	cut-off grade
CONAGUA	Comisión Nacional del Agua
ConfC	confidence code
CPF	Coarse Particle Flotation
CRec	core recovery
CRM	Certified Reference Material / Commercial Reference Materials
CSS	closed-side setting
CTW	calculated true width
Cu	copper
CuS	Acid soluble copper percent
CuT	total copper percent
CV	Certified Value
CVR	Common Voltrage Reference
D	day
DC	Direct current
DEM / DTM	Digital Elevation Model / Digital Terrain Model
DGPS	Differential GPS
DHDB	Drillhole Database
dia.	diameter
DUP	Duplicates
DVD	Digital Video Disk
EXA	Exploratory Data Analysis
FA	fire-assay
FDUP	Field Duplicate Samples
Ft	foot (feet)
ft ²	square foot (feet)
ft ³	cubic foot (feet)
G	gram
G&A	General and administrative
g/L	gram per liter
g/t	grams per tonne
Gal	gallon
g-mol	gram-mole
Gpm	gallons per minute
GPS	Global Positioning System®
H	hour
Ha	hectare

Abbreviation	Unit or Term
HDPE	Height Density Polyethylene
Hg	Mercury
High-mag	high magnetic intensity
hp	horsepower
HPGR	High Pressure Grinding Rolls
HTW	horizontal true width
ICP	Inductively Coupled Plasma
ICP	induced couple plasma
ID2	inverse distance squared
ID3	inverse distance cubed
IDW	Inverse distance to the 3rd power interpolation method
IDW2	Inverse Distance Weighted Squared
IDW3	Inverse Distance Weighted Cube
IFC	International Finance Corporation
ILS	Intermediate Leach Solution
IMU	Inertial Measurement Unit
INEGI	Instituto Nacional de Estadística y Geografía (National Institute of Statistics and Geography).
INS-GNSS	Inertial Navigation System-Global Navigation Satellite System ("GNSS aided INS")
IP	Induced Polarization
ITRF08	International Terrestrial Reference Frame 2008
IUGS	International Union of Geological Sciences
kA	kiloamperes
KEV	Key Economic Variables
kg	kilograms
km	kilometer
km ²	square kilometer
koz	thousand troy ounce
kt	Thousand (kilo) tonne
kt/d	thousand tonnes per day
kt/y	thousand tonnes per year
kV	kilovolt
kW	kilowatt
kWh	kilowatt-hour
kWh/t	kilowatt-hour per metric tonne
L	liter
L/sec	liters per second

Abbreviation	Unit or Term
L/sec/m	liters per second per meter
Lb	pound
LHD	Long-Haul Dump truck
LiDAR	Light Detection and Ranging
LLDDP	Linear Low Density Polyethylene Plastic
LOI	Loss On Ignition
LOM	Life-of-Mine
Low-mag	low magnetic intensity
M	meter
M&I	Measured and Indicated
m.y.	million years
m ²	square meter
m ³	cubic meter
m ³ /h/m ²	cubic meters per hour per square meter
m ³ /hr	Cubic meter per h
MA	Moving Average
MARN	Ministry of the Environment and Natural Resources
MDA	Mine Development Associates
mg/L	milligrams/liter
Min	minute
mm	millimeter
mm ²	square millimeter
mm ³	cubic millimeter
MME	Mine & Mill Engineering
Mo	molybdenum
Moz	million troy ounces
MRE	Mineral Resource Estimate
MSRDI	Mountain States Research and Development Inc.
Mt	million tonnes
Mt/y	million tonnes per year
MTW	measured true width
MW	million watts
NAD27	North America Vertical Datum 1927
NGO	non-governmental organization
NI 43-101	Canadian National Instrument 43-101
NNP	Net Neutralization Potential
nT	nanotesla (10 ⁻⁹ tesla), a unit of magnetism

Abbreviation	Unit or Term
OK	Ordinary Kriging
OSC	Ontario Securities Commission
OTV	Optical Televiewer
oz	troy ounce
P/F	pass/fail
PAX	Potassium Amyl Xanthate
PBLNK	Pulp Blank
PDL	Practical Detection Limit
PDUP	Pulp Duplicate Samples
PEA	Preliminary Economic Assessment
PL	Point Load
PLC	Programmable Logic Controller
PMA	Particle Mineral Analysis
PMF	probable maximum flood
ppb	parts per billion
ppm	parts per million
PRM	Public Registry of Mining
PRM	Public Registry of Mining
QA/QC	Quality Assurance/Quality Control
QAPF	Quartz-Alkali Feldspar-Plagioclase-Feldspathoid
QMP	Quartz Monzonite Porphyry
R&R	Resources and Reserves
RC	rotary circulation drilling
RMA	Reduction of the Major Axis
RoM	Run-of-Mine
RPEEE	Reasonable Propects for Eventual Economic Extraction
RQD	Rock Quality Designation
S&R	Smelting and Refining
S/R	Strip ratio
SAR	Synthetic Aperture Radar
SD	Standard Deviations
SEC	US Securities & Exchange Commission
sec	second
SEM	Scanning Electron Microscopy
SEMARNAT	The Secretariat of Environment and Natural Resources (in Spanish: Secretaría del Medio Ambiente y Recursos Naturales)
SG	specific gravity

Abbreviation	Unit or Term
SGA	Semi-autogenous grinding
SGM	Servicio Geológico Mexicano
SIRGAS	Geocentric Reference System for the Americas
SK	Simple Kriging
SMO	Sierra Madre Occidental
SMU	Selective Mining Unit
SOP	Standard Operating Procedures
SPT	standard penetration testing
st	short ton (2,000 pounds)
SWIR	Short Wave Near Infrared
t	tonne (metric ton) (2,204.6 pounds)
t/d	tonnes per day
t/h	tonnes per hour
t/y	tonnes per year
TMI	Total Magnetic Intensity ('TMI')
TSF	tailings storage facility
TSP	total suspended particulates
UCS	Uniaxial Compressive Strength
US\$	United States Dollar
UTM	Universal Transverse Mercator
V	volts
VFD	variable frequency drive
VLF-EM	Very low frequency - electromagnetics
W	watt
XRD	x-ray diffraction
y	year

3 RELIANCE ON OTHER EXPERTS

The QPs have relied upon the following other expert reports, which provided information regarding mineral rights, surface rights, property agreements, royalties, environmental, permitting and data generated by Oroco Resource Corp., for sections of this Report.

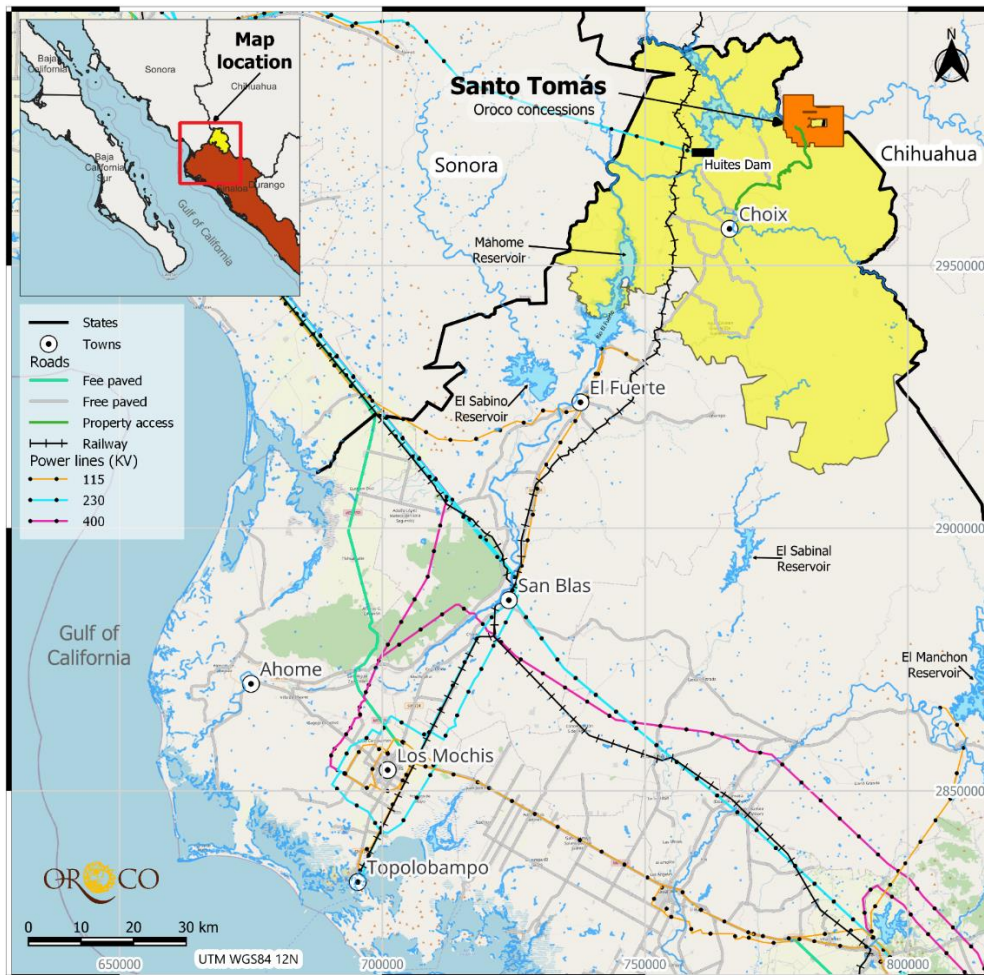
The authors have carefully reviewed, within the scope of their technical expertise, all the available information presented to them, however they cannot guarantee its accuracy and completeness. The authors reserve the right, but will not be obligated to revise the technical report and its conclusions if additional information becomes known to them, subsequent to the effective date of this report. The authors are not experts with respect to legal, socio-economic, land title, or political issues, and are therefore not qualified to comment on issues related to the status of permitting, legal agreements, and royalties.

4 PROPERTY DESCRIPTION AND LOCATION

4.1 Property Location

The Santo Tomás Project (the “Project”) is comprised of three zones (South Zone, North Zone and Brasiles Zone) within 13 mineral concessions (the “Project Property also described as Peripheral and Core Concessions”) in the municipality of Choix, straddling the northern border of Sinaloa State and the southern border of Chihuahua State, Mexico, centered at latitude 26°53’00” N and longitude 108°11’30” W (see Figure 4-1). The mineral resource which is the subject of this report is hosted in the North Zone and South Zone (the “Resource Property also described as Core Concessions”), which are entirely located in Sinaloa State on the south bank of the Río Fuerte in the Sierra Madre Occidental.

Figure 4-1: Property Location Map



Source: Oroco, 2023.

4.2 Mexican Mineral Tenure System

4.2.1 Governing Law and Regulations

Mexico (Estados Unidos Mexicanos) has a well-established system of mineral land tenure which is regulated by Article 27 of the Mexican Constitution and the Mining Law and its Regulations (the “Mining Law”). Article 27 of the Constitution establishes that the Federal Republic owns all minerals found in Mexican territory. Application of the Mining Law is the responsibility of the Federal Executive (the President’s office) through the Ministry of the Economy.

On April 29, 2023 (effective May 9, 2023), the Mexican Congress approved a decree amending the Mining Law and other national laws regarding mining and water concessions (the “Amendments”). The Amendments focus principally, but not exclusively, on the process of the granting of new concessions and their associated rights and obligations, which are not seen as being applicable to Oroco given that the Project comprises existing concessions. The amendment reducing the initial term of mineral concessions from 50 years to 30 years is not, therefore, thought to affect the term of current concessions.

Principal Amendments affecting existing concessions are: (1) the reduction of the term of renewal to a one-time period of 25 years, with the right to bid for the concession thereafter if the concessionaire matches 90% of the highest bid in a public bidding process; (2) the requirement of government approval for the transfer of mineral concessions; (3) the addition of grounds for cancellation, including: (i) failure to pay mining fees for two consecutive years; (ii) failure to submit verification reports for works for two consecutive years or five non-consecutive years; (iii) failure to initially commence work within one year; (iv) failure to carry out work for a period of two consecutive years; (v) failure to submit a mine closure plan within the time required; and (vi) lack of a valid water concession; and (4) the elimination of mining’s preferential nature and the related right to expropriate land when required.

4.2.2 Mexican Public Registry of Mining

The Mexican Public Registry of Mining (the “PRM”) is the central titles registration office under the Mexican Mines Bureau. All concessions must be registered with the PRM, with title being evidenced through such registration. Oroco’s subsidiary, Minera Xochipala, S.A. de C.V. (“Minera Xochipala”), has filed for registration of its interest in the six Peripheral Concessions (see “4-3 Mineral Tenures of The Project and the Resource Property” below), which registration is pending. The interest in the Resource Property held by Xochipala Gold, S.A. de C.V. (“Xochipala Gold”), an Oroco subsidiary, is fully registered in the PRM.

4.2.3 Assessment Work, Reporting and Mining Duties

Pursuant to the Mining Law, concession holders are obligated to either expend a minimum amount per year (subject to certain temporary, fact specific exemptions) on the exploration and assessment of each mineral concession, or to produce a minimum value of mineral products per year, and to pay, on a semi-annual basis, government mining concession duties. The amount of the minimum expenditure obligation and the mining duties are calculated based on the size and age of the concession and are updated each year to adjust for inflation. Oroco is up to date on the payment of all concession duties on the Project Property.

Concession holders are obligated to file an expenditure verification report by the end of May of the following year, and, for mineral concessions older than six years, a report of any mineral production from the concession within the first 30 days of the following year. Oroco is up to date on the filing of all assessment work verification and mineral production reports for 2023.

4.2.4 Valid Concession Holders & Surface Rights

Mexican mineral concessions may be held only by Mexican nationals or Mexican incorporated companies (there are no restrictions on foreign ownership of such entities) (El Congreso de Los Estados Unidos Mexicanos, 1992, updated 2014).

Mineral concessions do not grant any surface rights and the Amendments have repealed the right of expropriation of surface land. However, while concession holders are expected to negotiate the acquisition of surface rights with the landowner (El Congreso de Los Estados Unidos Mexicanos, 1992, updated 2014), a concession holder does have the right pursuant to the Mining Law to apply for orders of temporary occupation and easements when required for the exploration and exploitation of the concession.

The surface rights over the Resource Property are held by the Boca de Arroyo Ejido (communal land holding), which holds the surface rights over the South Zone and a portion of the North Zone, and the Mexican individual member of the Third Parties, who holds the surface rights over the balance of the North Zone. Oroco has a long-term surface rights lease agreement with the Boca de Arroyo Ejido (10 years commencing November, 2020, with a right of renewal for a further 10 years thereafter), and an informal interim lease agreement with the Mexican individual while it is advancing the acquisition of that individual's surface rights.

The Company also has a long-term surface rights agreement with the Macoribo Ejido which holds the surface rights over the Brasiles Zone north of the Río Fuerte in Chihuahua State, for a term of 10 years commencing November, 2020, with a right of renewal for a further 10 years thereafter.

4.2.5 Location Surveys

In Mexico, the location of a concession is determined by the location of a single claim monument, with all corners being located based on surveyed distances and bearings from that monument. A licensed surveyor (a "Perito Minero") must determine these distances and bearings. The monument may be placed outside of the surveyed claim boundaries. All meets and bounds of the concession boundaries are defined in metric dimensions.

Historically, coordinates cited in the Mexican Mineral tenure system are based on a UTM grid, North American Datum (NAD) 27 datum. The National Institute of Statistics and Geography (Instituto Nacional de Estadística y Geografía) under Article 26 of Part B of the Constitution of Mexico approved a change to the coordinate system used to display and publish geospatial data. This change is to improve the quality and accuracy of the geospatial data they present. This transition is from datum NAD27 (North America Vertical Datum 1927) to ITRF08 (International Terrestrial Reference Frame, 2008), which is compatible with WGS84 (World Geodetic System 1984) and SIRGAS (Geocentric Reference System for the Americas). The change was published in the Official Gazette on December 23, 2010, and entered into law the following day. All geospatial data from the Mexican Government since 2010 contains metadata detailing the coordinate system used and any transformations applied to the original data (Diario Oficial de la Federación, 2010).

4.3 Mineral Tenures of The Project Property and the Resource Property

The Project Property is comprised of 13 mineral concessions, of which seven (the "Core Concessions") are 100% owned by Xochipala Gold, and six (the "Peripheral Concessions") are 80% owned by Minera Xochipala and 20% owned by either of two, third party Mexican companies or a Mexican individual (the "Third Parties").

The "Santo Tomás Property" is the entire package of 13 concessions held as follows:

- Xochipala Gold - 7 "Core Concessions": Santo Tomás, Bob, Roberto Verde, Esme, Karisu, Karisu Fracc 1 and Tona;

- Minera Xochipala - 80% interest in 6 "Peripheral Concessions: La China II, Papago Fracc 1, Papago 17, Rossy, Rossy 1 and AMP STO Tomás Red 1.

Papago 17 covers a portion of the South Zone mineralization.

Oroco also holds various interests in abutting mineral concessions (the "Peripheral Concessions") that are not the subject of the mineral resource estimate of this Technical Report. The Peripheral Concessions are described herein and named above. Other third-party property and operations are described in the report section "Adjacent Properties."

Oroco initially acquired a 66.6% interest in Xochipala Gold, which interest has been increased to 95% with the expenditure of \$30,000,000 Canadian dollars in relation to the acquisition and development of the Santo Tomás Project. A Mexican individual holds the remaining 5% of Xochipala Gold.

The Third-Parties initially held a 15% contractual interest in the Core Concessions, which interest was also subject to dilution on the Santo Tomás Project-related expenditure of \$30,000,000, reducing the Third Parties contractual interest to the current 10%. Therefore, Oroco currently holds a net 85.5% interest in the Core Concessions (95% of Xochipala Gold's net 90% interest in the Core Concessions) and an 80% interest in the Peripheral Concessions. Both the Core Concessions and the Peripheral Concessions are subject to an aggregate 1.5% net smelter returns royalty interest held by various parties.

Santo Tomás Project expenditures made by Oroco exceeding CAD \$30 million are being made as a loan to the Santo Tomás Project, with the loan terms to be established.

Xochipala Gold's Core Concessions are listed in Table 4-1 and shown in Figure 4-2. Minera Xochipala's Peripheral Concessions are listed in Table 4-2 and shown in Figure 4-2 below.

Table 4-1: List of Xochipala Gold, S.A. de C.V.'s Santo Tomás Core Concessions

Concession Name	Title No.	Area (ha)	Expiry Date (d/m/y)
ESME	211954	326.3	27/07/2050
Karisu	209594	63.2	02/08/2049
Karisu Fraccion 1	209595	4.1	02/08/2049
Toña	215721	85.6	11/03/2052
Roberto Verde	149672	221.7	27/06/2018
Santo Tomás	212003	242.7	17/08/2050
Bob	149675	229.2	27/06/2018
Total Area (ha)	-	1,172.8	-

Table 4-2: List of Minera Xochipala, S.A. de C.V.'S Santo Tomás Peripheral Concessions (80% interest)

Concession Name	Title No.	Area (ha)	Expiry Date (d/m/y)
AMP STO Tomás Reducc 1	227732	6,660.4	20/01/2053
La China II	195050	168.0	24/08/2042
Rosy	224710	766.7	30/05/2055
Rosy 1	224711	13.1	30/05/2055
Papago Fracc 1	195147	40.3	24/08/2042
Papago 17	246416	212.8	18/06/2068
Total Area (ha)	-	7,861.3	-

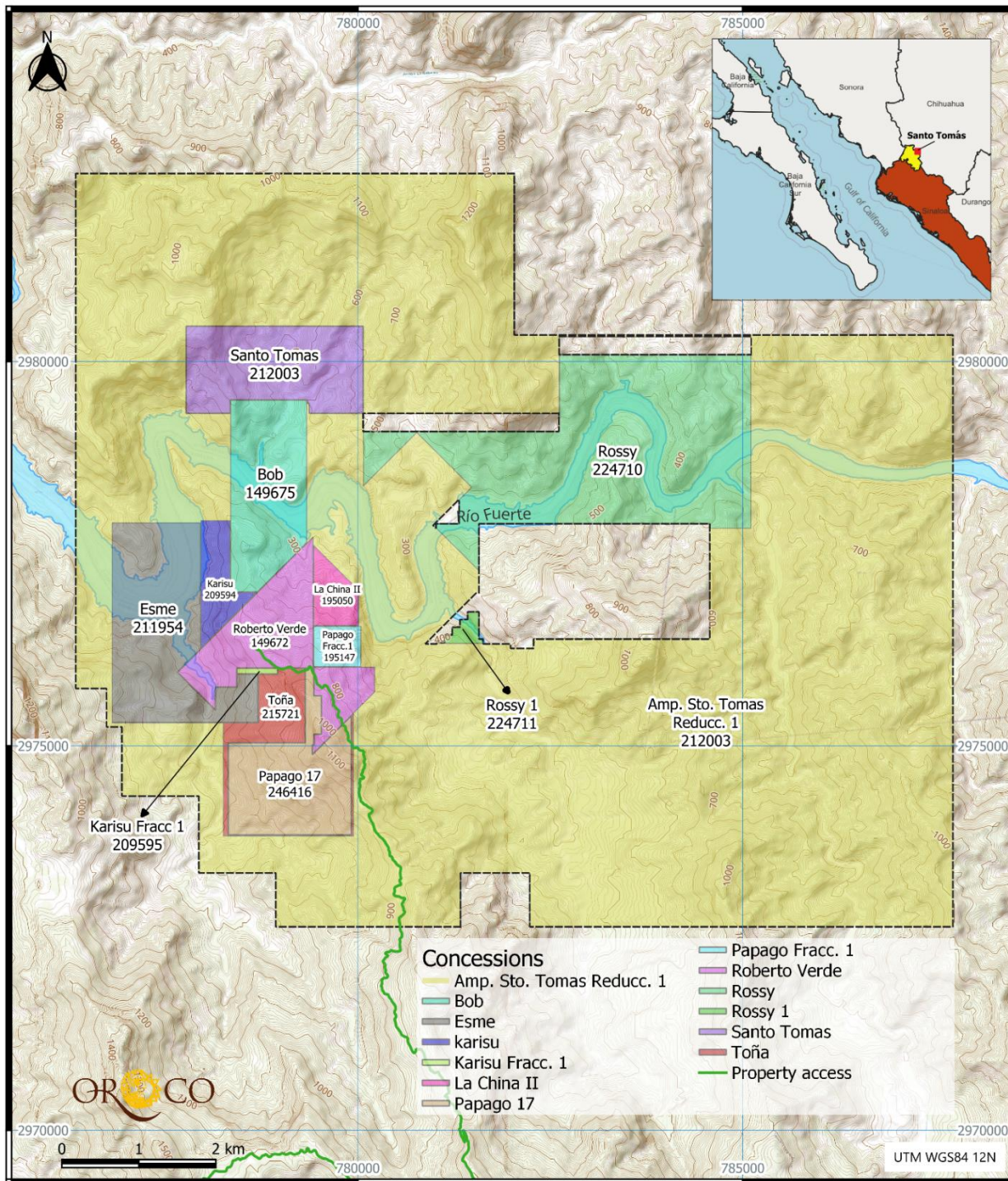
The Amendments do not affect the current term of the Core Concessions or the Peripheral Concessions, but do reduce the term of renewal to a one-time period of 25 years, with the right to bid for the concession thereafter if the holder matches 90% of the highest bid for the concession in a public bidding process.

The Resource Property is located on those six Core Concessions located in Sinaloa State south of the Río Fuerte (Bob, Roberto Verde, Karisu, Karisu Fracc 1, Esme and Tona) and one of the Peripheral Concessions (Papago 17) to the immediate south thereof (see Figure 4-2).

4.3.1 Legal Survey of the Property

Barney Green Lee Portillo and Israel Alejandro Iza Estrada, both Perito Mineros (Registered Surveyors) verified the positions of the concession monuments of the Project concessions. This work was commissioned by Oroco to obtain definitive information on the position of the concession monuments and key historical diamond drill hole collars. See a listing of the Project concessions in Table 4-1 and Table 4-2 and see Figure 4-2 for the Project map of the concessions.

Figure 4-2: Oroco Controlled Concessions: the "Property"



Source: Oroco, 2023.

4.3.2 Obligations to Maintain the Property

Concession duties payable for the Project concessions are fully paid and up to date as of the issuance of this report. All required assessment expenditure verification and production reports have been filed for the Project concessions.

Oroco has no obligation to any third party required to maintain Oroco's interest in the Santo Tomás Project concessions.

4.3.3 Surface Rights

The lands over the Project Property are largely rugged, unimproved, unutilized or lightly ranched areas with xerophilous scrub vegetation. Surface rights over the Oroco areas of operation in the Project Property are held by two Ejidos (Macoribo and Boca de Arroyo) and the individual member of the Third Parties. Surface rights over the Resource Property are held by the Boca de Arroyo Ejido (South Zone and part of the North Zone) and the Mexican individual member of the Third Parties (the balance of the North Zone).

Oroco has surface rights agreements with Macoribo and Boca de Arroyo Ejidos and the individual member of the Third Parties covering the current areas of operation (Brasiles Zone, North Zone and South Zone) of the Project Property, including all of the Resource Property (see "4.2.3 Valid Concession Holders & Surface Rights" above). The surface rights agreements with the Mexican individual and Boca de Arroyo Ejido fully cover the Resource Property. The surface rights agreement with the Macoribo Ejido covers the Brasiles Zone.

Oroco anticipates no impediment to the future acquisition on fair commercial terms of any other surface rights which may be required, principally for waste rock storage and tailings, as the area is of limited utility for any other purpose other than very light ranching.

Oroco can legally access the property via publicly accessible roads that connect from the southwest, originating in Choix. The road from the local public highway continuing northward to the Project Property's North Zone is a public municipal road administered from Choix. The local residents, Ejidatarios and ranchers look to the municipality to maintain their access to the region, the maintenance of which the Company has agreed with the municipality to support. For example, Oroco has funded the construction of several retaining walls on this municipal road to improve safety and continuity of access.

Figure 4-3: Access Road Stability Retaining Walls Built by Community Members with Oroco Financial Support



Source: Ubaldo Trevizo Ledezma, 2022.

4.4 Permits and Liabilities

Prior to the acquisition by Oroco of the Core Concessions, the Project Property had not been drilled since the Exall drill program completed in 1994. The Company obtained an exploration permit for the Brasiles Zone from SEMARNAT in 2021. Permit applications and notices of work with regard to the South Zone and North Zone were filed with SEMARNAT in 2021 and 2022, providing Oroco with the necessary approvals and rights to conduct its 2021-2023 exploration program.

No outstanding environmental liabilities have been reported to the Author, and none is expected to have arisen from fieldwork performed since 1994 on the Property.

Additional drilling may necessitate the construction of new access roads and mechanized construction work which may require permits from SEMARNAT. Additional drilling from existing drill pads using existing access roads is an option under consideration.

4.5 Risks

Uncertainties and changes regarding the new Mining Law introduced on May 8th, 2023, will be assessed as the project moves forward. As the industry in general considers the implications, it is likely that legal action for relief will be initiated at the Mexican Supreme Court.

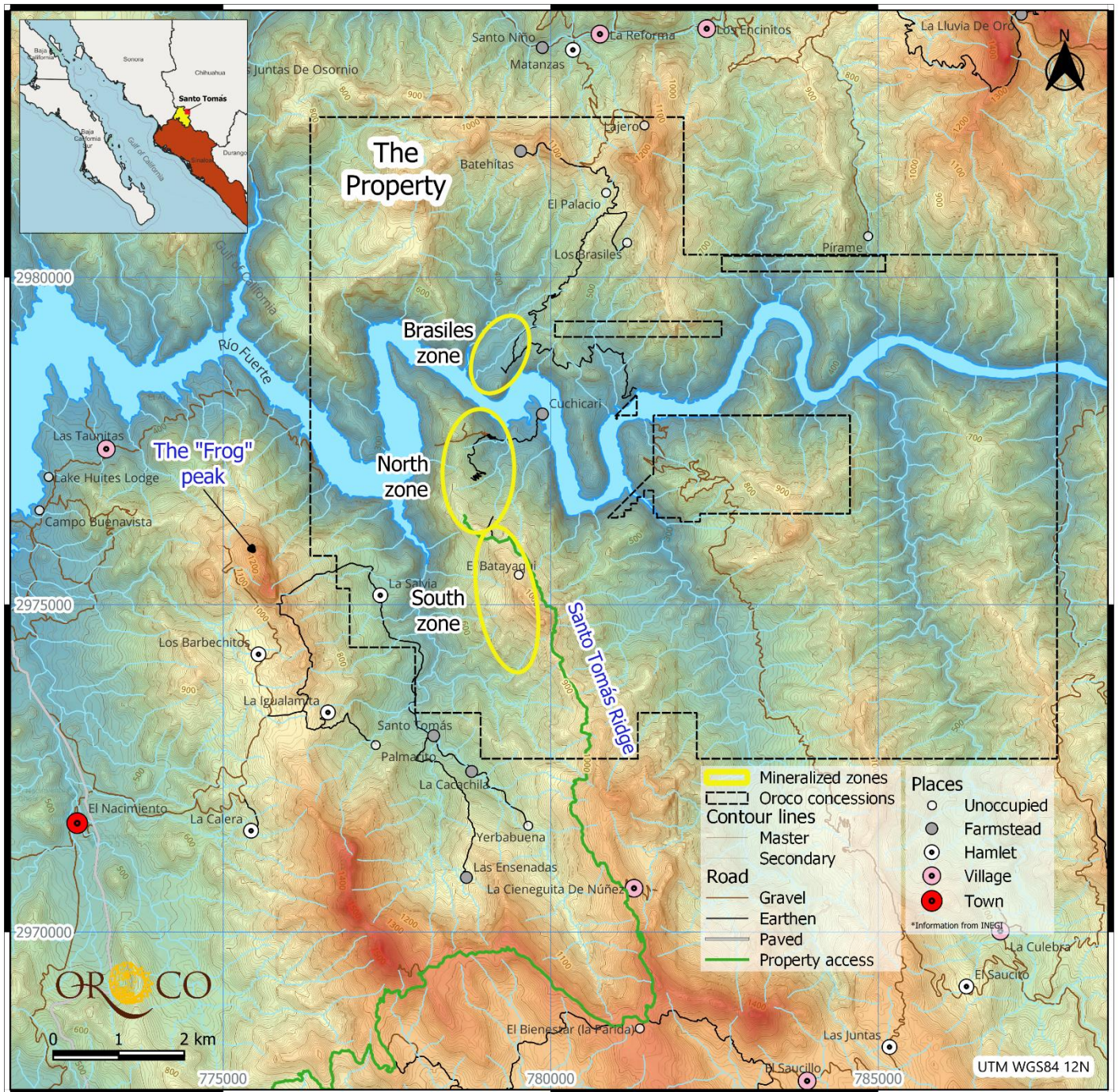
5 ACCESSIBILITY, CLIMATE, LOCAL RESOURCES, INFRASTRUCTURE AND PHYSIOGRAPHY

5.1 Physiography

The Santo Tomás area is mountainous and part of the southwestern slopes of the SMO Mountain range. The area is characterized by deeply incised, steep-walled valleys that rise in elevation from Río Fuerte valley at 225 m elevation, to approximately 1,340 m at El Bienestar Ranch. Vegetation changes gradually southward and to higher elevations through brush and scrub-covered woodlands, and climate transitions to a temperate zone at elevations between 1,100 to 1,300 m. Pine and oak forests characterize the temperate climatic zone (Borovic, 2006). Figure 5-1 illustrates the following place names on and around the Property that are referred to in this report:

- El Bienestar Ranch, old site of the Santo Tomás core storage facility. It is serviced by an existing powerline.
- El Ranchito, current offices, core processing and storage and pulp/reject storage facility in Choix, State of Sinaloa, México.
- Santo Tomás Village located NNW of El Bienestar by road. It is serviced by a powerline.
- Santo Tomás Ridge that is the prominent north-south trending ridge connecting the village of Santo Tomás to Río Fuerte.
- South Zone is the mineralized zone that previously was studied by Bateman (1994) and falls within the current economic pit. It largely falls on and under the western slopes of the Santo Tomás ridge.
- North Zone is the main mineralized zone on the Property that previously was studied by Bateman (1994) and falls within the current economic pit. The zone lies on the eastern flank of the Santo Tomás ridge and extends westward towards the western bounding valley under post mineral rocks and limestones. The eastern expression of the North Zone mineralization is defined by oxide copper mineralization at surface, hosted in quartz monzonites and andesites.
- Brasiles is a mineralized zone to the north of the Río Fuerte/ Huites Reservoir. It is probable that the mineralized zone encountered in seven drill holes is a continuation of the mineralized system defined to the south. The Brasiles Zone (a.k.a. Brasiles Prospect) is excluded from the MRE.
- Huites Reservoir that inundates Río Fuerte at the Property for most of the year. When flooded, the water way provides alternate access to the project for exploration activities.
- Cuchicari is the village on the south side of the Río Fuerte and east of the North Zone that was abandoned due to the flooding of the Huites Reservoir.
- The “Frog” that is a prominent peak lying on the ridge to the west of the Santo Tomás Ridge. It was the site of a limestone quarry in the 1990s.

Figure 5-1: Local Physiography with Mineralized Zones

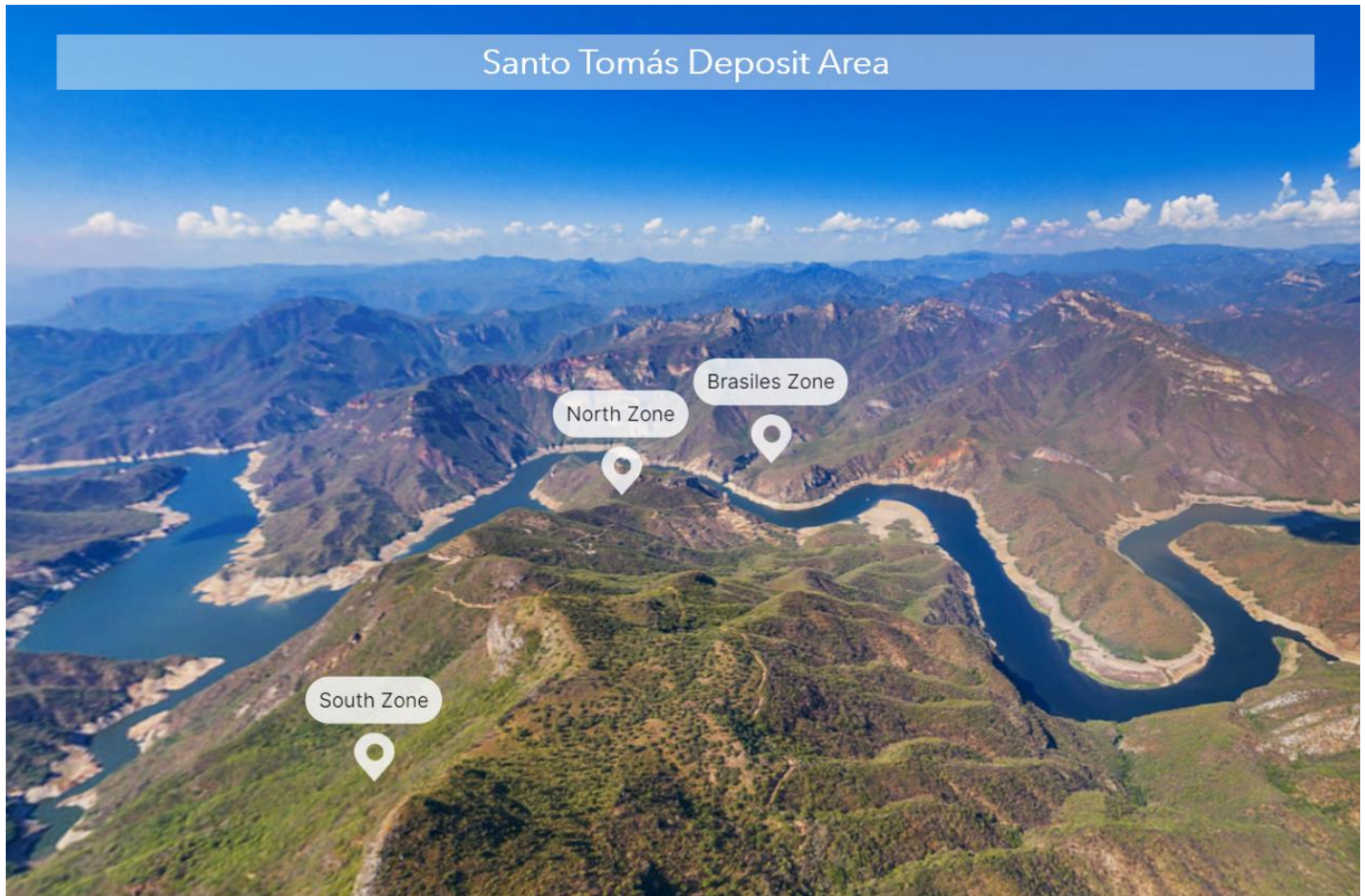


Source: Oroco, 2023. Note: Occupancy classifications based on population: 0 occupants = unoccupied, <10 = farmstead, 10-40 = hamlet, 40-200 = village, >200 = town.

Lying on the same ridge is the Microwave Tower that is serviced by a power line. The site is accessed by roads from the Frog: mainly from the south by the access road to El Bienestar. The tower now provides cell phone and internet connectivity between El Ranchito and the Project Site. It is suitable for installing additional communications infrastructure for the project.

An aerial view of the three mineralized zones is shown in Figure 5-2.

Figure 5-2: View of the Santo Tomás Deposit Area indicating North Zone, South Zone, and Brasiles towards the Northeast.



Source: Oroco/VRIFY, 2022.

5.2 Local Resources

The nearest supply center is the town of Choix, with a population of 10,300, located 39 km to the SW of project. The town of El Fuerte and the city of Los Mochis are well-served with industrial supply and repair facilities, due to the region's port, agricultural, and mining activities.

Labor and experienced mining technicians and equipment operators are available in northwestern México, a consequence of the region's long mining history.

5.3 Accessibility

Access to the Property is by way of a 169 km paved highway from the Port of Topolobampo, through the city of Los Mochis to the northern town of Choix. From El Ranchito to the project area via the current access road it a further 38 km along mostly unimproved dirt roads via Cajón de Cancio. From the Chihuahua Pacific highway, access is by secondary, unsurfaced roads that are usable in all seasons.

Historically, the Property was explored from an exploration camp located on the El Bienestar Ranch (La Parida Ranch) that is located on a ridge south of the Property. The ranch and camp buildings remain on-site and include a core storage building where diamond drill core and rotary drilling cuttings were stored. All operations and core storage were subsequently moved the El Ranchito Facility, north of Choix in the summer of 2021.

Access to the project is either via the El Sauzal Mine access road turning off at Km 38 or via the Cajón de Cancio village route. For the MRE the latter access is considered the probable future project access route.

Access to the North Zone of the Property is also afforded from the end of the Chihuahua-Pacific highway at the Huites Reservoir. From there, a boat is used to access the northern area of the Property. Access is now available from the western side of the North Zone, thus eliminating the truck use on the switchback access from the north. On-going road repair is required to maintain access during the monsoon season.

5.4 Climate

Elevation effects on the climate over the property boundaries are dramatic. The climate varies from subtropical at the northern end of the Property to temperate climates at higher elevations in the south at El Bienestar Ranch. The deep river valley is hot and humid.

Excluding the river valley surrounds, the overall climate is dry and arid for most of the year and with heavy, monsoon rains during the period from July to September. Levels of Río Fuerte are highly variable during this period. Localized flooding may also occur requiring engineering of access and roadways to mitigate erosion and landslides in the steep terrain.

The operating season is effectively 365 days a year. Some access restrictions may occur during the monsoon season.

5.5 Infrastructure

5.5.1 Regional Infrastructure

Facilities for ocean shipping of concentrate would need to be arranged at the Port of Topolobampo (see Figure 4-1); a distance of 183 km from the Property via the Chihuahua Pacific Highway. The Port has recently completed significant upgrades to berth-side storage including the installation of additional berths, cranes, and ship-handling tugboats (Secretaría de Comunicaciones y Transportes, 2014). Containerized concentrate shipping is the preferred option. This would eliminate port contamination with concentrate spillage.

The nearby international airport at Los Mochis (Aeropuerto Federal del Valle del Fuerte: IATA Code LMM; ICAO Code MMLM) services scheduled commercial jet aircraft.

The Port of Topolobampo and Los Mochis are serviced by several rail lines, including the Chihuahua Pacific railroad that connects to El Paso, Texas. The latter line passes within 12 km of the west of the Property. Alternate port facilities are located to the north at Guaymas in Sonora though this is a significantly longer truck haul for concentrates.

The Chihuahua Pacific Highway is currently under construction with plans to improve the route between the Huites Reservoir and El Paso, Texas, USA Work is complete from Topolobampo to the Huites Reservoir, passing within 6 km of the Property. Bridge construction to cross the Huites Reservoir / Río Fuerte is permitted but has not commenced.

5.5.2 Local Infrastructure

Adequate water for mining operations is available from Río Fuerte and Huites reservoir if a suitable allotment is arranged by permit. However, if that permitted allotment is not available, drilling of local aquifers for well-field water would be required.

The large Huites dam (officially known as the Luis Donaldo Colosio Dam) was constructed for irrigation and power generation (422 megawatt capacity) and is located on the Río Fuerte 20 km from the Property. The dam produces an average of 911 million kWh annually. The Colosio dam is connected to the main power transmission grid of northwestern México, via a 230kV power line.

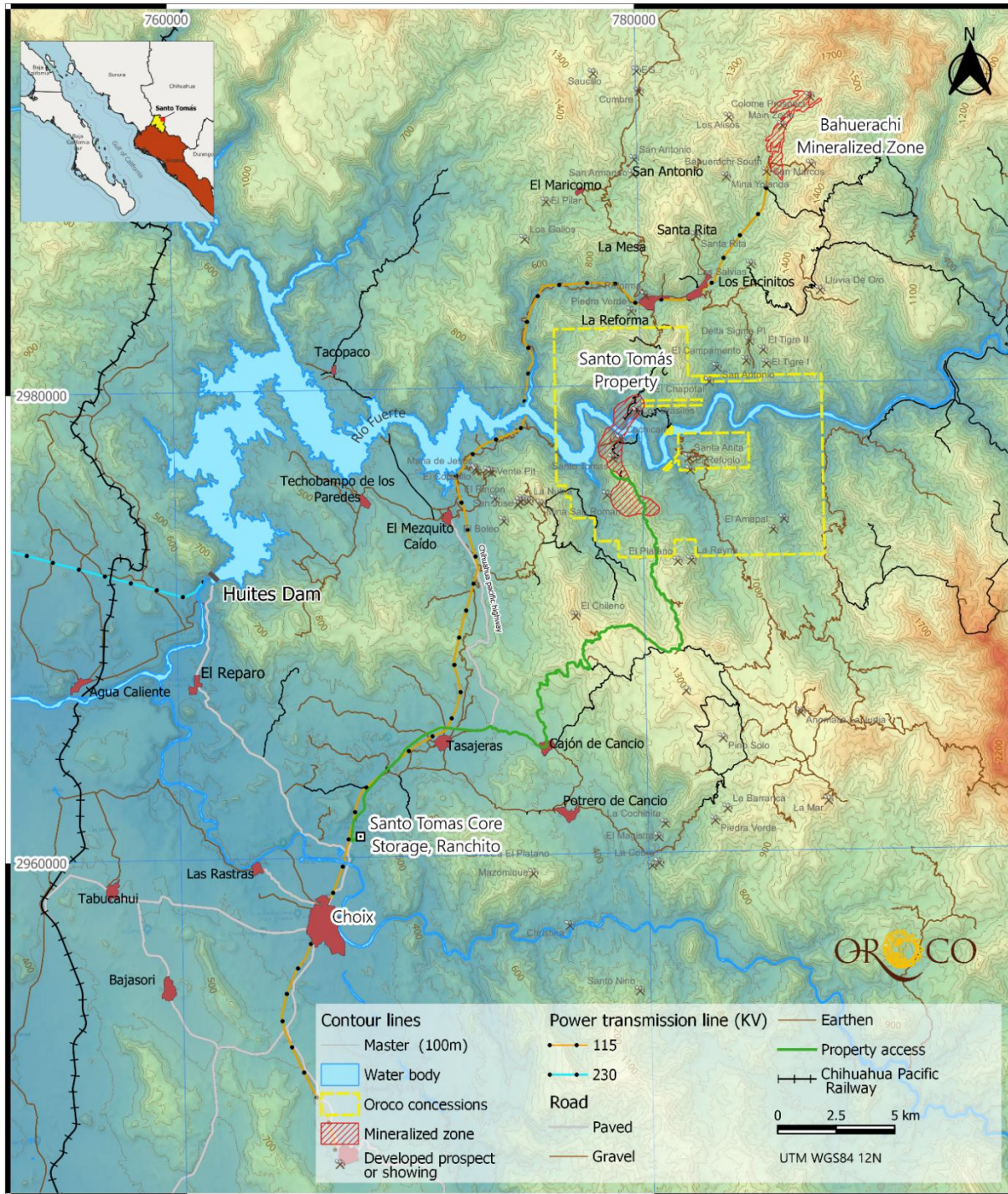
A smaller 110kV power transmission line to the former La Reforma Mine and Jinchuan's Bahuerachi property passes within 4 km west of the Property. A smaller powerline services the ranch houses located on the Esme mineral concession proximal to the areas of exploration and drilling on the Property. The line is suitable for servicing camp facilities in support of work on the Property, though to date camp power has been delivered by diesel generator.

A 115 kV line to the south of the property is still in service. The line provided power to the now closed El Sauzal Gold mine.

TransCanada Pipelines brought a large capacity natural gas pipeline into service on June 29, 2018, that connects the city of Ahome and the Port of Topolobampo with existing pipelines in the State of Chihuahua. The pipeline has a capacity of 670 million cubic feet (19.0 million cubic m) per day. The pipeline passes within 20 km of the Property and offers a very significant alternate energy supply to any mine or infrastructure development in the area.

A representation of the local infrastructure is shown in Figure 5-3.

Figure 5-3: Local Infrastructure



Source: Oroco, 2023.

5.5.3 Infrastructure for Exploration

Oroco has acquired access to project surface land through the execution of a series of lease agreements with the surface landowners. The lands over the Property are largely unimproved and are comprised of unutilized or lightly ranched pasture only. Land rights are held by several owners, both Ejido groups and private ranchers. Oroco anticipates no impediment to the future acquisition of these surface rights on fair commercial terms for the possible construction of mine related infrastructure.

A fit for purpose field camp was constructed on the project site between the North and South Zones. Upwards of 40 people can be accommodated at camp, cutting out the 3 hours round trip transit time from Choix to site via an unimproved road. An upgraded core processing facility was constructed at El Ranchito (Figure 5-4 and Figure 5-5).

Figure 5-4: South Camp Aerial View (left), and El Ranchito Core Processing Facility Inside View (right).



Source: Oroco Photo, El Ranchito Core Processing Facility. May 5, 2023.

Figure 5-5: The El Ranchito Secure Core and Sample Pulp Storage Facility



Source: Oroco, 2023.

6 HISTORY

6.1 Exploration History

Most of the historical drill holes were collared in the northern area of the Property, in what has subsequently been referred to as the “North Pit” area (Bateman,1994), located directly south of Río Fuerte. Additional drilling was conducted on more widely spaced locations 2 km to the south where additional copper-bearing mineralization was found in an area named the “South Pit” (Bateman, 1994). In this report, these “pits” will be called the North and South Zones, respectively.

The history of the Project has been summarized in Table 6-1.

Table 6-1: Historical Exploration Programs

Year	Company	Work	Results
Early 1900's	Artisanal Miners	High grade Ox Cu Mining	No information on tonnes of material removed
1968 to 1971	ASARCO	Road Building and drilling, 43 vertical diamond core holes and 16 vertical rotary percussion holes, 15,088 m total drilling	Property relinquished in 1973 after spending 1 million dollars
1973 to 1977	Tormex - Peñoles	26 ASARCO holes re-logged. 5,336m of 1/2 core split and assayed. 2,401m of new drilling in 7 holes.	New resource estimation undertaken. No information available. Property relinquished
1973	Government supported mapping by Davidge and Clark	Preliminary Geology and Mineralization of the Choix Area	presumably data collected was capture by the governmental mapping program
1990	Esmeralda Group	Review and updating geological sections and plans	No information available
1991	Minera Real De Ángeles	Re-logged 12 ASARCO holes and re-assayed 2 holes.	Good correlation between assay results reported
1992	Exall	Acquired property	-
1993	Exall	4,000m of 33 reverse circulation drill holes and 7 diamond drill holes.	MRE completed
1993	Exall	Bateman Engineering Inc. retained to undertake a PFS	-
1994	Exall	Metallurgical test work. Minetek S.A. de C.V. and	Test work indicates a 90% copper recovery rate using standard concentration

Year	Company	Work	Results
		Mountain States Research and Development	methods, resulting in a 28% copper concentrate.
1994	Exall	Preliminary pit constrained Mineral Resource developed on previous Tormex and ASARCO drilling	Deposit evaluated as two pits: North and South. An estimate of the mineral resources was reported.
2011	Thor Resources LLC	Technical Report and mineral resource estimation (historical)	MRE completed

Informal miners have been working at the Santo Tomás site sporadically since the early 1900s resulting in several small excavations and two small adits in the North and South Zones. (Davidge 1973) reported that local villagers were working the property in the 1970s and that approximately 1 tonne of mineral material was being removed per week.

The first systematic exploration at Santo Tomás was initiated by ASARCO Mexicana S.A. (“ASARCO”). Commencing in 1968 ASARCO constructed an access road to the Property from El Bienestar Ranch and conducted a predominantly drill-based exploration program. A total of 43 vertical diamond-drill holes totaling 13,697 m and 16 vertical rotary percussion holes totaling 1,391 m were completed by 1971. Most of the ASARCO drill holes were in the North Zone.

Tormex Mining Developers Ltd. (Contratista Tormex S.A.) and Industria Minera Peñoles (“Tormex”) optioned the Property in 1973 and conducted exploration and re-sampling to 1977, mainly on the North Zone. Twenty-six ASARCO core holes from the North Zone were re-logged, and 5,336 m of half-core was re-split and sent for assay. Tormex completed an additional 7 drill holes totaling 2,401 m in 1974. A new mineral resource estimation was made, and a revised geological interpretation depicted a shallowly west-dipping mineralized zone.

In the 1980’s and 1990’s, the Santo Tomás deposit region was included in a series of regional airborne magnetic surveys, helicopter surveys, LANDSAT imagery and geological mapping by Mexican government agencies. The Esmeralda Group and Minera Real de Ángeles S.A. de C.V. interpreted existing data and produced mineral resource calculations. However, the results of these studies are not available.

Exploration activity on the Property resumed in 1990 when the Esmeralda Group produced a new set of geologic sections and plan-maps, which summarized the previous exploration work and provided a new Mineral Resource calculation.

In 1991, Minera Real de Ángeles S.A. de C.V. re-logged 12 ASARCO drill holes and re-assayed two holes. A block model resource calculation was produced, but the results of this study are not available.

A Canadian Company – Cerro de Cobre Inc. (“CDCI”) entered into a purchase agreement with the Esmeralda Group for the Property and then optioned the Property to Exall Resources Ltd. (Exall) in 1992. Exall focused on the higher-grade near-surface oxide zone. Exall engaged Watts, Griffis and McOuat Ltd (“WGM”) to review the available data. WGM recommended that on-going exploration was warranted with a focus on higher-grade, near-surface oxide mineralization.

In 1993, Exall conducted a 4,000 m drill program composed of 33 reverse circulation drill holes and 7 diamond drill holes. A new resource estimate based on 14,881 m of drilling information was completed. (49 ASARCO/Tormex and 40 Exall drill holes). Exall retained Bateman Engineering Inc. (“Bateman”) of Phoenix, Arizona, to prepare a Pre-feasibility study and contracted metallurgical testing from Mintek S.A. de C.V. and Mountain States Research and Development Inc. of Tucson, Arizona (“MSRDI”). Also, Mintec, Inc. of Arizona (“Mintec”), was retained to prepare a MRE and a mining study, as part of the Bateman studies.

The MSRDI testing included flotation tests, bottle roll leaching tests, and concentrate bioleaching tests. They concluded that the Santo Tomás mineralization responds favorably to flotation but is not amenable to direct leaching using sulfuric acid. The test work shows that approximately 90% of the contained copper is recoverable through standard concentration methods, yielding a concentrate of 28% Cu.

During and after the Exall drilling programs, in the period 1992 to 1995, the Luis Donaldo Colosio Dam (“Huites Dam”) was constructed 15 km downstream from the property on Río Fuerte. The maximum water level was raised approximately 70 m after the dam completion. The new water level of the reservoir impinges on the northern flank of the Santo Tomás deposit.

In 1997, Exall relinquished its option on the Santo Tomás property.

In 1997-1998, Morgain Minerals Inc. (“Morgain”) and its wholly owned Mexican subsidiary Minera MGM S.A. de C.V. (“MGM”) signed an agreement with Mr. Rubén Rodríguez for the acquisition of 100% interest in the Property. Morgain evaluated the Santo Tomás Project technical data in conjunction with consultants and with Cominco Engineering Services Ltd. (“CESL”) regarding bench-scale testing of copper concentrates and produced a series of north-facing vertical sections at 1:1,000 scale. The Author was not able to locate any further information regarding this agreement.

In 2002, Rubén Rodríguez Villegas (“Rodríguez”) transferred 100% ownership of the Property to Compañía Minera Ruero, S.A. de C.V. (“CMR”), a private registered mining company in México. CMR is owned 99.998% by Ruero International Ltd. (“Ruero International”), a Bahamas company, and 0.002% by Rodríguez.

In 2002, Fierce Investments Ltd., a USA company, entered into a Share Purchase agreement with Rodríguez to acquire the shares of Ruero International.

IGNA Engineering and Consulting Ltd. (“IGNA”) was engaged to conduct a geological study and evaluation of the Santo Tomás property in 2002. IGNA conducted field examinations of the project in 2002 and 2006. Eight complete holes and a few partial holes were re-logged and verification samples collected. Examination of the drill core led to a new interpretation of the geology that the mineralized quartz monzonite is quartz monzonite dike, is striking NNE and dipping steeply to the NW, rather than shallowly dipping.

IGNA noted that Tormex, Minera MGM and Exall interpreted the geology and structure in different ways. IGNA concluded that the mineral resource calculations completed by various companies appeared to be acceptable within the limitations of the drill spacing. Additional drilling and exploration were recommended to improve and upgrade the Mineral Resources for both the North and South Zones.

Re-logging and selective resampling of drill core were done by Tormex in 1977 on 1971 ASARCO core, in 1991 by Minera Real de Ángeles S.A. de C.V. on ASARCO core and by IGNA in 2002. Good correlations have been obtained from all the past re-sampling programs.

In 2003, Bateman prepared an update to the completed Prefeasibility Study of 1994. The report focused on plant design and metallurgical test work and incorporated the 1994-dated MREs. Later in 2003, Mintec conducted a review of potential target areas for additional drilling and suggested that the area lying to the south and west of the South Zone was open for finding additional copper mineralization. A systematic drill program at 250 m spacing was recommended.

Cambria Geological Ltd. (in 2005) and Cambria Geosciences Inc. (together, “Cambria”) (2006-2009) conducted several technical reviews of the Santo Tomás property throughout 2005 to 2009.

In 2010, John Thornton, P.Eng. of Thor Resources LLC, prepared a revised report (Thornton, 2011) summarizing the MREs for all mineral resource classifications, scoping the project with current costs, and metal prices to determine a pit-constrained MRE, now classified as an historical resource.

In 2015, 100% ownership of Ruero International reverted to Rodríguez under a decision of the Supreme Court of the Commonwealth of the Bahamas. Ruero International is currently owned 50% by Altamura and 50% by Rodríguez.

In June 2016, XG acquired a 100% interest in the Property from CMR. Registration of the sale agreement and transfer of title to XG was impeded by a court judgment which was nullified in 2019.

CMR was the prior registered holder of title to the 7 "core concessions" until December, 2019, at which time a 2016 concession assignment agreement between CMR and Xochipala Gold assigning 100% of title to Xochipala Gold, was finally registered in the Public Registry of Mining (PRM).

Exploration from 2017 to 2019 by Oroco consisted of access road rebuilding, surveying, limited outcrop and structural field mapping, acquisition of Synthetic Aperture Radar data, and structural interpretation based on a digital terrain model and an orthophoto; the structural interpretation was supplemented field mapping and structural measurement in 2019.

6.2 Historical Mineral Resource Estimates

The Current MRE presented in this report represents the only compliant estimation of the Santo Tomás Project under the CIM 43-101 rules and guidelines. A qualified person has not done sufficient work to classify the historical estimate as current mineral resources or mineral reserves; and the issuer is not treating the historical estimate as current mineral resources or mineral reserves. They are reported to maintain the project history. The historical estimates have been superseded by the mineral resource in Section 14.

Early MREs included estimation work by ASARCO and Tormex. However, the reporting as described in Spring (1992) lacks the details of the methods and geological controls to mineralization. The results are not acceptable under the current standards of disclosure. Therefore, these historical mineral resources estimates are not cited here. In 1993, Mintec Inc. was retained to review the MREs, to assess the project's overall potential and to design conceptual pit phases, as part of the Prefeasibility Study requested by Exall Resources (Bateman, 1994). The Author does not cite herein the historical MRE included in Bateman (1994) and Mintec (1994).

Thornton (2011) Technical Report: John Thornton, P. Eng., of Thor Resources LLC prepared the most recent Mineral Resource and Reserve calculation of the Santo Tomás deposit. Summary of Thornton (2011) Historical Estimate Results

At a 0.15% total copper percent (CuT) cut-off grade (CoG), the results showed a large historical Measured and Indicated (M&I) MRE consisting of 211.2 million tonnes at 0.35% Cu (measured) and 610.6 million tonnes at 0.31% Cu (indicated) for a total of 822 million tonnes at an average grade of 0.32% CuT, for a total of 5.8 billion contained pounds of copper.

The results were presented in the document titled: "Santo Tomás Copper Project, Choix, Sinaloa, México, Technical Report" dated September 23, 2011 (Thornton, 2011).

The MRE prepared by Thornton (2011) is a Historical Estimate as defined under NI 43-101 - Standards of Disclosure for Mineral Projects ("NI 43-101"). Thornton (2011) addressed certain important limitations of the 1994 MRE released by Bateman (1994). Thornton (2011) revised the block modeling scheme to better accommodate the structural geology by using a 3D volume of the main mineralized zones to constrain his Historical Estimate.

An important conclusion of the Bateman (1994, 2003) studies was that gold, silver and molybdenum report to the concentrates during processing (Bateman, 1994; Thornton, 2011), notwithstanding that the recovery rates for these metals were not determined in the initial metallurgical test work conducted for either of the 1994 or 2003 reports.

7 GEOLOGICAL SETTING AND MINERALIZATION

7.1 Regional Geology

The Project area is covered by the 1:50 000 scale Tasajeras map (Sheet G12-B59) from Servicio Geológico Mexicano (SGM). SGM's notes on the map, along with their respective map unit abbreviations, are used as the basis for the regional geology description.

Western México developed from allochthonous terranes accreted to the continental margin of North America in the Mesozoic and earliest Cenozoic (Dickinson and Lawton, 2001; Keppie, 2004), the largest represented by the Guerrero Composite Terrane (Campa and Coney, 1983; Centeno-García et al., 2008). The Tasajeras area is underlain by the Tahue Terrane, a subterrane of Guerrero Composite Terrane. This comprises a basement of Paleozoic accreted arc and eugeoclinal sedimentary rocks and Triassic rift-related meta-igneous rocks. These strata are unconformably overlain by arc-related rocks interpreted as part of the Guerrero Arc (Ortega-Gutiérrez et al., 1979; Henry and Fredrikson, 1987; Roldán-Quintana et al., 1993; Freydier et al., 1995). Mesozoic arc-related strata comprise volcanic and volcanoclastic sequences of oceanic affinity associated with island arcs of Middle Jurassic and Early Cretaceous age that accreted onto North America in the Late Cretaceous during the Laramide Orogeny (Campa and Coney, 1983; Centeno-García et al., 1993). Numerous batholiths, forming a NW-SE trending belt, were emplaced between 90 and 40 Ma during the Laramide orogeny and subduction, the most extensive represented by the Sinaloa-Sonora Laramide batholith complex (Anderson and Silver, 1969; Gastil and Krummenacher, 1977; Valencia Moreno et al., 2003; Ramos-Velázquez et al., 2008). Laramide contraction was followed by Basin and Range extension and deposition of an extensive middle Cenozoic (Tertiary) volcano-sedimentary sequence. This comprised andesitic volcanoclastic rocks and flows; rhyolite ignimbrites; and intercalated sediments including polymictic conglomerates and breccia termed the SMO) volcanic province.

The following summary presents a brief description of the of the geology according to the Tasajeras map sheet area, and the Geology, Mineralization, and Exploration of the Santos Tomás Cu-(Mo-Au-Ag) Porphyry Deposit, Sinaloa, Mexico: NI 43-101 Technical Report (Bridge, 2019) published in 2019 for the Santo Tomás area.

7.1.1 Stratified Rocks

7.1.1.1 Mesozoic Volcanic and Sedimentary Rocks

These Mesozoic strata consist of carbonate-rich sediments, including limestone, marble bodies, sandstones, and large volumes of andesitic volcanic rocks (Borovic, 2006). The Tasajeras map sheet refers to the lower greenschist metamorphosed Mesozoic intermediate volcanic, and volcanic-sedimentary rocks as Jurassic-Cretaceous Meta-andesite (JtKapMA). Thick limestone, marl and marble beds are common, enclosed by andesitic rocks, termed Jurassic-Cretaceous Meta-Limestone (JtKapMCz). Similar limestone units, that are floored and enclosed by the Late Cretaceous Sinaloa-Sonora Batholith, are locally termed Meta-Limestone (KaMCz) although they are likely equivalent to the unit JtKapMCz.

7.1.1.2 Cenozoic (Tertiary) SMO Volcanic Rocks

The SMO extends from the southwestern United States to central México representing the largest continuous ignimbrite province in the world (Aguirre-Díaz et al., 2008), a result of result of Cretaceous-Cenozoic magmatic and tectonic episodes related to the subduction of the Farallon plate beneath North America and opening of the Gulf of California. In the northern

part of its distribution, the SMO is composed of silicic ash-flow tuffs and rhyolitic lavas with minor amounts of andesitic lavas. The average thickness exceeds 1 km (McDowell and Clabaugh, 1979) and the ages cluster in two discrete periods of Eocene and Oligocene age.

In the Tasajeras map sheet, the oldest SMO units are Oligocene Sandstone and Polymictic Conglomerate (TeoAr-Cgp) and Andesite and Rhyolite Tuff (ToA-TR, TomTR). Dacitic volcanic rocks at the Bahuerachi deposit, located 15 km northeast of the Property, are dated as 59 Ma (approximately Eocene in age) and importantly, are termed “post-mineralization.” Younger SMO units comprise the largest volumes of silicic ash-flow tuffs and rhyolitic lavas, termed Rhyolite Tuff and Ignimbrite (TomTR-Ig). Feeder dikes and small felsic intrusions coeval with the SMO are locally termed Rhyolite intrusions (TmR). SMO volcanism is ascribed to fractional crystallization of mantle-derived basalts (Johnson, 1991; Wark, 1991) with volcanism contemporaneous with the waning of Laramide orogenesis and initiation of Basin and Range extension (Wark et al., 1990; Aguirre-Díaz and McDowell, 1991, 1993). The oldest Eocene SMO units may represent the extrusive components of the youngest Laramide intrusive events, as indicated by age data from the Bahuerachi deposit.

7.1.2 Intrusive Rocks

Intrusive rocks consist of batholiths and stocks, and dikes of several varieties and ages.

7.1.2.1 Late Cretaceous: Sinaloa-Sonora Batholith

The Late Cretaceous Sinaloa-Sonora Batholith is contemporaneous with the Jurassic and Cretaceous accretion of the terranes that make up much of the North American Cordillera. The batholith contains multiple phases of intrusive rocks ranging in composition from diorite and tonalite to granite and quartz-monzonite. The emplacement of intrusions was partially controlled and subsequently offset by several phases of faulting dating from Late Cretaceous to the Cenozoic. In the region near the Property, the Sinaloa-Sonora Batholith is mostly Granodiorite (KsGd) and Tonalite (KsTn).

7.1.2.2 Late Cretaceous to Paleocene: Laramide Intrusions

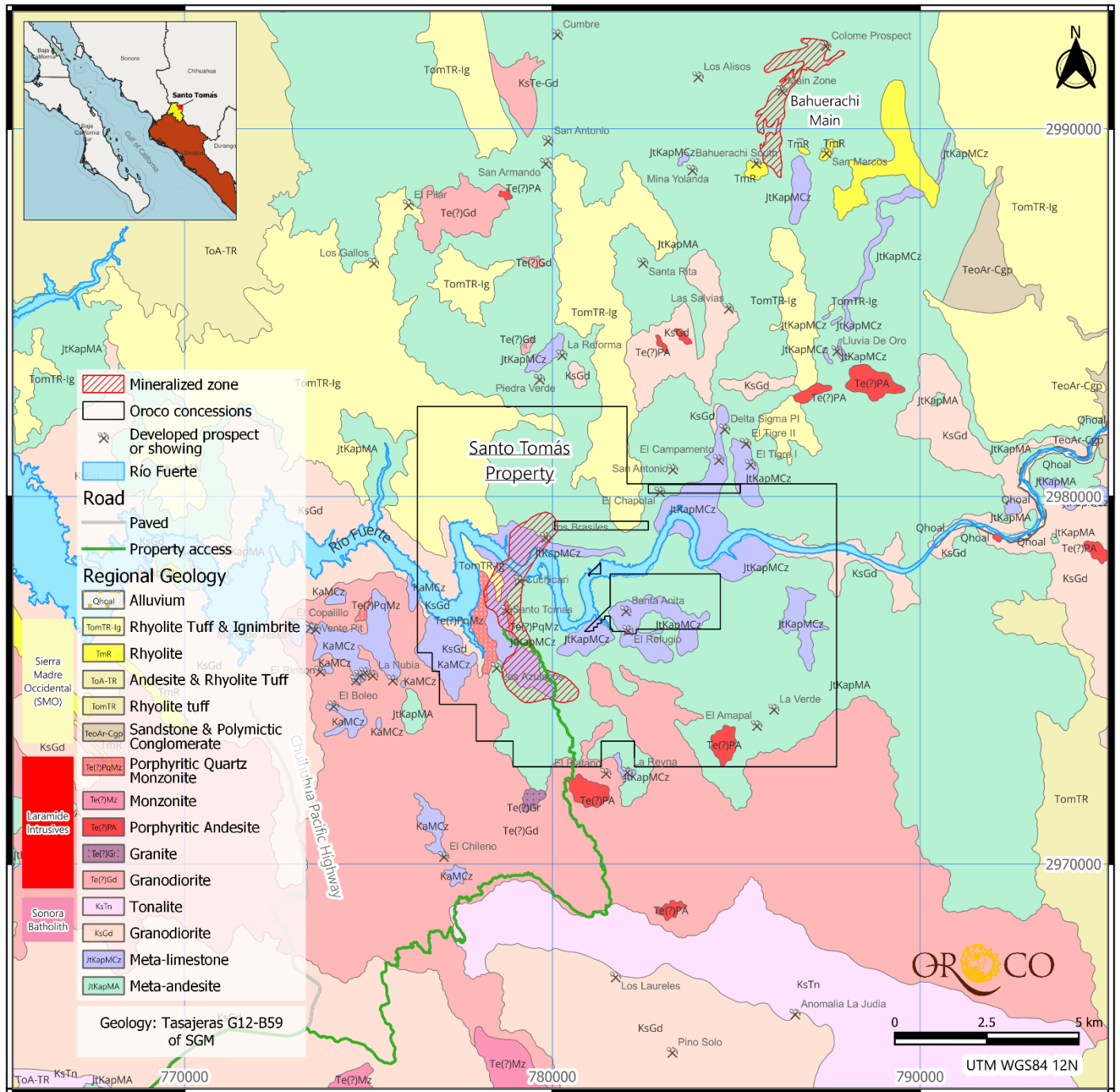
Locally, the Laramide-age intrusive rocks are emplaced in north and north-east trending fault zones and clearly post-date the Sinaloa-Sonora Batholith. The Laramide intrusions in the region of the Property are Paleocene age.

On the Tasajeras map sheet, Granodiorite (Te(?)Gd & KsTe-Gd) is of uncertain age. The intrusive felsic rocks are more certainly of Laramide-age and are designated as Porphyritic Quartz Monzonite (Te(?)PqMz), Porphyritic Andesite (Te(?)PA) and Granite (Te(?)Gr).

7.1.2.3 Late Dikes

Younger Mid- to Late-Cenozoic intrusive rocks, mostly in the form of dikes cut the older sedimentary rocks and early intrusive rocks. Reported dike rocks include Rhyolite and Trachyte (TmR) and mafic (basalt equivalent) varieties.

Figure 7-1: Regional Geology



Source: Oroco, 2023.

7.1.3 Structural Geology & Mineralization

Regional mapping indicates that the older, Mesozoic sedimentary and volcanic sequence is folded to varying degrees by regional Laramide deformation and deformation related to the emplacement of the Late Cretaceous NW-SE trending Sinaloa-Sonora Batholith. Locally, these older stratified rocks tend to occur as wedges between intrusive bodies or as roof pendants. Recrystallization of limestone by heat derived from plutonism has produced marble bodies, contact-type hornfels alteration and skarns. On the Tasajeras map sheet, gently dipping “rafts” of marble (KaMCz) are locally floored by granodiorite of the Sinaloa-Sonora Batholith. Contact metamorphism lithologies include marble, magnetite-epidote-wollastonite exoskarn, and locally, endo-skarn in the Cretaceous granodiorite.

Near the Property, and in the vicinity of the La Reforma and Bahuerachi deposits, the style of deformation is indicated by the distribution of the thick Mesozoic limestone units. Meta-andesite (JtKapMA) and limestone beds are gently dipping. Near the Property, massive fault bounded, rotated limestone/marble (JtKapMCz) blocks dip gently northwards and westwards. They serve as markers to trace the effect of several stages of brittle fault deformation. See the Property Geology section of this report for details of the stages of brittle deformation.

NNE and NE trending normal faults and broad, transcurrent wrench-fault zones likely controlled Laramide dike swarms, hydrothermal brecciation, hydrothermal alteration, and sulphide mineralization. NNE and NE trending intrusive bodies and hydrothermal breccia have been documented at Bahuerachi (e.g., Tyler Resources Technical Report: Jutras and McCandlish (2003)), in the barren Santa Rita hydrothermal breccia body, and on the Property within the Santo Tomás North, South, and Brasiles Zones.

Late-Stage deformation is characteristically normal listric style faulting of the younger Choix horst and graben structures which represents a period of extensional deformation dating to the Oligocene-Miocene and part of the Basin and Range Province. These structures have offset and modified the contact relationships between the older phases of intrusive rocks, metasedimentary host rocks and mineralization.

Locally, late-stage faulting has served to control and localize the emplacement of younger, Miocene-aged SMO rhyolitic volcanic rocks.

At the Santo Tomás, late-stage faulting also displaces SMO volcanic strata and appears to exploit certain of the early-stage fault planes of the Santo Tomás deposit.

7.2 Property Geology

7.2.1 Introduction

The Santo Tomás Cu(-Mo-Au-Ag) porphyry deposit is associated with Laramide-age porphyritic quartz monzonite (Te(?)PqMz, QM) stocks and dikes (K-Ar age of 57.2 ± 1.2 Ma) (Bridge, 2020). These were emplaced into Jurassic-Cretaceous strata comprising metamorphosed andesite, limestone and minor argillaceous and clastic units. Mineralization is strongly structurally controlled and associated with the Laramide-age Santo Tomás fault and fracture zone (an “Early-Stage Structural zone”) which provided the pathway for the quartz monzonite dikes swarm and related hydrothermal alteration, hydrothermal breccias, and sulphide mineralization. Sulphides dominated by pyrite-chalcopyrite-(molybdenite) are distributed in quartz monzonite and altered andesite. Mineralization forms a tabular, SE striking, NW dipping zone primarily defined by finely disseminated sulphides and fracture-fillings with subordinate sulphides hosted in stockwork quartz veinlets. Minor mineralization is associated with skarn and replacement-style mineralization in the hanging wall limestone. Oroco together with SRK undertook a detailed mapping campaign on the Property to update the

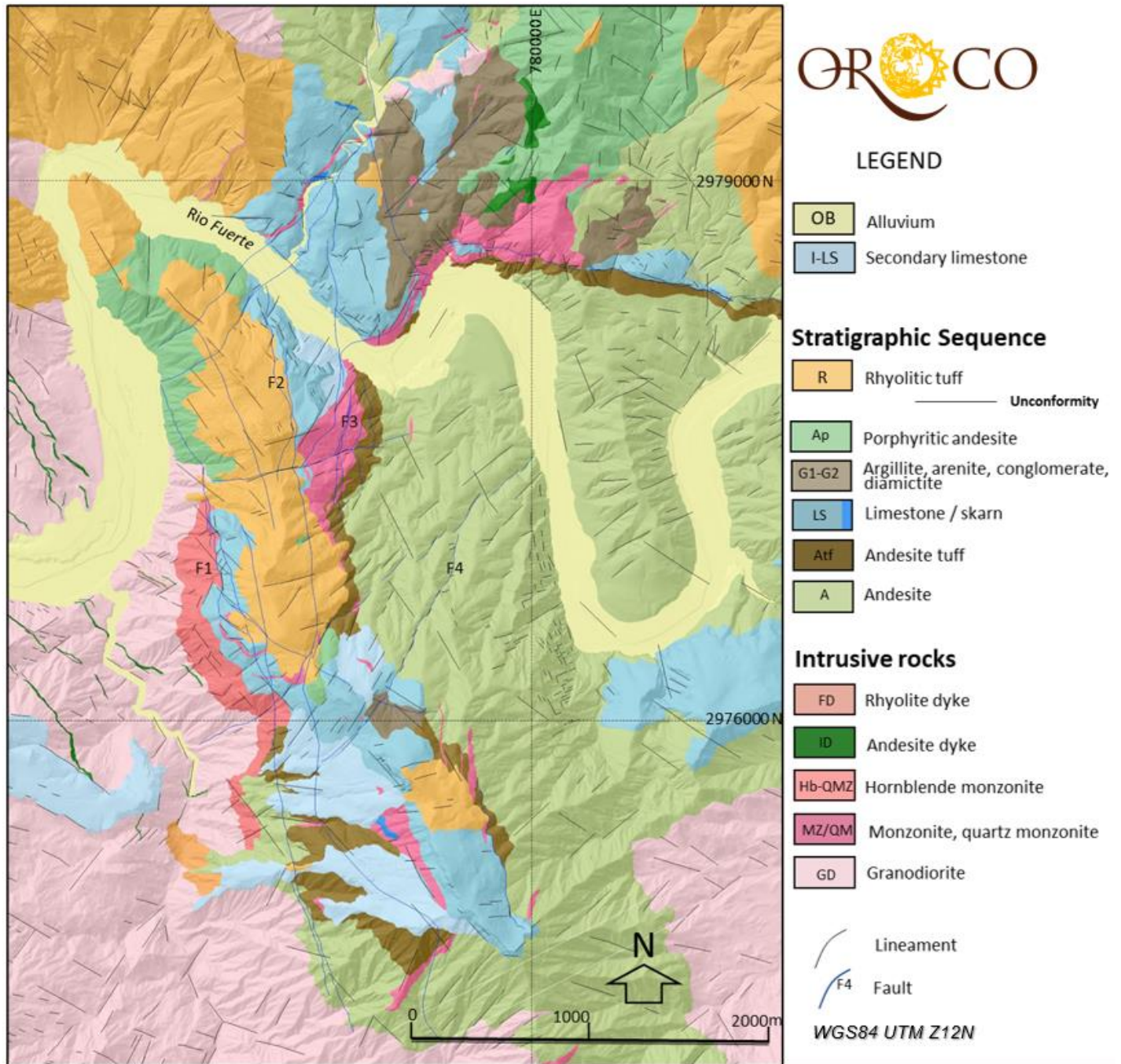
map presented in the previous Technical Report (Bridge, 2020). All mapping data were compiled into an Arc GIS project. This comprised lithology and structural orientation data, line work and contacts, and included active links to field photographs. Mapping data and Arc GIS shape files were also imported into 3D space (Leapfrog Geo) software. In Leapfrog Geo the data were integrated with high-resolution drone data, lineament analysis data, geophysics data and drill hole data to further constrain lithology domains, contacts and structures and inform the lithostructural modeling and resource modeling process. In addition, a database with 1027 field stations, a total of 17 samples (Table 7-1), from surface (8 samples) and drill holes (9 samples) were selected for geochronological analysis (Ar40/Ar39, U/Pb and Re-Os) to support stratigraphic interpretation and timing of alteration-mineralization. The results of the field mapping campaigns are represented in the geological map and stratigraphic column (Figure 7-1 and Figure 7-2), while structural data and interpretations are presented in the structural chapter.

Table 7-1: List of Samples from the Santo Tomás Porphyry Deposit Selected for Geochronological Analysis

Sample ID	Hole/Station	Method	Code	Sample Material	Age	Location	Weight kg
300221	ST176	U-Pb/Zr	U-ISTP02	Intrusive Monzonite	Late Cretaceous - Early Tertiary	Surface	2.4
300222	B414	U-Pb/Zr	U-ISTP02	Andesite Porphyry	Late Cretaceous - Early Tertiary	Surface	1.6
300223	ST29	U-Pb/Zr	U-ISTP02	Intrusive Hornblende Quartz Monzonite	Late Cretaceous - Early Tertiary	Surface	2.1
300224	B004	U-Pb/Zr	U-ISTP02	Intrusive Monzonite	Late Cretaceous - Early Tertiary	Core	2
300225	S019	U-Pb/Zr	U-ISTP02	Intrusive Monzonite	Late Cretaceous - Early Tertiary	Core	2
300226	N004	U-Pb/Zr	U-ISTP02	Granodiorite - Sonora Batholith	Late Cretaceous	Core	2.8
300227	S006	U-Pb/Zr	U-ISTP02	Granodiorite - Sonora Batholith	Late Cretaceous	Core	3.6
300228	ST75	Ar-Ar /Micas	Ar-ISTP01	Andesite Trachyte	Jurassic	Surface	1.6
300229	ST288	Ar-Ar /Micas	Ar-ISTP01	Felsic Dike	Mid-to-Late Tertiary	Surface	2.1
300230	B188	Ar-Ar /Micas	Ar-ISTP01	Intermediate Dike	Mid-to-Late Tertiary	Surface	0.9
300231	SW-1	Ar-Ar /Micas	Ar-ISTP01	Hornblende Volcanic	Late Cretaceous - Early Tertiary	Surface	2.6
300232	S018	Ar-Ar /Micas	Ar-ISTP01	Andesite Tuff	Jurassic	Core	2.1

Sample ID	Hole/Station	Method	Code	Sample Material	Age	Location	Weight kg
300233	N021	Ar-Ar /Micas	Ar-ISTP01	Andesite Porphyry	Late Cretaceous - Early Tertiary	Core	2.7
300234	N018	Ar-Ar /Micas	Ar-ISTP01	Alteration (Phyllic - Sericitic)	Late Cretaceous - Early Tertiary	Core	2.6
300235	ST241	Re-Os / Mo	Re-ISTP01	Mineralization	Late Cretaceous - Early Tertiary	Surface	0.3
300236	B003	Re-Os / Mo	Re-ISTP01	Mineralization	Late Cretaceous - Early Tertiary	Core	0.7
300237	N018	Re-Os / Mo	Re-ISTP01	Mineralization	Late Cretaceous - Early Tertiary	Core	0.5

Figure 7-2: Project Geology, mapped by Oroco Project and SRK Geology Personnel



Source: Oroco, 2023.

7.2.2 Stratified Rocks

7.2.2.1 Andesite (A)

The Jurassic-Cretaceous andesite (JtKap) comprises an extensive undifferentiated andesitic succession exposed to the east of the Santo Tomás ridge. Surface mapping indicates that the thickness exceeds 500 m with the thickest intercept of 394.62 m, recorded by drill hole ST21-N001. The andesites are mostly massive flows with poorly developed bedding. The rocks are medium to dark gray colored, aphanitic to fine-grained, and may be porphyritic containing 10%, 1-3 mm subhedral plagioclase phenocrysts. The lower part of the sequence is represented by gray to gray-reddish andesite with a trachytic texture defined by oriented plagioclase laths (av. 40%) in an aphanitic matrix that often contains secondary quartz amygdales.

7.2.2.2 Andesite Tuff (Atf)

A unit of andesite tuff was recognized within the regional andesite (JtKap) sequence. The tuff overlies the more massive andesites and immediately underlies the limestone. Thickness is highly variable with a maximum thickness of 370.85 m recorded in drill hole S003. The rock typically fine-grained, medium to dark gray in color with a greenish tint. The texture varies from massive and aphanitic to fine-grained porphyritic. Phenocrysts include plagioclase up to 8mm in size which may be locally aligned and scattered mafic phenocrysts up to 2 mm in length.

7.2.2.3 Limestone (LS)

The limestone (JtKap) at Santo Tomás and Brasiles forms prominent cliff faces and scarps. The limestones are typically massive, fine to coarse-grained, and frequently recrystallized to a marble. In places bivalves, ostracods and coral fragments are preserved. Bedding is poorly defined on outcrops but in places a crude layering may be observed. The preserved erosional thickness of this unit varies, with a maximum thickness of 352.47 m recorded in drill hole B005.

7.2.2.4 Siltstone (G1) – Conglomerate (G2)

The units G1 (argillaceous) and G2 (arenaceous, pebbly quartz conglomerate and sandstones) refer to a clastic sequence KsTpa? that immediately overlies and may be interbedded with the upper parts of the Limestone unit. The most extensive outcrops are found at Brasiles with smaller occurrences at North and South Zone. Strata dip to the E-SE in the Brasiles area and drill hole intercepts indicate a thicker sequence in Brasiles with 98.86 m in drill hole B002 and 111 m in drill hole B003.

G1 is represented by pale brown to greenish, fine to medium grained siltstone-sandstone that may be laminated with occasional normal graded bedding preserved.

G2 is a pale greenish gray colored, mature mainly clast-supported quartz conglomerate. Clasts are moderately to well sorted, composed mainly of subrounded to rounded quartz less than 2 cm in size with occasional igneous clasts of silicified monzonite and andesite. The unit is generally massive by graded bedding may be visible in places.

7.2.2.5 Sierra Madre Occidental Volcanic Rocks

Miocene Rhyolite Tuff and Ignimbrite (TomTR-Ig, V) form a discontinuous blanket over the tops and flanks of the ridges on the Property. Two units are recognized on the Property, a lower unit (Rbx) characterized by debris flow deposits and

rhyolite breccias, and an upper unit largely comprising rhyolite tuff (R). The SMO paleosurface had significant relief in places and comprised the exhumed, eroded, and weathered lower succession and pre-SMO deformation and the Santo Tomás mineralization but also preserving the mineralization from post-SMO erosion.

7.2.2.5.1 Diamictite and Rhyolitic Breccia (Rbx)

This lower unit comprises diamictite overlain by rhyolitic breccia.

Diamictite directly overlies the unconformity and marks base of the SMO. Diamictites are typically red-hematite stained and matrix-supported. Clasts are polymictic, poorly sorted, angular to rounded, usually less than 15 cm in size but locally up to 30 cm. Clasts commonly comprise fragments of the underlying limestone with porphyritic rhyolite, andesite, altered monzonite, and quartz identified. Clasts may be elongated and aligned, and in places are normally graded.

The rhyolite breccia, overlying the diamictite, is medium red to pale pink in color with a fine-grained matrix containing clasts that are mostly matrix-supported but locally clast-supported. Clasts are moderately to poorly sorted and aligned in places and subangular to rounded. Clast types are dominated by rhyolitic compositions, up to 8 cm in size, with subordinate andesite clasts up to 4 cm in size and subhedral xenocrysts of feldspars and anhedral quartz. A Rbx thickness of 145.15 m was intersected in drill hole N040 in the North Zone with the unit thickening northwestward of the North Zone and northeastward of Brasiles.

7.2.2.5.2 Rhyolite Tuff (R)

The rhyolite tuff unit (R) overlies the Rhyolite breccia. It is a pale to dark pink colored, fine-grained, crystal-rich, tuffaceous rock with an ash-lapilli matrix. Crystals are typically less than 2 mm in size and include subhedral to anhedral biotite, amphibole, quartz, and plagioclase. Angular to subangular volcanic fragments up to 4 cm, mainly of rhyolitic composition, are common with oxidized fiamme. The unit is mostly massive but some intervals may show flow texture and normal graded intervals. The thickest interval of 156.5 m was recorded by drill hole ST21-N009.

7.2.3 Intrusions

Intrusive rocks were emplaced into the older Mesozoic sedimentary and volcanic rocks and consist of several varieties and overlapping phases of granodiorite, quartz monzonite, granite, and tonalites.

7.2.3.1 Late Cretaceous: Sinaloa-Sonora Batholith

7.2.3.1.1 Granodiorite (GD)

Granodiorite (KsGD) of the Late Cretaceous Sinaloa-Sonora Batholith mainly crops out to the west of the Santo Tomás Ridge and extends northward into Brasiles Zone. This unit is light to medium gray, medium grained, with a phaneritic texture comprising subhedral feldspars, anhedral quartz and dark brown euhedral biotite (hexagonal/rectangular) and euhedral hornblende, disseminated magnetite and traces of pyrite. Some plagioclases are visibly zoned and have a sieve texture.

7.2.3.2 Late Cretaceous to Paleocene: Laramide Intrusions

7.2.3.2.1 Monzonite/Quartz-Monzonite (MZ/QM)

The Santo Tomás Cu (-Mo-Au-Ag) porphyry deposit is associated with Laramide-age MZ and QM porphyry stocks and dikes (K-Ar age of 57.2 ± 1.2 Ma) (Bridge, 2020), emplaced into Jurassic-Cretaceous andesite and limestone strata (Fig. 3a-b). On the Property, the MZ/QM (Te(?)) is exposed in windows through the overlying LS cap rocks and the younger SMO volcanics.

The MZ intrusions are typically pinkish pale-gray varying from a porphyritic texture with a very fine-grained groundmass to a crowded crystal-texture. Phenocrysts include feldspar, usually 3 mm in size but may be up to 9 mm in size, subhedral to euhedral biotite, amphibole and anhedral quartz.

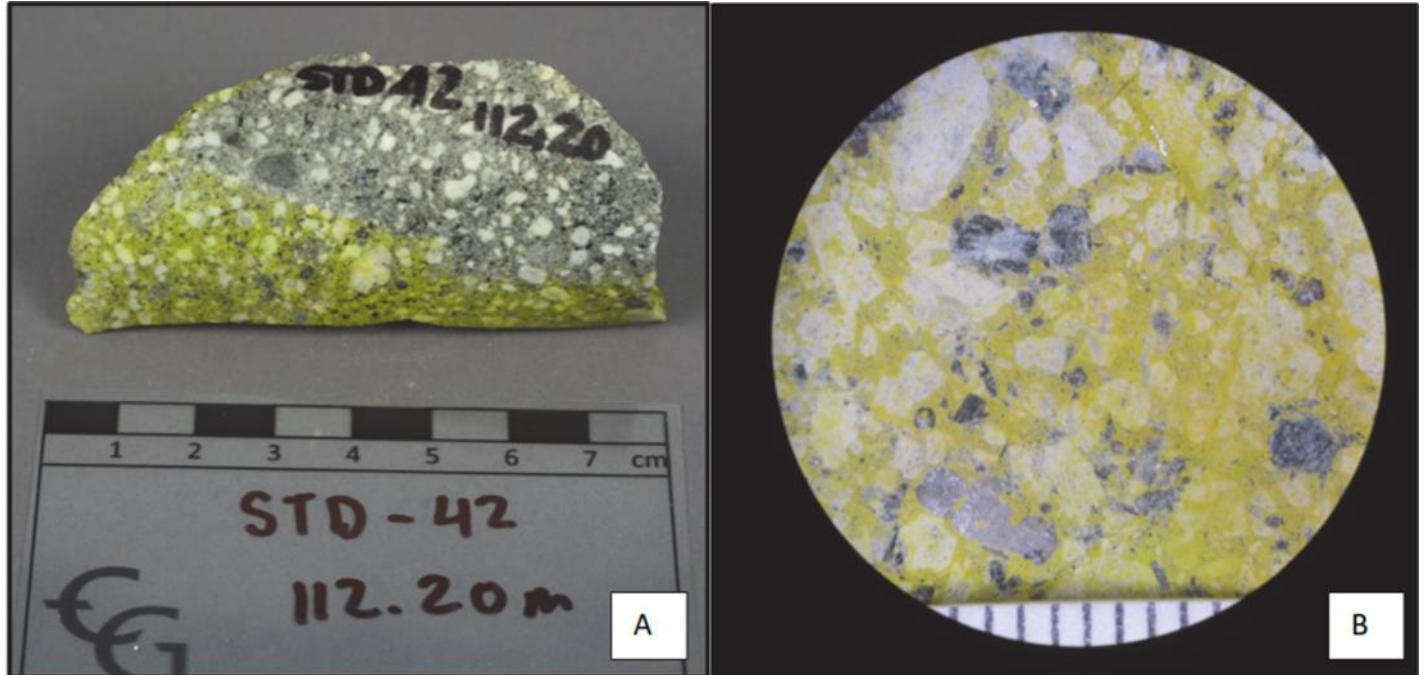
The QM is pale-gray and porphyritic with a variable phenocryst percentage from 45 to 60%. Feldspar phenocrysts are subhedral to euhedral up to 5 mm in size with sporadic 1.5 cm zoned plagioclase. Mafic phenocrysts include subhedral to euhedral biotite and amphiboles up to 4 mm in size. Quartz is typically anhedral constituting less than 10% of the rock.

Previously calculated (Bridge, 2020), the average modal mineralogy for the QM intrusions as:

- Plagioclase 35%
- K-feldspar 43%
- Quartz 8%
- Mafic minerals (mostly hornblende, biotite) 11%
- Sulphides 0.5%
- Other 2.5%

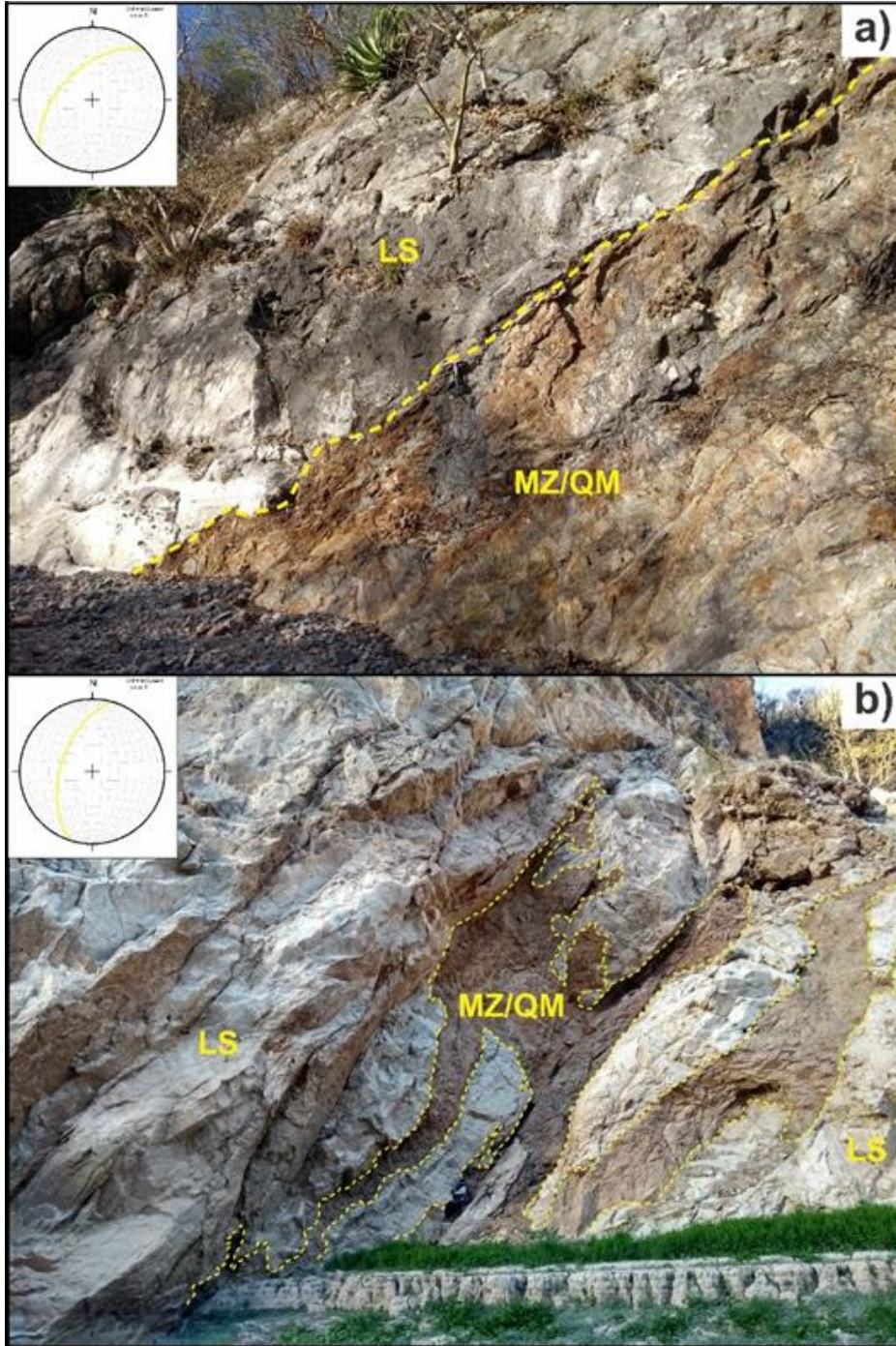
The above-listed percentages normalize to 41% plagioclase, 50% K-feldspar and 9% quartz, yielding a composition of quartz monzonite under the IUGS (International Union of Geological Sciences) plutonic rock classification scheme following the Quartz-Alkali Feldspar-Plagioclase- Feldspathoid ("QAPF") diagram (Walker and Cohen, 2009).

Figure 7-3: Core Sample of Quartz Monzonite from STD-42 Note Core sample of the quartz monzonite (the yellow is a stain for K-feldspar) (A), host to the mineralization at Santo Tomás. A magnified photograph of the sample showing the porphyritic texture of the rock (B), the scale is in millimetres



Source: Oroco, 2023.

Figure 7-4: A) MZ/QM intruding LS northwestward to the B003-B004 drill holes; B) QM/QM sills emplaced along the bedding planes of LS next to El Río Fuerte southwestward to the B005 drill hole. The direction of the contacts is represented in the stereonets



Source: Oroco, 2023.

7.2.3.2.2 Hornblende Quartz-Monzonite (HbQM)

The unit HbQM (Te?) crops out along the western side of the Santo Tomás ridge. This rock is gray in color, inequigranular and hypidiomorphic. Visual estimates indicate that K-feldspar exceeds plagioclase, and quartz composition is greater than 8%. Mafic minerals include amphiboles and biotite and scattered magnetite. Contact relationships between the MZ/QM and the HbQM are not clear, however the MZ/QM intrusions dip westerly while the HbQMz is interpreted to dip easterly.

7.2.3.2.3 Porphyry Andesite (Ap)

This unit is classified as an intermediate intrusion characterized by a high plagioclase phenocrysts content. It is typically medium green to gray in color with a porphyritic texture. Phenocrysts comprise subhedral to anhedral plagioclase up to 5 mm in size and scattered subhedral biotite, up to 3 mm in size. Large sporadic plagioclase porphyroblasts up to 2 cm in size are observed.

7.2.3.3 Late Hypabyssal Intrusions

7.2.3.3.1 Hornblende Trachy-Andesite (TAhbl)

A late hypabyssal intrusion (Te?), intruding the GD was mapped west of Santo Tomás ridge. The rock is light to medium brown colored with a porphyritic to trachytic texture. It is characterized by elongated and tabular hornblende with lesser euhedral to subhedral feldspars, up to 5 mm in size and very fine-grained disseminated magnetite.

7.2.3.3.2 Fine-Grained Granodiorite (Fg-GD)

A phase of late fine-grained granodiorite intrusion occurs in the southeastern portion of the area. It is light gray in color, with a composition similar to the more extensive GD unit. The rock has a phaneritic texture and usually contains disseminated pyrite, and tourmaline.

7.2.3.3.3 Felsic Dike (FD)

Felsic dikes up to 3 m wide are pale pink to light gray in color. They are porphyritic to aphanitic texture with sporadic subhedral to euhedral biotite and amphiboles, less than 2 mm in size and anhedral feldspar, less than 1 mm in size. Felsic intrusions were seen in several sites at Santo Tomás, with the most significant intrusion outcrops noted on the El Río Fuerte valley extending northwest towards the North Zone. The felsic dikes intrude the LS G1/G2 units, suggesting a probable Oligocene-Miocene age, coeval to the SMO volcanoclastic deposits.

7.2.3.3.4 Intermediate-Mafic Dikes (ID)

A series of andesitic-basaltic dikes were mapped in the area. These typically display a dark gray color, have an aphanitic texture, and in some cases fine-grained plagioclase crystals are visible. The rocks have moderate magnetism containing disseminated magnetite and thin veinlets. ID intrusions post-date the FD suggesting a very young age, possibly linked to several Pliocene-Quaternary magmatism represented by scoria cones approximately 20 km west of Santo Tomás.

7.2.3.4 Overburden (OB)

Quaternary unconsolidated and semi-consolidated deposits comprise talus deposits and alluvium valley fill. Thick talus is locally developed below cliffs, and where these are of limestone, talus may include secondary limestone and tufa aprons. Thick alluvial valley fill is developed along the Río Fuerte with more recent silt accumulations associated with impoundment by the (Huites) Luis Donaldo Colosio Dam.

7.2.4 Alteration

Alteration of the country rocks includes contact metamorphism and hydrothermal alteration. Hydrothermal alteration is recognized by zones of hydrothermal breccia, and zones of propylitic, sodic-calcic, potassic, phyllic and argillic alteration.

7.2.4.1 Contact Metamorphism: Hornfelsed Andesite

Thermal metamorphism of host lithologies, mostly andesite, in contact with quartz monzonite is widely reported on the Property. Andesitic lithologies described as hornfels are aphanitic to very fine-grained, commonly light-colored and mottled with sections of medium- to dark-gray color with a bleached or slightly waxy, baked appearance. In addition to the bleached appearance, is the absence of identifiable mafic or chlorite grains in the groundmass compared to the unaltered andesite protolith. The light-colored hornfelsed andesite may be slightly albitic, biotitic, potassic or silicified. Hornfelsed andesite commonly has moderate to intense micro-fracturing with cm to mm spaced fractures.

7.2.4.2 Hydrothermal Breccia

Hydrothermal breccias are developed in MZ/QM, A and Atf units. The breccias are medium gray in color and comprise variable sized lithic fragments usually less than 8 cm in size in a cement of quartz, clay, disseminated pyrite, and locally tourmaline. The breccia may have an overprint of weak to moderate silicification. The geometry and thickness of hydrothermal breccia domains are highly variable, with the most volumetric zone recorded in the South Zone with 143.78 m intercepted in drill hole S016 and 100 m intersected in drill hole S018.

Hydrothermal breccias developed in andesite consist of well-rounded clasts, mainly 2-3 cm to 10 cm, locally up to 15 cm in size in a fine-grained granular matrix. They vary from packed clast-supported to matrix-supported with 75% matrix. No hydrothermal pervasive alteration is apparent, but some clasts may contain a thin, light gray alteration rim.

Limestone hydrothermal breccias consist of angular 1 to 10 cm sized, matrix-supported limestone clasts in a recrystallized limestone matrix that may have been derived from a comminuted limestone rock-flour matrix but is texturally similar to the limestone clasts. They have a similar off-white to light gray color as the massive, recrystallized limestones.

7.2.4.3 Veining

Pervasive veining within the main mineralized zone is represented by a series of vein types that along with hydrothermal alteration provide important vectors to mineralization.

Detailed logging at Santo Tomás has revealed ten vein types (Table 7-2) most notably are copper-bearing vein stages that characterize the main mineralization zone, specifically the Early Dark Micaceous (EDM), A and B veins.

EDM veins are hosted in the Quartz Monzonite and characterized by dark micas (muscovite with secondary biotite) along with anhydrite, quartz and chalcopyrite and typically have a coarse subhedral biotite halo. EDM veins are known to characterize the proximal zones of porphyry copper deposits (e.g., Haquira, Peru; Resolution Copper, Arizona; Batu Hijau, Indonesia; Los Pelambres, Chile).

Type A veins are characterized by anhydrite-bornite with a chalcopyrite median line and disseminated biotite-magnetite and are usually pervasive.

Type B veins cut the Type A veins and are hosted within both the Quartz monzonite and Andesite. Vein mineral assemblage is dominated by quartz and chalcopyrite with fine molybdenite on vein margins or in vein sutures with a K-feldspar and illite halo.

High densities of A & B-type veins characterized by chalcopyrite-molybdenite (minor bornite) are typically associated with the Potassic and Phyllic (QSP) alteration zones. Preliminary fluid inclusion analysis have reported the A-B vein types associated with fluids up to 53.6 NaCl (wt%) and temperatures up to 442 °C.

Type E vein are represented by a late-stage mineralizing event that cuts the A & B veins. Veins are characterized by a quartz-calcite pyrite veins with associated chalcopyrite-sphalerite in proximal zones and sphalerite-galena in distal zones.

Table 7-2: Oroco Vein Type Classification at Santo Tomás

Code	Description
EDM	Early Dark Micaceous: Biotite + Anhydrite + Chalcopyrite
LG	Quartz + Biotite + Chlorite ± Magnetite
M	Magnetite Veins
A	First Mineralized Veinlets: Quartz + Chalcopyrite ± Bornite ± Magnetite
B	Second Mineralized Veinlets: Quartz + Molybdenite ± Chalcopyrite + Pyrite ± k-feldspar
D	Forth Mineralized Veinlets (QSP): Quartz + Sericite + Pyrite
E	Firth Mineralized Veinlets: Quartz + Sericite + Pyrite + Carbonate ± Sphalerite ± Galena
DX	Pyrite + Cobalt / Pyrite / Pyrite + Chlorite
QTP	Quartz-Tourmaline- k-feldspar ± Pyrite

7.2.4.4 Propylitic Alteration

Propylitic alteration is the distal or peripheral alteration phase at Santo Tomás. Propylitic alteration generally occurs in two stages; the epidote stage and the epidote-free stage. The epidote-stage reveals mineral assemblages of epidote-chlorite-sericite, chlorite-sericite and chlorite-epidote-calcite (with or without albite and quartz) whereas epidote-free stage assemblages include calcite, chlorite and sericite (Seki, 1973).

7.2.4.5 Sodic-Calcic Alteration

Albitic alteration is an early-stage, high-temperature alteration that is a deeper or core alteration in porphyry systems. At Santo Tomás sodic-calcic or albitic alteration is very poorly defined and may be mainly overprinted by later potassic alteration.

In STD-45, silica-albite alteration in quartz monzonite occurs in part of the 328.2-351.7 m interval, at 315.5 m, and in STD-44 at 333 m. It is a uniformly light-colored, off-white groundmass consisting of 50% opaque to semi-translucent albite (?) and 50% transparent to translucent, colorless quartz as distinct, very fine, separated, sand-like grains. Minor euhedral remnants of the original plagioclase phenocrysts and quartz phenocrysts attest to a quartz monzonite precursor.

Irregular tourmaline patches and minor remnants of chlorite are common. The overall character is a whiter lithology compared to normal quartz monzonite and absent to minor, wispy to indistinct chlorite, but with the chlorite appearing brighter green, possibly because of the whiter groundmass.

Very localized potassic alteration occurs with the silica-albite alteration and may indicate that the albitic alteration of plagioclase phenocrysts and groundmass predates potassic alteration.

Silica-albite alteration is associated with higher-than-normal sulphide concentrations.

7.2.4.6 Potassic Alteration

Potassic alteration is characterized by the exchange of K for Ca and Na ions, leading to the replacement of Ca- Na bearing mineral phases by potassic minerals; typical assemblages are orthoclase and biotite after plagioclase and hornblende. It is commonly developed in the core of porphyry Cu-systems.

Very thin potassic alteration halos occur along the margins of quartz and quartz-sulphide veins as indicated by staining for potassium. However, in unstained rock, there is little color contrast between these halos and the rock, so the presence of potassic alteration is near impossible to detect unaided by staining.

Potassic altered andesite: Potassium feldspar (Potassic) alteration in andesite locally alters the groundmass from an aphanitic texture to a uniform and very fine-grained hypidiomorphic granular texture and imparts a slight translucency to the groundmass.

Potassic altered andesite is commonly medium gray in color and does not display any potassium feldspar coloration. Individual mineral grains are indistinct due to potassic alteration, and the rock appears to consist of weakly translucent plagioclase and altered plagioclase with minor chloritic remnants of mafic minerals. Staining for potassium indicates abundant speckling, up to 50-60%, of potassic alteration that results in slightly indistinct grain boundaries. Locally the groundmass contains abundant fine-grained black tourmaline.

Fracture and veining intensity vary from minor to intense with some correlation of higher copper values with a higher fracture intensity.

Biotite altered andesite: Biotite alteration in andesite or hornfels imparts a black to a nearly black color and an aphanitic to very fine-grained texture. The rock is slightly softer to a scratch with a steel point, but the hardness is variable and is not a reliable indicator.

Some andesite may be biotite altered, especially at monzonite contacts where it is locally near black, rather than dark gray. From observations limited to selected core samples from STD-44 and 45, biotite alteration appears to be less common than other potassic alteration suites.

Potassic altered quartz monzonite: The Santo Tomás quartz monzonite is mainly uniform, medium to coarse-grained with 30-35% euhedral to subhedral plagioclase phenocrysts, 10% quartz phenocrysts and 5% chlorite after primary hornblende. Locally it is in part porphyritic with a relatively fine-grained groundmass and may be transitional to feldspar and quartz-feldspar porphyry. The plagioclase phenocrysts are chalky off-white, partly kaolinized, to pale pinkish when strongly potassic altered.

Potassic alteration varies from weak alteration along vein margins and speckling in the groundmass to total groundmass replacement and partial replacement of the plagioclase phenocrysts. Weak to moderate potassic alteration is commonly identifiable by spotty and slight pink coloration in the groundmass.

Potassic dominated alteration at Santo Tomás affects most of the mineralized quartz monzonite and andesites and extends to the up-dip edge of the dike at its contact with limestone and limestone related sedimentary rocks and local skarn assemblages.

7.2.4.7 Phyllic Alteration

Phyllic alteration is commonly associated with sericite-quartz-pyrite-chlorite assemblages in porphyry Cu settings. It typically forms by the decomposition of feldspars as replacement of feldspars on low pH (acidic) conditions. Phyllic alteration commonly occurs at higher levels than potassic alteration or peripheral to potassic alteration. The relatively narrow dike morphology at Santo Tomás compared to the more common stock or batholithic shape to many porphyry systems may account for the restricted development of phyllic alteration at Santo Tomás.

Phyllic altered quartz monzonite on the Property is uniformly medium gray, slightly translucent, with a weak color contrast between plagioclase phenocrysts and groundmass. The rock is firm but scratches with a knife, looks silicified but is too soft, is slightly waxy as opposed to lustrous. Chlorite after hornblende is present, but grains are less euhedral and less distinct. From the STD-44 and 45 selected core samples and descriptions, there are sharp contacts between possibly later-stage, less-altered monzonite and sericitic quartz monzonite.

Quartz monzonite in drill hole STD-44, at 221.4 m and 237 m has been historically logged as silicified, but the lithology here is dominantly sericite altered. Phyllic alteration is rarely described in andesites in drill core. It may constitute part of the alteration assemblage in bleached hornfelsed andesites, but there has not been any thin section work to confirm the case.

Much of the phyllic alteration described in the core at Santo Tomás appears to be confined to the zone of early-stage faulting and fracturing and the quartz monzonite intrusion.

Figure 7-5: Outcrop of Phyllic Altered Quartz Monzonite Porphyry



Source: Oroco, 2023. The view is looking south, located in the North Zone.

7.2.4.8 Argillic Alteration

Argillic alteration plays a key role in the formation of clay minerals, including kaolinite, smectite and illite. Argillic alteration is generally a low-temperature event alteration stage. The earliest signs of argillic alteration include the bleaching out of feldspars. Advanced argillic alteration, a subcategory of argillic alteration, consists of kaolinite + quartz + hematite + limonite, feldspars leached and altered to sericite. The presence of this assemblage indicates low pH (highly acidic) conditions and temperatures of less than 220°C. At higher temperatures, the mineral pyrophyllite (white mica) forms in place of kaolinite.

There does not appear to be any significant upper-level argillic assemblage on the Property. Argillic alteration is described in core in many of the fault zones in intrusive and andesitic rocks, but it is generally not described in the adjacent lithologies. This argillic alteration likely refers to fault gouge rather than a zone of pervasive hydrothermal alteration. Outcrops of mineralized quartz monzonite appear to be argillic altered, but the surface indications of clay mineralogy may be related to weathering and leaching of phyllic and potassic alteration. For similar reasons, argillic alteration is commonly mentioned in the upper portions of drill holes where the rock is fractured, broken, and weathered.

Figure 7-6: Outcrop of Contact between Hornfelsed Andesite (left) and a Quartz Monzonite Dike (right)



Source: Oroco, 2023. The view is looking towards Azimuth 200° (Contact is 020°/50°W), the site is near STE-27, North Zone.

7.2.5 Structure

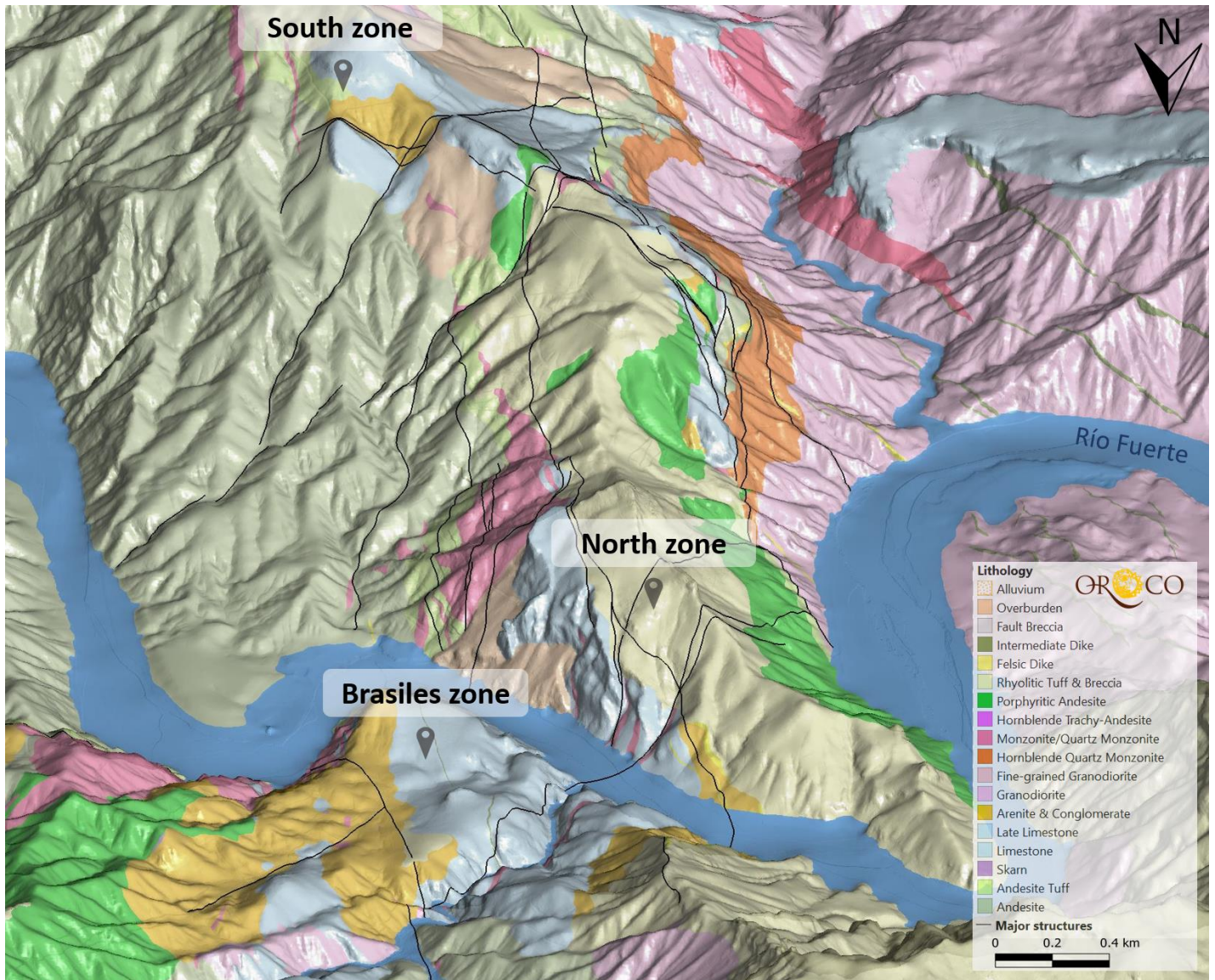
7.2.5.1 Deposit Morphology

The Santo Tomás – Brasiles porphyry copper system is atypical of porphyry deposits in that it consists of a 300- 400 m wide dike complex with a strike extent of at least 5 km. This gives it a very high aspect ratio in the range of 12 to 17:1. Consequently, it exhibits strong structural control rather than the more typical stock or batholith control evident in many porphyry systems. The permeability and fluid flow that produced the alteration and mineralization were the results of multiple faults and an extensive set of fractures related to the faults, that developed in response to hydraulic fracturing. The Santo Tomás deposit has the structural characteristics of porphyry deposits that are broadly related to regional and pull-apart structures at dilational bends, strike-slip faults, shear zones, duplexes, pull-apart basins, and grabens such as described by Berger et al., (2008).

7.2.5.2 Structural Geology – Results from the 2022-2023 Field Work

The field mapping campaigns during 2022 and 2023 generated a significant structural database with a total of 2116 structural measurements. 1275 of these were collected on tectonic structures (faults, shear zones, fault zone, shear-mylonite/cataclasites, fault breccias, fault gouge). An oblique view of the geology and mapped faults are shown in Figure 7-7.

Figure 7-7: Oblique View of Geology and Faulting Looking to the South



Source: Oroco, 2023.

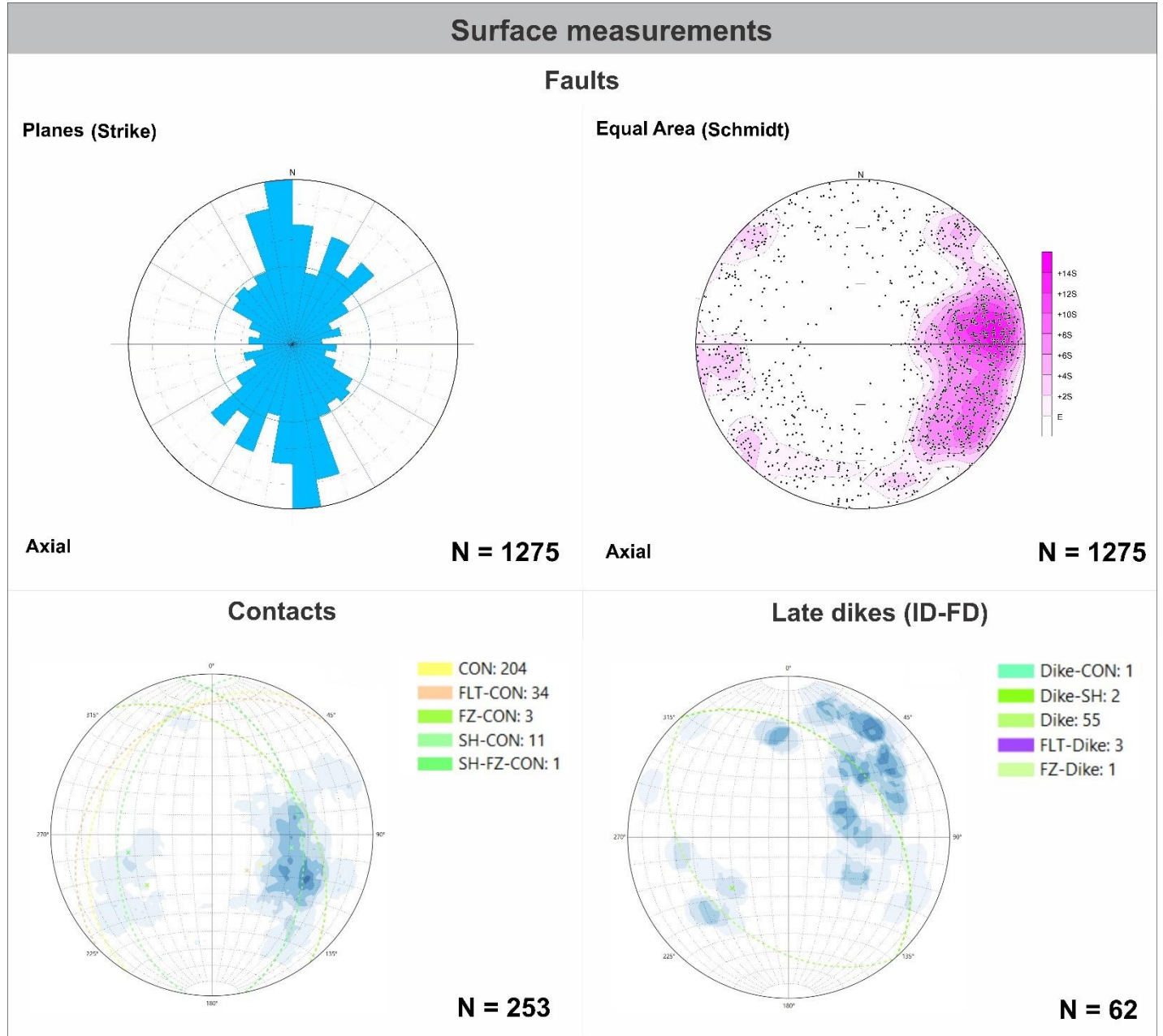
Data analysis indicates three main fault systems:

1. The principal fault system trending NNW-SSE (azimuth N160-N190), composed by structures dipping mainly to the WSW with angles $>40^\circ$.
2. The secondary system trending NE-SW (azimuth N200-N230), composed by structures dipping to the NW and SE (less density) usually with angles $>45^\circ$.

3. Subordinate system composed of NW-SE trending faults.

Structural data of lithology contacts have NNE-SSW trends with a WNW dip-direction (Figure 7-8). These orientations conform to the MZ/QM dike orientations and support a conformable intrusion along the andesite-limestone contact orientation. The minor NW-SE trending fault system is best represented by the late intrusions (ID-FD), which usually dip to the SW Figure 7-9 suggesting that this fault set is the youngest structural system of the area.

Figure 7-8: Orientation data plots from the geological mapping campaign. Histogram and stereonet poles to faults measured in the area: stereonet showing the main orientation of the lithological contacts including faulted and non-faulted contacts: stereonet showing the main trends



Source: Oroco, 2023.

Figure 7-9: System of ID intruding the GD next to the El Río Fuerte and west of the N032-41 drill holes. The orientation of the dikes is represented in the stereonet. View looking South.



Source: Oroco, 2023.

7.2.5.2.1 Kinematic Analysis

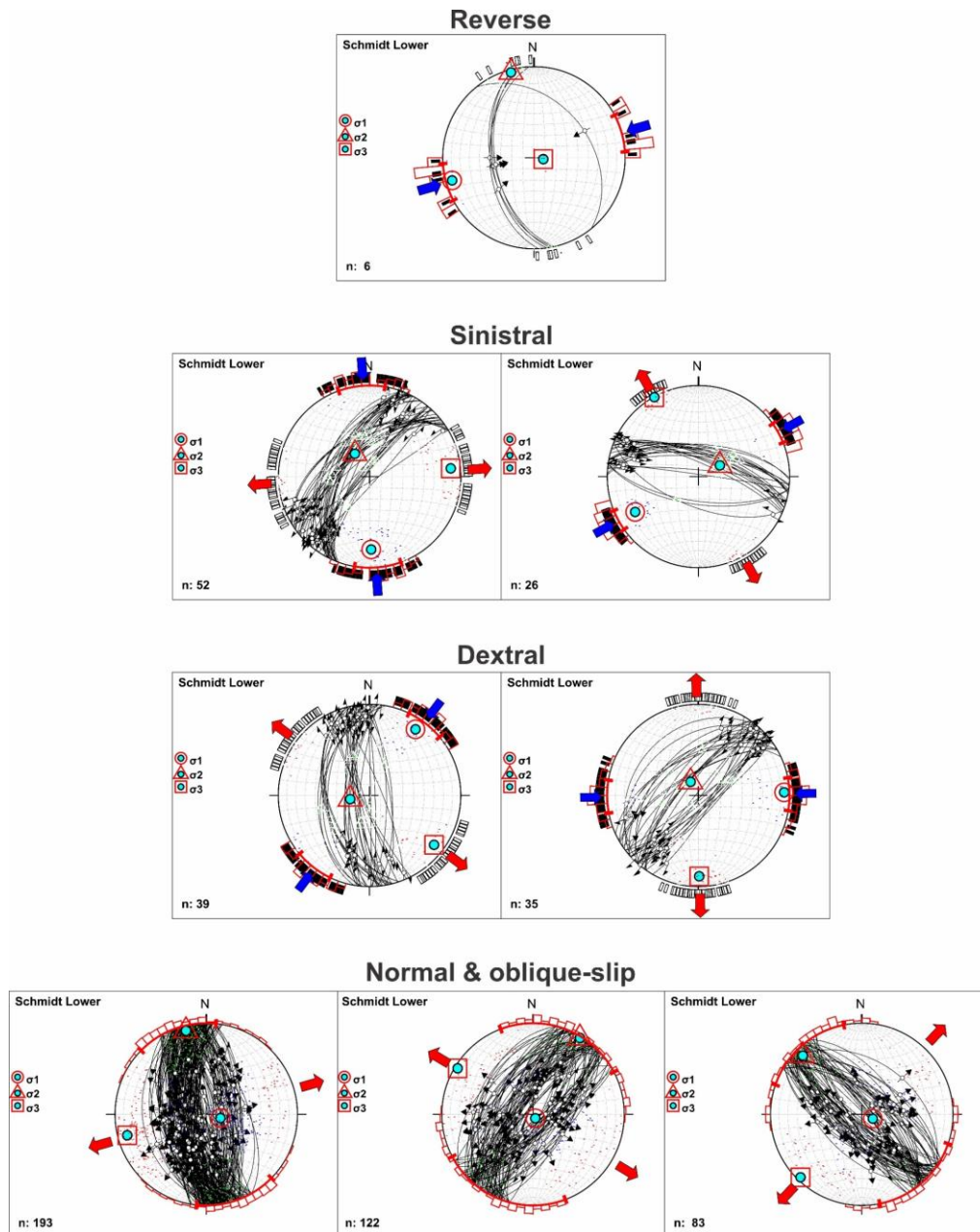
Kinematic analysis was performed for faults in which kinematic indicators had been recorded (slip directions). Fault systems were defined considering the orientation and movement of the structures. Reverse, strike-slip and normal oblique slip faults were recognized (Figure 7-10).

Reverse Faulting

Reverse faulting in the area, considered the earliest phase of deformation, is difficult to recognize due to missing subsequent reactivation events. In the Brasiles Zone, a reverse fault between marble and limestone was mapped,

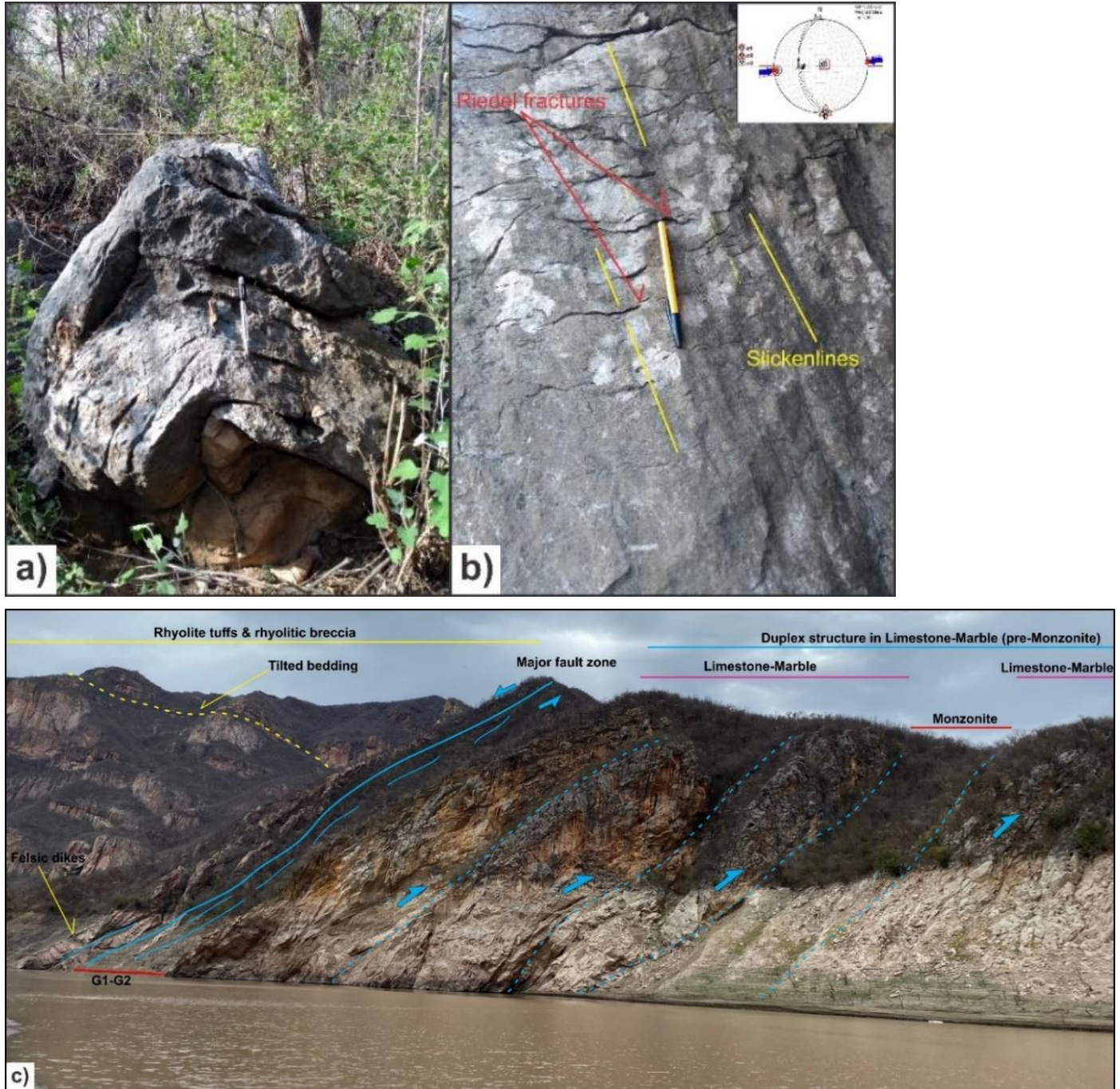
developing local drag folds. A duplex structure was interpreted in Limestones (LS) in the El Río Fuerte outcrops, postdated by MZ/QM intrusions and the younger extensional and strike-slip faulting that tilted the rhyolitic tuffs of the SMO (Figure 7-11). Additional data on reverse structures were measured in the North Zone on faults cutting the Atf unit.

Figure 7-10: Stereonets showing the main fault systems of the Santo Tomás area in terms of orientation and kinematics; note the paleo-stresses calculated for every stereogram



Source: Oroco, 2023.

Figure 7-11: Compressional structures identified in the Brasiles area: a) drag fold related to the reverse fault showed on “b”, b): reverse fault plane, c): view looking north of duplex type structure cropping out next to El Río Fuerte: view looking N. Felsic dikes emplaced on the fault zone



Source: Oroco, 2023.

Sinistral Strike-slip Faults

Sinistral faults occur in two main trends NNE-SSW and ESE-WNW trending (Figure 7-10).

- NNE-SSW trending set: These set dips to the NW (45° - 90°) and comprises transtensive and transpressive structures. These orientations match those of the main system of veins/veinlets of the Santo Tomás porphyry.
- ESE-WSW trending set: This set dips to the SSW. This set is subordinate to the NNE-SSW trend although it is represented by major fault-shear zones in Brasiles (surface and drill holes logging), North Zone (logging), and the South Zone (logging).

Dextral Strike-slip Faults

Dextral strike-slip faults are subdivided in two main systems, a dominant NNW-SSE trending set and secondary NNE to NE trending set.

- NNW-SSE trending set: This set is represented by low to high dips angles ($>25^{\circ}$ - 90°) to the WSW. Some major faults contain both strike-slip and normal oblique kinematics. NNW-SSE dextral faults were observed to cutting and displace mineralized structures in the Brasiles area (Figure 7-12).
- NNE to NE trending set: This set is represented by moderately to steeply dipping structures with angles usually $>50^{\circ}$ to both the NW and SE.

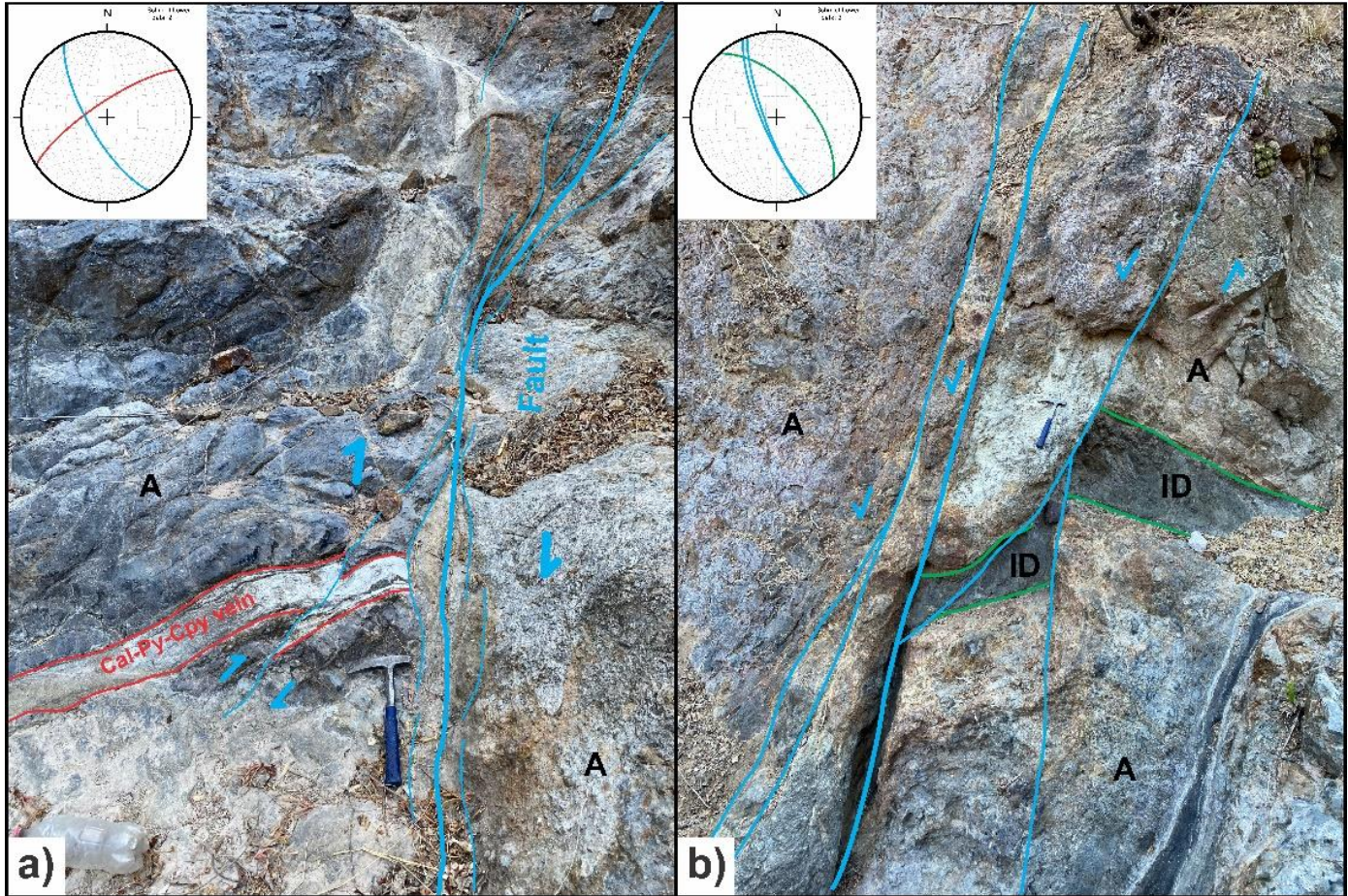
Normal Oblique-slip Faults

Extensional structures are the most common features of the area. Three fault systems, characterized by normal to oblique-slip kinematics were identified, trending NNW-SSE, NW-SE, and NE-SW:

- NNW-SSE trending set: These faults represent the dominant normal fault system in terms of data density. Faults (Figure 7-10) dip to the WSW and ENE. Normal and oblique-slip is usually associated with high angle fault planes (60° - 90°).
- NW-SE trending set: These faults dip to the SW and NE with angles between 50° and 90° .
- NE-SW trending set: This system has dips usually $>60^{\circ}$ to the NW and SE.

The NNW-SSE and NW-SE trending normal fault sets represent some of the youngest structures in the area. This is indicated by the emplacement of ID and FD along these features and by a NNW-SSE normal fault cutting an ID in the northern section of Brasiles Zone (Figure 7-12). A NE-SW directed extensional setting was likely associated with the development of both the NNW-SSE and NW-SE trending normal faults, synchronous with, and after dike emplacement.

Figure 7-12: a) Plan view of dextral fault cutting and displacing vein mineralized with calcite-pyrite-chalcopyrite. b) Section view looking NNE of normal fault cutting and displacing intermediate-mafic dike and andesitic rocks. ID: intermediate-mafic dike; A: andesite. The structures measured on the faults, contact and vein are plotted in the stereonet. The color of the lines in the stereonets represents the color of the structure on the image

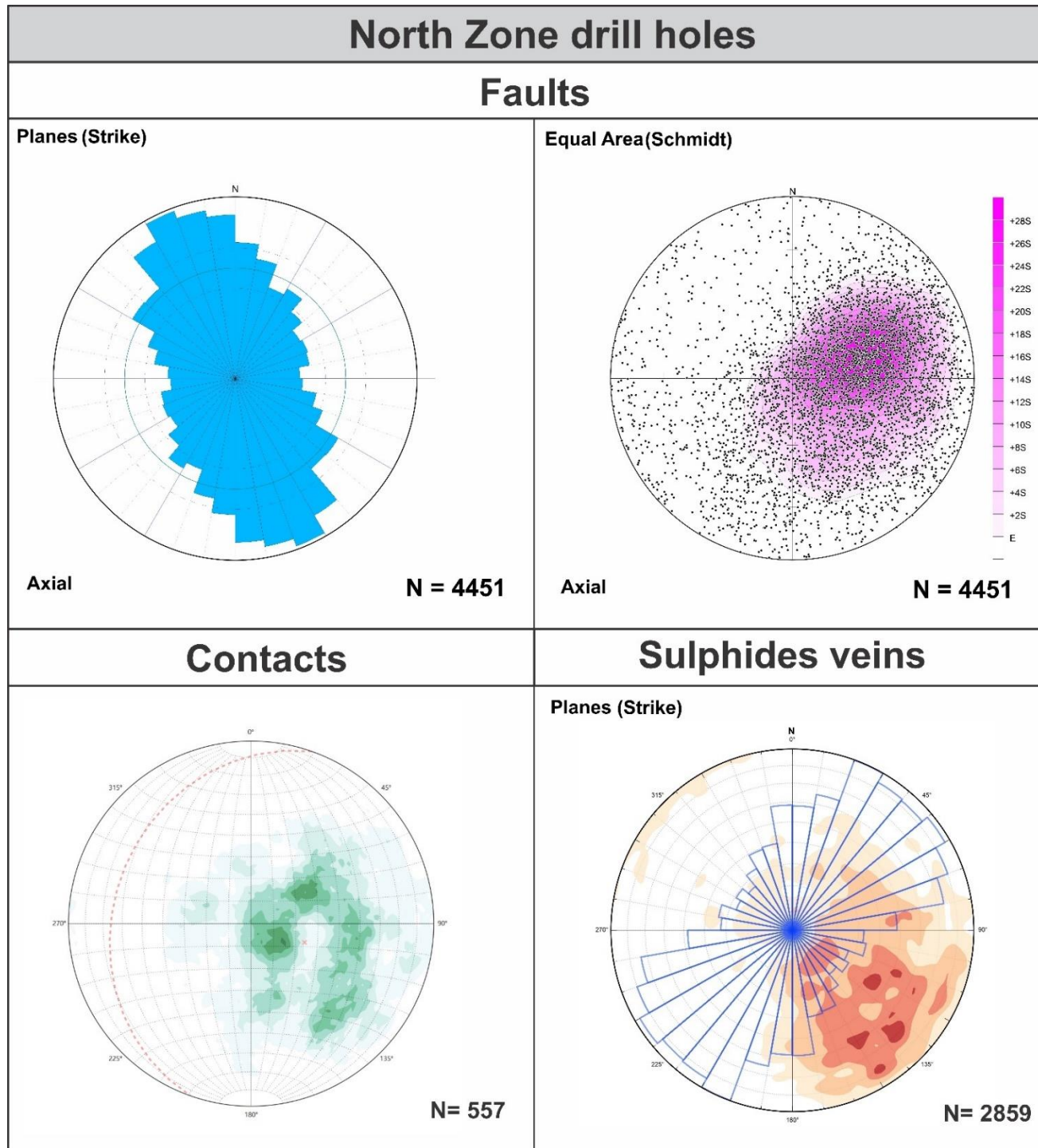


Source: Oroco, 2023.

7.2.5.2.2 Drill holes Structural Geology

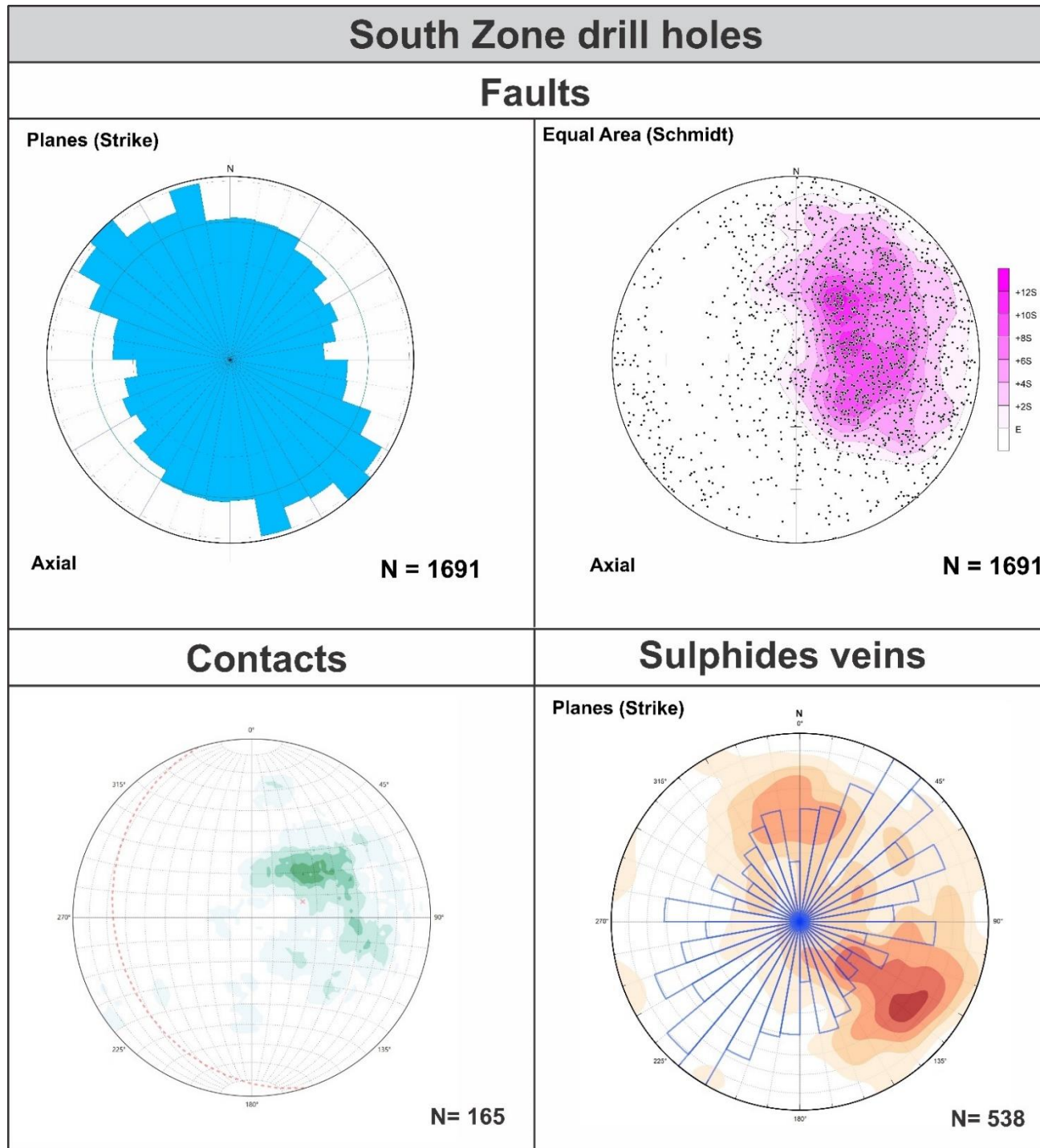
Structural logging generated a data base with 7412 oriented structural measurements, in North Zone, South Zone and Brasiles (Figure 7-13, Figure 7-14 and Figure 7-15) represented primarily by orientation of faults, contacts and mineralized veins.

Figure 7-13: Stereonets Calculated or the Oriented Structural Data Collected on Drill holes from North Zone



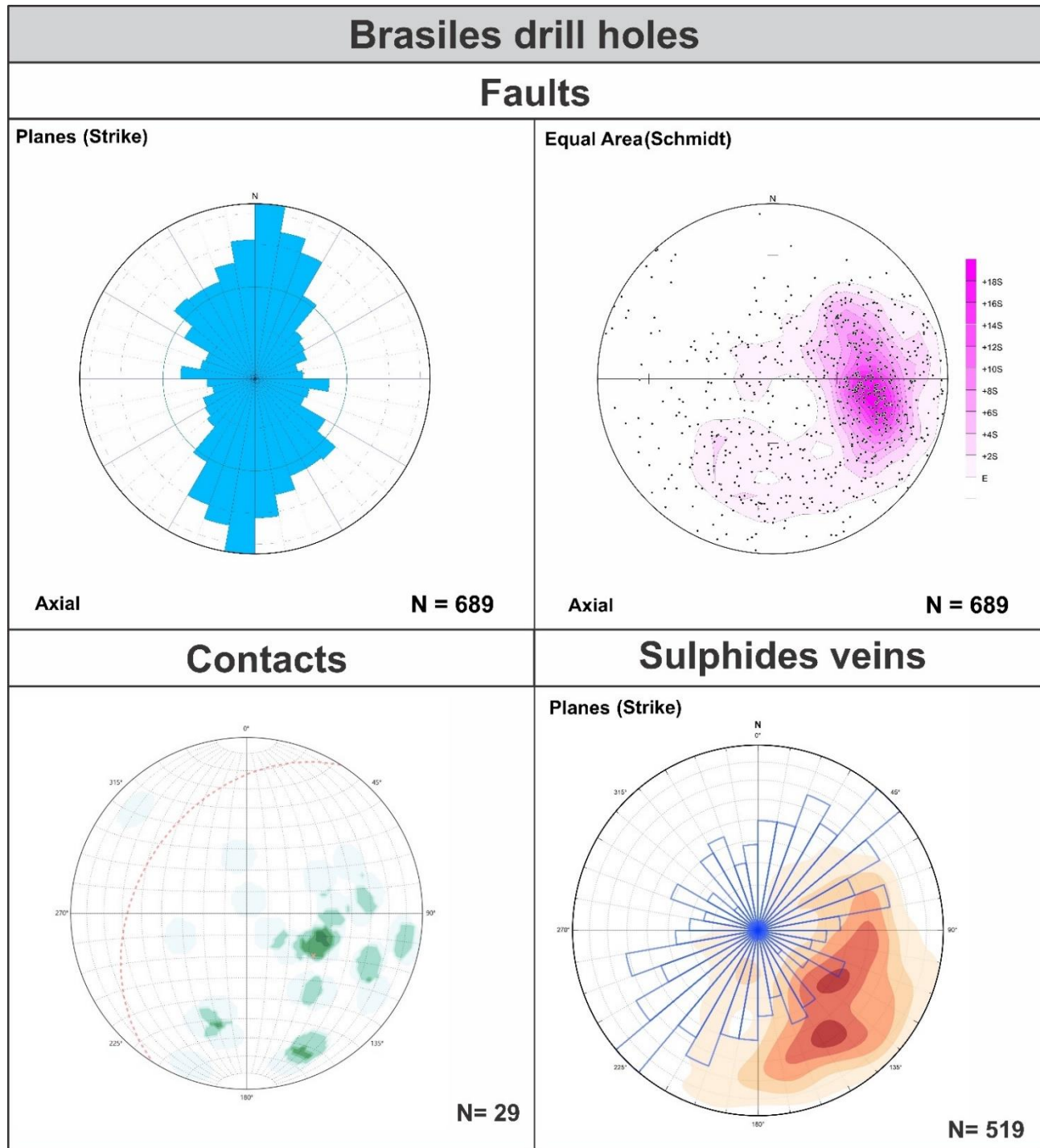
Source: Oroco, 2023.

Figure 7-14: Stereonets Calculated or the Oriented Structural Data Collected on Drill holes from South Zone



Source: Oroco, 2023.

Figure 7-15: Stereonets Calculated or the Oriented Structural Data Collected on Drill holes from Brasiles Prospect



Source: Oroco, 2023.

North Zone

Structural analysis of drill holes data from North Zone (Figure 7-13) indicates the following:

- The main fault system is represented by NNW-SSE trends with dips mainly to the WSW.
- Contacts dip at low to moderate angles to the W, with dispersion to the WNW and WSW.
- Mineralized veins are dominated by NE-SW to NNE-SSW trends dipping to the north westerly.

South Zone

- Fault data for the South Zone (Figure 7-14) is more dispersed in comparison to Brasiles and North Zone, with NW-SE and NNW-SSE trends and dips to the SW and WSW.
- Lithology contacts show a major NW-SE trend with SW dip-direction.
- Mineralized veins exhibit a high dispersion in terms of orientation, dip-direction, and inclination, although, two sets are prominent: i) the principal set corresponds to a NNE-SSW trend dipping to the WNW, ii) the secondary set is represented by an E-W trend dipping to the S.

Brasiles

Structural analysis for the data collected in Brasiles drill holes (Figure 7-15) shows a good correlation between fault data, lithological contacts and mineralized veins:

- The main fault system is NNE-SSW trending and dips mainly to the WNW.
- Measured contacts highlight a main group of structures with NNE-SSW trends (slightly more NE than the faults) with overall WNW dip-direction.
- Mineralization veins are dominated by NE-SW trends dipping to the NW.

Major structures

The major structures were defined using the surface structural data and lineament interpretation in combination with the structural logging database.

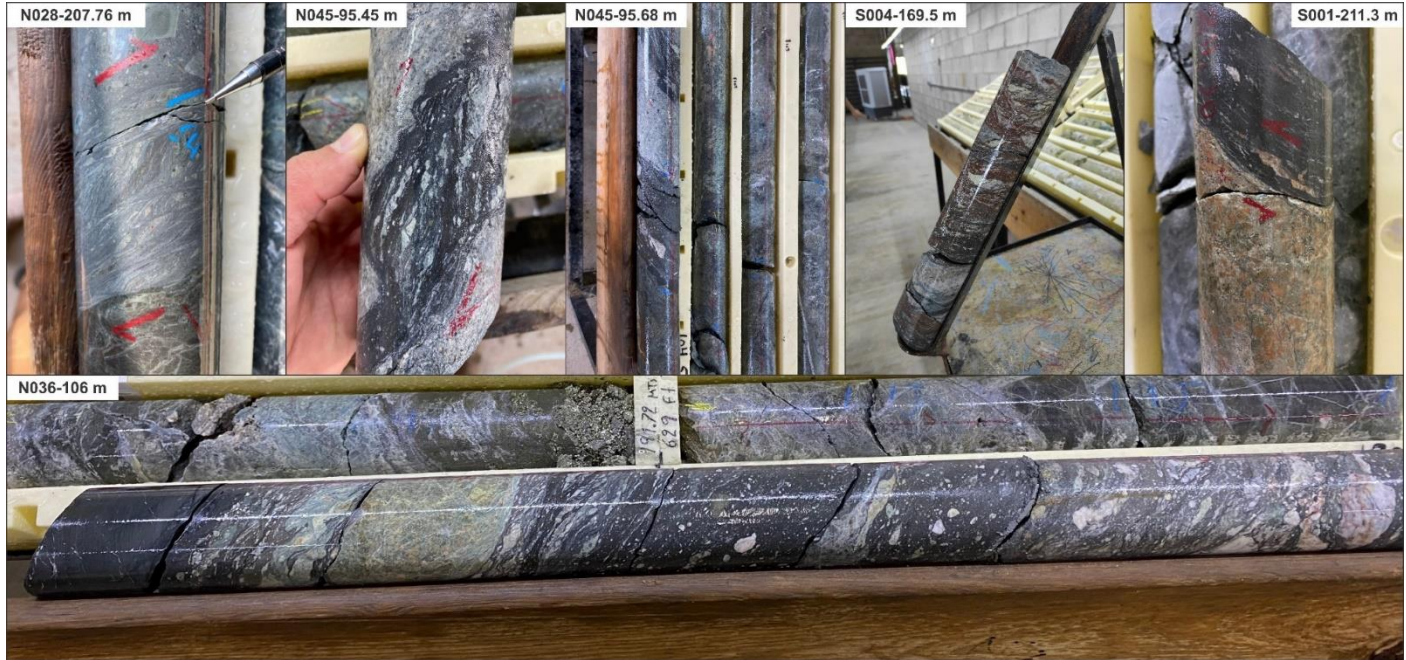
The dominant and primary fault system is characterized by brittle- ductile shear zones (usually up to 30 m wide) occasionally with development of mylonites (Figure 7-16). Logging confirmed that these structures occur mainly along lithological contacts that have been repeatedly reactivated under different stress fields, resulting in a complex kinematic history.

Faults identified with a significant influence on the geometry of the mineralization in the North Zone are indicated in the geological map (Figure 7-16) as F1, F2, F3 and F4.

- F1 is a sheared contact developed between the GD and Mesozoic cover. It marks the western limit of the mineralization. It has a NNW-SSE trend and ENE dip.
- F2 corresponds to the western fault usually intercepted at the base of the R-Rbx. It has a NNW-SSE trend and dips to the WSW.
- F3 is shear zone contact developed along the lower contact of LS. It has a NNE-SSW trend and dips to the WNW.

- F4 is represented by a shear zone in the footwall of the mineralization. It trends parallel to F3.

Figure 7-16: Core of major structures intercepted in different drill holes: all the structures correspond to shearing structures with development of cataclasites-mylonites under brittle-ductile deformation regime. SC-Type structures, rotated clasts, enlarged clasts and offsets are observed in the deformation zones. The code in the corner of every photograph indicates the drill hole number and the depth of intersection



Source: Oroco, 2023.

7.2.6 Mineralization

Santo Tomás is characterized by copper porphyry and skarn/replacement style mineralization linked to the Laramide Orogeny (80-40 Ma age). The Santo Tomás Cu (-Mo-Au-Ag) porphyry deposit lies mostly on the Property and is associated with a NNE-trending zone of quartz monzonite porphyry stocks and dikes (K-Ar age of 57.2 ± 1.2 Ma), hosted in strongly faulted and fractured Cretaceous meta- andesite and limestone. The deposits are similar in age, host rocks and mineralization styles to the Cananea deposits, in Sonora, and other Laramide-age deposits of the southwestern USA.

The Santo Tomás mineralogy comprises chalcopyrite, pyrite and molybdenite with minor bornite, covellite, and chalcocite. Sulphides occur as fracture fillings, veinlets, and fine disseminations together with potassium feldspar, quartz, calcite, chlorite, and locally, tourmaline. Minor copper oxides occur near the surface.

Chalcopyrite is the main copper mineral. It occurs with pyrite both as fine-grained disseminations throughout altered rock types and along with the central or marginal parts of microfractures that have been filled with quartz and potassium feldspar, and locally with black tourmaline crystals within the intrusive and adjacent andesite. The microfractures host mm to 2-3 mm thick quartz and potassium feldspar veins. The hairline fractures produce surfaces with scattered very fine sulphide grains that have the appearance of randomly disseminated grains. Some mm to 2-3 mm quartz-sulphide veins contain chlorite or magnetite.

The veining paragenesis and composition along with hydrothermal alteration are used as important vectors to mineralization. Potassic and Phyllic (QSP) alteration is one of the most common assemblages, and substantial zones of mineralization are closely related to extant “white micas” and the density of A & B-type veins characterized by chalcopyrite-molybdenite (minor bornite). Veins up to 2.5cm, also characterize higher-grade zones of mineralization.

B-type veinlets are the most common and important micro-structures in Santo Tomás for Cu-Mo mineralization. Main features:

- Hosted by Quartz monzonite and Andesite.
- Proximal: Vein quartz-chalcopyrite, fine molybdenite at border, suture, with Kspar -illite halo.
- Distal: Vein quartz- with molybdenite-cpy-py, with illite halo (green sericite?)
- Often visible suture of fine molybdenite and grains of chalcopyrite.
- The width goes from mm to cm, as well as twinned veins.

Most of the PCD veins show a strong structural control, clearly indicating a right-lateral component. Resulting in larger veins with multiples appendices that favorize the efficiency to precipitate the sulphides.

Strong structural control provided a very efficient mechanism for precipitating the metal content of mineralized hydrothermal magmatic fluid. Locally layered/laminated veins with accumulation of fine sulphides layers. Such texture testifies a crack-n-seal texture, testify a dynamic environment with multiple re-opening of the same fracturation system, filled by the same hydrothermal source. In central zone, these layered veins system with fine chalcopyrite dissemination were observed at 25m from a skarn zone, close to the contact between the strongly chloritized monzonite and the limestone.

The mineralization is hosted mainly by Laramide-age quartz monzonite intrusions and strongly fractured and faulted Mesozoic-age andesitic volcanic rock. Both sets of Early-Stage faulting and fracturing act as a host for the dikes. Screens of andesite between dikes are strongly hornfelsed.

The quartz monzonite dikes, and screens of andesite can be mapped together as a definable Early-Stage fracture zone unit (Property Map unit, Mx) comprised of sheeted quartz monzonite dikes, and screens of highly fractured, hornfelsed andesite, and lesser limestone. Related sulphides occur as disseminations, in fractures, and in quartz veinlets.

The Santo Tomás deposit is exposed in discontinuous outcrops along a 5 km strike length. The mineralization is continuous though there is a lower grade area that splits the south of the river mineralization into the North and South Zones. South of the Río Fuerte, Mineralization that lies on the eastern flank of the prominent N-S ridge is referred to herein as the “North Zone.” To the south, similar mineralization on the west flank of the Santo Tomás ridge is termed the South Zone.” In the North Zone, the mineralized zone dips westward from the eastern flank exposures on the ridge. In the South Zone, the mineralized zone dips sub-parallel to the western flank erosional surface of the Santo Tomás ridge. The mineralized zone lying north of Río Fuerte is termed the Brasiles Zone.

The main mineralized zone varies in thickness between approximately 100 to 400 m (locally 600 m) in true thickness and dips moderately to the west at 50° in the North Zone. Similar moderate angle dips are apparent in the southerly portion of the South Zone where mineralization dips sub-parallel, or slightly steeper than, the west-facing slope of the Santo Tomás ridge. Interpretation of the moderate westerly dip of the mineralized zone is complicated by stepwise down-dropping of the mineralized zone along the west side of both the North and South Zones, due to the influence of late faulting of the Western Fault zone.

The deposit only partly crops out at the surface. The deposit is formed beneath a blanket of Cretaceous limestone beds and later covered by young felsic volcanic rocks. These rock formations conceal much of the strike length of the deposit on the Property. The main area of surface exposure is in the North Zone on the east flank of the prominent ridge of 500 to 700 m relief, above the Río Fuerte.

7.2.7 Geological Chronology and Controls to Mineralization

Understanding the distribution of economic copper sulphide mineralization in the Santo Tomás deposit requires consideration of the chronological sequence of the mineralization events and their structural controls on the Property.

Successful geological modeling of the Santo Tomás deposit requires a resolution of the early Laramide-age intrusive and mineralizing events and their displacement across later, post-mineralization faults.

The chronological sequence of the Santo Tomás mineralized zone is broadly described as follows, from the oldest events to the youngest.

7.2.8 Guerrero Terrane – Jurassic – Cretaceous Arc Volcanics, Intrusions, and Sediments

- Jurassic-Cretaceous volcanic and sedimentary strata of the Guerrero terrane are weakly deformed and gently tilted to the west-northwest. Map Units andesite (A), andesite tuff (Atf) and limestone (LS) are the most common in the local bedrock.
- Cretaceous intrusions of the Sonoran Batholith invaded the Guerrero sequence and are coeval with the arc-related volcanic strata. Map Unit and KsGd belongs to this association.

7.2.9 Laramide Orogeny – Late Cretaceous to Paleocene (80 to 55 Ma)

Laramide orogenic movement is marked by oblique subduction, transpression, and intrusion that is distinctly younger and separate from the Guerrero volcano-sedimentary arc terrane and the formation of the Sonoran Batholith. Laramide deformation in the Tasajeras map sheet area is dominantly brittle faulting and fracturing.

- Laramide wrench-faulting: Laramide faulting in the Tasajera map sheet is oriented North and Northeasterly, and dips are moderately westward. Age of the wrench faulting is indicated by the Laramide-age of intrusions emplaced syn- and post-fault movement.
- Displacement of Limestone Marker Beds: At Santo Tomás, the wrench faulting imparted significant normal dip-slip and oblique-slip displacements, marked by relative movements on thick beds of Cretaceous limestone in the South, North and Brasiles Zones. Individual blocks of limestone drop- down, stepwise on the west side of NNE-trending faults, and down on the north side of NE and ENE trending cross-faults. Large displacements are seen across the Western Fault.
- Early-Stage ~N-S to NNE Faulting: Structural mapping demonstrated that the Laramide brittle deformation of the Santo Tomás is marked by early N-S to NNE-trending faults and fracture sets. Branching and somewhat younger fault sets are more northeasterly striking. A system of av. E-W faults with sinistral kinematics was recognized, which could represent the conjugated structures, coeval to the NNE dextral faults: this is mainly appreciated in the South Zone where a system of veins striking ~E-W was identified.

- **Laramide Quartz Monzonite Intrusions:** Laramide intrusions at Santo Tomás are mostly branching, sub-parallel dikes of quartz monzonite. Host pathways for the dikes include both sets of Early-Stage faulting and fracturing. Screens of andesite between dikes are strongly hornfelsed. At Santo Tomás, the drill hole spacing does not allow confident correlation of individual sub-parallel dikes. However, taken together, the dikes and screens can be mapped as a definable Early-Stage fracture zone unit (Property Map unit, Mx) comprised of sheeted quartz monzonite dikes, and screens of highly fractured, hornfelsed andesite and lesser limestone. Related sulphides occur in disseminations, fractures and quartz veinlets.
- **Cu-Mo-Au-Ag Porphyry Mineralization:** After the displacement of limestone, coeval quartz monzonite intrusion, hydrothermal brecciation, veining, stockworks, and sulphide mineralization were emplaced in linear zones along and within the early-stage wrench-fault systems, tension fractures, and hybrid shear-extension structures striking overall NE-SW. The Santo Tomás mineralized zones (Te(?)MZ/QM) yield age determinations of Laramide-age, common with Bahuerachi and La Reforma deposits.
- **Related Alteration:** Widespread propylitic alteration in andesite is common. In the core of the mineralized zone at Santo Tomás is an early K-feldspar alteration. Later phyllic alteration is partially developed. The strong structural overprint and its likely control on fluids preclude the development of classic porphyry alteration halos found in other districts.

Santo Tomás fault system is interpreted to represent a regional-scale, anastomosing fault zone with inferred Laramide-age dextral displacement and likely a long-lived fault mesh with several episodes of movement. The NE faults are interpreted as normal-motion flower structure faults linking to a master-fault structure. The interpreted translational and tensional zone is the zone of weakness responsible for hosting intrusive bodies of Laramide quartz monzonite intrusions and related sulphide mineralization.

7.2.10 Pre-Basin and Range – SMO Volcanic Province Faulting

Prominent across all the geology maps of the NW México, including the Tasajeras map sheet, are late NW- trending lineaments and faults. Locally, the structural province is termed the Choix Graben and Horst province. The onset of the extensional basin and range event was marked by rhyolite tuff and ignimbrite (TomTR-Ig) of the SMO Volcanic Province and related sub-volcanic intrusions (ID and FD). The chronology of the onset of SMO formation likely predates the formation of the SW USA / NW México Basin and Range tectonism but shares a similar geometry.

At Santo Tomás the field structural data and observations document a reactivation of the N~S dextral system as normal and oblique faults, also appreciated along NW-SE striking structures, although sinistral faults are present as well. A NNW fault and fracture set with a prominent N20°W trend that cuts the Early-Stage faulting and fracturing. Data is sparse, but a cluster of orientations of approximately 140-180°/35- 60°W characterize the set. NW to NNW faulting was triggered by a NE to E-W extension, that also yielded the reactivation of the NE structures as transfer faults.

- **Brasiles:** The data in the Brasiles Zone shows little of the late, NW brittle deformation, except for a fault zone that crops out on the north bank of the Río Fuerte that is invaded by rhyolite dikes (TmR, RD). The fault defines the western extremity of the Brasiles limestone and places that limestone in fault contact with SMO Volcanic strata (TomTR-Ig). That fault is provisionally correlated with the Western Fault 2 of the South and North Zones.
- **SMO Volcanic Strata & Related Intrusions:** Andesite and rhyolite (TmR, FD) form dikes and small stocks, aligned with the NW fault and fracture set but also following some older NNE fault sets. The NW fault set is also seen displacing the overlying ignimbrite and felsic volcanic strata (TomTR-Ig) in the North Zone and the western side of Brasiles.

No other significant easterly faults are observed.

8 DEPOSIT TYPES

The Santo Tomás exploration programs have primarily focused on Cu-Mo-Au-Ag porphyry deposit types. Herein, exploration recommendations continue with this deposit-type target.

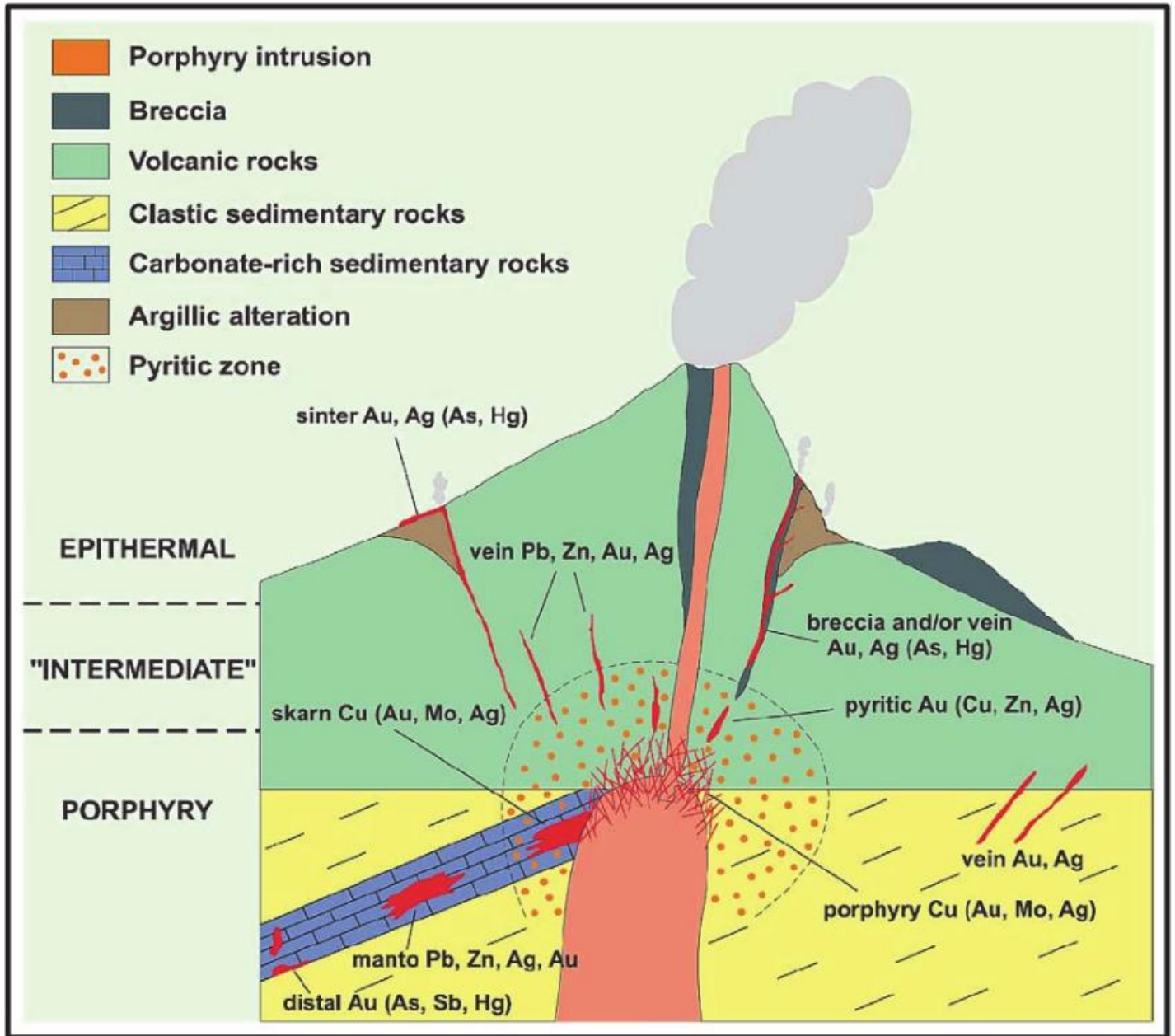
8.1 Porphyry Deposits

Porphyry deposits are large, low- to medium-grade deposits in which primary (hypogene) minerals are dominantly structurally controlled and which are spatially and genetically related to felsic to intermediate porphyritic intrusions (Sinclair, 1996). The generalized geological setting of porphyry-related deposits is shown in Figure 8-1. The large size and structural control exhibited by veins, vein sets, stockworks, fractures, 'crackled zones' and associated hydrothermal breccias serve to distinguish porphyry deposits from a variety of deposits that may be peripherally associated, including skarns, high-temperature mantos, breccia pipes, peripheral mesothermal veins, and epithermal precious metal deposits.

Lowell and Guilbert (1970) proposed a relatively simple model characterized by lateral and vertical zoning of the primary and alteration mineralogy, which is centered on an intrusive body characterized by a porphyritic texture. Sillitoe (1973) proposed that the mineralizing porphyries are calc-alkaline stocks emplaced at depths of 1.5–3 km in the crust, which grade downward to stockwork mineralization and potassic alteration zones in a larger equigranular intrusive.

In general, the longevity and dynamism of the hydrothermal activity, as well as the presence of favorable physical-chemical conditions in the fluid-rock relation, are important factors for producing economic deposits (e.g., Clark, 1993). Along with these factors, the repetition and superimposition of the mineralizing events in a system produce a progressive enrichment of the deposit, which is particularly important for the concentrations of copper (Gustafson et al., 2001). Evidence includes multiple stages of vein- and fractured- controlled mineralization, and the overprinting of alteration assemblages.

Figure 8-1: Schematic Diagram of a Porphyry Cu System from Sinclair (2007)



Source: Sinclair, 2007. Note: Porphyry Cu system in the root zone of an andesitic stratovolcano showing mineral zonation and possible relationship to skarn, manto, "mesothermal" or "intermediate" precious- metal and base-metal vein and replacement, and epithermal precious- metal deposits.

8.2 Laramide-Age Porphyry Deposits of NW México

Most of the known porphyry copper deposits in México lie along a 1,500 km-long, NW trending belt sub-parallel to the western coast of México (Hammarstrom et al., 2010). This belt extends from the US border through the states of Sonora (the Cananea and La Caridad deposits), western Chihuahua, Sinaloa, Michoacán (the Inguarán deposit), and Guerrero. The deposit at Cananea (>20 Mt contained copper) in Sonora is among the 15 largest porphyry copper deposits in the world. These deposits are part of a globally important belt of porphyry copper deposits in the southwestern United States and México that is Laramide (80 to 40 Ma) in age. This information is not necessarily indicative of mineralization on the Property that is the subject of this technical report.

Deposits and intrusions of the Laramide orogeny in NW México are shown in Figure 8-2.

These Laramide-age deposits formed in a continental arc tectonic setting related to the subduction of the Farallon Plate beneath the North American Craton. Laramide igneous rocks in the western part of the Cordillera arc (within 500 km of the paleo-trench) are calc-alkalic, whereas the igneous rocks farther inland (700 to 1,000 km) tend to be alkalic (Damon et al., 1983).

The Laramide porphyry copper deposits of southwestern US and northern México are one of the great concentrations of porphyry deposits, rivaling the Tertiary age deposits in the southern Andes or the Philippines. The Laramide porphyry copper belt is interpreted as being a result of an Andean-type arc that evolved as high-angle subduction of the Farallon oceanic plate under the North American continental block. The angle of subduction flattened at the end of the Cretaceous, possibly due to an increase in the rate of plate convergence (Valencia-Moreno et al., 2007).

The porphyry copper systems of México, including some associated skarn and hydrothermal breccia pipe deposits, occur along a NNW-SSE-oriented belt exposed along most of the western side of the country. Approximately 60 deposits are recognized in this belt, approximately 70% of which occur in northwestern México, particularly in the states of Sonora and Sinaloa.

The porphyry copper deposits of México can be classified in two main geographic groups (Valencia-Moreno et al., 2007).

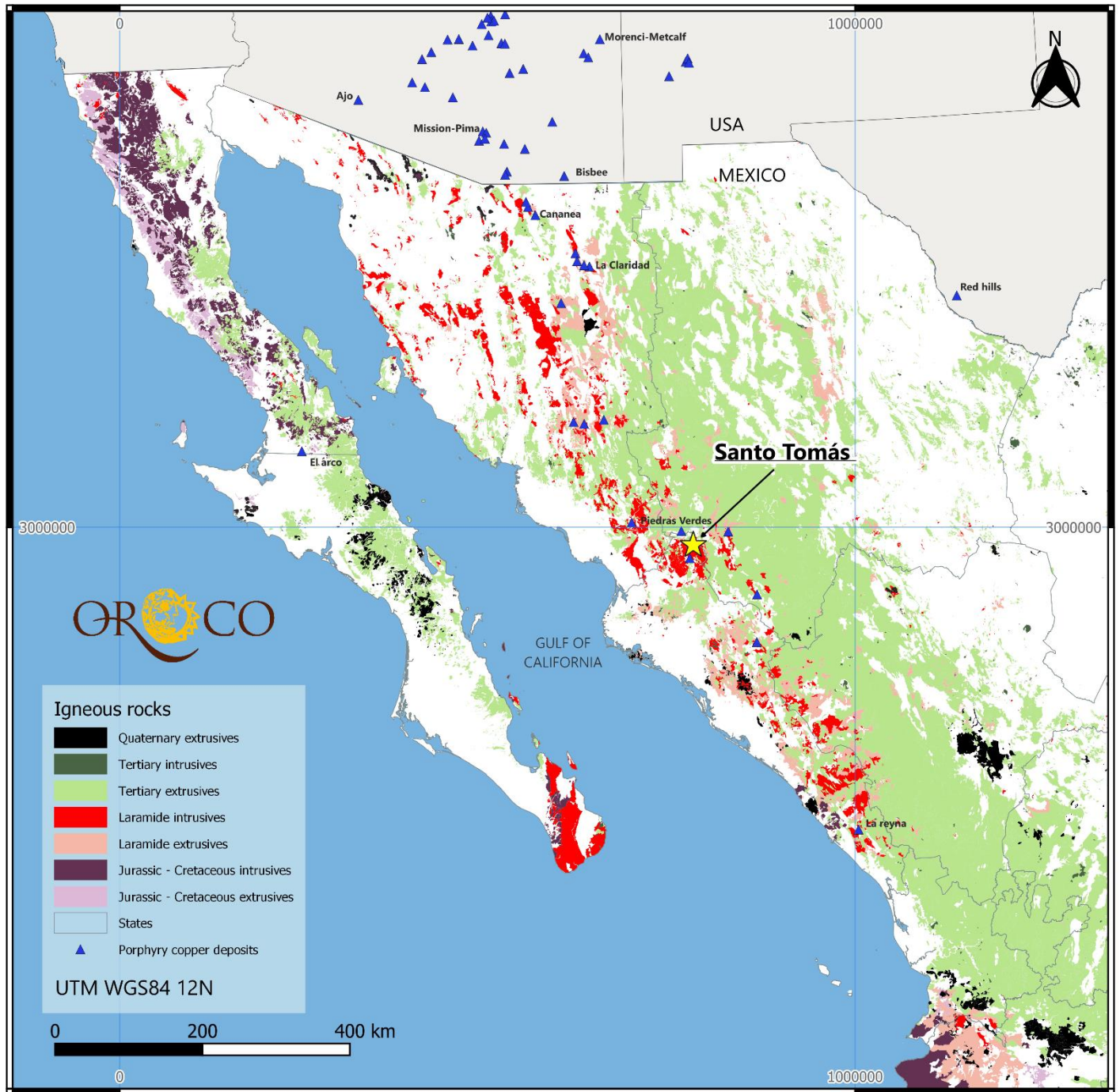
1. A first group, which comprised the northern and central domains and was developed under the significant influence of old continental crust, is characterized by Cu-Mo-W deposits and includes the world-class deposits of Cananea and La Caridad.
2. The second group comprises the southern domain of the belt and exhibits clear genetic relations with a relatively young oceanic basement. It is dominated by Cu-Au mineralization and has a significant number of deposits, but most are relatively small for the size commonly observed for this type of mineralized deposit system. Two exceptions are the large El Arco deposit in Baja California and Santo Tomás at the junction of Sonora, Sinaloa, and Chihuahua.

The intrusive rocks related to porphyry copper deposits include granite, quartz monzonite, monzonite, granodiorite, tonalite, and diorite for the general porphyry copper deposit model, and syenite in addition to the preceding rock types for the Cu-Au porphyry copper deposit subtype.

There are many general classifications of porphyry copper systems, but the Laramide deposits can be grouped into three main categories: a) those dominated by a stock or batholithic intrusive body, b) those dominated by a structurally controlled intrusive body within a structural domain and c) and those dominated by hydrothermal breccias.

The model described by Lowell and Guilbert (1970) was developed to apply mainly to the stock or batholithic type, with or without hydrothermal breccias. The Laramide deposits are commonly characterized by extensive zones of potassic, phyllic, propylitic, and argillic hydrothermal alteration, associated with subvolcanic stocks of monzonitic to quartz-dioritic compositions. The mineralization mainly occurs as stockwork zones or is disseminated, especially when hosted in Laramide volcanic rocks of intermediate composition, as well as in the subvolcanic plutons themselves. The porphyry copper deposits can be described as zones of copper and molybdenum sulphides occurring as disseminations and stockworks of veinlet sulphides emplaced in various host rocks that have been altered by hydrothermal solutions into concentric zonal patterns when the mineralizing system is dominated by a stock or batholithic intrusion.

Figure 8-2: Late Cretaceous to Early Tertiary “Laramide” intrusion-related deposits of Northwestern México



Source: Modified of United States Geological Services. (2010). Porphyry Copper Assessment of México. Reston, VA: US Geological Survey.

In contrast, most of the porphyry copper deposits in the western part of the Sierra Madre Occidental (in Sonora and Sinaloa) were emplaced in structurally controlled, highly fractured rocks during the Paleocene to Eocene (Ferrari et al., 2007). Hydrothermal breccias are important components of the Mexican deposits and, in some cases; copper mineralization is restricted to breccias (Sillitoe, 1976). Barton et al. (1995) noted the association of porphyry copper deposits with breccia pipes as well as with numerous small copper skarns in the states of Sonora, Guerrero, and Michoacán.

9 EXPLORATION

Historical exploration programs are described in the History section of this report. Since 2019, Oroco has conducted an exploration program of remote sensing and airborne and ground geophysical surveys in preparation for a resource drilling campaign at North and South Zones. A small exploration drilling initiative was campaigned at Brasiles. In the course of Phase 1 drilling, from mid-2021 through early 2023, geology mapping has been selectively campaigned in key areas of the project.

The location of each major contracted remote sensing and geophysical survey is displayed in Figure 9-1, including the outline of a vegetation study undertaken in support of site permitting.

9.1 Remote Sensing

In preparation for field work Oroco commissioned an airborne LiDAR survey to update and improve the resolution, accuracy and precision of the existing 2017 project digital elevation model and orthophotography record. The earlier satellite-derived dataset was based upon Synthetic Aperture Radar (SAR) data acquired for Oroco by Auracle Geospatial Science, Inc. and MacDonald, Dettwiler and Associates Ltd. using the RADARSAT-2 acquisition platform (Bridge 2020).

9.1.1 2021 LiDAR Survey

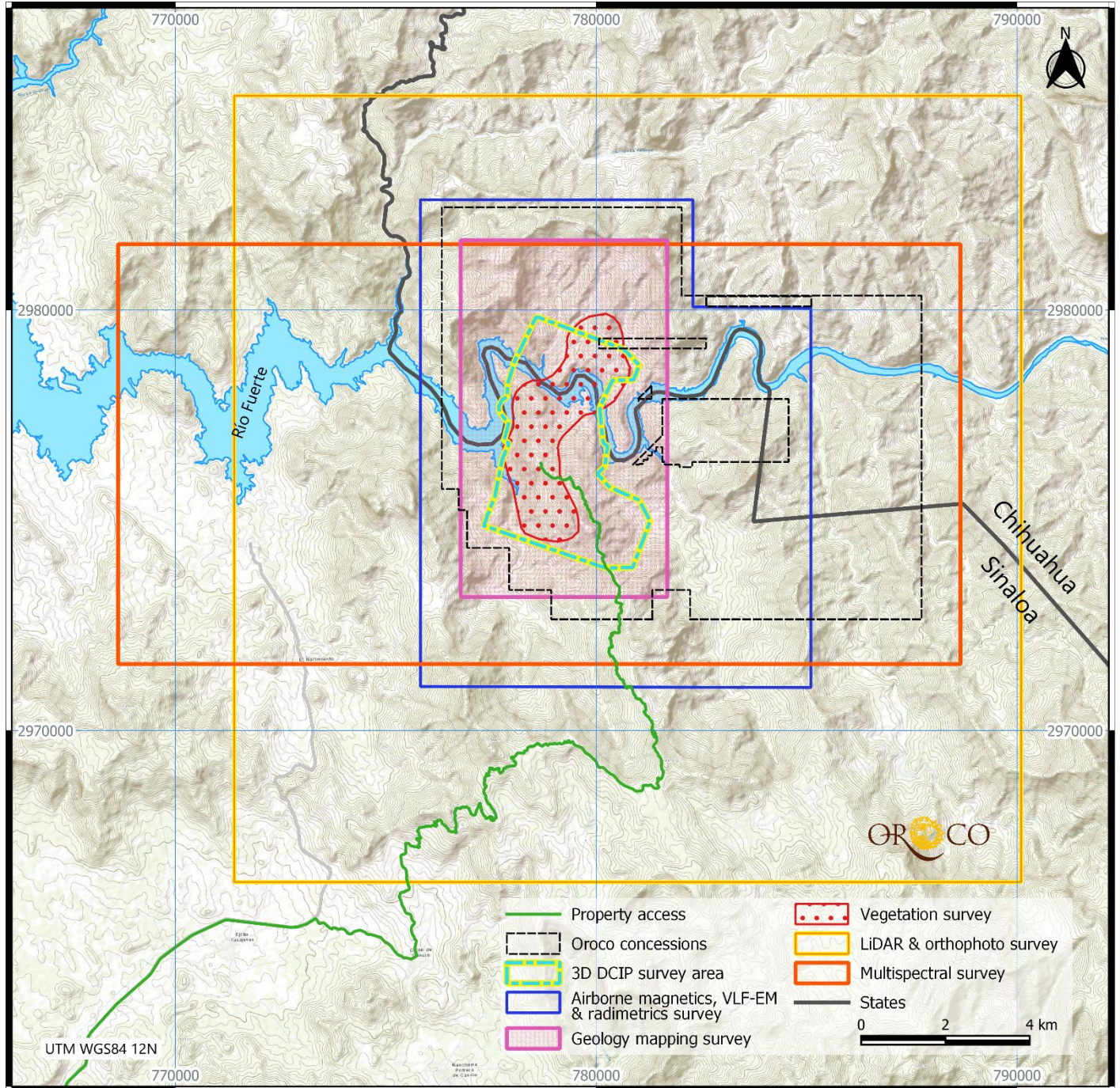
Eagle Mapping Ltd., ('Eagle') of Langley, BC, Canada, was contracted by Oroco to fly a 342 km² airborne LiDAR survey over the Project during the April dry season of 2021 to minimize foliage interference for both laser ranging and visible spectrum data acquisition of ground surface features. The survey was flown at 1,600 m AGL on April 6th and 7th, 2021, using a Riegl VQ780II LiDAR unit and a PhaseOne iXM-150F camera, to produce 10 pulse / m² LiDAR density and 20 cm pixel photo imagery (Eagle Mapping, 2021). The survey was not co-ordinated from ground markers, with navigation and positioning based upon an Applanix POS AV610 (IMU 57) coupled INS-GNSS, processed using POSpac MMS v8.6 software.

Post delivery of the LiDAR survey, ground-based DGPS surveys of features that were clearly visible in the processed, tiled LiDAR product confirmed that at seven (7) points the DGPS coordinates agreed to within 30cm (range 11 to 29 cm) in the X-Y plane and to within 25cm (Z).

The LiDAR data was delivered to Oroco in LAS (.las) point cloud format, with 1,000 m project tiles of ASCII (.txt) DEM, band tone and 1m contour Shape (.shp) files, and Hillshade and Orthophoto GeoTiff (.tif) files in EPSG 6367 map projection (UTM 12N, ITRF08 epoch 2010.0 horizontal datum, NAVD88 vertical datum, on the GGM10 geoid). In all 400 tiles of up to 1 km² were generated and delivered to Oroco by Eagle.

Oroco has used the products of the LiDAR survey to comprise the master DEM / DTM for the Project, where it has been used in the Project GIS and other technical software platforms, including the 3D Leapfrog (Edge/Geo) instances of the Project that are used for the modeling of drilling information and surface mapping in support of the resource work. The LiDAR products have also been used with the site standard DGPS applications to corroborate the spatial locations of *inter alia* DGPS injection and recording stations, sample sites, roads, drill pads and drill hole collars. The Company has also used the LiDAR to search for evidence of disturbance to locate overgrown roads, former drill sites, remnants of old farm walls and the like.

Figure 9-1: Location outlines for the project LiDAR, airborne magnetics (plus radiometrics and VLF-EM), ground 3D DCIP survey, geological mapping and vegetation survey coverage



Source: Oroco, 2023.

The LiDAR survey raw data, and certain Oroco generated map products, have been filed (by Eagle and Oroco respectively) with the Mexican Government Geoinformatics branch, for reference by government agencies. The SEMARNAT and CONAGUA (Environment and Water Affairs agencies) have both made reference to the LiDAR-derived shaded topographic maps in consultation with Oroco.

The Company has generated a number of topographic map bases, including themed slope and elevation maps for internal use. The DEM / DTM and contour products are presently being used for engineering and site design purposes by Ausenco and Mining Plus in their PEA work efforts.

The Project has in general replaced the prior 2019 project 'AW3D Enhanced DTM' referenced in Bridge (2020), except in some online applications where the lower resolution of the historical product allows for faster viewing.

9.1.2 Satellite Multispectral Review

During the course of late 2021 and 2022, Rodrigo Díaz Martínez of Díaz Remote Sensing Geology ('Díaz') commenced a satellite multispectral data compilation of NW México and the project area for Oroco, with a view to evaluating structural and alteration features detectible using the various sensors deployed on orbital satellite platforms. Though the project was started, it has not advanced past early evaluation owing to the ill-health of Mr Díaz Martínez, Díaz' principle technical service professional. Alternative services may be contracted for this work.

9.2 Geophysical Surveys

Oroco has focused its geophysical data collection on an airborne survey for project magnetometry (with surface radiometric emission sensors and VLF-EM transmissions receivers), and a targeted (area-constrained) ground-based electrical 3D DCIP survey.

The selection of methods targets geophysical products that can specifically assist with broad geological definition of lithologies (passive magnetics and radiometric measurements, especially of potassium ('K')), major geological structures (VLF and resistivity contrasts) and targeting of metal-sulphide mineralized units (chargeability). Secondary alteration may also be evidenced in electrical data sets (resistivity) and in alteration forming secondary magnetic iron oxides (magnetics, magnetic remanence effects).

9.2.1 Airborne Magnetics Survey

Oroco contracted Terraquest Ltd of Markham, ON, Canada ('Terraquest') to fly a Helicopter-borne High-Resolution Aeromagnetic, Radiometric, Matrix VLF-EM/Resistivity Survey over the Santo Tomás Project. The project was flown between February 20th - 27th, 2021 with the Bell 206 L4 Long Ranger helicopter, owned and operated by Heliservicios Internacionales. The helicopter was based at the then in-construction El Ranchito Core Storage facility for the duration of the survey.

The survey comprised of approximately 2,022-line km of traverse line flying at a line spacing of 50 m by 500 m tie-line flying totaling approximately 252 km where the 233 traverse lines were flown on Azimuth 090°/270° and the 19 tie lines on Azimuth 000°/180° (nominal, true), for approximately 2,231-line km of data collected. Some traverse lines were locally double flown to correct for excessive terrain clearance on some lines in very steep sections of the survey (Figure 9-2).

The primary airborne geophysical equipment included one high sensitivity cesium vapor magnetometer (Scintrex CS-3 Cesium Vapor), a gamma ray spectrometer system (Radiation Solutions: RS-500 Advanced Digital Spectrometer Gamma

Ray Detector Pack and Radiation Solutions RSX-4 1024 in3 (16.8 liters)) and a proprietary Matrix VLF-EM (Terraquest Ltd: Matrix Digital VLF-EM) system. Ancillary support equipment included a tri-axial fluxgate magnetometer (Billingsley: TFM100-LN), data acquisition system, radar altimeter, barometric altimeter, GPS receiver with a real-time correction service, and a navigation system.

Oroco received WGS 84, UTM Zone 12N projected final data and maps to be delivered in Geosoft™ database (.gdb) and grid (.grd) formats with PDF / PNG images of all printed map products. Additionally, geophysical data and associated vector overlays (flight path, contours, etc) were delivered in GeoTiff (geo-referenced .tif) image format. Products included Total Magnetic Intensity ('TMI'), Vertical Magnetic Gradient (calculated vertical derivative of the TMI), Total Count, K, Th, U & Ternary radiometric data, and a Digital Terrain Model derived from GPS and radar altimeter data. The data were provided as an Archive Data Set, delivered on DVD, including all map products and a database of all measured and calculated data in a Geosoft format. An Operations Report (Dias Geophysical Limited, 2021) was also delivered on the DVD.

Oroco has used the magnetics data maps to assist with surface mapping and to help define surface expressions of the major magnetically distinct lithologies. VLF-EM structural lineament maps supplied by Terraquest have also been considered with other evidence of apparent structural discontinuities in the evaluation of evidence for major faults or structural fabric features on the project property. The potassium radiometrics locally reflect potassic alteration and monzonitic intrusive rock outcrop as these rocks contain potassium feldspars.

The Terraquest survey suffered from some local deviation from the terrain clearance specifications defined for the survey. In general, the instances of out-of-spec terrain clearance occurred distal from the central area of the project where work is focused on the occurrence of mineralization. However, a desire to build an inversion model based on magnetic susceptibility required some post processing and inversion modeling, discussed following.

9.2.1.1 Inversion of the Magnetic Survey and Review of VLF-EM

Oroco retained the services of Condor Consulting, Inc of Lakewood, Colorado, USA ('Condor') to assist with some flight line clearance corrections and build a magnetic susceptibility inversion model to help interpret the airborne magnetic data over and surrounding the Santo Tomás project and so to assist in exploration and targeting of porphyry Cu mineralization.

Condor work was also undertaken to characterize magnetic lineaments, magnetic domains, lineaments and domains associated with mineralization in the hope of defining potential prospective mineralized areas. The program included leveling and de-corrugating of magnetic data, production of magnetic filters and upward-continued grids, the compilation and assessment of published geology and mineralization over the study area in the context of interpretation of the magnetic data aimed at identifying major structures, magnetic domains, and exploration areas.

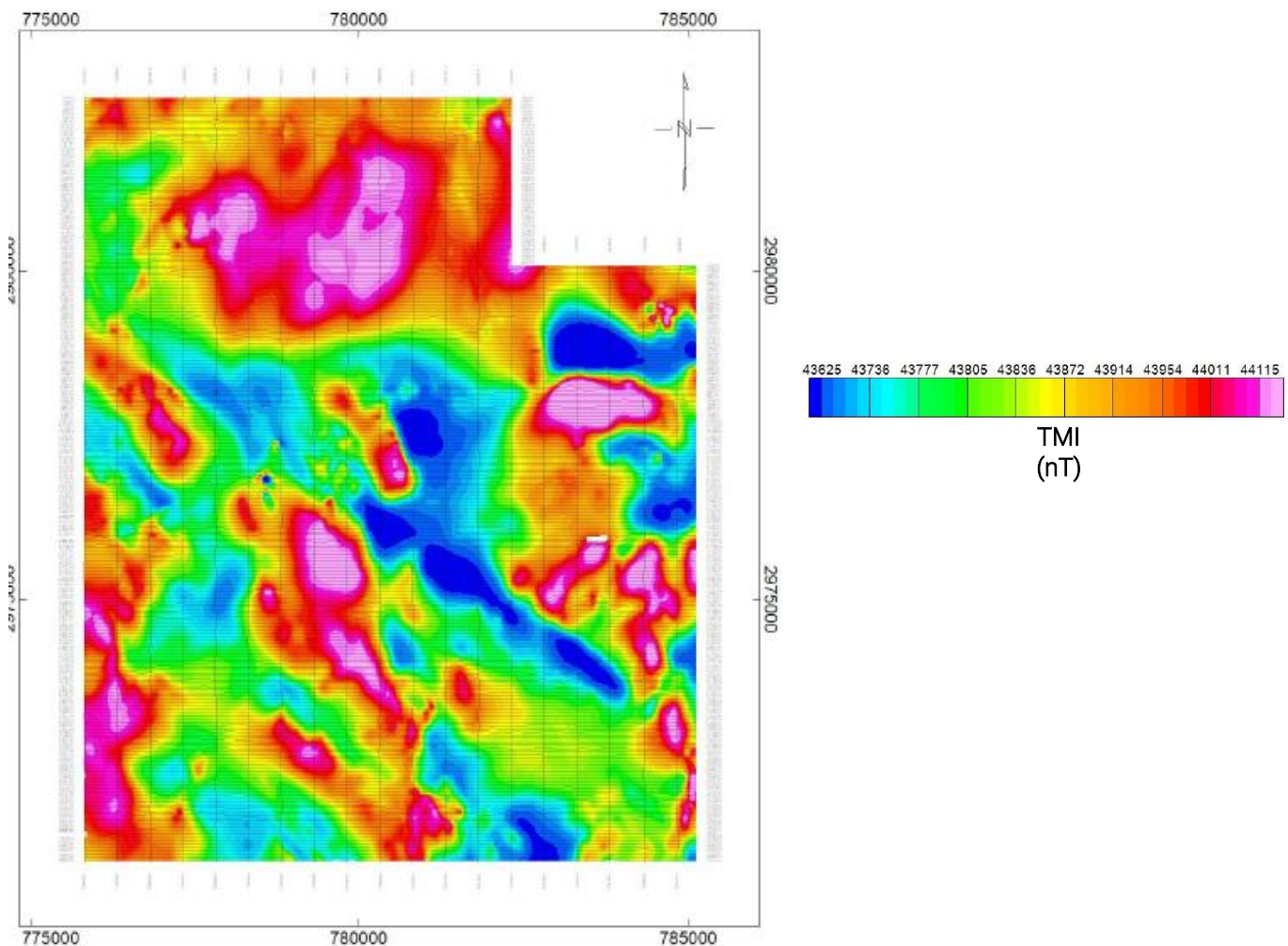
The products of the lineaments work program included a GIS data package, a PowerPoint summary report, and a poster-sized map. Airborne magnetic data has shown it can be utilized to identify domains associated with porphyry Cu mineralization at the Santos Tomás project. The work also showed that radiometric data can also be used to identify domains of mineralization, albeit more broadly, that government mapped lithology and structures do not correspond well with magnetic data, while the government lithology does correspond to radiometric data, while structures do not. The main magnetic fabric is SSE- and NNE-trending.

Historic mines and mineral showings and the porphyry mineralized zone at Santos Tomás tend to occur to within 100 m of SSE trending low-mag lineaments, within 100 m of the ends of high-mag lineaments, within 100 m of magnetic source

edges, and in radiometric domains relatively depleted in K, Th, U. The resulting magnetic-radiometric prospectivity map produced is sufficient for application in conjunction with other geologic data, but expressly not in isolation, for targeting.

Condor North Consulting ULC (also 'Condor') generated an unconstrained, smooth model, magnetic susceptibility inversion using Seequent VOXI software (Moul, 2021). The process required several model runs (allowed for 50 x 50 x 25 m cells size at altered centers to capture the 50 m line separation constraints and maximum VOXI inversion runs) on a de-trended and heading corrected TMI file. This file required corrections to the source TMI data set for diurnal effect, heading effect and removal of a 1Mst order polynomial regional trend in the data to produce the input file for the magnetic inversions (Figure 9-3 and Figure 9-4).

Figure 9-2: The Microlevelled TMI Grid

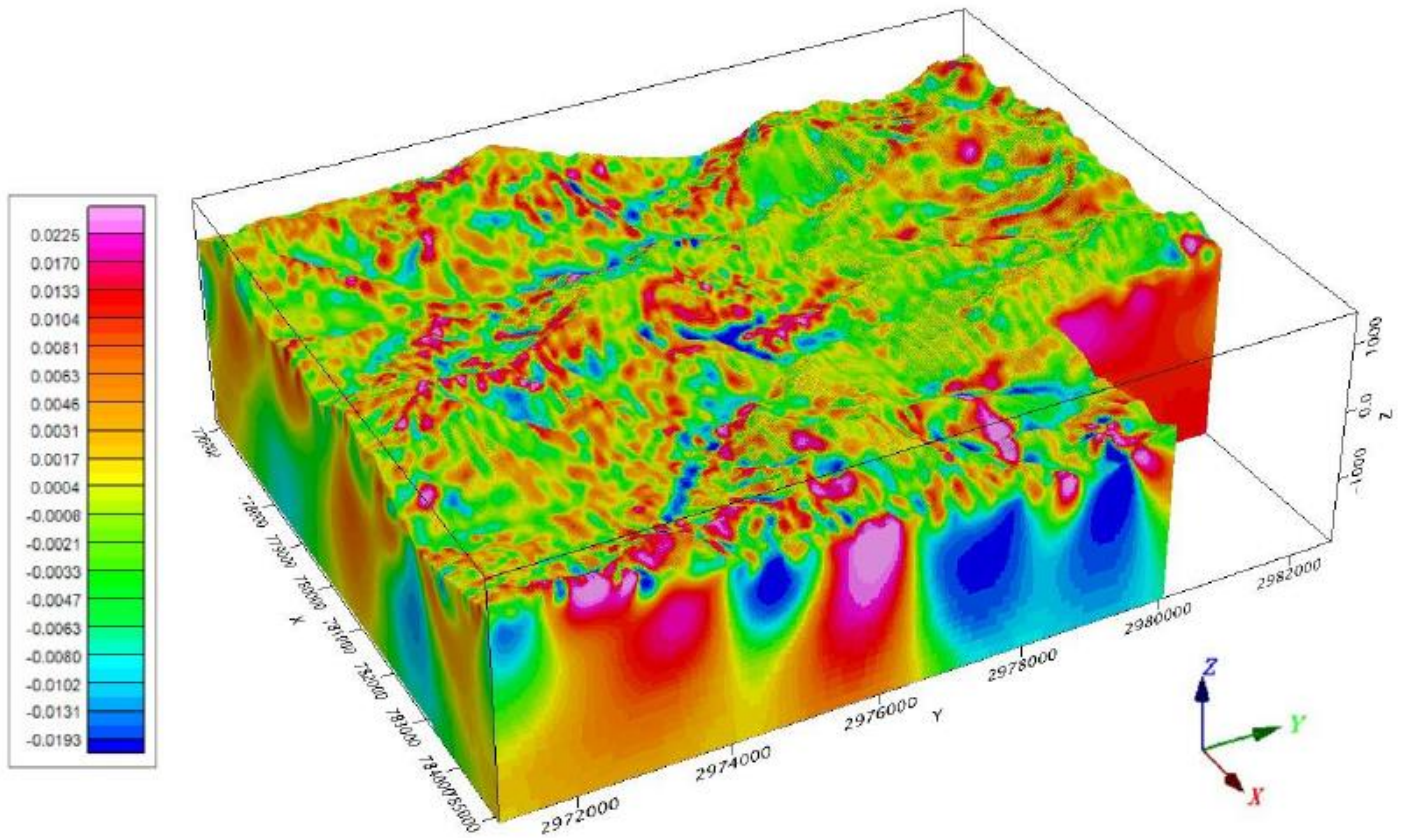


Source: Oroco, 2023.

The process defined certain 3D domains of magnetic susceptibility. Good coherence between the shallower parts of the model and known geological domains have been observed, while some deeper domains are locally inconsistent with the

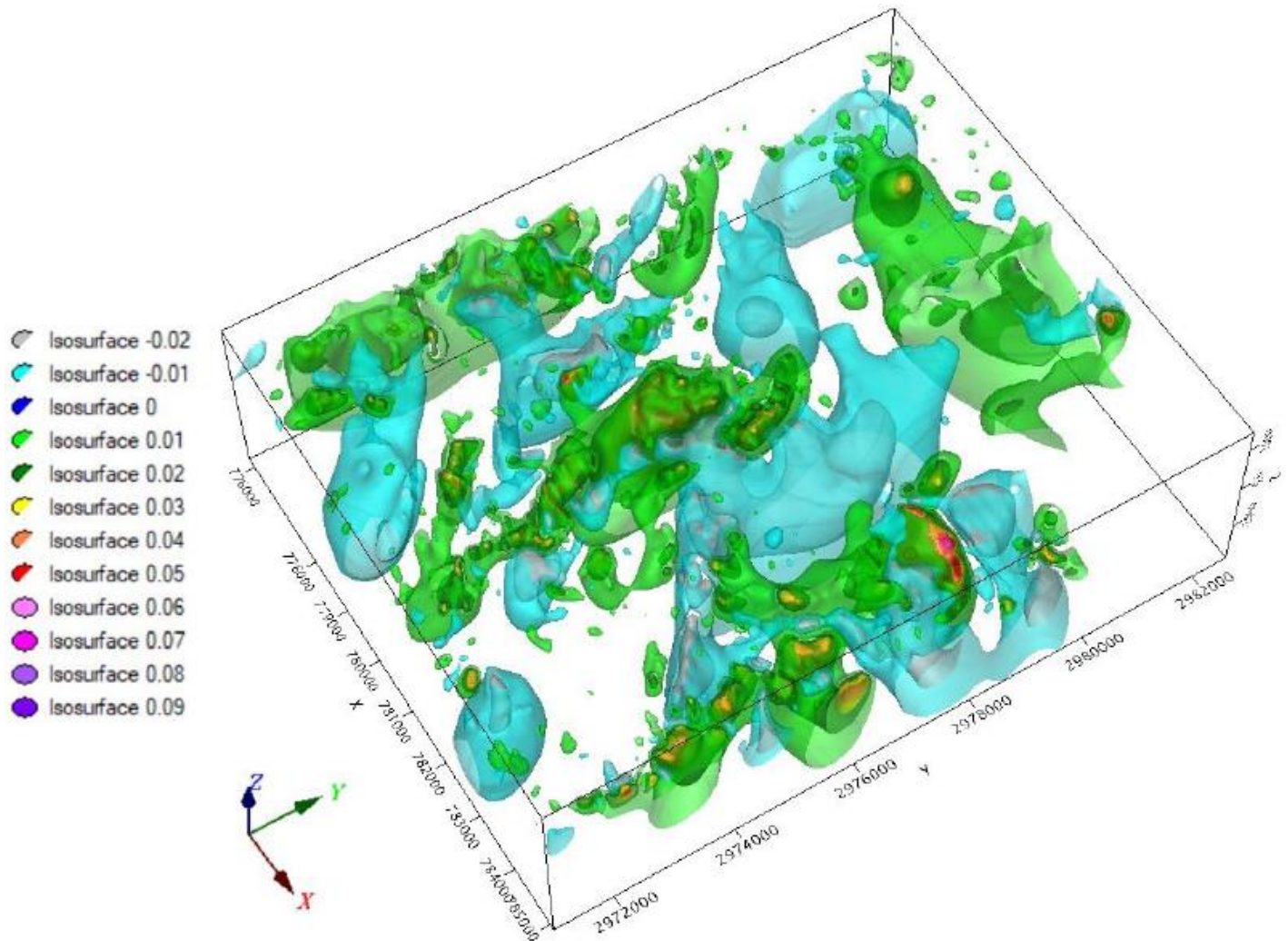
now known magnetic susceptibility characteristics of those rock units (as measured in drilling) or have been untested. However, downhole magnetic susceptibility surveys on some holes (refer to Section 10 of this report) and the routine collection of point source magnetic susceptibility data on drill core, will permit a constrained (re-) inversion of the data.

Figure 9-3: VOXI Susceptibility Inversion Model



Source: Oroco, 2023.

Figure 9-4: Iso-surfaces Generated from VOXI Magnetic Susceptibility Inversion Model



Source: Oroco, 2023.

9.2.2 Surface 3D DCIP Survey

Dias Geophysical Limited of Saskatoon, SK, Canada ("Dias") was contracted by Oroco (through Minera Xochipala, S.A. de C.V., a Mexican subsidiary of Oroco, 'XG') to undertake a 3D DC resistivity and induced polarization ('3D DCIP') survey of the Project. The survey fieldwork continued from September 1st, 2020, until March 16th, 2021

The survey, with a 2D DCIP extension to the east of South Zone, was undertaken using the DIAS32 system (Dias, 2021). The geophysical program was carried out to detect the electrical resistivity and chargeability signatures associated with potential targets of interest. This was achieved using the DIAS32 acquisition system in conjunction with one of Dias' proprietary GS5000 transmitters. The survey was completed using a rolling distributed partial 3D DCIP array and a 2D distributed array, each with a pole-dipole configuration. The full survey covered an area spanning approximately 20 km²,

and was carried out in two phases, a first phase spanning from September 1st until December 5th, 2020, and a second phase carried out between February 10th and March 16th, 2021.

Dias Geophysical completed a 3D rolling distributed pole-dipole array survey in common voltage reference ('CVR') mode where the main grid, surveyed using a 3D rolling array, was comprised of 26 receiver lines alternating with 27 transmitter lines. These lines were oriented ESE with an azimuth of 110°. All lines were 2.4 km long and separated by 100 m, with receiver line (L10100N through L15100N) receiver stations spaced 100 m apart. Five additional receiver stations were setup at 100 m spacing off the eastern end of the three northern-most receiver lines (L14500N, 14700N and 14900N) in order to provide extra coverage over an area of interest at Brasiles. Along the transmitter lines (lines L10000N through L15200N) injection stations were spaced 200 m apart: when access allowed, at least one extension injection was carried out 200 m off both ends of each transmitter lines. Additionally, up to 5 extensions were carried out at 200 m spacing off the ends of five select transmitter lines (10800N, 11400N, 12400N, 13000N, 132000N, 134000N and 13600N) in order to offer greater depth of investigation along the edge of the grid in these areas. Current (injection) extensions at lines 12400N through 13600N were strategically carried out along the opposite riverbank from the survey lines to provide coverage beneath the riverbed (Figure 9-5).

The results of the first phase of the survey identified a sizable IP feature of interest in the southeast corner of the grid. As a result, decision was made to add four 2D survey lines to follow this IP feature east. These 2D lines were spaced 400 m apart and extended south-southwest-north-northeast, perpendicularly to the main grid, with an azimuth of 20°. The first line, Line 140E, started at the level of station 140E on the main grid and all lines extended in grid latitude between main grid lines 10100N and 11900N, except for the eastern-most 2D line L260E that extended between main grid L10300N to 11500N only. Along the 2D lines receiver and transmitter stations were spaced 200 m apart. The transmitter stations were setup at midpoint between consecutive receiver stations. For the 2D survey the full receiver line was setup and remained active for all current injections, leading to N=8 dipoles being collected for each injection (Figure 9-5), except for line 260E where N=6 was collected.

The same 'remote' local current electrode reference station was used for the entire program and was established ~3.5 km southeast of the main survey grid at 780762E, 2970462N and was comprised of 8 steel cylindrical 1.2-meter rods. The rods were placed in damp ground and in the shade. A barrier dam was placed around the electrodes maintain dampness for as long as possible. Both the local current and current remote were deployed using 16 AWG transmission wire connected to the transmitter site.

Survey procedures required careful safety co-ordination to ensure safety during all current injections and field activities in some very steep country. The Dias GS5000 transmitter used for the project provided output up to 10.0 kW and 4000 V, and the transmitted current ranged from 0.2 A to 4.8 A. The current transmission was maintained for a recording time of 4-6 minutes per station. Where the current varied by more than 10% during this recording time, the transmission was terminated, the injection electrode contact was improved, and the transmission re-started to provide a stable current for the duration of the recording. Whenever the injected current caused the nearest receivers to overvoltage, double injections were carried out: the first injection was carried out at maximum current and the closest receivers were disconnected, and a second injection was carried out at lower current and with all receivers active. For the Santo Tomás Project, a total of 439 current injections were carried out, including 18 double injections were carried out.

The receiver stations measure integrated normalized secondary voltages (i.e., chargeability) in milliseconds (ms) over a standard 2-second time base with 20 sample intervals. The total integrated chargeability is computed as the sum of each normalized secondary voltage multiplied by the length of its sample interval, divided by the total sample interval (i.e., 1.88 s for the 2 seconds time-base data). In the case of the Santo Tomás data and in concertation with the client, the apparent chargeabilities were calculated using a reduced integration window (480-1120ms).

For the Santo Tomás Project, dipoles of lengths varying between ~100 m and ~850 m were generated using a blanket dipole generation approach. In the case of the Santo Tomás 3D part of the grid, for each injection with up to 4 active receiver lines, approximately 2000 receiver dipoles were generated, yielding a final dataset with approximately 715,000 pole-dipole data points over the entire grid.

9.2.2.1 Inversion of the 3D DCIP Survey

After a thorough quality control, all the “accepted” data were used to produce a set of unconstrained 3D DC and IP models using the SimPEG inversion code (version 2.0 -<https://www.simpeg.xyz/>). A coarse model unconstrained inversion series to establish inversion parameters is run, with final unconstrained inversion using a fine mesh to yield the final 3D models following further data trimming suggested by the coarse modeling runs. The fine mesh size is 1/4 of the closest nominal spacing between receiver electrodes in the horizontal and vertical directions. The inversion parameters are further modified as needed to improve the model results until the fine models are considered acceptable.

The parameters used for the Santo Tomás grid DC and IP fine inversions are detailed in Dias, 2021. A flat standard deviation error combined with a floor were assigned as uncertainties for both DC (error = 5% and floor = 10th percentile) and IP (error = 5% and floor = 2.5e-5mV/V) inversions. The DC inversion was carried out first followed by the IP inversion and both inversions used a uniform background (for DC 241.42 Ohm-m; and for IP 1e-5 mV/V). The final DC model was used for the IP inversion.

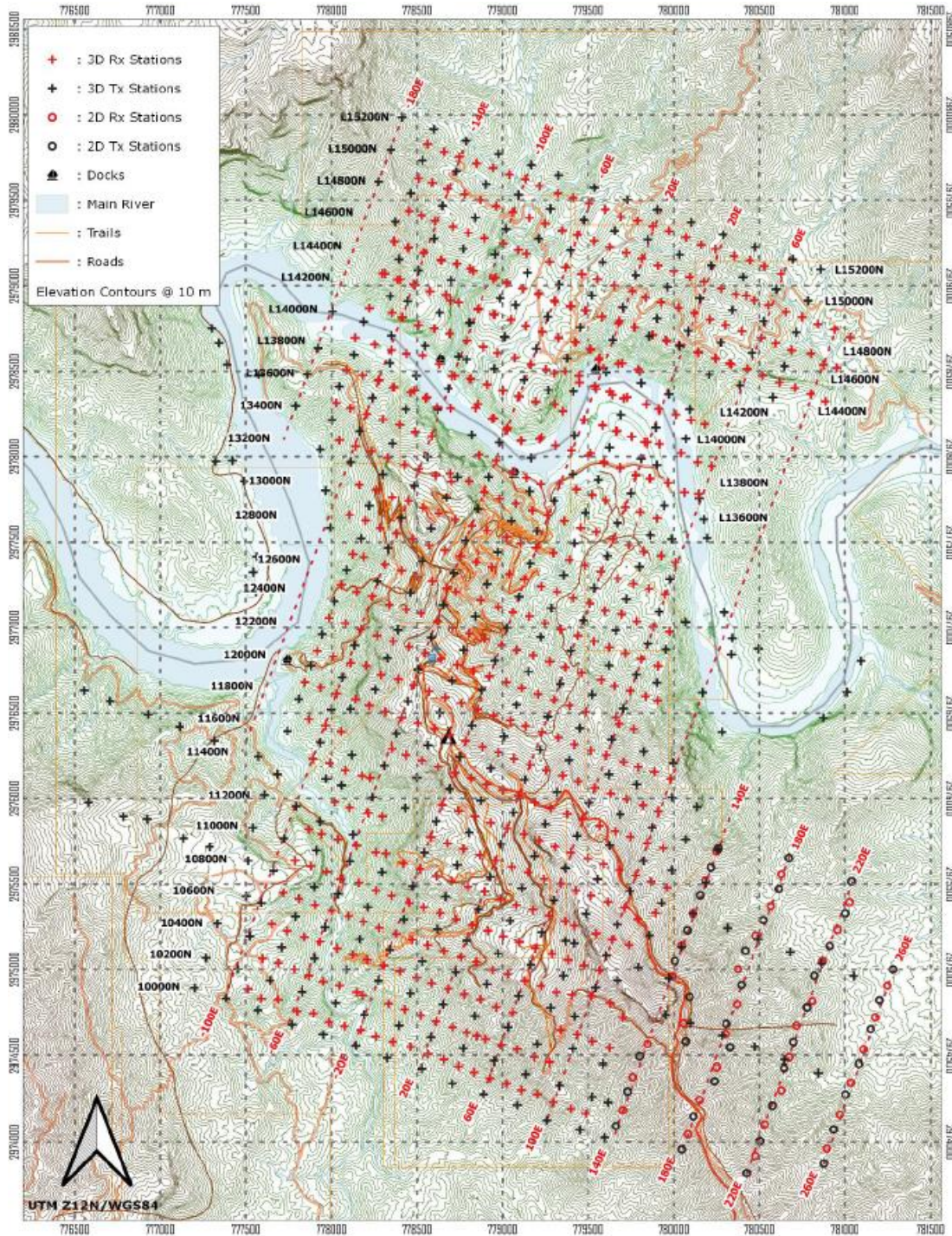
The inversions were carried out in UTM coordinates, and given its relative proximity to the grid, the current remote was included in the inversion calculation. The Eagle Mapping LiDAR DEM was used for the harmonization of the survey station elevations and was also the topographic file for the inversion.

9.2.2.2 Application of the DCIP Inversion Models

The unconstrained inversion models have been extensively used by Oroco as the primary targeting tool for the resource and exploration drilling.

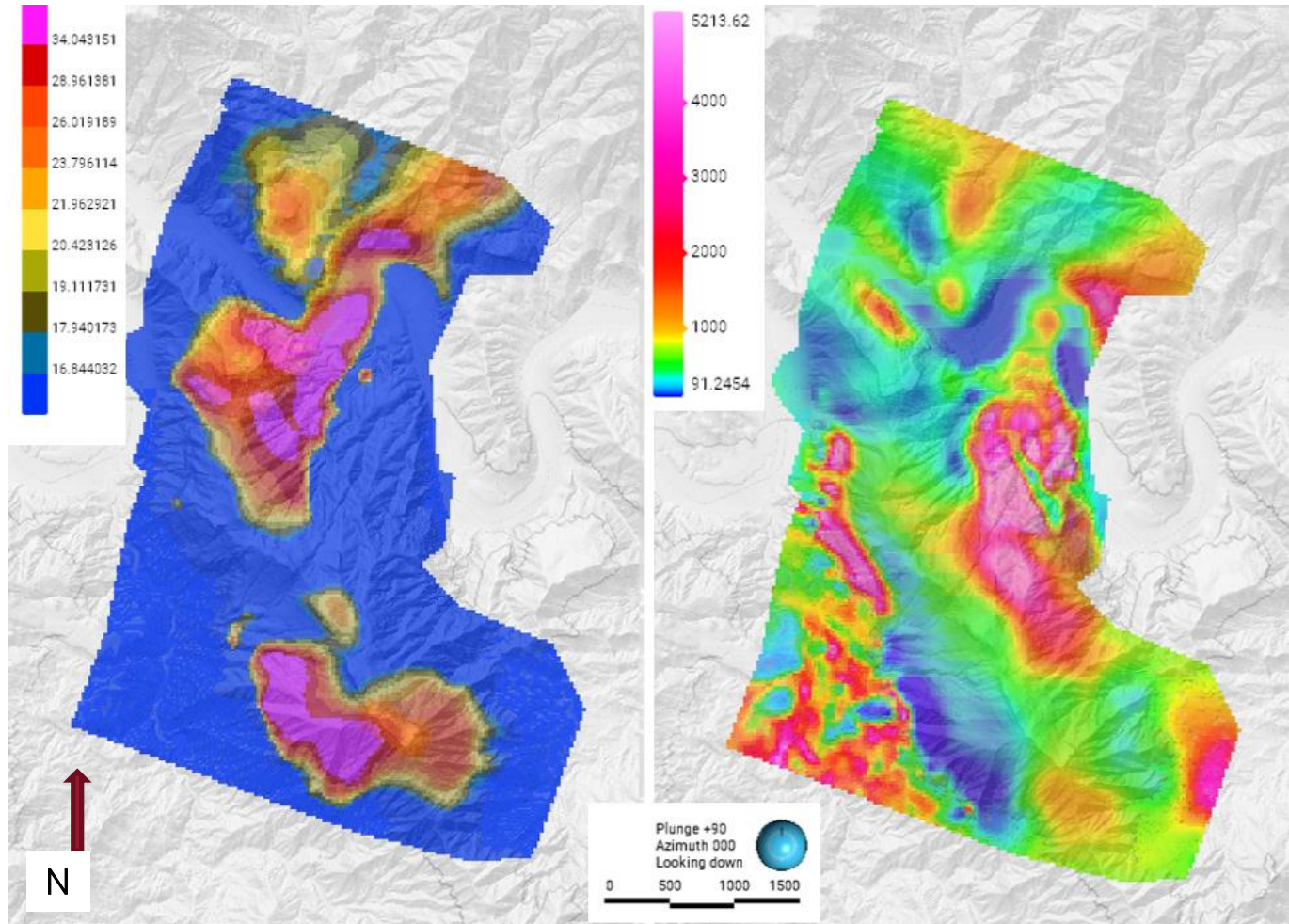
Copper mineralization has been found to commonly occur in areas of intermediate chargeability (+14.4 mV/V to <40 mV/V). Areas in which coarser pyrite is developed, and most commonly associated with low copper mineralization, are characterized by zones of highest chargeability. In general, no metal-sulphide mineralization of interest has been found associated with areas of low chargeability. Oroco has included color-ramp chargeability inversion model backgrounds in cross-sections used in the public disclosure of drilling assay data (Figure 9-6).

Figure 9-5: DCIP Survey coverage on the Santo Tomás Project, showing the locations of the transmitter/injection station sites and the receiver station locations (2D and 3D)



Source: Oroco, 2023.

Figure 9-6: Plan view of the Santo Tomás chargeability inversion model (left, in mV/V) and the resistivity inversion model (right, in Ohm-m) where the inversion model in each case is sub-horizontally plan sectioned by a plane dipping north at 10°. The section trace is demarcated by the gray ‘inclined contour’ line intersecting with the LiDAR-derived shaded topography



Source: Oroco, 2023.

In addition, areas of low resistivity commonly correlate with areas of extensive hydrothermal potassic alteration that are also well correlated with copper mineralization of interest, particularly in areas of shallower (< 300 m depth) low resistivity zones. The Company has used chargeability, resistivity and where relevant the results of historical drilling to guide drill targeting.

In the course of drilling, Oroco collected downhole IP data in a number of drill holes. This data was particularly collected for deeper holes, and holes that intersected a wide range of modeled chargeability. It is expected that the downhole chargeability and resistivity data will be aid in the planned constrained (re-)inversion of the DCIP data set. A listing of the specific methods used in each of the holes drilled by Oroco is available in Table 10-5.

9.2.2.3 Detailed Interpretation from the DCIP Models

A 2D geological interpretation of the project area was conducted based on geophysical data, geological mapping, and drilling data by Mira Geoscience of Vancouver, BC, Canada ('Mira'). The purpose of the interpretation was to identify important geophysical and geological domains for modeling and to construct a fault network to support interpretation of geophysical data (Mira Geoscience, 2022). The interpreted structural history and setting were interpreted and reconciled with other proprietary and public information about the project area. Fault dips were interpreted based on unconstrained geophysical inversion results, geological mapping, and structural measurements. A 3D fault network was constructed and used as a framework for geological interpretation and modeling. Geological surfaces were constructed based on constraints generated from mapping, drill hole data, and interpretations from geophysical data. Geological surfaces and faults were used to define a lithology property on a 3D block model ("voxet") for use during geophysical inversion.

9.2.2.3.1 Fault Network

Faults were interpreted from geological mapping, drilling data, magnetic and 3D IP data and models, satellite imagery, and lidar data. Two main families of faults occur in the project area. The first family is a series of predominantly NNW-striking moderately to steeply dipping faults. They are interpreted to have a predominant strike-slip or dip-slip sense of motion. These structures are interpreted to have formed during the Laramide orogeny.

The first set of faults are cut by NW-striking normal faults with extensive strike lengths that define a series of grabens in the project area. These grabens appear to control the location and thickness of SMO volcanics and sediments. They offset Laramide intrusions and are interpreted to offset both the porphyry dyke complex and mineralization at the North Zone. The normal faults are related to the end of Laramide compression and beginning of basin and range tectonism and extension.

9.2.2.3.2 Alteration and Lithology

Mira used unconstrained DCIP and magnetics inversion models with other public and Oroco data to construct a geological/alteration voxet model for the distribution of major rock types and rock type <> alteration associations. This voxet model was used to run theoretical constrained inversion models with a view to focusing on the structural implications of the models and possibly the recognition of deeper features.

Well developed zoning in the 3D IP data and to a lesser extent the magnetic data does not coincide directly with lithological units and are interpreted by Mira to partially represent alteration systems related to mineralization. A zone of irregular conductivity and moderate chargeability is related to the mineralization at the North Zone. There are broad trends in the magnetic data that may correspond to portions of a porphyry alteration system. A linear, NNW-striking magnetic low feature is interpreted to represent a key fluid pathway within the hydrothermal alteration system at the North Zone. A broad magnetic high feature east of the North Zone is interpreted to represent either propylitic alteration (as observed in core logging) or preserved magnetite in country rocks.

In addition to the observed lateral zonation, alteration signatures are expected to be zoned vertically, which combined with the "telescoping" effect of normal faulting in the area implies that geophysical anomalies must also be interpreted with respect to their expected vertical position within the system.

9.2.2.3.3 Recommendations

Mira recommended that petrophysical study of all rock types in the project area would improve further use of geophysical data: this recommendation encouraged Oroco to continue to collect the downhole *in-situ* geophysics in selected holes.

The continued collection of magnetic susceptibility data was recommended to help in discriminating intrusive phases and alteration zones. Quantitative measurement of alteration data using a portable X-ray fluorescence (XRF) or short wave near infrared (SWIR) device would enable 3D modeling of alteration zones and improve future inversions as well as conceptual targeting models – this data has been systematically collected (refer to Section 10).

The geological model was recommended to be reviewed against new drilling data collected in areas of sparse information and updated to reflect known geology so that the inversions can be rerun using the updated geological model when sufficient data has been collected.

9.3 Geological Mapping, and Mineral Sampling

Mapping and surface sampling as well as the location of historical artisanal mining adits has been undertaken in support Project exploration. This work is detailed in other sections of this report, with general mapping cover illustrated in Figure 9-1.

Oroco together with SRK undertook a detailed mapping campaign on the Property to update the map presented in the previous Technical Report (Bridge, 2020). All mapping data were compiled into an Arc GIS project. This comprised lithology and structural orientation data, line work and contacts, and included active links to field photographs. Mapping data and Arc GIS shape files were also imported into 3D space (Leapfrog Geo) software. In Leapfrog Geo the data were integrated with high-resolution drone data, lineament analysis data, geophysics data and drill hole data to further constrain lithology domains, contacts and structures and inform the lithostructural modeling and the resource modeling process.

The field work developed by Oroco geologists produced a database with 1027 field stations (518 in North and South Zones, and 509 Brasiles) and 1190 structural measurements, additionally to the 926 field stations and 926 measurements of SRK. A group of 17 samples (Table 7-1) from surface (8) and drill holes (9) were selected for geochronological analysis (Ar40/Ar39, U/Pb and Re-Os) to support stratigraphic interpretation and timing of alteration-mineralization. The results of the field mapping campaigns are represented in the geological map and stratigraphic column (Figure 7-2), while structural data and interpretations are presented in the structural chapter.

9.4 Site Access for Exploration

The Santo Tomás project site access has been improved since the commencement of drilling to improve road stability and access using boats. In particular, over a km of new access road was constructed in collaboration with and at the request of the Cieneguita del Núñez community, to avoid poor quality access along the unstable west side of the ridge near the El Bienestar Ranch site.

10 DRILLING

10.1 Drilling on the Property

Drilling campaigns were conducted by ASARCO, Tormex and Exall between 1968 and 1993, with the most recent pre-Oroco drilling completed by Exall in 1993. 106 drill holes (reverse circulation, percussion, and diamond-drill holes, collectively the 'historical' or 'legacy' drill holes) were completed on the Property (Thornton, 1994). ASARCO completed sixteen percussion holes in the late 1960s to early 1970s, but the logs and results for these holes have not been identified (Spring, 1992). Therefore, the 16 percussion holes are not included in the drill hole database assembled by Exall.

Commencing on 28th July 2021 and continuing through March 28th, 2023, Oroco completed 76 diamond drill holes for 48,481 m of diamond core drilling. This campaign represents the entirety of Phase 1 drilling by Oroco. Seven (7) of these holes were drilled for exploration purposes at the Brasiles prospect (5,116.4 m) and have been excluded from consideration in the MRE presented in this report (Section 14). Table 10-1 displays Oroco Phase 1 drill holes and reports total meters that were included and excluded in the present MRE.

At the time the MRE was developed (effective date - April 21, 2023), assays for one (1) drill hole (N047) and QA/QC check assay data for two (2) drill holes (N045 and N046) at North Zone had not been received. The MRE was therefore made using assay data from 65 (40,978.92 m) of the Phase 1 Oroco drill holes combined with legacy results (Table 10-1). Geotechnical Hole GT001 was also excluded.

Table 10-1: Oroco Drill hole Inclusion / Exclusion Table

Inclusion status	Drill holes	Meters
Included	ST21-N001 to ST21-N010 N11 to N044 S001 to S021	40,978.92
Excluded	N045 to N047 GT001 B001 to B007	7,501.96
Total	76	48,480.88

Oroco's entire updated drill hole database (with MRE excluded holes) contains 166 new and legacy drill holes (reverse circulation and diamond drill holes) totaling 69,556 m with lithological logging data and 29,992 Cu assays. The assay database statistics used to develop the MRE are presented in Table 10-2. This database was supplied to SRK to develop the MRE.

Table 10-2: Oroco and Historical Drilling and Assaying as used in this MRE

Phase of Drilling	No. of Cu Assays	No. of Drill holes	Total Length (m)	Average Length (m)
Pre-Exall, STD Series, to 1991 ^a	4,707	50	16,004	320
Exall STE Series ^a	2,537	40	5,071	127
Oroco MRE ^b ST21, N and S series	19,135	65	40,978	630
Total (MRE)^c	26,379	155	62,054	-

Note: ^a Historical / legacy drilling as recorded in the Exall database acquired by Oroco.
^b Drill holes statistics for holes included in the MRE, excluding N045, N046, N047, the Brasiles series holes and GT001.
^c Total meter values may not sum due to rounding.

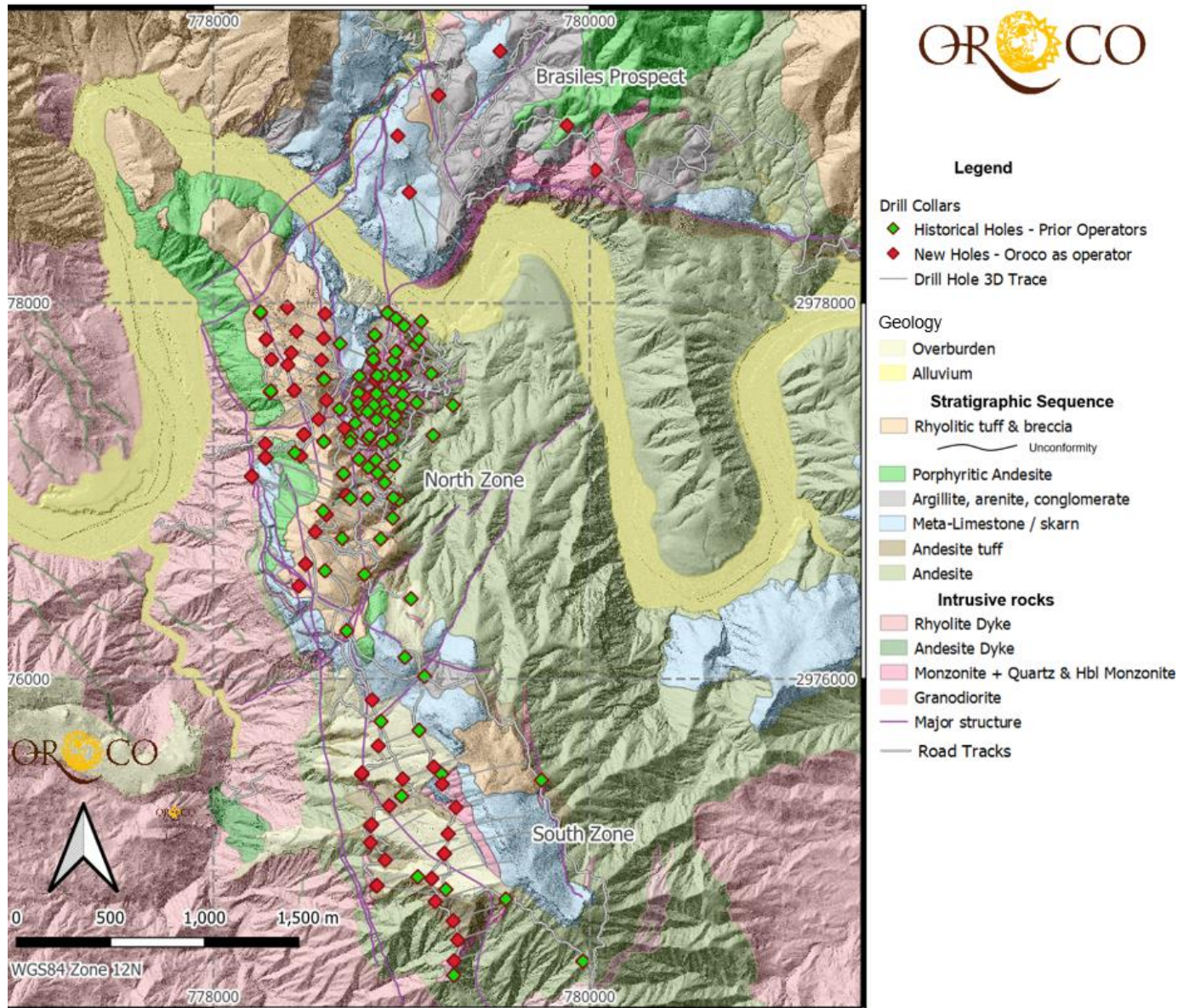
All of the legacy drill holes are vertical except for five Exall drilled holes (STE-28, STE-51, STE-61, STE-62, and STE-63), for which the dip ranges from -60° to -70°. No downhole surveys have been located for any of the legacy drill holes (Thornton, 2011). Figure 10-1 through Figure 10-4 present maps of the drill collars with drill traces for inclined drill holes.

The STE series drilling employed wireline diamond drilling methods, and samples for analysis taken from a ½ split of the core using a Longyear core splitter. The STD holes were sampled using a rotary drill and a split of the cuttings obtained for analysis.

During the Exall drilling program, every 1 in 5 samples in the drill sample sequence was analyzed for Mo, Au, Ag and Fe, in addition to the Cu analyses, yielding a total of 534 samples analyzed for the suite of Cu, Mo, Au, Ag and Fe. Exall assembled the database of historical drilling during the 1992-1993 exploration program. Review of the historical reports and drill logs indicate there are no known drilling, sampling or recovery factors that could materially impact the accuracy and reliability of the historical drilling results.

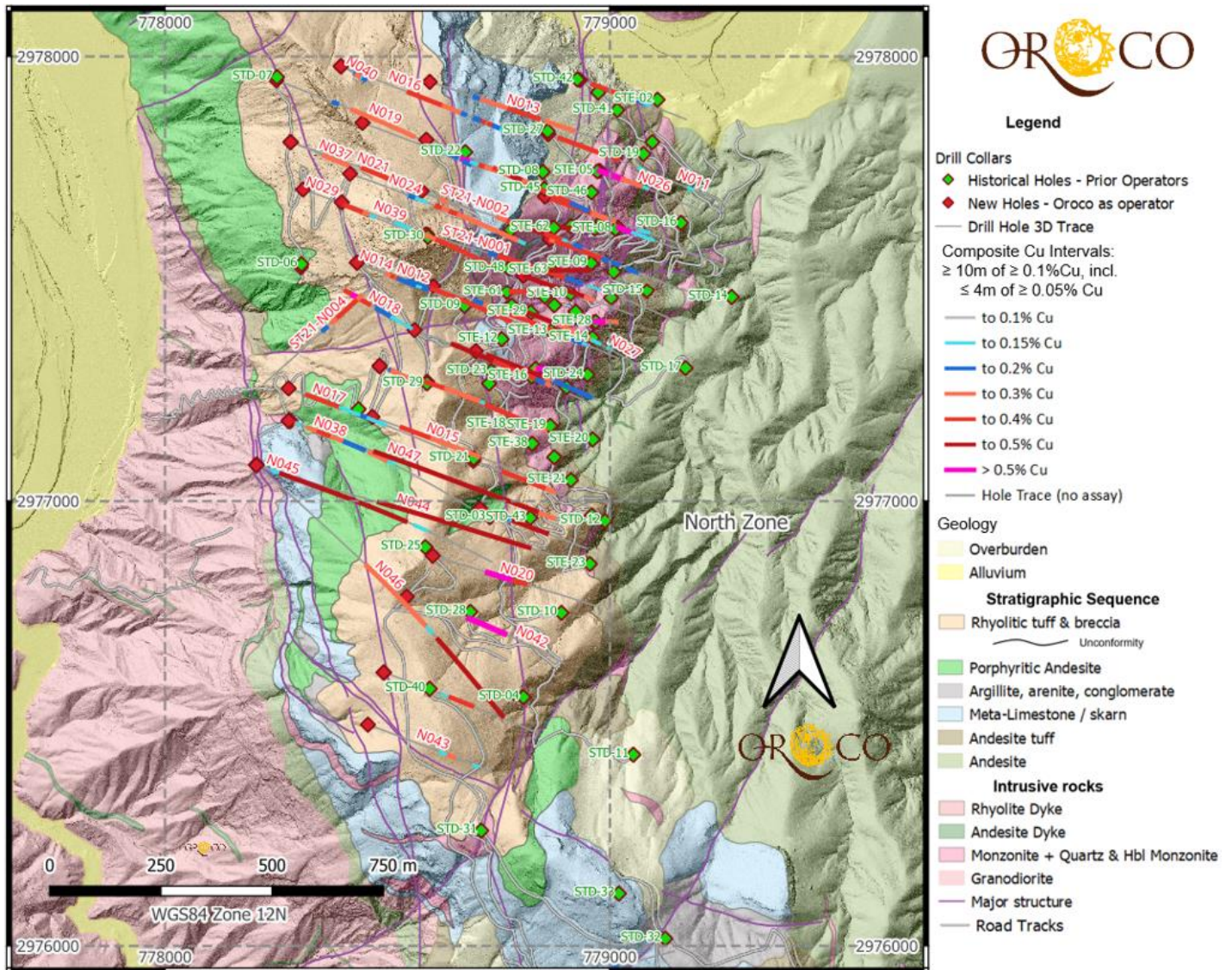
Oroco’s Phase 1 drilling sampling and assay protocols are reviewed in greater detail in Section 11 of this report. Drill holes ST21-N001 through ST21-N010 and N011 through N047 are located in the Project’s North Zone. Holes S001 through S021 are located in the South Zone. Holes B001 through B007 are exploration holes drilled at the Brasiles Prospect. B003 is the first significantly mineralized hole for which Oroco has copper assays in this zone, and also represents the discovery hole on the Brasiles Prospect. Hole GT001 is the first (and so far the only) designated geotechnical drill hole on the project. It is located in the southern part of the North Zone (Figure 10-2, same collar location as N038).

Figure 10-1: Santo Tomás Project drill collar and hole trace locations for North and South Zones resource drilling, and exploration drilling at Brasiles



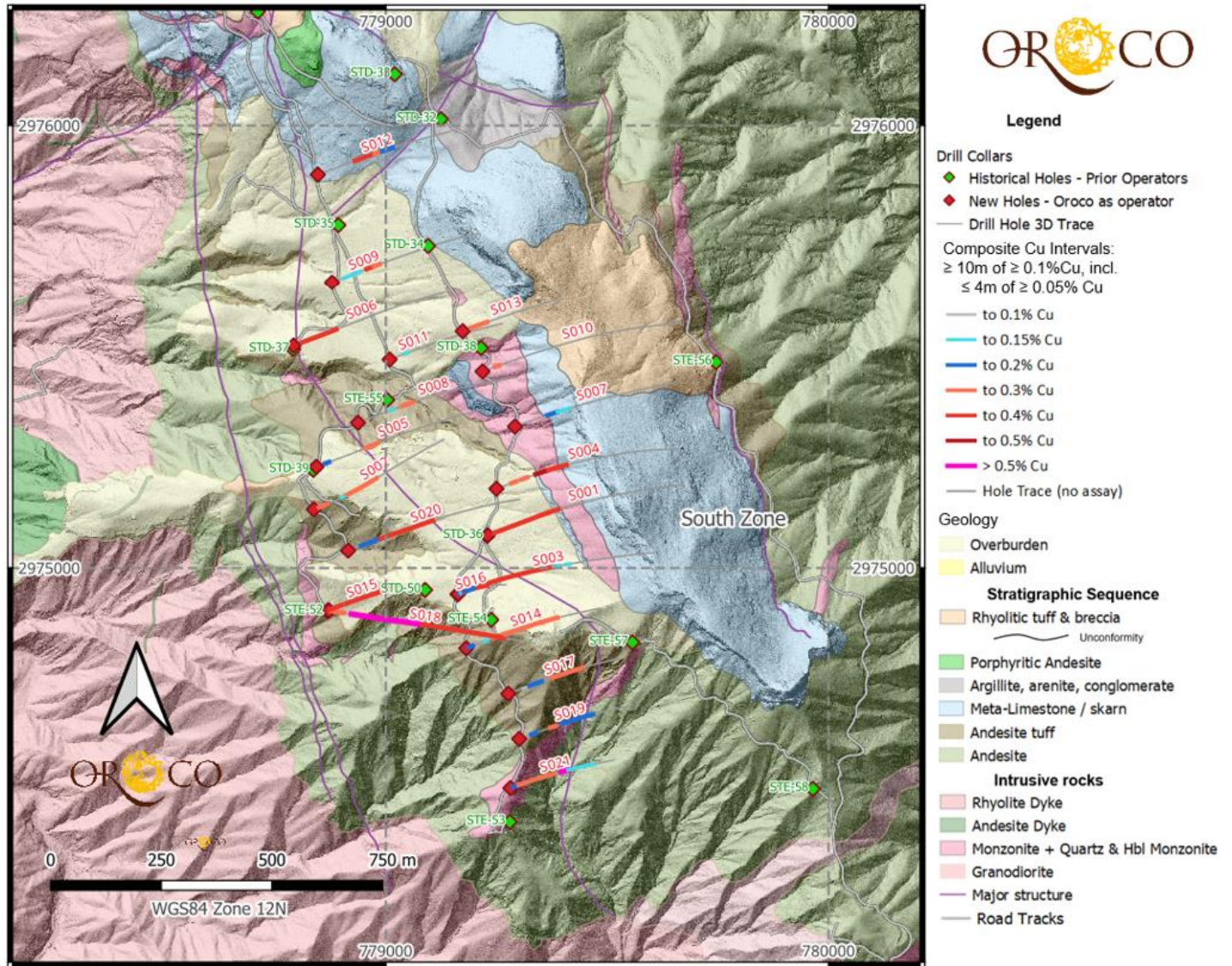
Source: Oroco, 2023.

Figure 10-2: North Zone drill hole collar locations and drill hole traces showing composite intervals > 0.1% Cu



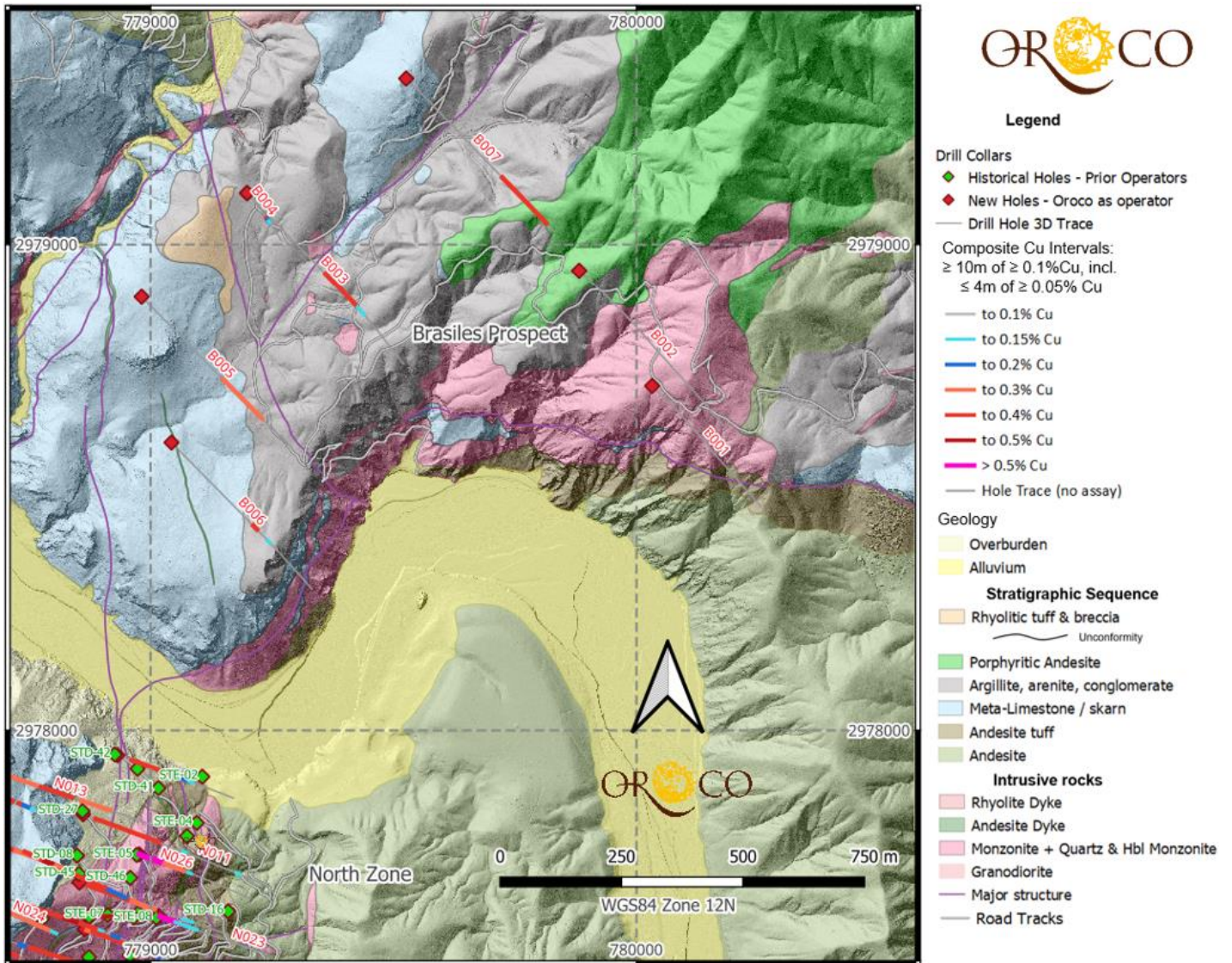
Source: Oroco, 2023.

Figure 10-3: South Zone drill hole collar locations and drill hole traces showing composite intervals > 0.1% Cu



Source: Oroco, 2023.

Figure 10-4: Brasiles exploration drill hole collar locations and drill hole traces showing composite intervals > 0.1% Cu



Source: Oroco, 2023.

Table 10-3: Project Drill Collars – Coordinates in WGS84 UTM Zone 12N

Hole_ID	UTM_E	UTM_N	RL	Az	Dip	TD
ST21-N001	778,588	2,977,601	580	110	-55	1,024
ST21-N002	778,576	2,977,698	555	110	-55	829
ST21-N003	778,586	2,977,814	515	110	-55	881
ST21-N004	778,585	2,977,601	580	225	-55	856
ST21-N005	778,864	2,977,590	443	110	-55	37
ST21-N006	778,864	2,977,590	443	110	-55	621
ST21-N007	778,602	2,977,484	526	110	-55	753
ST21-N008	778,560	2,977,384	526	110	-55	692
ST21-N009	778,443	2,977,852	524	110	-55	911
ST21-N010	778,588	2,977,267	526	110	-55	609
N011	778,860	2,977,826	371	110	-55	685
N012	778,431	2,977,538	508	110	-55	734
N013	778,594	2,977,944	480	110	-62	920
N014	778,431	2,977,538	508	110	-74	740
N015	778,465	2,977,188	488	110	-55	710
N016	778,394	2,977,979	482	110	-62	1,002
N017	778,277	2,977,252	396	110	-55	713
N018	778,304	2,977,528	416	120	-55	625
N019	778,249	2,977,947	407	110	-55	871
N020	778,601	2,976,876	654	110	-55	658
N021	778,281	2,977,809	412	110	-55	683
N022	778,853	2,977,686	444	110	-55	597
N023	779,016	2,977,617	383	110	-55	390
N024	778,415	2,977,737	481	110	-55	719
N025	778,805	2,977,508	445	110	-55	475
N026	778,976	2,977,744	367	110	-55	399
N027	778,775	2,977,436	450	110	-55	533
N028	778,931	2,977,948	271	110	-55	439
N029	778,310	2,977,702	431	110	-65	725
N030	778,697	2,977,336	510	110	-55	469
N031	778,692	2,977,090	546	110	-55	503
N032	778,491	2,976,614	667	110	-55	643
N033	778,481	2,977,303	471	110	-80	484
N034	778,481	2,977,303	471	110	-55	615
N035	778,707	2,976,982	560	110	-80	463

Hole_ID	UTM_E	UTM_N	RL	Az	Dip	TD
N036	778,707	2,976,982	560	110	-50	402
N037	778,281	2,977,809	412	110	-75	728
N038	778,277	2,977,179	381	110	-50	710
N039	778,396	2,977,673	488	110	-55	753
N040	778,394	2,977,979	482	110	-85	923
N041	778,491	2,976,614	667	0	-90	478
N042	778,542	2,976,784	670	110	-55	606
N043	778,455	2,976,496	655	110	-55	509
N044	778,205	2,977,081	383	110	0	706
N045 ^a	778,204	2,977,081	382	110	-25	624
N046 ^a	778,205	2,977,080	383	131	0	796
N047 ^a	778,281	2,977,179	383	110	0	664
S001	779,229	2,975,073	826	70	-55	736
S002	778,836	2,975,131	691	70	-55	617
S003	779,161	2,974,940	818	70	-55	702
S004	779,249	2,975,178	825	70	-55	701
S005	778,842	2,975,228	703	70	-55	656
S006	778,790	2,975,501	646	70	-55	623
S007	779,291	2,975,319	828	70	-55	608
S008	778,936	2,975,327	693	70	-55	636
S009	778,877	2,975,646	658	70	-55	592
S010	779,217	2,975,443	808	70	-55	693
S011	779,007	2,975,470	690	70	-55	465
S012	778,845	2,975,890	677	70	-55	531
S013	779,172	2,975,534	798	70	-55	416
S014	779,180	2,974,817	814	70	-55	558
S015	778,869	2,974,904	674	70	-55	310
S016	779,162	2,974,940	818	70	-80	696
S017	779,275	2,974,715	809	70	-55	483
S018	778,870	2,974,903	674	100	-35	581
S019	779,300	2,974,613	797	70	-55	468
S020	778,914	2,975,038	677	70	-55	693
S021	779,280	2,974,502	775	70	-55	393
GT001 ^a	778,277	2,977,179	380	110	-75	301
STD-01	778,974	2,977,623	404	0	-90	227

Hole_ID	UTM_E	UTM_N	RL	Az	Dip	TD
STD-02	778,826	2,977,289	471	0	-90	307
STD-03	778,729	2,976,963	562	0	-90	303
STD-04	778,804	2,976,558	665	0	-90	310
STD-05	778,962	2,977,401	399	0	-90	331
STD-06	778,306	2,977,534	445	0	-90	95
STD-07	778,251	2,977,955	449	0	-90	302
STD-08	778,848	2,977,741	418	0	-90	306
STD-09	778,672	2,977,438	492	0	-90	400
STD-10	778,890	2,976,748	598	0	-90	421
STD-11	779,051	2,976,429	630	0	-90	353
STD-12	778,987	2,976,954	472	0	-90	403
STD-13	778,874	2,977,098	469	0	-90	452
STD-14	779,275	2,977,458	278	0	-90	292
STD-15	779,082	2,977,473	324	0	-90	362
STD-16	779,159	2,977,627	293	0	-90	359
STD-17	779,169	2,977,298	349	0	-90	240
STD-18	778,776	2,977,612	496	0	-90	412
STD-19	779,074	2,977,782	285	0	-90	304
STD-20	778,874	2,977,439	407	0	-90	285
STD-21	778,693	2,977,095	564	0	-90	317
STD-22	778,674	2,977,786	503	0	-90	303
STD-23	778,732	2,977,291	481	0	-90	318
STD-24	778,948	2,977,283	395	0	-90	202
STD-25	778,584	2,976,896	655	0	-90	244
STD-26	778,434	2,977,206	489	0	-90	41
STD-27	778,859	2,977,833	365	0	-90	334
STD-28	778,685	2,976,750	639	0	-90	314
STD-29	778,588	2,977,264	547	0	-90	289
STD-30	778,590	2,977,596	580	0	-90	288
STD-31	778,710	2,976,258	748	0	-90	275
STD-32	779,123	2,976,016	801	0	-90	310
STD-33	779,019	2,976,117	810	0	-90	318
STD-34	779,094	2,975,729	770	0	-90	376
STD-35	778,892	2,975,776	666	0	-90	332
STD-36	779,228	2,975,072	826	0	-90	368
STD-37	778,790	2,975,493	645	0	-90	329

Hole_ID	UTM_E	UTM_N	RL	Az	Dip	TD
STD-38	779,214	2,975,496	803	0	-90	426
STD-39	778,835	2,975,221	703	0	-90	352
STD-40	778,594	2,976,577	710	0	-90	380
STD-41	779,015	2,977,880	266	0	-90	356
STD-42	778,926	2,977,950	272	0	-90	305
STD-43	778,820	2,976,961	535	0	-90	362
STD-44	778,870	2,977,616	441	0	-90	352
STD-45	778,852	2,977,704	444	0	-90	370
STD-46	778,957	2,977,696	405	0	-90	277
STD-47	778,872	2,977,533	411	0	-90	298
STD-48	778,772	2,977,524	463	0	-90	383
STD-49	778,778	2,977,438	450	0	-90	352
STD-50	779,088	2,974,949	802	0	-90	371
STE-01	778,972	2,977,920	270	0	-90	98
STE-02	779,106	2,977,904	205	0	-90	80
STE-04	779,094	2,977,809	277	0	-90	80
STE-05	778,971	2,977,743	366	0	-90	80
STE-07	778,911	2,977,619	422	0	-90	80
STE-08	779,011	2,977,613	385	0	-90	80
STE-09	778,957	2,977,536	372	0	-90	80
STE-10	778,910	2,977,465	385	0	-90	100
STE-11	779,001	2,977,456	367	0	-90	100
STE-12	778,756	2,977,363	489	0	-90	82
STE-13	778,867	2,977,381	442	0	-90	80
STE-14	778,960	2,977,366	402	0	-90	80
STE-15	778,727	2,977,263	476	0	-90	80
STE-16	778,823	2,977,279	471	0	-90	80
STE-17	778,901	2,977,255	408	0	-90	90
STE-18	778,774	2,977,171	467	0	-90	76
STE-19	778,865	2,977,168	443	0	-90	80
STE-20	778,960	2,977,138	403	0	-90	80
STE-21	778,911	2,977,046	464	0	-90	80
STE-22	778,958	2,976,967	500	0	-90	80
STE-23	778,954	2,976,858	514	0	-90	80
STE-24	778,965	2,977,614	404	0	-90	150
STE-25	778,922	2,977,425	403	0	-90	126

Hole_ID	UTM_E	UTM_N	RL	Az	Dip	TD
STE-26	778,853	2,977,459	408	0	-90	120
STE-27	779,008	2,977,517	335	0	-90	80
STE-28	778,967	2,977,402	399	90	-65	110
STE-29	778,821	2,977,423	435	0	-90	130
STE-38	778,824	2,977,128	476	0	-90	70
STE-51	778,832	2,977,297	473	90	-70	56
STE-52	778,867	2,974,901	674	0	-90	268
STE-53	779,279	2,974,425	747	0	-90	250
STE-54	779,237	2,974,882	867	0	-90	227
STE-55	779,002	2,975,379	695	0	-90	250

Hole_ID	UTM_E	UTM_N	RL	Az	Dip	TD
STE-56	779,745	2,975,464	868	0	-90	174
STE-57	779,556	2,974,831	966	0	-90	250
STE-58	779,966	2,974,500	946	0	-90	250
STE-59	780,134	2,974,093	899	0	-90	250
STE-61	778,767	2,977,470	453	90	-70	197
STE-62	778,873	2,977,616	441	90	-65	201
STE-63	778,868	2,977,520	410	90	-60	166
STE-64	780,117	2,978,647	442	0	-90	1
STE-65	780,040	2,978,839	431	0	-90	1
STE-66	779,956	2,978,967	463	0	-90	1

Notes:

^a Holes GT001, N045, N046 and N047 are not included in the MRE calculation.

The Brasiles exploration prospect, also sometimes referenced as the Brasiles Prospect, was drilled as part of the Oroco Phase 1 drilling campaign to explore the area located north of the North Zone. The hole location data are presented in Table 10-4.

Table 10-4: Brasiles Prospect Exploration Drill Hole Collar Information (WGS84 UTM Zone 12N)

Hole_ID	UTM_E	UTM_N	RL	Az	Dip	TD
B001	780,031	2,978,708	437	135	-55	557
B002	779,881	2,978,947	424	135	-55	752
B003	779,198	2,979,107	332	135	-55	822
B004	779,198	2,979,107	332	135	-80	740
B005	778,981	2,978,892	342	135	-55	789
B006	779,042	2,978,591	302	135	-55	700
B007	779,525	2,979,343	427	135	-55	755

Note: These holes are excluded from the MRE.

10.2 Downhole Surveys

There is no record of downhole surveys being conducted as part of any of the historical drilling work at Santo Tomás.

Drilling by Oroco at Santo Tomás has included the collection of hole attitude surveys Table 10-5, initially using an EZ-Trac magnetic azimuth tool (holes ST21-N001 and -N002). The magnetic declination adjustment was made by the site team post data collection during the drill program.

Subsequently, downhole surveys were completed using the north-seeking EZ-Gyro equipment for holes ST21-N003 to N016 and B001-B004. For drill holes N017 onwards, all South Zone holes and B005 to B007 a Sprint-IQ (also by Reflex™) downhole tool, which also includes a north-seeking gyro.

Drill holes were aligned at setup using a gyro-equipped Reflex TN14 device from Hole ST21-N006 onward. Only the holes measured with Sprint-IQ have the azimuth adjusted using the TN14 tool.

The QL40-GR and EZ-Gamma instruments are used for detecting gamma radiation. The QL40-IP instrument is used to measure induced polarization, while the QL40-ELOG instrument measures resistivity. The QL40-MGS and KT instruments are used to measure magnetic susceptibility. The QL40-ABI serves as an acoustic televiwer, while the QL40-OBI is an optical televiwer. Both televiwers are utilized for identifying rock structures.

Table 10-5: In-hole Attitude and Geophysical Surveys by Drill Hole, including Set-out method and number of Samples Taken

DDH	Drill Rig	Collar Orient	Hole Survey	Gamma	IP/ Res	Mag Susc	Tele viewer	Samples
ST21-N001	H6	-	EZ-Trac	IDS	IDS	KT	-	853
ST21-N002	H5	-	EZ-Trac	-	-	KT	-	523
ST21-N003	H5	-	EZ-Gyro	IDS/EZ-Gamma	IDS	KT	-	577
ST21-N004	H6	-	EZ-Gyro	IDS/EZ-Gamma	IDS	KT	-	331
ST21-N005	H5	-	-	-	-	KT	-	21
ST21-N006	H5	TN14	EZ-Gyro	IDS/EZ-Gamma	IDS	KT	-	414
ST21-N007	H6	TN14	EZ-Gyro	IDS/EZ-Gamma	IDS	KT	-	500
ST21-N008	H5	TN14	EZ-Gyro	IDS/EZ-Gamma	IDS	KT	-	382
ST21-N009	H6	TN14	EZ-Gyro	IDS/EZ-Gamma	IDS	IDS/KT	-	484
ST21-N010	H5	TN14	EZ-Gyro	IDS/EZ-Gamma	IDS	IDS/KT	-	316
N011	H6	TN14	EZ-Gyro	IDS/EZ-Gamma	IDS	IDS/KT	-	431
N012	H5	TN14	EZ-Gyro	IDS/EZ-Gamma	IDS	IDS/KT	-	389
N013	H6	TN14	EZ-Gyro	IDS/EZ-Gamma	IDS	IDS/KT	-	563
N014	H5	TN14	EZ-Gyro	IDS/EZ-Gamma	IDS	IDS/KT	-	385
N015	H2	TN14	EZ-Gyro	IDS/EZ-Gamma	IDS	IDS/KT	ATV	373
N016	H5	TN14	EZ-Gyro	IDS/EZ-Gamma	IDS	IDS/KT	ATV/OTV	543
N017	H2	TN14az	Sprint-IQ	IDS/EZ-Gamma	IDS	IDS/KT	ATV/OTV	417
N018	H5	TN14az	Sprint-IQ	IDS/EZ-Gamma	IDS	IDS/KT	ATV/OTV	389
N019	H2	TN14az	Sprint-IQ	IDS/EZ-Gamma	IDS	IDS/KT	ATV/OTV	449
N020	H5	TN14az	Sprint-IQ	EZ-Gamma	-	KT	-	343
N021	H2	TN14az	Sprint-IQ	IDS/EZ-Gamma	IDS	KT	ATV/OTV	349
N022	H5	TN14az	Sprint-IQ	EZ-Gamma	-	KT	-	383
N023	H4	TN14az	Sprint-IQ	EZ-Gamma	-	KT	-	240
N024	H2	TN14az	Sprint-IQ	IDS/EZ-Gamma	IDS	KT	ATV/OTV	382
N025	H5	TN14az	Sprint-IQ	EZ-Gamma	-	KT	-	301
N026	H4	TN14az	Sprint-IQ	EZ-Gamma	-	KT	-	253
N027	H5	TN14az	Sprint-IQ	EZ-Gamma	-	KT	-	334
N028	H4	TN14az	Sprint-IQ	EZ-Gamma	-	KT	-	228
N029	H2	TN14az	Sprint-IQ	EZ-Gamma	-	KT	-	367

DDH	Drill Rig	Collar Orient	Hole Survey	Gamma	IP/ Res	Mag Susc	Tele viewer	Samples
N030	H5	TN14az	Sprint-IQ	EZ-Gamma	-	KT	-	287
N031	H4	TN14az	Sprint-IQ	EZ-Gamma	-	KT	-	266
N032	H4	TN14az	Sprint-IQ	EZ-Gamma	-	KT	-	386
N033	H5	TN14az	Sprint-IQ	EZ-Gamma	-	KT	-	300
N034	H5	TN14az	Sprint-IQ	EZ-Gamma	-	KT	-	364
N035	H4	TN14az	Sprint-IQ	EZ-Gamma	-	KT	-	286
N036	H4	TN14az	Sprint-IQ	IDS/EZ-Gamma	IDS	IDS/KT	ATV	222
N037	H2	TN14az	Sprint-IQ	EZ-Gamma	-	KT	-	362
N038	H5	TN14az	Sprint-IQ	IDS/EZ-Gamma	IDS	KT	ATV	370
N039	H2	TN14az	Sprint-IQ	EZ-Gamma	-	KT	-	401
N040	H6	TN14az	Sprint-IQ	EZ-Gamma	-	KT	-	446
N041	H4	TN14az	Sprint-IQ	IDS/EZ-Gamma	IDS	KT	ATV/OTV	281
N042	H5	TN14az	Sprint-IQ	EZ-Gamma	-	KT	-	215
N043	H4	TN14az	Sprint-IQ	EZ-Gamma	-	KT	-	301
N044	16021	TN14az	Sprint-IQ	EZ-Gamma	-	KT	-	412
GT-001	H5	TN14az	Sprint-IQ	EZ-Gamma	-	KT	-	192
N045	16021	TN14az	Sprint-IQ	EZ-Gamma	-	KT	-	348
N046	16021	TN14az	Sprint-IQ	EZ-Gamma	-	KT	-	429
N047	16021	TN14az	Sprint-IQ	EZ-Gamma	-	KT	-	405
S001	MX-79	TN14az	Sprint-IQ	EZ-Gamma	-	KT	-	453
S002	15001	TN14az	Sprint-IQ	IDS/EZ-Gamma	IDS	IDS	ATV	319
S003	MX-79	TN14az	Sprint-IQ	EZ-Gamma	-	IDS	ATV/OTV	422
S004	MX-79	TN14az	Sprint-IQ	IDS/EZ-Gamma	IDS	KT	ATV	432
S005	15001	TN14az	Sprint-IQ	EZ-Gamma	-	KT	ATV/OTV	320
S006	15000	TN14az	Sprint-IQ	IDS/EZ-Gamma	IDS	KT	ATV	209
S007	MX-79	TN14az	Sprint-IQ	EZ-Gamma	-	KT	ATV/OTV	373
S008	15001	TN14az	Sprint-IQ	IDS/EZ-Gamma	IDS	KT	ATV/OTV	280
S009	15000	TN14az	Sprint-IQ	IDS/EZ-Gamma	IDS	KT	ATV/OTV	305
S010	MX-79	TN14az	Sprint-IQ	IDS/EZ-Gamma	IDS	KT	ATV	305
S011	15001	TN14az	Sprint-IQ	IDS/EZ-Gamma	IDS	KT	ATV	250
S012	15000	TN14az	Sprint-IQ	EZ-Gamma	-	KT	-	289
S013	MX-79	TN14az	Sprint-IQ	IDS/EZ-Gamma	-	KT	-	227
S014	15001	TN14az	Sprint-IQ	EZ-Gamma	-	KT	-	322
S015	15000	TN14az	Sprint-IQ	IDS/EZ-Gamma	IDS	KT	ATV	178
S016	MX-79	TN14az	Sprint-IQ	EZ-Gamma	IDS	KT	ATV/OTV	290
S017	15001	TN14az	Sprint-IQ	EZ-Gamma	-	KT	-	302
S018	15000	TN14az	Sprint-IQ	EZ-Gamma	-	KT	-	361
S019	15001	TN14az	Sprint-IQ	IDS/EZ-Gamma	IDS	KT	ATV/OTV	296
S020	MX-79	TN14az	Sprint-IQ	IDS/EZ-Gamma	IDS	KT	ATV/OTV	408
S021	MX-79	TN14az	Sprint-IQ	EZ-Gamma	IDS	KT	ATV/OTV	243
B001	H7	TN14	EZ-Gyro	IDS/EZ-Gamma	IDS	IDS/KT	-	367
B002	H7	TN14	EZ-Gyro	IDS/EZ-Gamma	IDS	IDS/KT	ATV/OTV	478
B003	H7	TN14	EZ-Gyro	IDS/EZ-Gamma	IDS	IDS/KT	-	523
B004	H7	TN14	EZ-Gyro	IDS/EZ-Gamma	IDS	IDS/KT	ATV	462
B005	H7	TN14az	Sprint-IQ	IDS/EZ-Gamma	IDS	IDS/KT	ATV/OTV	503
B006	H7	TN14az	Sprint-IQ	IDS/EZ-Gamma	IDS	IDS/KT	ATV/OTV	318
B007	H7	TN14az	Sprint-IQ	EZ-Gamma	-	KT	-	296

Note:

In the "Gamma," "IP/Res," "Mag Sus," and "Televiewer" columns, the abbreviation "IDS" corresponds to the instrument names. The instrument names are as follows: QL40-GR for Gamma, QL40-IP for IP, QL40-ELOG for Resistivity, and QL40-MGS for Mag Sus. In the Televiewer column, the ATV corresponds with instrument type QL40-ABI and OTV corresponds with instrument type QL40-OBI.

10.2.1 Downhole Geophysical Survey

Oroco undertook downhole electrical and magnetic surveys on selected holes at the Santo Tomás project. The collection of these geophysical datasets has identified distinct petrophysical units, which has assisted the Company with focusing its geological logging of the drill core. In addition, these data will be used to help with plans to re-invert the airborne magnetics and ground 3D DCIP surveys (Section 9). Detail regarding which holes were surveyed by method is presented in Table 10-5.

10.2.2 Downhole Televiewer Survey

Oroco surveyed a select number of holes using Acoustic Televiewer (ATV) and Optical Televiewer (OTV) technologies with the intention of using the results to help calibrate the effectiveness of the Company's oriented core program and to supplement the core geotechnical data collection program. The drill holes surveyed with ATV and OTV techniques are shown in the Table 10-5. The televiewer service provider is currently generating structural interpretations from some of these surveys. The results have yet to be integrated with the structural and rock quality data sets.

10.3 Summary and Interpretation of Relevant Results

The North and South Zone drilling is characterized by broad zones of sulphide mineralization and mineralized zones where copper grades greater than 0.10% Cu. The mineralized zones are proximal to quartz monzonite dikes that intruded the host andesites and limestones. Areas of higher-grade copper mineralization commonly show (post mineral) fault and fracture structural opening caused by tectonic stresses in addition to syn-mineral hydrothermal brecciation resulting from intrusion.

Summarized in Table 10-6 and Table 10-7 is a listing of drill intersections of composite sample intervals where the length-weighted average grade of each composite is equal to or greater than (\geq) 0.4% Cu. These intervals of mineralization comprise ≥ 10 m of contiguous samples with a minimum grade of 0.1% Cu, but may include up to 4 m of samples of $\geq 0.05\%$ Cu in grade. Such intervals are considered to represent intercepts of significant mineralization at the Santo Tomás Project.

Table 10-6 presents such intervals sorted for their location in the North Zone or South Zone, but are otherwise listed by Hole ID. Included in the composite calculations are the molybdenum, gold and silver values for each composite, and a calculation of the "Copper Equivalent" as CuEq%. The CuEq% is calculated as:

$$\text{CuEq} = ((\text{Cu grade} * \text{Cu recovery} * \text{Cu price}) + (\text{Mo grade} * \text{Mo recovery} * \text{Mo price}) + (\text{Au grade} * \text{Au recovery} * \text{Au price}) + (\text{Ag grade} * \text{Ag recovery} * \text{Ag price})) / (\text{Cu price} * \text{Cu recovery})$$
It is assumed that the Santo Tomás Project would produce a conventional (flotation) copper concentrate based on metal recoveries of 84.3% Cu, 66% Mo, 57% Au, and 54% Ag, derived from recent preliminary metallurgical test work on samples from the North Zone (refer Section 13). The commodity prices used are in \$US: Cu \$3.80 /lb, Mo \$12.00 /lb, Au \$1,650 /troy oz and Ag \$22 /troy oz.

In addition, the tables present an estimate of the approximate true width of the presented intercepts. The true width estimate is based upon a generalized estimated attitude of the mineralization (including consideration of lithology and alteration), of $\sim 40^\circ$ to WNW at North Zone, $\sim 35^\circ$ to W at South Zone.

Table 10-7 presents composite intervals generated from the exploration drilling at the Brasiles Prospect. The attitude of mineralization for the calculation of approximate true width at Brasiles Prospect is $\sim 40^\circ$ to the NW.

10.4 Drill Methods

The historical drilling was a mix of diamond drilling for reverse circulation, percussion, and diamond-drill holes.

The drilling undertaken by Oroco has followed a common practice of starting holes in PQ diameter to break rock formations (limestone and faulted limestone contact intervals). This was then followed by a reduction to HQ diameter (HQ or HQ3), and the drill holes were completed with NQ3 diameter.

Owing to challenging access in the southern parts of North Zone, a modified underground rig capable of horizontal drilling was employed to drill holes N044 to N047.

Table 10-6: Listing of Significant Cu Composite Intervals from the North Zone and South Zone

Hole_ID	Zone	From	To	Length (m)	Est. Tr. Width	Cu %	CuEq %	Mo %	Au ppm	Ag ppm	Labels
ST21-N001	North	365	419.2	54.2	53.99	0.55	0.58	0.0073	0.0969	2.568	54.20m @ 0.55 % Cu
ST21-N001	North	439	460.89	21.89	21.81	0.46	0.51	0.0137	0.0527	2.182	21.89m @ 0.46 % Cu
ST21-N001	North	474	523	49	48.81	0.49	0.55	0.0154	0.0294	3.162	49.00m @ 0.49 % Cu
ST21-N002	North	393	407	14	13.95	0.46	0.48	0.0042	0.0601	2.186	14.00m @ 0.46 % Cu
ST21-N002	North	436	451.4	15.4	15.34	0.45	0.5	0.0115	0.0228	3.552	15.40m @ 0.45 % Cu
ST21-N002	North	506	580	74	73.72	0.46	0.51	0.0142	0.0175	3.493	74.00m @ 0.46 % Cu
ST21-N002	North	600	616	16	15.94	0.45	0.49	0.0065	0.0093	4.413	16.00m @ 0.45 % Cu
ST21-N003	North	370	384.3	14.3	14.25	0.5	0.54	0.0085	0.0263	3.329	14.30m @ 0.50 % Cu
ST21-N003	North	456	470	14	13.95	0.46	0.53	0.0209	0.0241	3.857	14.00m @ 0.46 % Cu
ST21-N003	North	476	495	19	18.93	0.55	0.63	0.0227	0.0161	3.947	19.00m @ 0.55 % Cu
ST21-N003	North	510.6	597.7	87.1	86.77	0.45	0.5	0.0123	0.0167	2.972	87.10m @ 0.45 % Cu
ST21-N004	North	434.33	456.2	21.87	21.79	0.46	0.51	0.0113	0.0188	2.809	21.87m @ 0.46 % Cu
ST21-N004	North	468	483	15	14.94	0.46	0.52	0.0171	0.0214	2.341	15.00m @ 0.46 % Cu
ST21-N006	North	65	163	98	97.63	0.51	0.54	0.0025	0.0637	2.885	98.00m @ 0.51 % Cu
ST21-N006	North	171	187	16	15.94	0.46	0.48	0.0041	0.0706	2.631	16.00m @ 0.46 % Cu
ST21-N007	North	335	351.9	16.9	16.84	0.46	0.49	0.003	0.0339	3.96	16.90m @ 0.46 % Cu
ST21-N007	North	352.9	364	11.1	11.06	0.48	0.52	0.0053	0.0392	4.793	11.10m @ 0.48 % Cu
ST21-N007	North	386.2	405.15	18.95	18.88	0.46	0.52	0.0186	0.0262	3.09	18.95m @ 0.46 % Cu
ST21-N008	North	233	319	86	85.67	0.62	0.64	0.0026	0.095	3.248	86.00m @ 0.62 % Cu
ST21-N008	North	325	351	26	25.9	0.49	0.53	0.0136	0.0353	3.008	26.00m @ 0.49 % Cu
ST21-N008	North	411	442	31	30.88	0.46	0.52	0.0127	0.0161	5.062	31.00m @ 0.46 % Cu
ST21-N009	North	438	470	32	31.88	0.68	0.73	0.011	0.0214	4.897	32.00m @ 0.68 % Cu
ST21-N009	North	655.2	665.6	10.4	10.36	0.45	0.5	0.0131	0.01	2.206	10.40m @ 0.45 % Cu
ST21-N009	North	671.35	685	13.65	13.6	0.47	0.52	0.0133	0.0235	2.752	13.65m @ 0.47 % Cu
ST21-N010	North	181	200	19	18.93	0.45	0.47	0.0029	0.0722	2.647	19.00m @ 0.45 % Cu
ST21-N010	North	205.9	286.05	80.15	79.85	0.5	0.54	0.0076	0.0544	3.025	80.15m @ 0.50 % Cu
ST21-N010	North	307	357	50	49.81	0.47	0.54	0.0224	0.0227	3.279	50.00m @ 0.47 % Cu
N011	North	51	63	12	11.95	0.46	0.49	0.0036	0.039	3.55	12.00m @ 0.46 % Cu
N011	North	83	115	32	31.88	0.45	0.48	0.0045	0.083	3.167	32.00m @ 0.45 % Cu
N011	North	150	219	69	68.74	0.52	0.56	0.0079	0.0338	3.902	69.00m @ 0.52 % Cu
N012	North	345	362	17	16.94	0.47	0.52	0.0142	0.0751	3.129	17.00m @ 0.47 % Cu
N012	North	366	382	16	15.94	0.45	0.48	0.0057	0.0553	2.563	16.00m @ 0.45 % Cu
N012	North	386	410.77	24.77	24.68	0.46	0.51	0.0142	0.0287	3.428	24.77m @ 0.46 % Cu

Hole_ID	Zone	From	To	Length (m)	Est. Tr. Width	Cu %	CuEq %	Mo %	Au ppm	Ag ppm	Labels
N012	North	456	497	41	40.84	0.46	0.54	0.0233	0.0174	3.435	41.00m @ 0.46 % Cu
N012	North	529	539	10	9.96	0.46	0.5	0.0104	0.0193	2.645	10.00m @ 0.46 % Cu
N013	North	417	427.32	10.32	10.09	0.46	0.51	0.0117	0.0586	3.964	10.32m @ 0.46 % Cu
N013	North	485	534	49	47.93	0.47	0.53	0.019	0.0185	2.835	49.00m @ 0.47 % Cu
N013	North	584	598	14	13.69	0.47	0.52	0.0157	0.0221	2.971	14.00m @ 0.47 % Cu
N015	North	184.46	253.56	69.1	68.84	0.49	0.52	0.0063	0.0596	3.39	69.10m @ 0.49 % Cu
N015	North	279	304	25	24.9	0.46	0.54	0.0256	0.021	2.999	25.00m @ 0.46 % Cu
N016	North	398	420	22	21.52	0.47	0.5	0.0061	0.0508	2.945	22.00m @ 0.47 % Cu
N016	North	426.61	446.38	19.77	19.34	0.48	0.51	0.0054	0.0429	2.295	19.77m @ 0.48 % Cu
N016	North	481	505	24	23.48	0.47	0.53	0.0151	0.0266	4.925	24.00m @ 0.47 % Cu
N016	North	726	736	10	9.78	0.47	0.51	0.0084	0.035	3.48	10.00m @ 0.47 % Cu
N017	North	109	126.16	17.16	17.09	0.46	0.5	0.0125	0.0306	2.287	17.16m @ 0.46 % Cu
N017	North	153.83	177.09	23.26	23.17	0.49	0.52	0.0096	0.0434	2.458	23.26m @ 0.49 % Cu
N018	North	212	222	10	9.96	0.47	0.52	0.0144	0.0222	3.14	10.00m @ 0.47 % Cu
N018	North	273	290.92	17.92	17.85	0.46	0.52	0.0154	0.0239	2.602	17.92m @ 0.46 % Cu
N019	North	389	409	20	19.92	0.46	0.51	0.0098	0.0234	3.62	20.00m @ 0.46 % Cu
N020	North	223.36	308.23	84.87	84.55	0.53	0.55	0.001	0.1014	2.683	84.87m @ 0.53 % Cu
N020	North	313	331.28	18.28	18.21	0.52	0.56	0.0088	0.0237	2.974	18.28m @ 0.52 % Cu
N021	North	353	380.38	27.38	27.28	0.49	0.53	0.0092	0.0384	4.592	27.38m @ 0.49 % Cu
N021	North	397.52	408.59	11.07	11.03	0.78	0.82	0.0104	0.0362	3.706	11.07m @ 0.78 % Cu
N022	North	50.6	69	18.4	18.33	0.47	0.51	0.0129	0.0991	1.562	18.40m @ 0.47 % Cu
N022	North	95	130	35	34.87	0.51	0.54	0.0079	0.1068	1.919	35.00m @ 0.51 % Cu
N022	North	199	217	18	17.93	0.45	0.48	0.0049	0.0622	2.429	18.00m @ 0.45 % Cu
N023	North	4	55	51	50.81	0.59	0.62	0.0055	0.0571	2.924	51.00m @ 0.59 % Cu
N025	North	24	41.95	17.95	17.88	0.46	0.49	0.0043	0.0494	2.114	17.95m @ 0.46 % Cu
N025	North	67	175	108	107.59	0.51	0.53	0.002	0.0643	2.49	108.00m @ 0.51 % Cu
N025	North	189	216	27	26.9	0.45	0.48	0.003	0.0443	3.388	27.00m @ 0.45 % Cu
N025	North	222	232	10	9.96	0.48	0.51	0.0064	0.0387	3.254	10.00m @ 0.48 % Cu
N026	North	14.9	91	76.1	75.81	0.67	0.71	0.011	0.0644	2.139	76.10m @ 0.67 % Cu
N027	North	93	153	60	59.77	0.56	0.58	0.0012	0.0793	4.25	60.00m @ 0.56 % Cu
N027	North	179	212.2	33.2	33.07	0.52	0.56	0.0031	0.0387	4.899	33.20m @ 0.52 % Cu
N028	North	55	121	66	65.75	0.49	0.53	0.0066	0.0437	3.545	66.00m @ 0.49 % Cu
N029	North	313	337	24	23.18	0.45	0.5	0.0134	0.0218	3.025	24.00m @ 0.45 % Cu
N030	North	103	120.2	17.2	17.13	0.46	0.48	0.0031	0.0744	1.694	17.20m @ 0.46 % Cu
N030	North	136	238	102	101.61	0.52	0.54	0.0008	0.1011	2.937	102.00m @ 0.52 % Cu
N031	North	228.05	240	11.95	11.9	0.45	0.5	0.0117	0.022	2.498	11.95m @ 0.45 % Cu
N032	North	280.34	294	13.66	13.61	0.46	0.48	0.0022	0.0361	3.039	13.66m @ 0.46 % Cu
N032	North	299	315	16	15.94	0.46	0.48	0.0049	0.0356	2.488	16.00m @ 0.46 % Cu
N034	North	192	206	14	13.95	0.45	0.47	0.0037	0.0621	2.3	14.00m @ 0.45 % Cu
N034	North	212	240	28	27.89	0.47	0.5	0.0038	0.0569	3.365	28.00m @ 0.47 % Cu
N034	North	248	287	39	38.85	0.46	0.51	0.0136	0.0517	2.988	39.00m @ 0.46 % Cu
N034	North	329	341	12	11.95	0.48	0.55	0.0219	0.0137	4.35	12.00m @ 0.48 % Cu
N035	North	114	222	108	93.53	0.47	0.5	0.003	0.0679	2.894	108.00m @ 0.47 % Cu
N036	North	110.36	168	57.64	57.64	0.55	0.57	0.0007	0.16	2.822	57.64m @ 0.55 % Cu
N036	North	197	220	23	23	0.46	0.48	0.0019	0.0676	2.975	23.00m @ 0.46 % Cu

Hole_ID	Zone	From	To	Length (m)	Est. Tr. Width	Cu %	CuEq %	Mo %	Au ppm	Ag ppm	Labels
N038	North	314	324	10	10	0.47	0.61	0.0511	0.016	3.02	10.00m @ 0.47 % Cu
N039	North	318	330	12	11.95	0.72	0.77	0.0081	0.0238	5.417	12.00m @ 0.72 % Cu
N039	North	383	393	10	9.96	0.48	0.5	0.0005	0.0114	3.78	10.00m @ 0.48 % Cu
N039	North	473	485	12	11.95	0.45	0.51	0.0178	0.0132	2.726	12.00m @ 0.45 % Cu
N039	North	526	557	31	30.88	0.45	0.48	0.0063	0.0247	2.819	31.00m @ 0.45 % Cu
N039	North	558.75	572	13.25	13.2	0.45	0.5	0.012	0.0187	2.543	13.25m @ 0.45 % Cu
N040	North	526	548	22	18.02	0.45	0.51	0.0142	0.0177	4.191	22.00m @ 0.45 % Cu
N041	North	251	305	54	41.37	0.58	0.6	0.0031	0.0532	3.109	54.00m @ 0.58 % Cu
N042	North	260	381	121	120.54	0.56	0.59	0.0044	0.0798	3.158	121.00m @ 0.56 % Cu
N044	North	289.55	312	22.45	14.43	0.46	0.48	0.0021	0.0472	2.668	22.45m @ 0.46 % Cu
N044	North	328	390	62	39.85	0.51	0.54	0.0033	0.0417	4.457	62.00m @ 0.51 % Cu
N044	North	402	472	70	45	0.59	0.62	0.0013	0.0714	4.329	70.00m @ 0.59 % Cu
N044	North	556	606	50	32.14	0.46	0.49	0.0095	0.0177	2.751	50.00m @ 0.46 % Cu
N045 ^a	North	79	159	80	72.5	0.53	0.57	0.0083	0.0425	3.134	80.00m @ 0.53 % Cu
N045 ^a	North	180	284	104	94.26	0.5	0.53	0.0043	0.0529	3.434	104.00m @ 0.50 % Cu
N045 ^a	North	320	391	71	64.35	0.47	0.55	0.0268	0.018	3.392	71.00m @ 0.47 % Cu
N046 ^a	North	492.55	504	11.45	6.57	0.46	0.48	0.006	0.0301	1.776	11.45m @ 0.46 % Cu
N046 ^a	North	572	607	35	20.08	0.46	0.47	0.0017	0.0449	2.191	35.00m @ 0.46 % Cu
N046 ^a	North	628	730	102	58.5	0.51	0.53	0.0035	0.0429	3.05	102.00m @ 0.51 % Cu
N047 ^a	North	219	322	103	66.21	0.62	0.65	0.0029	0.0855	3.303	103.00m @ 0.62 % Cu
N047 ^a	North	330	440	110	70.71	0.51	0.54	0.0018	0.0461	3.889	110.00m @ 0.51 % Cu
N047 ^a	North	449	464	15	9.64	0.46	0.49	0.0064	0.0272	3.319	15.00m @ 0.46 % Cu
N047 ^a	North	471.5	487	15.5	9.96	0.45	0.49	0.0049	0.0173	4.389	15.50m @ 0.45 % Cu
STD-01	North	15.5	83.6	68.1	52.17	0.67	-	-	-	-	68.10m @ 0.67 % Cu
STD-01	North	97.4	132.3	34.9	26.73	0.46	-	-	-	-	34.90m @ 0.46 % Cu
STD-02	North	65.4	168.5	103.1	78.98	0.52	-	-	-	-	103.10m @ 0.52 % Cu
STD-02	North	258	276.5	18.5	14.17	0.46	-	-	-	-	18.50m @ 0.46 % Cu
STD-02	North	285.7	297.9	12.2	9.35	0.47	-	-	-	-	12.20m @ 0.47 % Cu
STD-03	North	123.4	234.4	111	85.03	0.53	-	-	-	-	111.00m @ 0.53 % Cu
STD-03	North	252.1	279.5	27.4	20.99	0.54	-	-	-	-	27.40m @ 0.54 % Cu
STD-04	North	145.1	182	36.9	28.27	0.48	-	-	-	-	36.90m @ 0.48 % Cu
STD-05	North	9	78.9	69.9	53.55	1.04	-	-	-	-	69.90m @ 1.04 % Cu
STD-05	North	235.5	268.8	33.3	25.51	0.45	-	-	-	-	33.30m @ 0.45 % Cu
STD-08	North	104.2	140.1	35.9	27.5	0.54	-	-	-	-	35.90m @ 0.54 % Cu
STD-08	North	190.2	202.1	11.9	9.12	0.47	-	-	-	-	11.90m @ 0.47 % Cu
STD-08	North	227.2	238	10.8	8.27	0.46	-	-	-	-	10.80m @ 0.46 % Cu
STD-08	North	276.2	306.4	30.2	23.13	0.45	-	-	-	-	30.20m @ 0.45 % Cu
STD-09	North	278.6	304.9	26.3	20.15	0.45	-	-	-	-	26.30m @ 0.45 % Cu
STD-09	North	371.1	384.4	13.3	10.19	0.46	-	-	-	-	13.30m @ 0.46 % Cu
STD-12	North	3.1	20.5	17.4	13.33	0.5	-	-	-	-	17.40m @ 0.50 % Cu
STD-13	North	15.3	47.3	32	24.51	0.46	-	-	-	-	32.00m @ 0.46 % Cu
STD-13	North	211.6	225.4	13.8	10.57	0.45	-	-	-	-	13.80m @ 0.45 % Cu
STD-18	North	195.2	218.2	23	17.62	0.6	-	-	-	-	23.00m @ 0.60 % Cu
STD-18	North	284.3	354.3	70	53.62	0.5	-	-	-	-	70.00m @ 0.50 % Cu
STD-18	North	393.7	411.9	18.2	13.94	0.47	-	-	-	-	18.20m @ 0.47 % Cu

Hole_ID	Zone	From	To	Length (m)	Est. Tr. Width	Cu %	CuEq %	Mo %	Au ppm	Ag ppm	Labels
STD-19	North	20	77.9	57.9	44.35	0.55	-	-	-	-	57.90m @ 0.55 % Cu
STD-20	North	3	22.9	19.9	15.24	0.97	-	-	-	-	19.90m @ 0.97 % Cu
STD-20	North	23.3	131	107.7	82.5	0.64	-	-	-	-	107.70m @ 0.64 % Cu
STD-20	North	131.3	175.4	44.1	33.78	0.47	-	-	-	-	44.10m @ 0.47 % Cu
STD-20	North	215.1	247.4	32.3	24.74	0.49	-	-	-	-	32.30m @ 0.49 % Cu
STD-21	North	149.5	199.6	50.1	38.38	0.5	-	-	-	-	50.10m @ 0.50 % Cu
STD-21	North	205.2	309	103.8	79.52	0.48	-	-	-	-	103.80m @ 0.48 % Cu
STD-23	North	53.5	215.2	161.7	123.87	0.58	-	-	-	-	161.70m @ 0.58 % Cu
STD-23	North	296.8	318.1	21.3	16.32	0.49	-	-	-	-	21.30m @ 0.49 % Cu
STD-27	North	50.1	73.9	23.8	18.23	0.52	-	-	-	-	23.80m @ 0.52 % Cu
STD-27	North	169.3	198.8	29.5	22.6	0.51	-	-	-	-	29.50m @ 0.51 % Cu
STD-27	North	234.5	257.9	23.4	17.93	0.46	-	-	-	-	23.40m @ 0.46 % Cu
STD-27	North	262.8	304.5	41.7	31.94	0.58	-	-	-	-	41.70m @ 0.58 % Cu
STD-27	North	304.8	333.9	29.1	22.29	0.57	-	-	-	-	29.10m @ 0.57 % Cu
STD-28	North	177.9	279.2	101.3	77.6	0.49	-	-	-	-	101.30m @ 0.49 % Cu
STD-29	North	214.5	225.9	11.4	8.73	0.48	-	-	-	-	11.40m @ 0.48 % Cu
STD-29	North	254.9	273.4	18.5	14.17	0.5	-	-	-	-	18.50m @ 0.50 % Cu
STD-40	North	233.7	246.5	12.8	9.81	0.46	-	-	-	-	12.80m @ 0.46 % Cu
STD-40	North	281.6	373.1	91.5	70.09	0.52	-	-	-	-	91.50m @ 0.52 % Cu
STD-41	North	3	41.7	38.7	29.65	0.53	-	-	-	-	38.70m @ 0.53 % Cu
STD-41	North	51.8	64.8	13	9.96	0.47	-	-	-	-	13.00m @ 0.47 % Cu
STD-41	North	124	137.8	13.8	10.57	0.48	-	-	-	-	13.80m @ 0.48 % Cu
STD-42	North	32.5	102.9	70.4	53.93	0.69	-	-	-	-	70.40m @ 0.69 % Cu
STD-42	North	159.5	171.6	12.1	9.27	0.52	-	-	-	-	12.10m @ 0.52 % Cu
STD-42	North	197.1	223.5	26.4	20.22	0.5	-	-	-	-	26.40m @ 0.50 % Cu
STD-42	North	261.2	273.4	12.2	9.35	0.49	-	-	-	-	12.20m @ 0.49 % Cu
STD-43	North	74.9	88.2	13.3	10.19	0.47	-	-	-	-	13.30m @ 0.47 % Cu
STD-43	North	118.7	159.1	40.4	30.95	0.47	-	-	-	-	40.40m @ 0.47 % Cu
STD-43	North	168.2	196.9	28.7	21.99	0.51	-	-	-	-	28.70m @ 0.51 % Cu
STD-44	North	144	328	184	140.95	0.51	-	-	-	-	184.00m @ 0.51 % Cu
STD-45	North	60	92	32	24.51	0.48	-	-	-	-	32.00m @ 0.48 % Cu
STD-45	North	144	248	104	79.67	0.57	-	-	-	-	104.00m @ 0.57 % Cu
STD-45	North	284	300	16	12.26	0.45	-	-	-	-	16.00m @ 0.45 % Cu
STD-45	North	312	370	58	44.43	0.59	-	-	-	-	58.00m @ 0.59 % Cu
STD-46	North	24	36	12	9.19	0.48	-	-	-	-	12.00m @ 0.48 % Cu
STD-46	North	52	212	160	122.57	0.6	-	-	-	-	160.00m @ 0.60 % Cu
STD-47	North	8	76	68	52.09	0.45	-	-	-	-	68.00m @ 0.45 % Cu
STD-47	North	84	108	24	18.39	0.45	-	-	-	-	24.00m @ 0.45 % Cu
STD-47	North	120	192	72	55.16	0.45	-	-	-	-	72.00m @ 0.45 % Cu
STD-47	North	216	276	60	45.96	0.5	-	-	-	-	60.00m @ 0.50 % Cu
STD-48	North	224	382.6	158.6	121.49	0.49	-	-	-	-	158.60m @ 0.49 % Cu
STD-49	North	132	144	12	9.19	0.48	-	-	-	-	12.00m @ 0.48 % Cu
STD-49	North	152	172	20	15.32	0.47	-	-	-	-	20.00m @ 0.47 % Cu
STD-49	North	180	324	144	110.31	0.52	-	-	-	-	144.00m @ 0.52 % Cu
STE-01	North	30	98	68	52.09	0.46	-	-	-	-	68.00m @ 0.46 % Cu

Hole_ID	Zone	From	To	Length (m)	Est. Tr. Width	Cu %	CuEq %	Mo %	Au ppm	Ag ppm	Labels
STE-05	North	16	32	16	12.26	0.47	-	-	-	-	16.00m @ 0.47 % Cu
STE-07	North	30	50	20	15.32	0.46	-	-	-	-	20.00m @ 0.45 % Cu
STE-07	North	56	80	24	18.39	0.46	-	-	-	-	24.00m @ 0.46 % Cu
STE-08	North	12	30	18	13.79	0.78	-	-	-	-	18.00m @ 0.78 % Cu
STE-08	North	40	66	26	19.92	0.46	-	-	-	-	26.00m @ 0.46 % Cu
STE-09	North	0	74	74	56.69	0.76	-	-	-	-	74.00m @ 0.76 % Cu
STE-10	North	10	54	44	33.71	0.52	-	-	-	-	44.00m @ 0.52 % Cu
STE-11	North	0	64	64	49.03	0.46	-	-	-	-	64.00m @ 0.46 % Cu
STE-13	North	6	80	74	56.69	0.48	-	-	-	-	74.00m @ 0.48 % Cu
STE-14	North	0	80	80	61.28	1.14	-	-	-	-	80.00m @ 1.14 % Cu
STE-15	North	48	80	32	24.51	0.67	-	-	-	-	32.00m @ 0.67 % Cu
STE-16	North	24	80	56	42.9	0.48	-	-	-	-	56.00m @ 0.48 % Cu
STE-17	North	12	24	12	9.19	0.47	-	-	-	-	12.00m @ 0.47 % Cu
STE-19	North	4	30	26	19.92	0.48	-	-	-	-	26.00m @ 0.48 % Cu
STE-21	North	2	40	38	29.11	0.58	-	-	-	-	38.00m @ 0.58 % Cu
STE-22	North	68	80	12	9.19	0.46	-	-	-	-	12.00m @ 0.46 % Cu
STE-23	North	56	70	14	10.72	0.45	-	-	-	-	14.00m @ 0.45 % Cu
STE-24	North	6	86	80	61.28	0.58	-	-	-	-	80.00m @ 0.58 % Cu
STE-24	North	98	122	24	18.39	0.46	-	-	-	-	24.00m @ 0.46 % Cu
STE-25	North	14	40	26	19.92	0.46	-	-	-	-	26.00m @ 0.46 % Cu
STE-25	North	46	114	68	52.09	0.52	-	-	-	-	68.00m @ 0.52 % Cu
STE-26	North	0	108	108	82.73	0.85	-	-	-	-	108.00m @ 0.85 % Cu
STE-27	North	0	30	30	22.98	0.46	-	-	-	-	30.00m @ 0.46 % Cu
STE-28	North	0	30	30	28.98	0.59	-	-	-	-	30.00m @ 0.59 % Cu
STE-28	North	36	62	26	25.11	0.95	-	-	-	-	26.00m @ 0.95 % Cu
STE-29	North	50	130	80	61.28	0.48	-	-	-	-	80.00m @ 0.48 % Cu
STE-38	North	52	70	18	13.79	0.66	-	-	-	-	18.00m @ 0.66 % Cu
STE-51	North	32	56	24	22.55	0.67	-	-	-	-	24.00m @ 0.67 % Cu
STE-61	North	142	154	12	11.28	0.46	-	-	-	-	12.00m @ 0.46 % Cu
STE-62	North	62	128	66	63.75	0.51	-	-	-	-	66.00m @ 0.51 % Cu
STE-62	North	150	164	14	13.52	0.46	-	-	-	-	14.00m @ 0.46 % Cu
STE-62	North	180	198	18	17.39	0.47	-	-	-	-	18.00m @ 0.47 % Cu
STE-63	North	0	84	84	82.72	0.47	-	-	-	-	84.00m @ 0.47 % Cu
STE-63	North	90	116	26	25.61	0.46	-	-	-	-	26.00m @ 0.46 % Cu
S001	South	186	234	48	48	0.46	0.49	0.0027	0.0364	4.091	48.00m @ 0.46 % Cu
S001	South	258	274	16	16	0.47	0.49	0.0039	0.0645	2.392	16.00m @ 0.47 % Cu
S002	South	268	279	11	11	0.47	0.59	0.0405	0.012	4.596	11.00m @ 0.47 % Cu
S003	South	315	377.2	62.2	62.2	0.57	0.6	0.0055	0.0286	4.001	62.20m @ 0.57 % Cu
S004	South	132	145	13	13	0.62	0.65	0.0015	0.0535	5	13.00m @ 0.62 % Cu
S004	South	167	215	48	48	0.47	0.49	0.0005	0.0836	2.787	48.00m @ 0.47 % Cu
S004	South	239	263	24	24	0.48	0.5	0.0037	0.0488	2.37	24.00m @ 0.48 % Cu
S006	South	109.8	182.1	72.3	72.3	0.46	0.48	0.0024	0.0792	2.824	72.30m @ 0.46 % Cu
S012	South	177	211	34	34	0.56	0.59	0.0022	0.0511	4.106	34.00m @ 0.56 % Cu
S015	South	23	45.7	22.7	22.7	0.48	0.52	0.0097	0.026	2.621	22.70m @ 0.48 % Cu
S015	South	78.4	126	47.6	47.6	0.53	0.61	0.0273	0.0341	2.335	47.60m @ 0.53 % Cu

Hole_ID	Zone	From	To	Length (m)	Est. Tr. Width	Cu %	CuEq %	Mo %	Au ppm	Ag ppm	Labels
S016	South	158	171	13	11.78	0.47	0.51	0.0025	0.055	5.927	13.00m @ 0.47 % Cu
S016	South	198	211	13	11.78	0.47	0.49	0.0036	0.02	3.499	13.00m @ 0.47 % Cu
S016	South	226	302	76	68.88	0.46	0.48	0.0019	0.036	2.629	76.00m @ 0.46 % Cu
S016	South	308	332	24	21.75	0.46	0.49	0.0047	0.028	2.658	24.00m @ 0.46 % Cu
S016	South	416	437.11	21.11	19.13	0.46	0.53	0.0215	0.0342	2.213	21.11m @ 0.46 % Cu
S018	South	80	252	172	161.63	0.52	0.56	0.0115	0.0401	2.451	172.00m @ 0.52 % Cu
S018	South	260	274	14	13.16	0.46	0.48	0.0049	0.0259	1.807	14.00m @ 0.46 % Cu
S018	South	312	326	14	13.16	0.47	0.5	0.0047	0.0241	2.243	14.00m @ 0.47 % Cu
S020	South	142.55	195	52.45	52.45	0.47	0.51	0.0109	0.0309	2.182	52.45m @ 0.47 % Cu
S020	South	254	264	10	10	0.46	0.51	0.0173	0.0399	2.59	10.00m @ 0.46 % Cu
S021	South	207	232	25	25	0.72	0.78	0.0141	0.0268	3.648	25.00m @ 0.72 % Cu
STD-31	South	147.4	175.4	28	22.94	0.65	-	-	-	-	28.00m @ 0.65 % Cu
STD-31	South	255.4	275.4	20	16.38	0.67	-	-	-	-	20.00m @ 0.67 % Cu
STD-35	South	94.4	106.4	12	9.83	0.5	-	-	-	-	12.00m @ 0.50 % Cu
STD-35	South	114.4	162.4	48	39.32	0.54	-	-	-	-	48.00m @ 0.54 % Cu
STD-36	South	144	180	36	29.49	0.45	-	-	-	-	36.00m @ 0.45 % Cu
STD-36	South	224	236	12	9.83	0.5	-	-	-	-	12.00m @ 0.50 % Cu
STD-36	South	240	256	16	13.11	0.47	-	-	-	-	16.00m @ 0.47 % Cu
STD-36	South	316	336	20	16.38	0.54	-	-	-	-	20.00m @ 0.54 % Cu
STD-36	South	344	368	24	19.66	0.49	-	-	-	-	24.00m @ 0.49 % Cu
STD-37	South	50	146	96	78.64	0.49	-	-	-	-	96.00m @ 0.49 % Cu
STD-39	South	135	203	68	55.7	0.47	-	-	-	-	68.00m @ 0.47 % Cu
STD-50	South	95	107	12	9.83	0.49	-	-	-	-	12.00m @ 0.49 % Cu
STD-50	South	151	179	28	22.94	0.45	-	-	-	-	28.00m @ 0.45 % Cu
STD-50	South	239	263	24	19.66	0.49	-	-	-	-	24.00m @ 0.49 % Cu
STD-50	South	271	303	32	26.21	0.45	-	-	-	-	32.00m @ 0.45 % Cu
STD-50	South	335	370.45	35.45	29.04	0.47	-	-	-	-	35.45m @ 0.47 % Cu
STE-52	South	56	68	12	9.83	0.45	-	-	-	-	12.00m @ 0.45 % Cu
STE-52	South	86	114	28	22.94	0.45	-	-	-	-	28.00m @ 0.45 % Cu
STE-53	South	108	118	10	8.19	0.45	-	-	-	-	10.00m @ 0.45 % Cu

Note:

^a These intercepts are not included in the MRE presented in Section 14 of this report.

The table lists composite sample intervals where the length-weighted average grade of each composite $\geq 0.4\%$ Cu. The composites ≥ 10 m of contiguous samples with a minimum grade of 0.1% Cu, but may include up to 4 m of samples of $\geq 0.05\%$ Cu in grade.

Table 10-7: Listing of Significant Cu Composite Intervals from the Braziles Prospect Exploration Drilling

Hole_ID	Zone	From	To	Length (m)	Est. Tr. Width	Cu %	CuEq %	Mo %	Au ppm	Ag ppm	Labels
B003	Bras	450	505	55	54.79	0.48	0.52	0.009	0.0702	4.657	55.00m @ 0.48 % Cu
B003	Bras	555	569	14	13.95	0.47	0.52	0.008	0.0241	5.17	14.00m @ 0.47 % Cu
B004	Bras	398	412	14	12.12	0.45	0.50	0.013	0.0314	2.729	14.00m @ 0.45 % Cu
B005	Bras	428	465	37	36.81	0.51	0.54	0.004	0.0573	3.996	36.95m @ 0.51 % Cu
B007	Bras	609	637	28	27.89	0.46	0.50	0.008	0.0718	4.257	28.00m @ 0.46 % Cu

B007	Bras	649	671	22	21.92	0.45	0.52	0.017	0.0665	4.333	22.00m @ 0.45 % Cu
------	------	-----	-----	----	-------	------	------	-------	--------	-------	--------------------

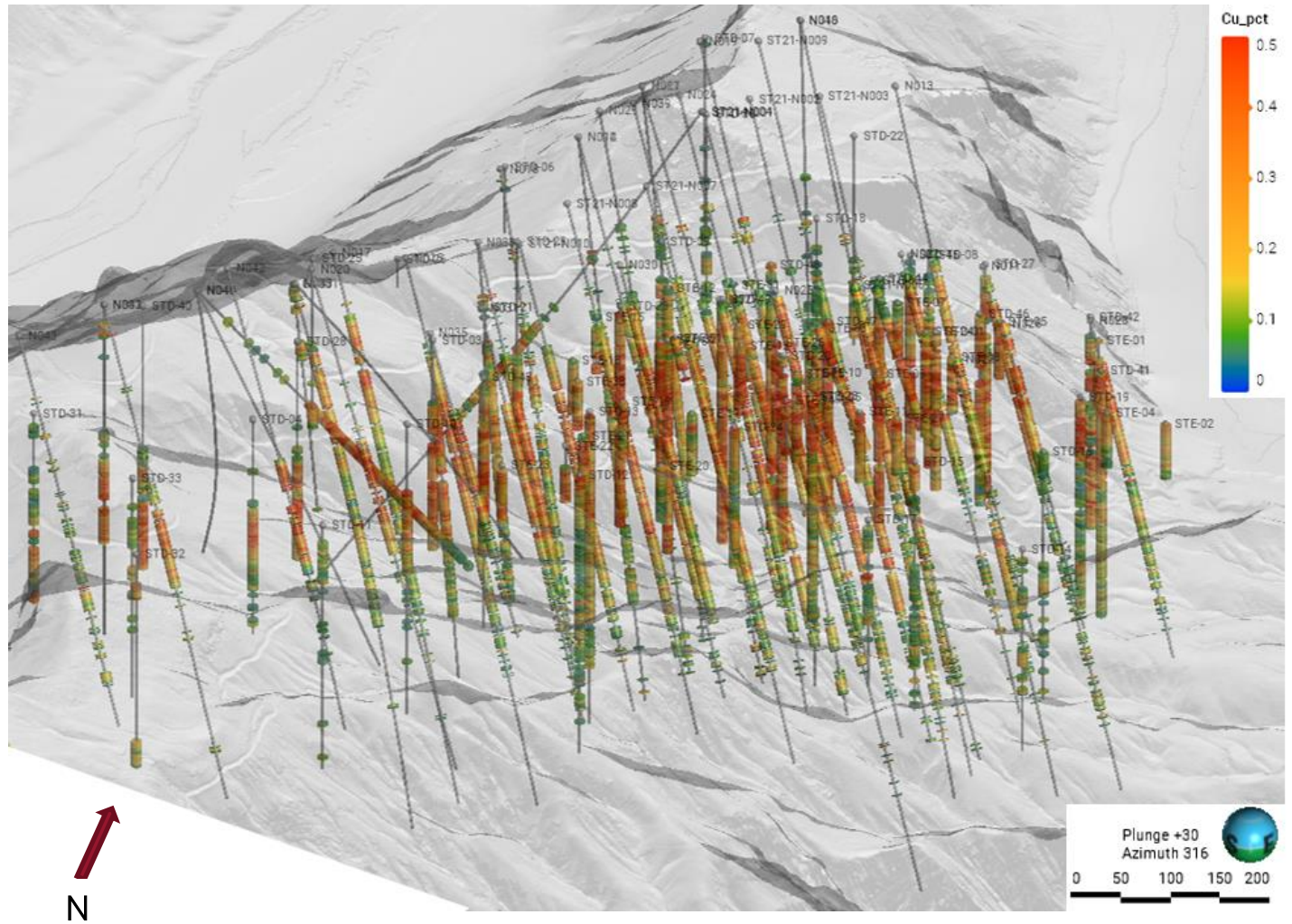
10.5 North Zone Drilling

The North Zone has been the focus of historical drilling campaigns and the contemporary program of drilling undertaken by Oroco. Historically prioritization was driven by the dominance of mineralized outcrop along the eastern ridge of the North Zone. Drilling by Oroco prioritized the North Zone to confirm and extend historical results, and to test the areas of highest interest indicated by chargeability determined from the 3D DCIP survey. The North Zone is drilled at the closest spacing on the Property. The along-strike continuity of the North Zone historical drilling results and the subsequent drilling by Oroco is best viewed from the SE toward the NE (Figure 10-5 and Figure 10-6).

Based upon historical geostatistics and a preliminary structural and lithological understanding of the North Zone (as presented in Bridge, 2020), the Oroco drill program sought to drill predominantly on azimuth 110° and most commonly angled at -55°. The intent was to generate near true width intercepts of the geology and mineralization. Drill holes were extended so that a significant number of holes would drill across the North Zone deposit from hanging wall, through mineralization and into the footwall. This pattern was maintained for the majority of the program, though hole ST21-N004 was drilled to the SW to infill an area for which collar locations due to access were not available. Drill hole ST21-N004 also tested an IP feature that suggested mineralization to the west of the mineralization known from historical work.

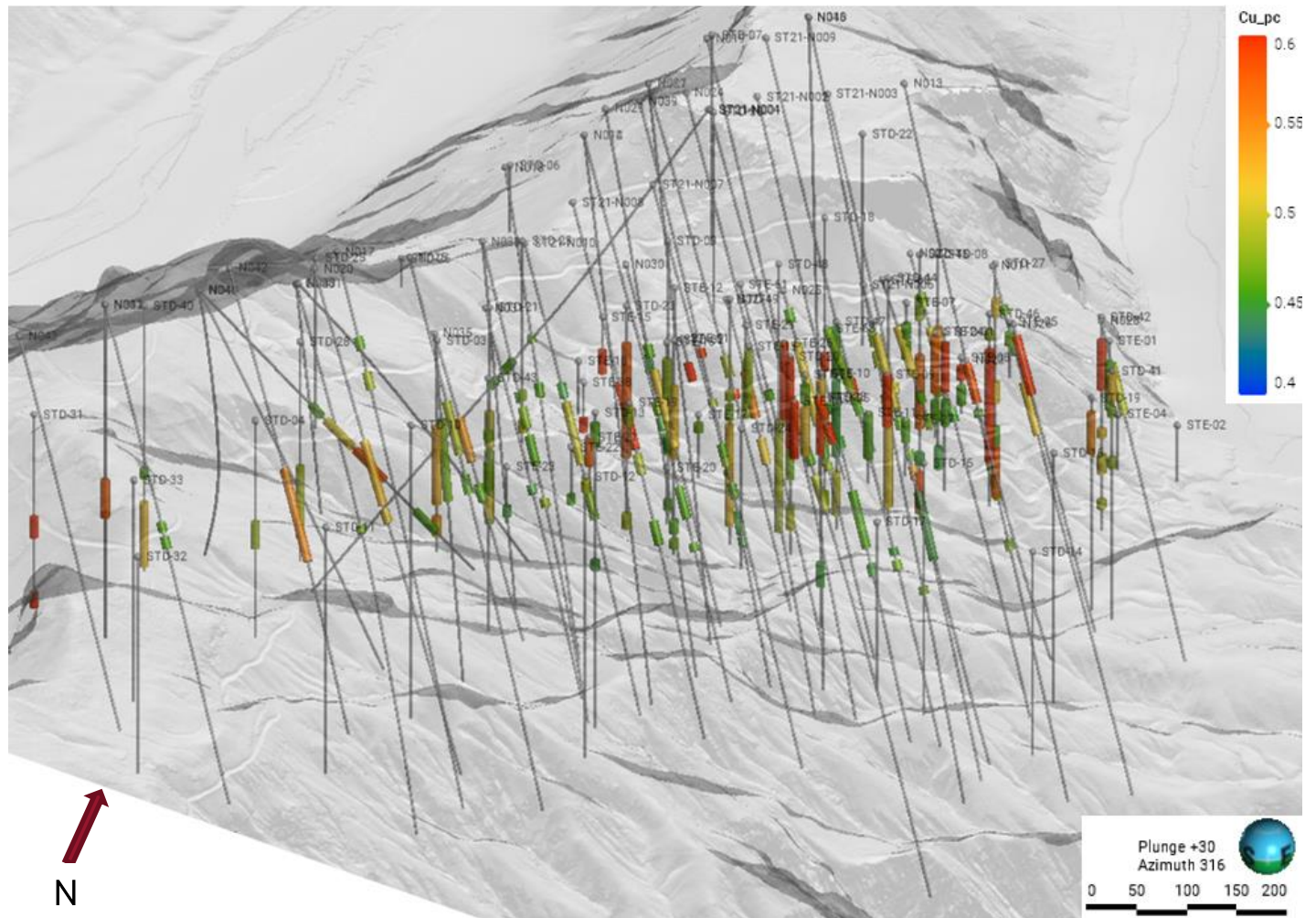
Holes N044 through N047 were drilled using a modified underground drill rig to allow flat and shallow angle drilling, also to solve the challenge of steep and inaccessible terrain at locations that would have maintained the general drilling pattern. Only the assay results of N044 are included in this MRE.

Figure 10-5: View of North Zone historical and contemporary drilling through topography showing thematic assay sample results. Data for GT001 and N045 through N047 are excluded



Source: Oroco, 2023.

Figure 10-6: View of North Zone historical and contemporary drilling through topography showing the disposition of the Significant Cu Composite Intervals from the North Zone as Listed in Table 10-5



Source: Oroco, 2023.

The layout of the North Zone drilling program also sought to intersect major structural features that had been mapped at surface. Hole ST21-N004 sought also to test the existence of a large monzonite body mapped/inferred by the SGM and to define a potential basement contact. Several of the historical drill holes were terminated while still in mineralization. The drill holes completed by Oroco continued into the footwall, allowing for appropriate domain limiting of mineralization and definition of the footwall alteration suite.

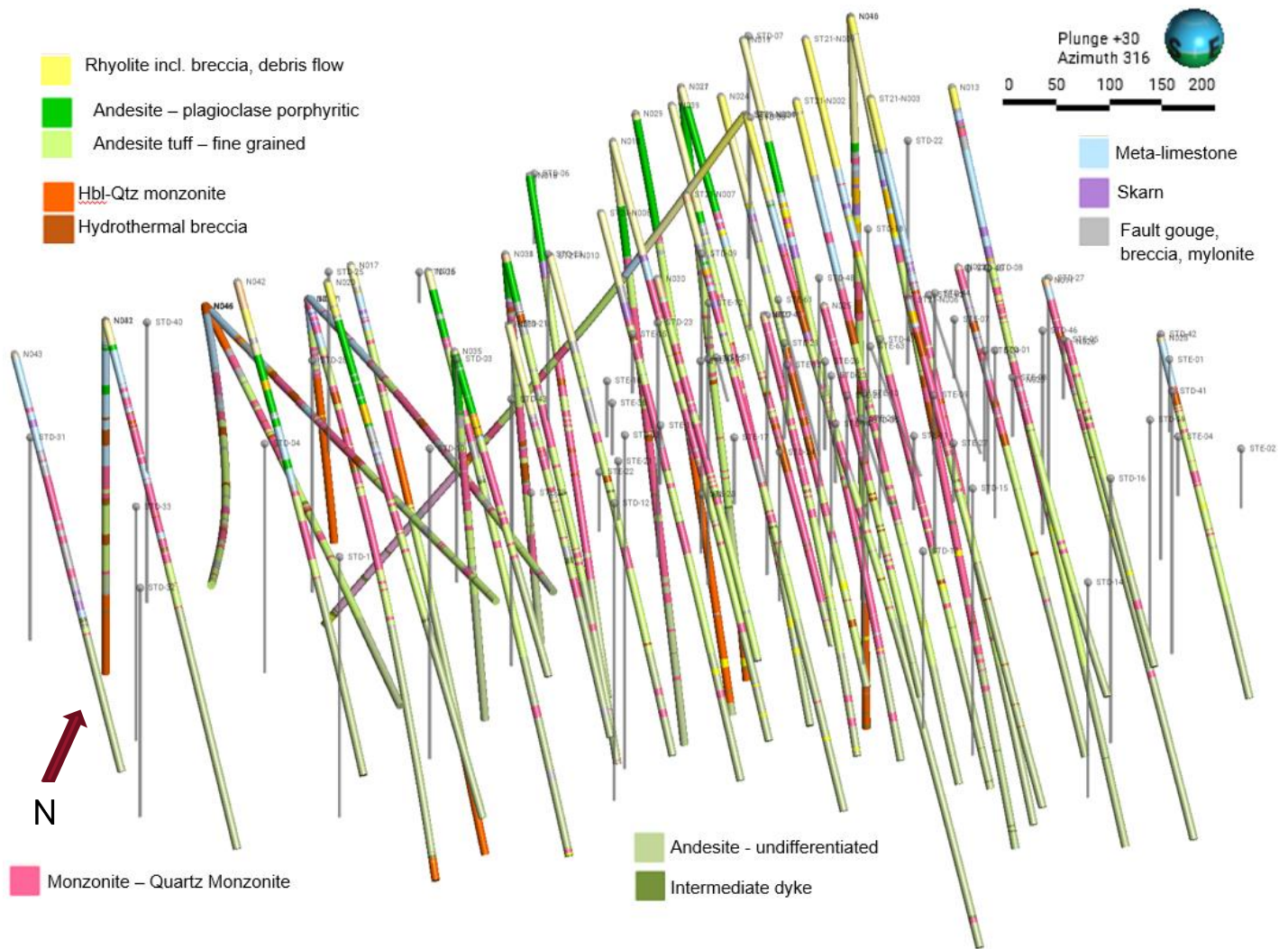
North Zone drilling commenced on the central part of the Zone and targeted the intermediate depth parts of the historically defined mineralized system, as defined by the historical grade shell (Bridge 2020). Drilling progressed northward and southward, and then began to test the areas of potential deeper development of the system as indicated by the chargeability by drilling from the western slope of the ridge and from the NNW-ern spine of the ridge (to test the deep mineralization at the north end of North Zone). Late in the program the shallower eastern ridge was angle drilled to

confirm and infill some of the historical work, and to properly drill into the footwall and so to define the base of mineralization to the north.

As work progressed, the good correlation between resistivity and areas of potassic alteration that host mineralization was recognized: this feature has become a factor considered in drill hole targeting.

Geological modeling of the North Zone is largely constrained by the geological logging by Oroco of the drill core. The Company also recovered and re-boxed some of the historical core that had been located at the El Bienestar Ranch location (as described in Bridge, 2020). The disposition of the logged lithologies in the North Zone drilling by Oroco is displayed in Figure 10-7.

Figure 10-7: View of North Zone historical and contemporary drilling absent topography and displaying key logged lithologies used to constrain geological modeling in the North Zone

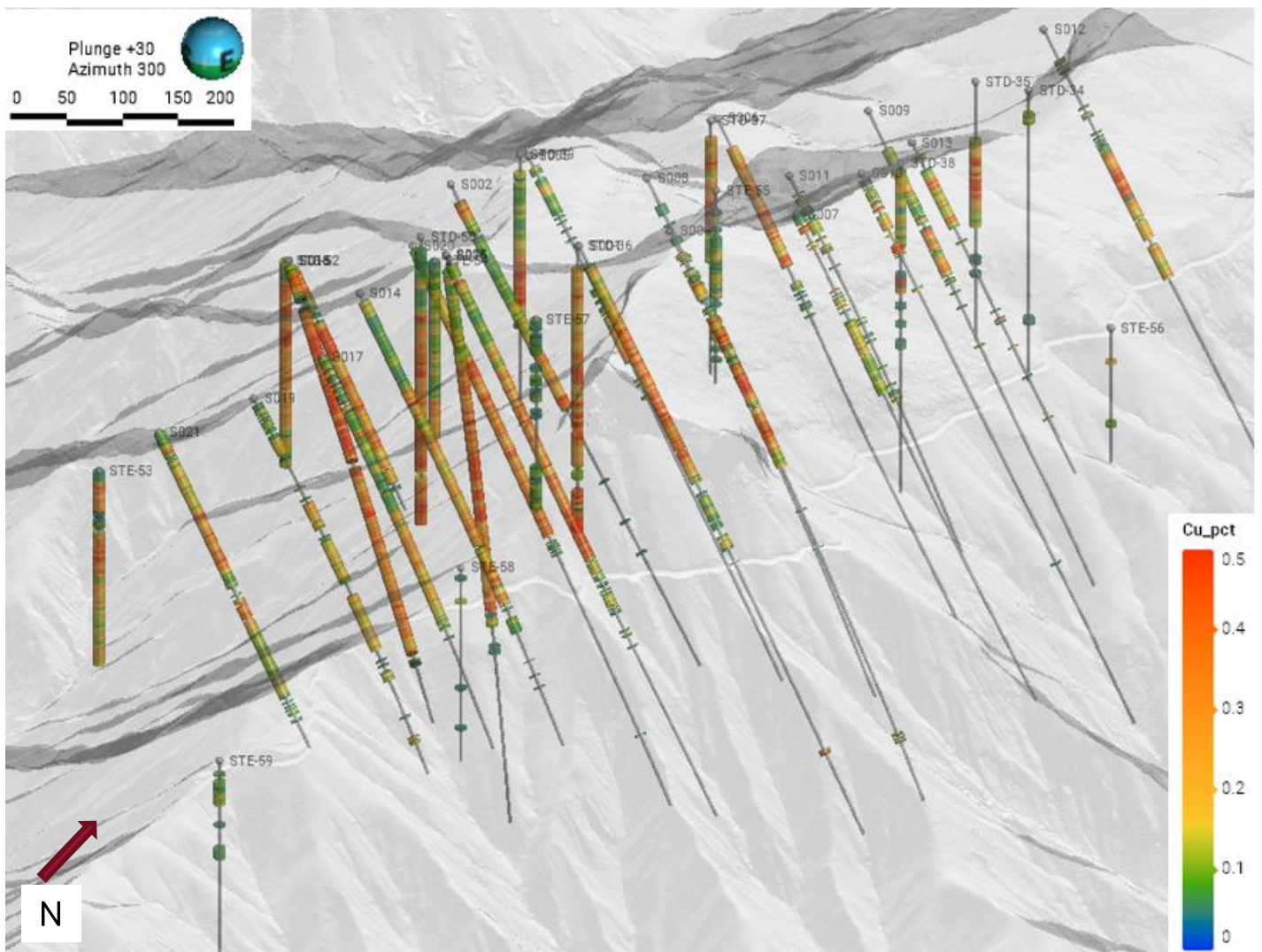


Source: Oroco, 2023.

10.6 South Zone Drilling

Historical drilling in the South Zone (Figure 10-8) was widely spaced and undertaken to explore for a potentially fault-displaced, southern extension of North Zone copper mineralization (Bridge, 2020). Two of the historical holes intersected good mineralization (STD-50 intersected 192m of 0.37% Cu at a 0.3% Cu Cut-off (from 111 m depth) and STD-36 intersected 208m of 0.32% Cu (from 28 m) and two deeper intercepts of 20.0 m of 0.54% and 24.0 m of 0.49% Cu at a 0.3% Cu cut-off: both holes bottomed in mineralization). The first intercept is longer than cited in Table 10-6, but of lower composite grade.

Figure 10-8: View of South Zone Historical and Contemporary Drilling through Topography showing Thematic Assay Sample Results Data



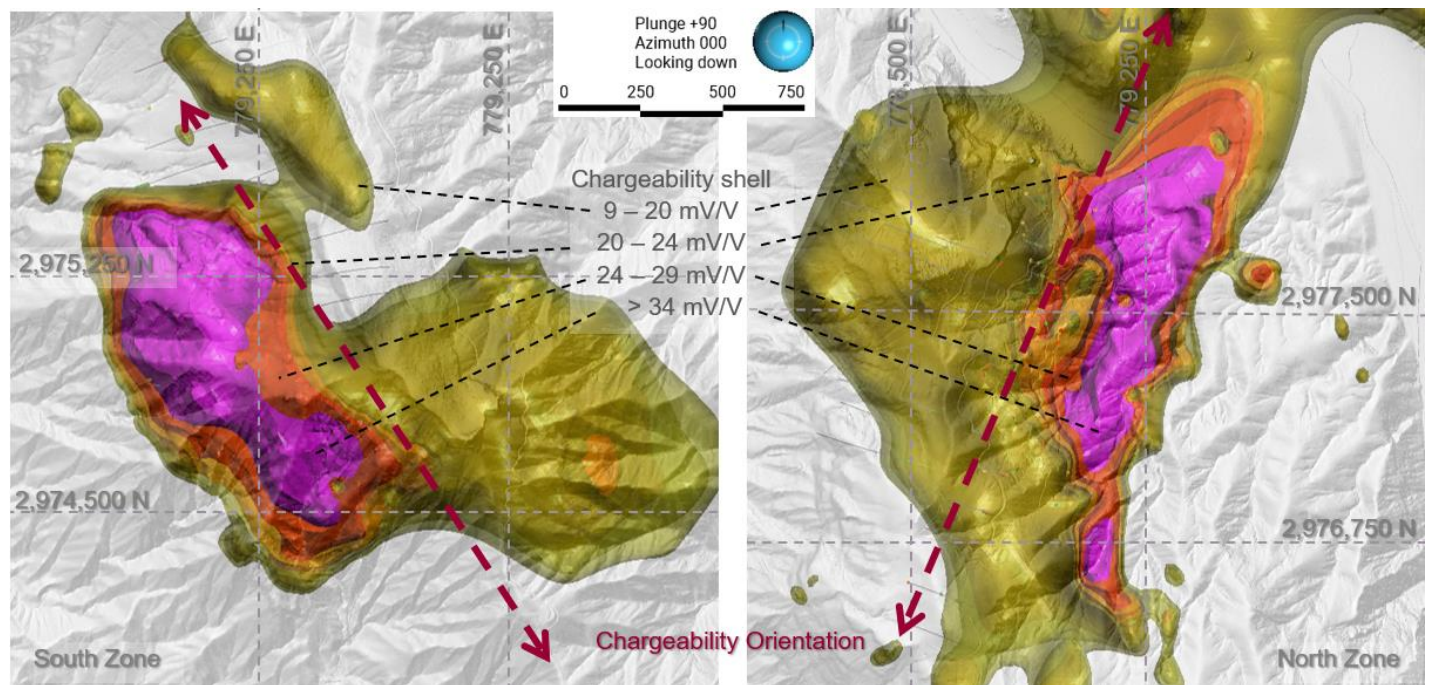
Source: Oroco, 2023.

These historical results strongly supported an Oroco drilling campaign at South Zone. Phase 1 drilling, comprising of 21 holes, was undertaken by Oroco at South Zone in 2022 and was completed in early 2023. The detection of extensive volumes comprising target chargeability and resistivity ranges that correlate well with areas of well developed and pervasive mineralization at North Zone were also isolated in the South Zone coverage by the 3D DCIP survey.

The South Zone drilling program successfully defined areas of mineralization in the north part of South Zone and in general confirmed buried chargeability features. Drilling has begun to delineate an area of more pervasive, extensive and coherent mineralization in the southern part of the South Zone that also correlates well with chargeability trends. Surface mapping and sampling has located strong zones of alteration and mineralization above the geophysical anomalies. This area of mineralization has not been fully defined or constrained by the Phase 1 drilling and remains open to the west and southwest.

The layout of the South Zone drilling program also sought to test structural features that had been mapped at surface, and to begin to define a lower (potentially structural) contact between the western extent of South Zone and basement granodioritic rocks. Based upon some preliminary observations of possible structures and the orientation of the 3D DCIP defined chargeability shells at South Zone – which differed from North Zone in apparent expression as is shown in Figure 10-9 below, the drilling at South Zone has been targeted on azimuth 070° and typically dipping at -55°. For reasons of ready access, hole S018 was drilled at 100° and -35° dip and S016 was drilled at -80° from the S003 setup.

Figure 10-9: View of South Zone (left) and North Zone (right) chargeability shells from the unconstrained 3D DCIP inversion, showing the apparent orientation of each zone



Source: Oroco, 2023.

Key historical drill holes, including STD-50 and STD-36 bottomed in good mineralization. The drill holes completed by Oroco continue well into the footwall, allowing for appropriate bracketing of mineralization and confident recognition of the footwall alteration suite.

Logging and consideration of the vein orientation data at South Zone are being reviewed with respect to the 070° drilling orientation azimuth. It is possible that future drilling will be oriented for a drill azimuth that targets a predominant vein orientation to the south of due east.

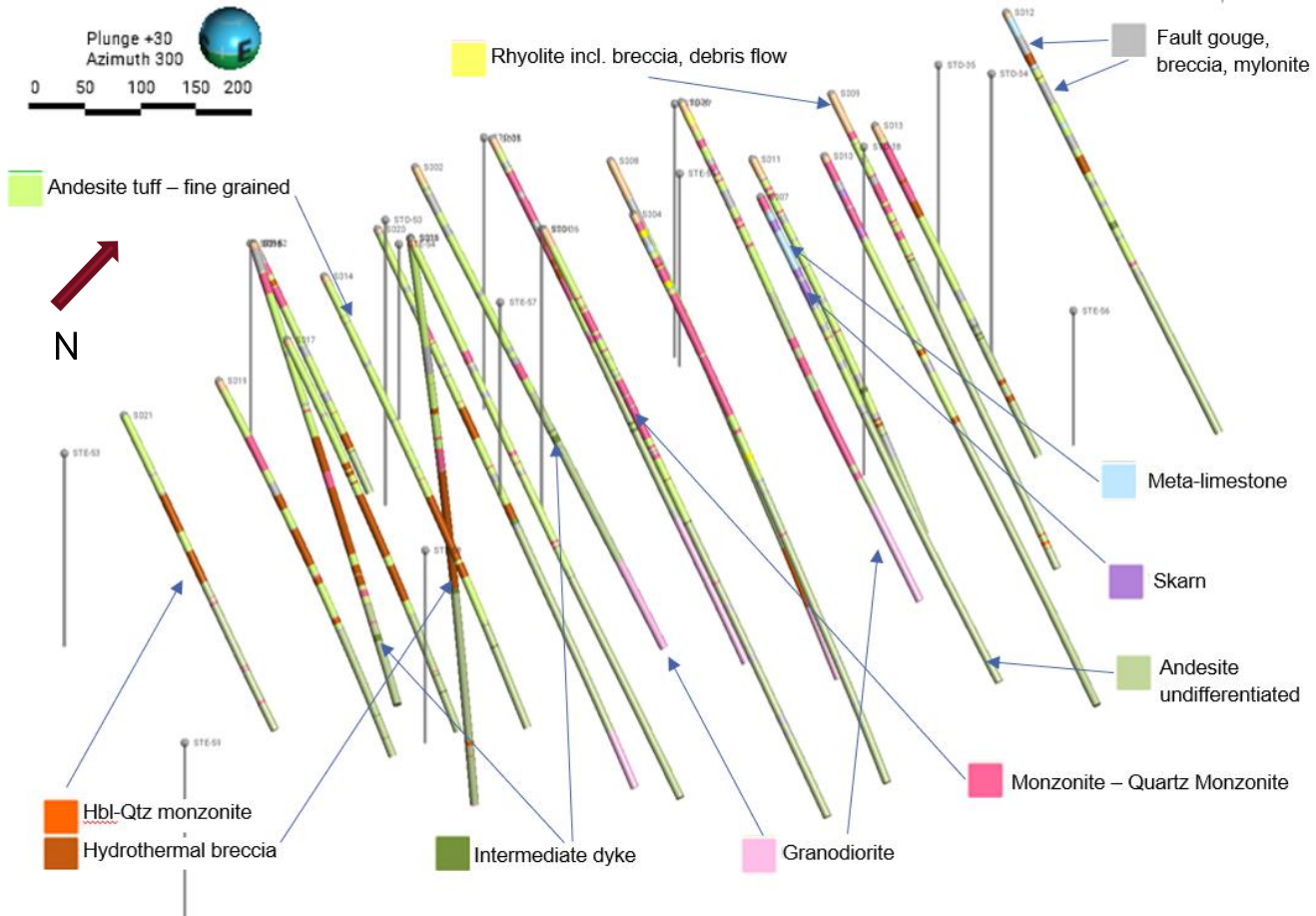
Drilling commenced in the central latitude of South Zone and initially progressed northward: some of the proposed holes in the northern sector were delayed once initial results suggested there may be greater promise southward, and holes N015 through N021 sought to define the potential south of the initial holes.

A program to confirm the locations of historical collars resulted in the discovery of collars for some of the South Zone holes at significant offset from the locations initially derived from the repositioning of historical grid locations as presented in Bridge. Hole STD-50 was found to be located significantly south (150 m) of the originally presumed location.

Drilling at South Zone intersected some compelling grade-width intersections using a 0.3% copper cut-off. Hole S016 intersected 349.2 m of 0.36% Cu; hole S018 returned two significant intersections of 187.9 m of 0.51% and 234.3 m of 0.34% respectively; hole S003 returned 277.4 m of 0.34% Cu; S001 drilled 271 m of 0.33% Cu; S020 returned 221.7 m of 0.37% Cu and S015 drilled 179.2 m of 0.36% Cu.

Geological modeling of the South Zone is largely constrained by the geological logging by Oroco of the drill core. The Company recovered and re-boxed some of the historical core that had been located at the El Bienestar Ranch location (as described in Bridge, 2020). The disposition of the logged lithologies in the South Zone drilling by Oroco is displayed in Figure 10-10. The existence of significantly brecciated zones in key holes of central latitude South Zone (S003, S016 and S018/15) has presented some challenges in modeling and will require some infill and drill section extensions to increase resolution of the preliminary MRE model.

Figure 10-10: View of South Zone historical and contemporary drilling absent topography and displaying key logged lithologies used to constrain geological modeling in the South Zone



Source: Oroco, 2023.

10.7 Geological Logging

Diamond core drill holes have been geologically logged for lithology, structure, alteration, vein types and mineralization. Select samples were stained to highlight feldspar compositions at an on-site rock staining facility. Particular attention was paid to structural geology feature logging. Much of the core on the project was oriented core, and structural and geotechnical data was recorded in true orientation where core orientation was achieved. All drill core was logged prior to sampling.

10.8 Recovery

Core recovery was systematically recorded from the commencement of coring to end of hole, by reconciling against driller's depth blocks in each core box. Core recoveries are typically between 90% to 100% with isolated zones of lower

recover. No sample bias has been identified associated with core loss. Core recoveries are typically between 90% to 100% with isolated zones of lower recovery associated with fault zones. Core loss is marked in the core box by the drillers at the time of drilling.

10.9 Geological and Hydrological Drilling

Geotechnical Rock Quality Designation (RQD) data was collected from the commencement of Oroco-supervised exploration drilling. The geotechnical data collection protocols were trained and implemented by SRK at the commencement of drilling. Owing to SARS-COV2 epidemic, initial training was done remotely: an audit by SRK early in the program showed that initial data is reliable for RQD, though some consistency improvements were made. UCS measurements were taken systematically through the program by on-site point load testing.

Preliminary recommendations for geotechnical and hydrogeological investigations have been received, but holes drilled on azimuths that would broaden the representativity of data for geotechnical purposes have not been drilled yet. A program for piezometer installation has been proposed for future implementation.

11 SAMPLE PREPARATION, ANALYSES AND SECURITY

11.1 Sampling Methods

11.1.1 Historical Sampling Methods

According to Spring (1992) and Thornton (2011), historically the drill core was logged at the El Bienestar Ranch facility south of the Santo Tomás deposit areas. Facilities for sawing the drill core and crushing and riffing the samples were maintained on-site (Thornton, 2011).

The drill core was oriented and marked for sampling by the geologist. For all diamond-drill core, the intervals selected for sampling were cut in half using either a diamond saw or with a mechanical splitter. The mechanical splitter was used on samples where it was suspected that the cooling water for the saw might wash out the copper minerals. One half of the core was retained in the core box for further consideration and the other half was placed in properly marked sample bags for shipment to the laboratory (Thornton, 2011).

Sample lengths varied to reflect the geology and mineralization. ASARCO assayed at various lengths, generally between 1 and 3 m (Spring, 1992). Where no visible mineralization was encountered, sample lengths of 4 m or greater were assayed. Exall prepared samples of 2 m lengths (Thornton, 2011) for assaying.

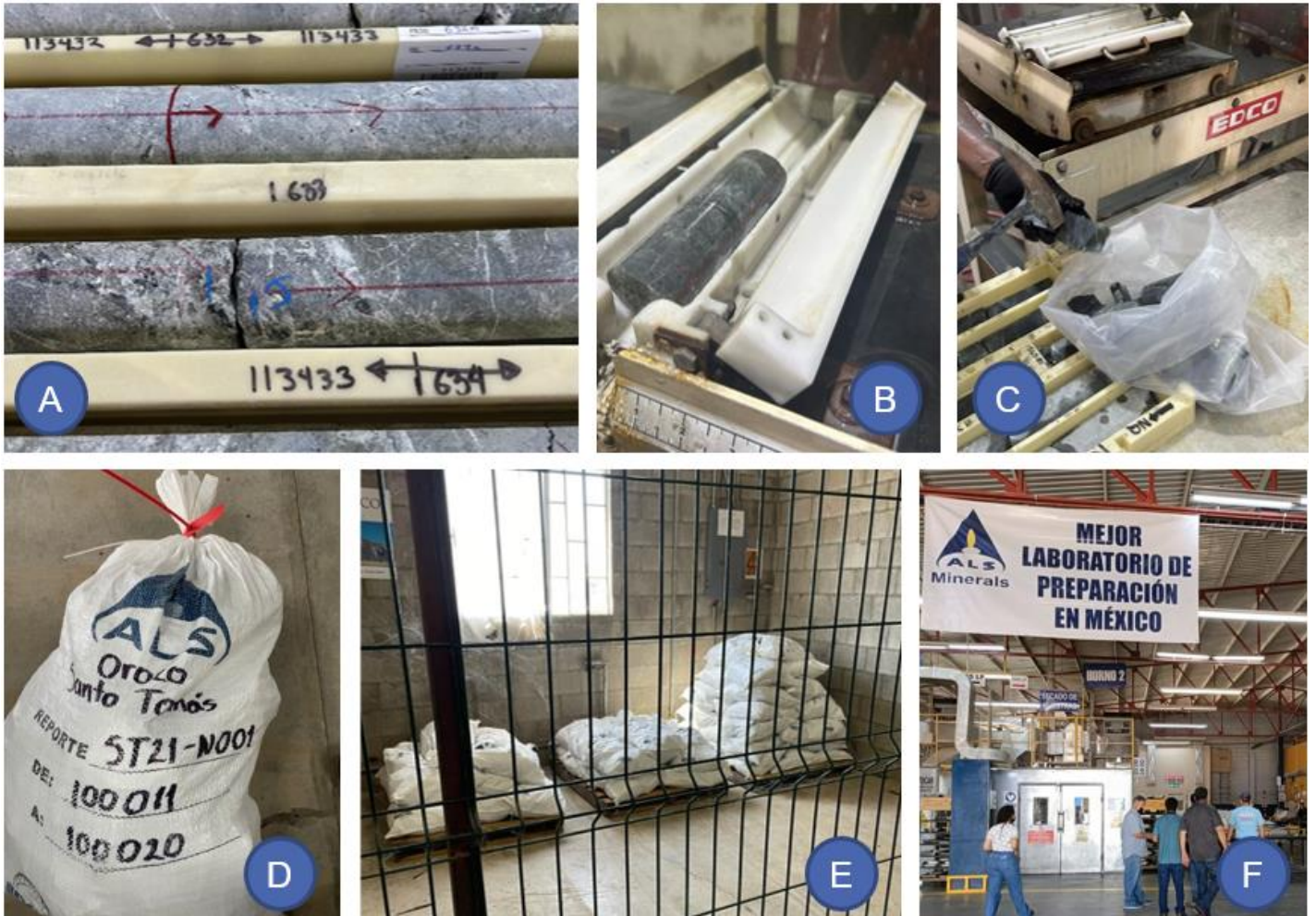
11.1.2 Oroco Sampling Methods

Figure 11-1 are photos illustrating Oroco's Phase 1 logging and sampling management. Phase 1 drilling by Oroco conducted core orientation and marking at the drill rig by drilling and geological staff. A quick log and mobile phone photograph of each core is taken before the core is transported to the core logging facility at 'El Ranchito'. Upon arrival at El Ranchito, core is washed, and a daily report quick log prepared. Staff review the core at this time to inform drilling decisions (e.g., hole termination). The diamond drill core is then processed through core photography (Figure 11-2), geotechnical markup and logging, structural geology measurement and geological logging. Specific gravity (SG, or density) samples are selected during logging.

Assay sample selections are based on visual observation of mineralization and lithological associations, and the sample intervals are marked on core boxes. An adhesive sample tag is attached to the core box by the geologist before being moved to the core cutting area. Tags for bagging are placed with the core to be sampled. In the core saw facility, the core is cut in half using a manually operated diamond-bladed saw. If the core is extremely fractured and/or composed of clays, it is not cut. A representative one-half split is taken using a spoon instead, leaving the remaining core in its original position in the core box. Sample lengths are nominally 2 m for HQ and NQ. Samples may be shorter depending on geological or mineralogical boundaries. For holes N001 to N018, the half-core was cut in half (quartered) to preserve core for initial metallurgical work. Core duplicates are either the second quarter fraction or the remaining half-core.

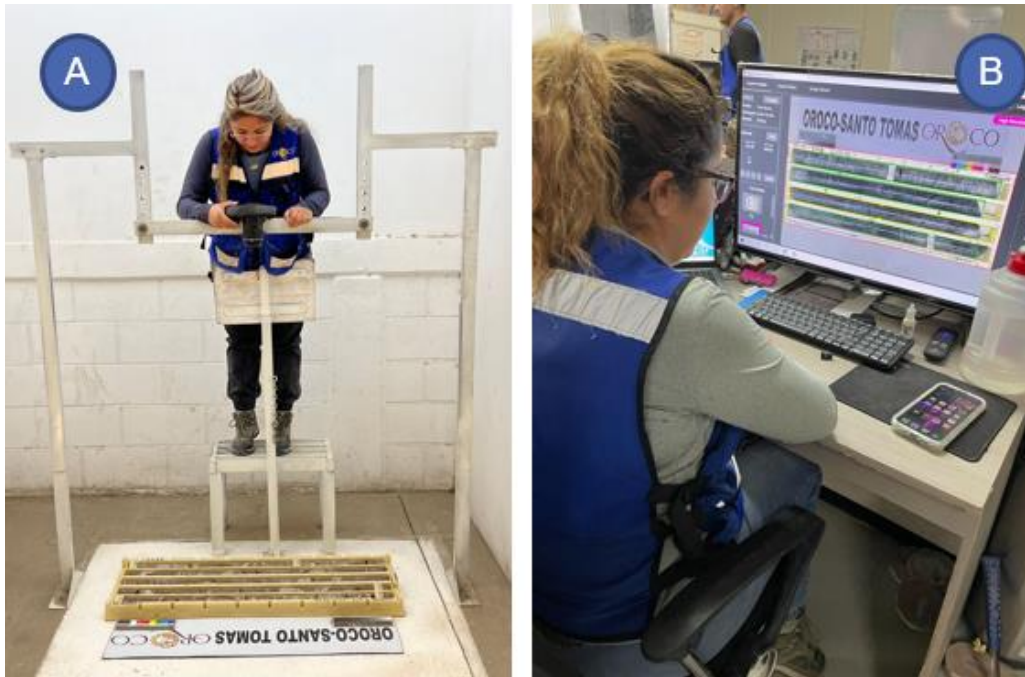
Cut core is placed in plastic bags direct from the saw with the remnant core placed back in the core box. The plastic bag is sealed with a cable tie and added to a gunny sack which contains 5 to 10 bagged samples. Each gunny sack is cable tied and sealed with a security zip-seal and labeled with indelible marker. Gunny sacks are placed on assay consignment pallets in a secure, access-controlled sample cage. Consignments of samples are collected at El Ranchito by ALS laboratory staff using their owned and operated trucks, commencing the laboratory chain-of-custody direct from the sample cage prior to the samples leaving the El Ranchito core processing facility.

Figure 11-1: Photos of Oriented Core Logging, CRM Storage and Samples for Shipping.



Source: Oroco, 2023.

Figure 11-2: A: Core Photo Capture Station at El Ranchito; B: Core Photo Preparation and QA in IMAGO®.



Source: Oroco, 2023.

11.2 Density (Specific Gravity) Determinations

11.2.1 Historical Density

A historical tonnage conversion factor of 2.6 t/m³ was applied universally to modeled blocks by Thornton (Thornton 2011).

11.2.2 Oroco Density Program

During Oroco's Phase 1 drilling campaign, some 2,351 density measurements were made using the weigh-in-air/weigh-in-water specific gravity technique. Samples were whole core, with dry weights of greater than 200 g averaging 684 g. Samples were selected from drill holes, their location, lithology, alteration, and mineralization type recorded. Selected samples were geologically intact but the occurrence of vuggy veins and the common occurrence of water absorbent clays in altered samples necessitated coating of samples with paraffin wax starting early in the program.

The mean density for the sampled SG for the Project is 2.68 g/cm³.

The weight-in-water measurement of the samples stabilized quickly, and no air bubbles were observed owing to the wax-sealed condition of each sample. QA/QC was maintained by measuring a reference zinc-nickel weight provided with the electronic scale (294.11 g, see item front-left of scale in Figure 11-3).

Figure 11-3: A: Specific Gravity Displacement Weight Equipment and Paraffin Wax Pot; B: UCS Point Load Tester



Source: Oroco, 2023.

11.3 Analytical and Test Laboratories

11.3.1 Historical samples

ASARCO used their professional laboratories in México for assaying. The laboratories were located at Nacozari in Sonora, San Luis Potosí in San Luis Potosí, and Parral in Chihuahua (Spring, 1992).

Tormex sent their samples to Ensayadores Quimicos del Noroeste in Hermosillo, México, with one sample in ten being sent for check assay to TSL Laboratories in Toronto, Canada (Spring, 1992).

Exall analyzed the Santo Tomás samples for total copper percent (CuT), acid-soluble copper (CuS), and assayed for copper, gold, silver, molybdenum and iron (Thornton, 2011). Exall also prepared several samples for metallurgical testing at Mountain States Research and Development Inc. (MSRDI) and at Minetek in 1993 and 1994 (Bateman, 1994).

In 2002, Borovic selected a total of 48.65 m of core (18 samples) and had them assayed at ALS Chemex, in Hermosillo (Borovic, 2002).

11.3.2 Phase 1 Drilling by Oroco

All of Oroco's Phase 1 drill assays were analyzed at ALS Limited in Hermosillo and Vancouver. Both laboratories are accredited under a group certificate issued to ALS Limited by SCC (Standards Council of Canada) File Number: 15722.

The laboratories comply with Accreditation Standard(s) ISO/IEC 17025:2017 satisfying the general requirements for the competence of testing and calibration laboratories for the Chemical/Physical Fields of Testing in the Mineral Analysis Program Specialty Area: (Initial Accreditation: 2005-05-18, Most Recent Accreditation: 2022-07-26, Accreditation Valid to: 2025-05-18). Both laboratories, ALS Minerals – Magnolia #16, Esq. Laurles Col. Libertad, Hermosillo, Sonora 83130 México and ALS Minerals - Unit 150 - 2155 Dollarton Hwy, North Vancouver, BC V7H 2B2 Canada, are covered under the same certificate.

The ALS Limited laboratories are accredited for the analytical code packages requested by Oroco:

- The Au-AA series assay package for the determination of gold in the samples - Determination of Au by Lead Collection Fire-Assay and Atomic Absorption.
- ME-ICP61 Multi-Element Determination by 4-Acid Digestion and Inductively Coupled Plasma-Atomic Emission Spectroscopy (ICP-AES) for assays of copper, molybdenum and silver and over-limits procedures.

11.3.3 Metallurgical Laboratory

ALS Canada Ltd. Metallurgy Services of Kamloops, BC, Canada undertook the Metallurgical Test work reported in Section 13. ALS Metallurgy Kamloops is a fully integrated mineral processing laboratory and is ISO 9001:2008 certified.

11.3.4 Laboratory Independence

The ALS group of companies and all of their laboratories are independent of Oroco Resource Corp., Ausenco, and SRK Consulting North America and all of their affiliates.

11.4 Sample Preparation and Analysis

Samples were submitted to the Mexican division of ALS Limited in Hermosillo, México, for sample preparation to pulps. Sample pulps were then sent to ALS Canada Ltd. in Vancouver, Canada, for analysis. Total copper, silver and molybdenum contents were determined by four-acid digestion with atomic absorption spectrophotometry finish. Gold was determined by fire-assay (Au-AA25) of a 50-gram charge or alternately by Au-AA23 of a 30-gram charge (1 Assay ton).

Sample preparation methods include crushing and pulverizing by ALS preparation code PREP-31Y using crushers with rotary splitter. The method crushes the material to 70 % passing 2mm, then rotary splits off 250 g, then pulverizes the split to 85% passing 75 microns (85% passing (P85) a -200 mesh (<75 µm) sieve).

The analytical package has consistently used ALS multi-element package code ME-ICP61 with over-limits re-assay. ALS method ME-ICP61 involves a 4-acid digestion (Hydrochloric-Nitric-Perchloric-Hydrofluoric) followed by ICP-AES determination. Samples that return 'over-limits' Cu grades >10,000ppm were analyzed by ALS "ore grade" method Cu-AA62, which is a 4-acid digestion, followed by AES measurement to 0.001%Cu.

11.5 Sample Security

11.5.1 Historical Sample Security

None of the historical procedures for sample and drill core security are available for review by the QP. Since 1994, data for the drill core sampling and logging has been in the continuous custody of John Thornton, P. Eng., formally a principal with Mintec, Inc.

Historical core was archived at the Bienstar Core Storage shed in 2008 by prior workers. The facility was not secured until 2021 and some core rack collapse occurred. Some rack metal and timber supports were disturbed by local ranchers, but in general core boxes were left in place. Oroco undertook a detailed core recovery and careful re-boxing in new, securely and individually strapped project standard core boxes in 2021. The re-boxed core was re-located to the El Ranchito core handling and storage facility, where it has recently begun to be re-logged and is securely stored.

The process of core re-boxing was done with utmost care. Where no reliable evidence of core identification was available for boxed core at Bienstar, the core was discarded. Fortunately, this impacted fewer than 30 cardboard boxes of historical core. To date, no further sampling of historical core has been undertaken. The Company intends to seek independent QP advice with respect to the further sampling of historical core following this MRE.

Historical assay pulps and coarse rejects have not been located.

11.5.2 Phase 1 Core Program Sample Security

Core material recovered from Phase 1 drilling was oriented at the drill site, marked by the drilling and geotechnical site crews, and checked by the site support field geologist before the core was telephone-photographed, foam-packed and security strapped for transport by pickup to El Ranchito. Phone core photographs were discarded once the core was received, intact, at El Ranchito.

Phase 1 drill core is secured within the access-controlled core logging facility on a 24/365 basis. Once core is sampled and bagged, it is added together with the QA/QC program sample bags to gunny sacks (refer to Section 11.1.2) and consigned to the access-controlled Project Sample Cage, where the security sealed gunny sacks are added to laboratory consignment pallets. The sample pallets are only removed from the Cage when loading onto ALS-provided secure laboratory sample shipment trucks under chain-of-custody (COC). The Cage is locked at all times except when the Sampling Supervisor is storing samples or retrieving Standards. Only approved personnel may enter the Cage, always under the supervision of the on-duty sampling manager. Oroco directors and officers and persons with a direct project interest are barred from entry to the Project Sample Cage.

Once assay samples are in the custody of ALS, the ALS collection team are required to remain with the truck when stopping for refreshments or refueling upon return to the laboratory. Once in Hermosillo, ALS locks trucks in a secure facility at the laboratory until the truck is unloaded and the samples are received into the Laboratory's management and tracking system. The same applies when sample pulps and coarse rejects are returned to the El Ranchito facility for long-term storage.

Remnant core is securely stored to ensure integrity in the event of future assay or metallurgical sampling requirements.

11.5.3 Commercial Reference Material Security

All of the CRM sample materials are stored prior to use at the access-controlled Project Sample Cage at El Ranchito.

11.6 Sample Storage

11.6.1 Historic Pulp and Coarse Reject Storage

There are no known remnants of historical assay sample pulps or coarse rejects.

11.6.2 Phase 1 Oroco Pulp and Coarse Reject Storage

Oroco sample pulps and coarse rejects returned from ALS under ALS’s secure sample COC and are stored securely at Oroco’s El Ranchito secure and access-controlled facility. Pulps are stored in metal lock-boxes that are in turn secured in locked pulp-box racks (Figure 11-4).

Figure 11-4: Sample Pulp Lockbox Secure Racking Storage (left); Coarse Reject Sample Offloading, (center); Cut Core Racking and Storage with Engraved Metal Box Tags (right) at the El Ranchito Secure Storage Facility.



Source: Oroco, 2023.

11.7 Quality Control and Quality Assurance

11.7.1 Historical QA/QC

The QPs have not been able to directly review the nature, extent, and results of historical quality control procedures employed and quality assurance actions taken during the drilling and sample analyses of the 90 historical drill holes for which Oroco has data (7,244 assays for Cu, of which 534 samples were also analyzed for the suite of Mo, Au, Ag and Fe). The historical drilling data is therefore too sparse for characterization of Mo, Au and Ag values in the Santo Tomás deposit. Due to the extant standards of reporting prior to 1994, the technical reports did not include data listings or detailed description of quality control procedures.

The Authors of this report are not aware of the sampling procedures at the laboratories used by any of the previous companies, nor are they aware of the use of any quality control samples in the sampling program. It is assumed that the laboratories performed their QA/QC for each sample batch analyzed, as this was common practice at the accredited laboratories used during the historical drill programs.

Since the original assay certificates are not available, it is not possible currently to determine whether there are transcription errors or inconsistencies between the assay certificates and the original drill logs for the historical drilling before 1992.

The QPs are relying on reported historical programs of quality control, documented as follows:

- Check assaying was conducted by Tormex on one in every ten samples (Spring, 1992).
- Check assay programs conducted by Tormex, Minera Real de Ángeles, and Exall showed an excellent correlation of results between the original assays reported by ASARCO and the re-assays (Thornton, 2011).
- Spring (1992) states "The considerable check assaying done, at different laboratories and at different times coupled with the very good agreement among the various investigators, suggests that the copper values as reported represent the drill core values."
- The most recent drill core sample intervals obtained from the El Bienestar core storage facility by Borovic in 2002 returned virtually identical results to the historical assays (Borovic, 2006).

Thornton (1994) prepared a mineral resource estimation and stated: "*With the amount of core removed from the drilling programs for re-assay and comparison to the previous assay results, the comparisons summarized leave the authors who have reviewed them with the view that extreme care was taken with the physical data, and they summarize very closely with each other.*" (Thornton, 2011)

These statements lead to a high degree of confidence in the historical copper analytical results in the Santo Tomás database. Thornton and Mintec, separately, have maintained a continuous COC of that data since 1994.

11.7.2 Oroco Phase 1 Program QA/QC

The Oroco Phase 1 QA/QC program is based upon the routine use of standards, duplicate samples and blanks inserted into the sample stream with the purpose of identifying analytical drift in accuracy and sample contamination by smearing from prior samples to assure a high level of confidence in assay values received from the laboratory, and to submit for re-assay samples that do not meet defined hurdle criteria to assure data reliability. Table 11-1 lists the duplicate and standard insertion scheme utilized.

“Blanks” are samples that do not contain significant amounts of base or precious metals, and check for possible contamination in the assay laboratory sample processing. CBLK.2 is a coarse blank, utilizing fragments of hammer-broken unmineralized fresh granodiorite, which is inserted into the sample stream every approximately 70th sample. This is done to check for potential contamination in the laboratory sample preparation process (crushing and pulverizing). Previously a coarse blank was prepared using marble, CBLK. However, this material is a poor matrix match for monzonite and andesite. A fine pulp blank (PBLNK), OR23b, is a certified CRM which is inserted into the sample stream every approximately 30th sample. This is done to check for potential contamination post the sample crushing and pulverizing circuit in the acid digestion and assay processes.

Duplicates (DUP) samples are additional samples taken for assaying from a particular drillhole interval, to measure the precision of assay results. The duplicates program includes the selection of certain Pulp Duplicate Samples (PDUP), where a duplicate pulp sample is split from the shatter box rock pulps prepared by the laboratory. The PDUP is requested to be done by the laboratory in the consignment instruction forms submitted by the project teams and is done on every (approximately) 60th sample. The PDUP process is performed to measure the precision in pulp sample splitting and assaying. A Course Duplicate Sample (CDUP) program is also conducted, wherein a duplicate sample that is split from coarsely crushed (≤ 2 mm) rock prepared by the laboratory is sampled by the laboratory and assayed. The process is requested to be done by the laboratory and is performed on every (approximately) 60th sample. The procedure measures the precision in coarse fraction splitting, pulping, pulp splitting and assaying.

To measure precision through the process, the Field Duplicate Samples (FDUP) is a duplicate assay of an equivalent fraction of the sawed sample over the matching interval is taken. On the Phase 1 drilling program this has been done every (approximately) 60th sample. At Santo Tomás the FDUP sample is the remnant half of the core for a selected sample interval. Up to hole N018, samples and duplicates comprised sawn quarter core: this approach was adopted to ensure an abundance of remnant core materials was available for re-assay and for metallurgical work. Observed stability in assays allowed for the program to transition to half-core samples wherein it is expected that an improvement in sampling variance may be captured. The FDUP process is performed to measure the precision in assay results from the same core interval, which confirms a largely natural variability in metal distribution.

A critical component of the QA/QC process is the introduction of ‘known’ standard materials into the sample stream. The standard materials used comprise of certified CRMs, which have been thoroughly tested by numerous laboratories (up to 21), to arrive at an accepted “true” or reference value for copper and select other metals. These CRM-based standards are inserted approximately every 16th sample on a staggered basis and is designed to measure the variance between the laboratory assay value and the accepted value, to identify potential assay process errors in the laboratory. Their selection is based on lithology and apparent degree of copper mineralization as estimated during logging.

The standards used by Oroco are OR505, OR506, OR701, OR151b and OR151a, sourced from OREAS North America Inc. of Sudbury, ON, Canada.

Table 11-1: QA/QC Duplicate and Standard Insertion Scheme

QA/QC Sample Inserts	Frequency
CBLK.2	One every $\pm 70^{\text{th}}$ sample
OR23b (PBlank)	One every $\pm 30^{\text{th}}$ sample
FDUP, PDUP, CDUP	One of each every 60^{th} sample - staggered
OR505, OR506, OR701, OR151b or OR151a	Four selected in runs of ± 60 sample intervals

Table 11-2: QA/QC Standard CRM Insertion Criteria

CRM Name	Use: Geological Basis
OR505	Medium to high Cu - altered monzonite & andesite
OR506	Medium to high Cu - altered monzonite & andesite
OR701	High Cu - skarn
OR151b (Out of stock) or OR151a	Low Cu - altered monzonite & andesite

The reference standard results are rigorously tracked upon the receipt of assay certificates from the laboratory, and deviation beyond pre-established tolerance levels from the anticipated results trigger immediate re-assay requirements under the Oroco QA/QC protocols.

11.7.2.1 QA/QC sample insertion detail

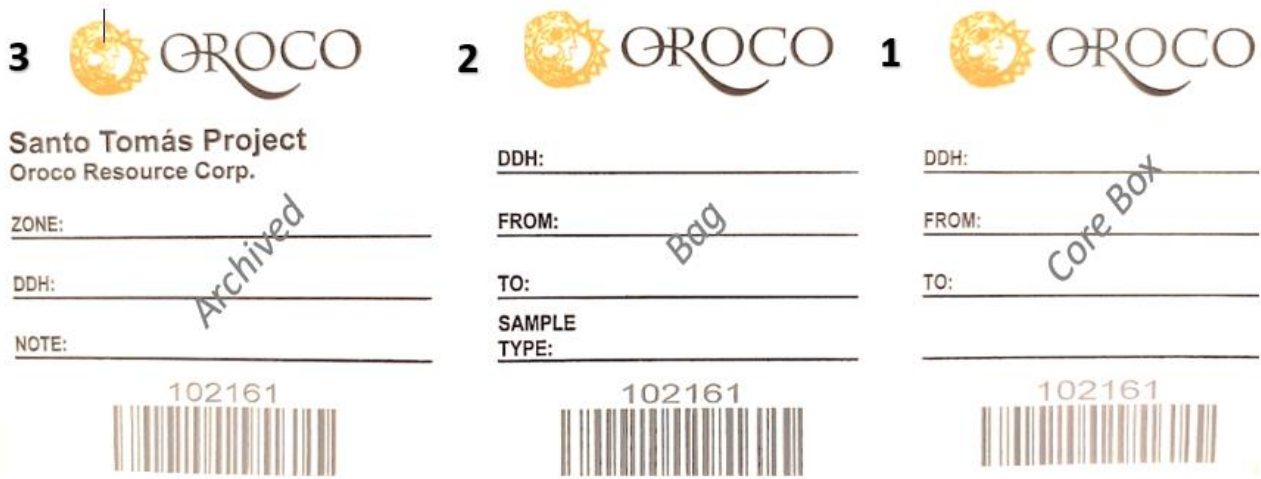
QA/QC sample insertions are included in each batch of samples as if each insertion is a sample of sawn core, and each is inserted according to the QA/QC criteria and verified by the geologist and sampling technician. Table 11-2 lists the QA/QC standard CRM insertion criteria. These QA/QC samples are placed into the sample sequence at their insertion frequency in any given run of core samples. An empty bag is placed at the appropriate position in the sequence indicating to the assay lab that a CDUP or PDUP sample is required. For the PDUP samples the type of sample is written on the Oroco Sample Number sticker tags 1, 2 and 3 (Figure 11-5). For the CDUP samples (material CBLK2), the sample name is written on sticker tags 1 and 3, while on sticker tag 2, which labels the bagged sample material, only the drillhole name and depth interval of the prior up-hole interval is written. Between 250-300 g of the broken granodiorite is placed into the bag.

The CRMs are maintained in the Controlled Access Sample Cage. Only the on-duty sampling manager has access to the Sample Cage and is responsible for removing CRMs for daily use in the sawing and sampling area. Every CRM standard packet removed from its box in the Cage is registered in the Standards Control List. Once selected, the CRM sample in its envelope is placed in a standard sample bag (Figure 11-5). Before the number of the OREAS sample is erased from its containing envelope, the sample ID is written over that envelope (Figure 11-6). The CRM identifier is erased after verification and comparison with the insertions list. For CRMs the standard number, and depth interval of the up-hole sample interval is written on sticker tags 1 and 3. Only the hole name and depth interval are written in sticker tag 2.

For the FDUP duplicates, FDUP is written on sticker tags 1 and 3, along with the corresponding drillhole name and depth interval. Sticker tag 2 is placed on an empty bag by the sampling supervisor, with the sample number written on the bag, and the remaining half of the sawn or spoon-split core is placed in the bag by the saw operator.

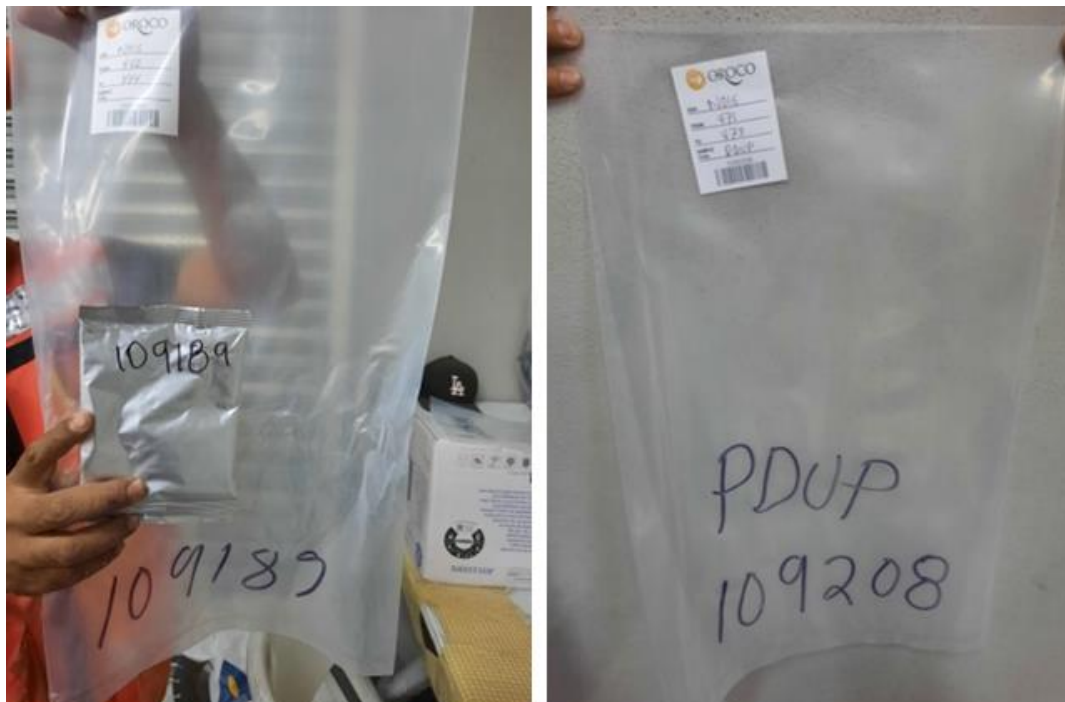
For PBLNK, only the CRM sample number (OR23b) is written on stickers 1 and 3. On sticker 2, only the drillhole name and depth interval of the prior up-hole interval is written. The sample number is added to the CRM container envelope, and the number compared with the number on the sample bag. Once confirmed by the sampling supervisor, the CRM identifier is erased from the envelope, and the CRM sample in its envelope is placed in the sample bag.

Figure 11-5: Oroco sample tag stickers



Source: Oroco, 2023.

Figure 11-6: Standard Envelope with Oroco Sample Number Added and Bagged (left) and empty PDUP (pulp duplicate marker) bag (right).



Source: Oroco, 2023.

11.8 Check and Re-Assay Programs

11.8.1 Historical Check and Re-Assay

The Authors are relying on historical programs of quality control, documented as follows:

- ex on one in every ten samples (Spring, 1992).
- Check assay programs conducted by Tormex, Minera Real de Ángeles, and Exall showed an excellent correlation of results between the original assays reported by ASARCO and the re-assays (Thornton, 2011).
- Spring (1992) states “The considerable check assaying done, at different laboratories and at different times coupled with the very good agreement among the various investigators, suggests that the copper values as reported represent the drill core values.”
- The most recent drill core sample intervals obtained from the El Bienestar core storage facility by Borovic in 2002 returned virtually identical results to the historical assays (Borovic, 2006).

11.8.2 Phase 1 Oroco Drilling Check Assay

A program of random check assays by a laboratory independent of ALS has not been undertaken ahead of the MRE that is the subject of this report.

A program of check assays is intended to be undertaken on a semi-random population of samples following the publication of a PEA that will utilize the resource included in this MRE. The check assays will be randomly drawn from subsets of higher, intermediate and lower grade assay class samples, and may comprise up to 5% of the samples assayed in each class (excluding DUP and Standard samples).

11.8.3 Oroco Re-Assays

Oroco has re-assayed samples that fall within a range of samples both up-hole and down hole of Standard and DUP series samples that do not meet the hurdle requirements on return of the assays. Oroco has treated the QA/QC review of returned sample consignment assays in some 16 ‘batches’ each comprising multiple certificates. CRM, pulp blank and other QA/QC DUP ‘failures’ are identified and are flagged for re-assay, usually in sample series windows of approximately 20 to 32 samples. The re-assays are returned by ALS in assay certificates and again reviewed for compliance: once the hurdle requirements are met, the re-assayed sample window batch is ‘passed’ for inclusion into the sample database. The Oroco QA/QC Manager writes QA/QC reports for each Batch of samples processed and writes follow-up reports for each Batch once the re-assays are received. The re-assay program has generally resulted in data that are included into the assay database, though a small number of failures have resulted in laboratory ‘incident’ reviews to detail causes and to implement corrective actions. The small incidence of identified issues is not material to this MRE.

11.9 Databases

Assay data are received from ALS by email from ALS.Reporting@ALSGlobal.com in an ALS standard assay certificate format (.csv, comma-separated-value) where the filename is the ALS-generated unique consignment identifier (e.g. HE23069419.csv). The emails are directed to the Oroco Data QA/QC and Database Manager, who receives and evaluates the contents of the certificates for QA/QC. Some QA/QC re-assays are reported via updated certificates of the same name; where the re-assays are more complex, ALS may assign a new ALS batch number. The order of qualification for

admission to the Oroco database is managed by the Oroco QA/QC and Database Manager and is reported in the QA/QC Batch reports and Batch update reports.

The Oroco database for drilling information and geochemical and assay data is archived in an industry specific database platform (Datashed 5) provide by MaxGeo. The core sample assays and QA/QC sample assays are warehoused in use-specific data tables, and project drill collar, downhole directional survey, downhole geophysical, core petrophysical, core geotechnical, core structural and lithological logging information are all stored in relational tables on the Datashed 5 platform. The datasets are provided to the Database Manager in .csv, MS-Excel .xlsx and geophysical standard .las formats for importation into Datashed 5.

To date the principal platforms used for 3D geological and resource modeling and management are not ODBC (Open Database Connectivity) linked to the Oroco Database: managed datasets are exported from Datashed as .csv files and are directly imported into Leapfrog and QGIS for application by technical users.

11.9.1 Santo Tomás Phase I Drilling – QA/QC Detailed Analysis

For Santo Tomás Phase I drilling, carried out between August 2021 and February 2023, Oroco Resource Corp. implemented a quality assurance and quality control (QA/QC) program consisting of standards, duplicates and blanks inserted into the regular sample stream. Duplicates included pulp, coarse and field duplicates (or twin samples) and blanks included both pulp and coarse blank material. The following QA/QC analysis is based on assay results from the sixty-five Phase I drillholes included in the MRE, consisting of 19,135 regular assays and 3,872 QA/QC assays. An additional five percent of total samples are currently being selected for an upcoming external check assay program. Sample preparation and analysis was carried out by ALS Global in Hermosillo, México and Vancouver, Canada.

The overall insertion rate of QA/QC samples for this program was 17% (Table 11-3). The insertion rate will increase to 22% with the addition of the check assays. Although there is no definite industry standard for QA/QC insertion rates, the recommendations for best industry practices by regulatory organizations as well as the preference of the mining industry is a QA/QC sample insertion rate close to 20%, including standards, duplicates, blanks, and external checks (Simon, A. Control Sample Insertion Rate, IAGS, June 2007).

Table 11-3: Santo Tomás Phase I Drilling (MRE) QA/QC Sample Insertion Rate

Sample Type		Count	% Total	
Standards	OREAS 151a	716	3.1	6.6
	OREAS 151b	56	0.2	
	OREAS 505	413	1.8	
	OREAS 506	291	1.3	
	OREAS 701	48	0.2	
Duplicates	PDUP	451	2	5.2
	CDUP	376	1.6	
	FDUP	374	1.6	
Blanks	OREAS 23b (Pulp)	702	3.1	5
	CBLK1, CBLK2 (Coarse)	445	1.9	
Regular Samples		19,135	83.2	
Total Assays		23,007	100	

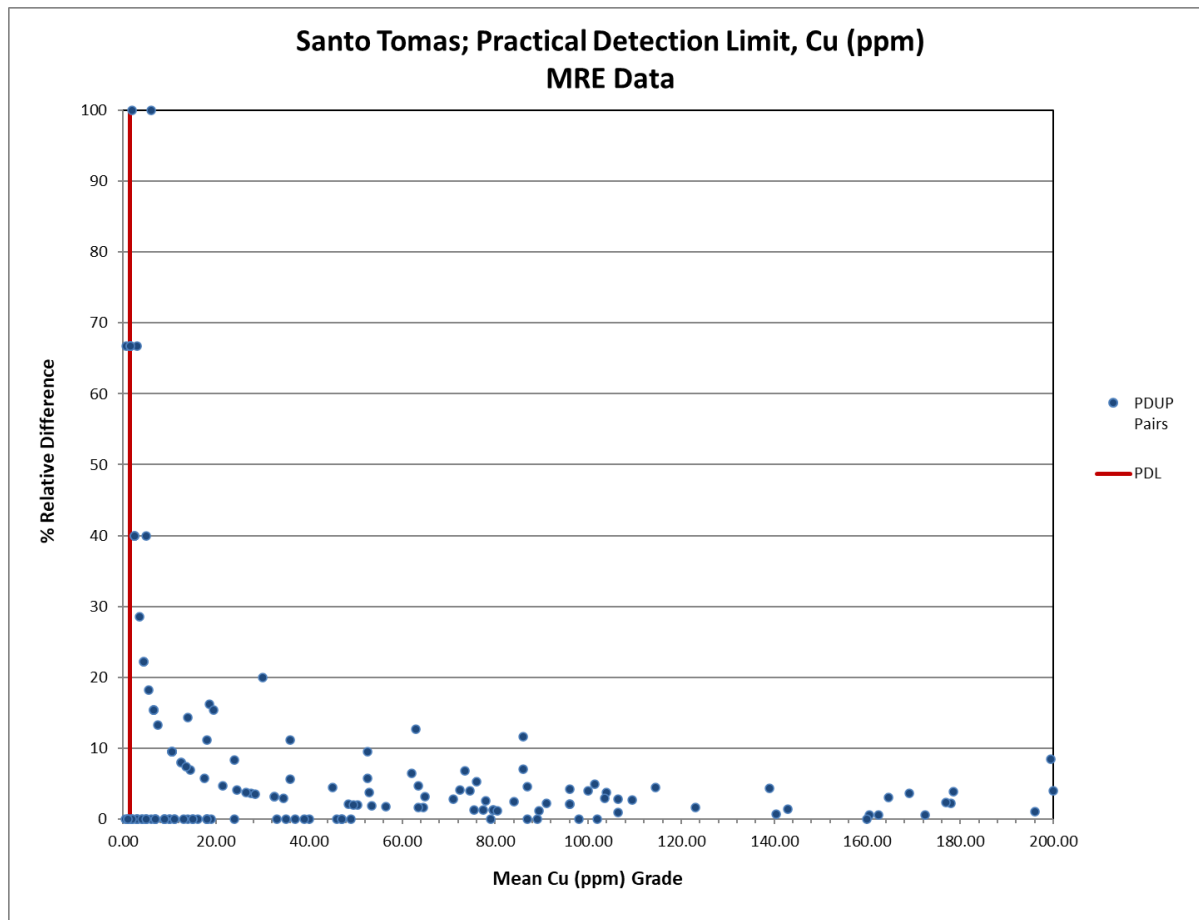
Samples were assayed at ALS using analysis methods (Table 11-4) ME-ICP61 (33 element suite with four-acid digestion and an ICP/AES finish) and Au-AA23 (30 g Au by Fire-Assay and an Atomic Adsorption Spectroscopy finish). Over-limits were analyzed with methods ME-OG62 and Au-GRA21. QA/QC analysis focused on the four main elements of interest for this deposit: Cu, Au, Ag and Mo, and used both the laboratory analytical detection limit (ADL) and a determined practical detection limit (PDL).

Table 11-4: ALS Methods and Analytical Detection Limits

Method	Analytical Detection Limits							
	Au (ppm)		Cu (ppm)		Ag (ppm)		Mo (ppm)	
	Lower	Upper	Lower	Upper	Lower	Upper	Lower	Upper
Au-AA23	0.005	100	-	-	-	-	-	-
Au-GRA21	0.05	10,000	-	-	-	-	-	-
ME-ICP61	-	-	1	10,000	0.5	100	1	10,000
ME-OG62	-	-	10	500,000	1	1,500	10	100,000

Lower PDLs were determined visually by plotting mean grade vs the relative difference of returned pulp duplicate pairs; the detection limit is defined by the asymptotic curve where the relative error between the paired data approaches 100% i.e., the assay results become very unreliable. See example plot in Figure 11-7 and the summary table of determined lower PDLs (Table 11-5).

Figure 11-7: PDL Determination, Mean Grade vs. Relative Difference, Cu (ppm)



Source: Oroco, 2023.

Table 11-5: Determined Lower Practical Detection Limits

Lower Practical Detection Limit			
Au (ppm)	Cu (ppm)	Ag (ppm)	Mo (ppm)
0.005	1.5	0.5	1.5

11.9.2 Standards

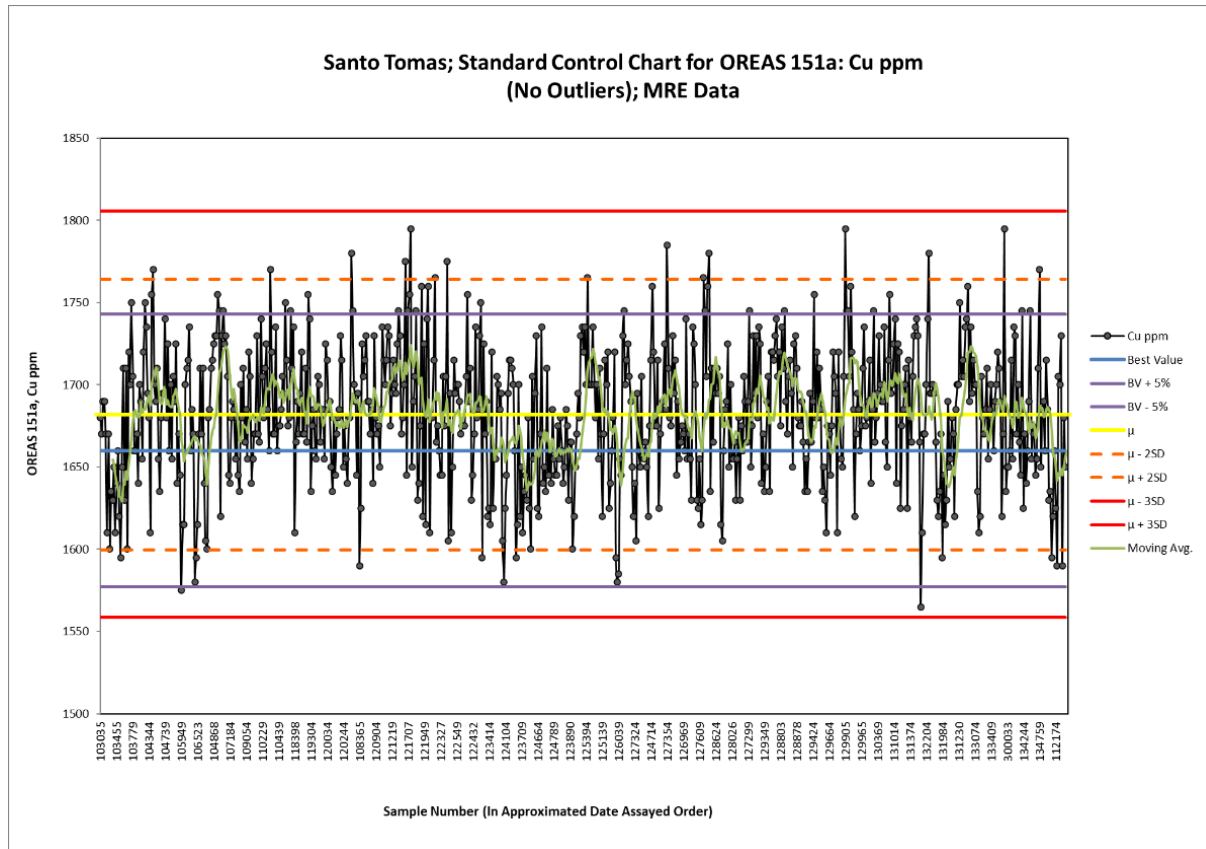
To assess the accuracy of the assay laboratory results, certified CRMs or “Standards” were inserted into the regular sample stream. Five different certified standards were purchased from ORE Research & Exploration Pty Ltd. (OREAS), of Victoria, Australia and used at Santo Tomás: OREAS 151a, OREAS 151b, OREAS 505, OREAS 506 and OREAS 701. These standards are comprised of a granodiorite matrix and cover the potential low-, mid- and high-grade ranges of the deposit (Table 11-6).

Table 11-6: CRM Best Values (BV), Based on 4-Acid Digest/ICP Finish (Cu, Ag, Mo) or Fire-Assay/ICP Finish (Au)

Element	OREAS 151a		OREAS 151b		OREAS 505		OREAS 506		OREAS 701	
	BV	SD	BV	SD	BV	SD	BV	SD	BV	SD
Au (ppm)	0.043	0.002	0.065	0.006	0.555	0.014	0.364	0.01	1.11	0.05
Cu (%)	0.166	0.005	0.182	0.005	0.321	0.008	0.444	0.01	0.491	0.012
Ag (ppm)	-	-	0.551	0.068	1.53	0.072	1.88	0.075	1.12	0.14
Mo (ppm)	40	3	55	2.2	66	2.1	87	3.6	254	21.4
S (%)	0.856	0.035	-	-	-	-	-	-	-	-

Standard results were plotted against the BV, the Best Value \pm 5%, the Mean (μ), \pm 2 Standard Deviations ($\pm 2SD$), \pm 3 Standard Deviations ($\pm 3SD$) and the Moving Average (MA) (Figure 11-8). Ideally, the MA should remain within $\pm 5%$ of the Best Value, and 95% of the samples should fall within ± 2 standard deviations of the mean (Simon, A and Long, S. of AMEC International, 2007). Failures outside of three Standard Deviations should be sent for re-assay. Refer to Table 11-7 and Table 11-8 for failure rates and calculated bias.

Figure 11-8: Standard Control Chart for OREAS 151a Cu (ppm)



Source: Oroco, 2023.

Table 11-7: Standard Failure Count and Calculated Bias for Cu and Au

Standard	Count	Cu					Au				
		2SD		3SD		Bias	2SD		3SD		Bias
		Failed	%	Failed	%		Failed	%	Failed	%	
OREAS 151a	716	31	4.3	0	0	1.33	15	2.1	0	0	2.33
OREAS 151b	56	3	5.4	0	0	2.2	4	7.1	0	0	1.54
OREAS 505	413	17	4.1	1	0.2	0.09	24	5.8	6	1.5	0
OREAS 506	291	15	5.2	1	0.3	-0.14	14	4.8	1	0.3	0.27
OREAS 701	48	2	4.2	0	0	0.1	3	6.3	0	0	-1.53

Table 11-8: Standard Failure Count and Calculated Bias for Ag and Mo

Standard	Count	Ag					Mo				
		2SD		3SD		Bias	2SD		3SD		Bias
		Failed	%	Failed	%		Failed	%	Failed	%	
OREAS 151a	716	20	2.8	2	0.3	-	15	2.1	0	0	-2.5
OREAS 151b	56	6	10.7	0	0	3.45	5	8.9	1	1.8	-1.82
OREAS 505	413	30	7.3	1	0.2	3.27	3	0.7	0	0	-1.52
OREAS 506	291	17	5.8	0	0	2.13	1	0.3	0	0	-3.45
OREAS 701	48	5	10.4	0	0	7.14	1	2.1	0	0	-2.36

*OREAS 151a is not certified for Ag.

For the majority of standards, $\geq 95\%$ of the samples fell within 2SD of the mean for all four elements of interest. Exceptions include Au, Ag and Mo for OREAS 151b, Au and Ag for OREAS 505 and Ag for OREAS 506.

For OREAS 151b, Au, Ag and Mo had 2SD failure rates of 7.1%, 10.7% and 8.9%, respectively. OREAS 151b was the initial low-grade standard and was replaced by 151a when the limited supply ran out. The small sample population is potentially contributing to the larger apparent failure rates due to a lack of robust statistics. In addition, the certified BV for Ag is only slightly above the lower ADL for Ag for the ME-ICP61 method, and the BV for Au is approximately 10x the lower ADL for Au for the Au-AA23 method. As increased variability and reduced precision is expected near the lower ADL, this is likely also contributing to increased failure rates for this standard.

OREAS 505 had 2SD failure rates for Au and Ag of 5.8% and 7.3%, respectively. Two of the flagged Au failures are missing or blank Au values, rather than actual failures. This is due to a different standard packet (OREAS 506) being used for the Au re-assays and the inability of the database to store mixed standard results for the same sample number. When reduced by two, the 2SD failure rate for Au is only 5.3%.

OREAS 505 has a 2SD failure rate of 7.3% for Ag. The Ag in this deposit is sometimes not fully digestible using the ME-ICP61 method, which may be contributing to an increased number of low 2SD failures, for not only OREAS 505, but OREAS 506, 701 and 151b as well.

All 3SD failures were sent for re-assay. Those that remained post re-assay and are noted in the above tables were reviewed and considered acceptable.

For OREAS 151a, the two remaining Ag failures reported a value of 0.8 ppm and are within a rounding error of the 3SD failure line at 0.77ppm. Ag is also not a certified element for OREAS 151a.

For OREAS 151b, the remaining Mo failure reported 58ppm which is 1ppm over the upper 3SD failure line. This sample is from early in the program, when there were fewer returned results and at the time of the initial QA/QC review, this sample was within range. As the pass/fail (P/F) limits for each standard are generated from all returned assay values, they are refined with additional analyses. As more results were accumulated over the duration of the program, the P/F window for OREAS 151b was narrowed and this sample was eventually bumped over the limit line.

For OREAS 505, there was a total of 8 remaining 3SD failures following re-assay. The Ag failure reported a value of 2ppm which is within a rounding error of the upper 3SD limit line of 1.97ppm. The one Cu failure reported a value of 3470ppm which is above the upper 3SD limit line of 3451.2ppm Cu. As with the Mo failure for OREAS 151b, this sample occurred earlier in the program and was not identified as a failure during initial QA/QC review. It was only later bumped over the limit line, as the P/F window was refined with additional analyses. Of the six Au failures, two are a result of a missing/blank value in the database (noted above) and the remaining four had values of 0.505, 0.5, 0.511 and 0.495 ppm, which fall below the lower 3SD limit line of 0.597ppm Au. Like the Cu failure, all four of these assays occurred early in the program and were not flagged as outliers during the initial QA/QC analysis. Looking at the OREAS 505 Au standard chart, there appears to have been a slight upwards shift in the reported Au results following this first batch of samples, possibly due to a recalibration of equipment or digestion issue at the lab.

For OREAS 506, there were two remaining 3SD failures. One Au failure reported 0.34ppm Au, which is below the lower 3SD cut-off of 0.389ppm Au. Like the Au failures for OREAS 505, this failure occurred early in the program and was not flagged as an outlier during the initial QA/QC analysis. The Cu failure reported 4090ppm Cu, which is below the lower failure limit of 4106.7ppm. The original assay for this sample did in fact pass QA/QC for Cu with a value of 4480ppm, but initially failed for Ag. Following re-assay, the sample was found in range for Ag, but low for Cu.

For all standards, although some minor areas of high or low bias were seen, the Moving Average generally remains within $\pm 5\%$ of the Best Value and data points fluctuate above and below the BV line. The most notable observed pattern was a high bias of 7% for Ag for OREAS 701. Across the other standards, Ag results displayed a slight high bias but all less than 5% and is therefore no cause for concern. Mo results displayed a low bias for all standards but again, less than 5%. A slight high bias was noted for both Cu and Au for OREAS 151a and 151b, and Au results displayed a slight low bias for OREAS 701 but also all less than 5%, which is considered acceptable.

11.9.2.1 Duplicates

Three different types of duplicate samples were inserted into the sampling stream at Santo Tomás: field duplicates (or twin samples) taken in the field and comprised of the other quarter of the half-cut core, coarse duplicates taken at the lab as a second split of material at the initial crush stage, and pulp duplicates taken as a second split of material following pulverization. The ALS standard crushing specifications are >70% passing a 2mm screen. This type of sample can be used to assess the variability due to the first stage of sample splitting at the laboratory. The ALS standard pulverizing

specifications are >85% passing a 75 µm screen (Tyler 200 mesh). This type of sample can be used to assess the variability due to the final stage of sample splitting at the laboratory.

The duplicate results were analyzed via Min/Max plots and AVR (Absolute Value of the Relative Difference) charts for all elements of interest. For the Min/Max plots, the maximum value of each pair was plotted against the minimum value, to reduce bias and have data points rotate above the y = x line. No more than 10% of sample pairs should fall outside the acceptable range bounded by the y = x line and the Pass/Fail (P/F) line for each type of duplicate (Simon, A. AMEC International, 2007). The P/F line is defined by the hyperbola $y^2 = m^2x^2 + b^2$, where slope m is calculated for b = 0 and relative errors for the different types of duplicates (Table 11-9).

Table 11-9: Relative Error and Calculated Slope for Different Duplicate Types

Duplicate Type	Relative Error	Slope (m)
PDUP	10%	1.11
CDUP	20%	1.22
FDUP	30%	1.35

In order to account for the reduction in precision close to the detection limit, b is defined as a factor (x)*the detection limit, in this case a factor of 3 was used. Failure lines for both the ADL and PDL were plotted (see Table 11-5) for determined PDL values).

The precision of duplicate pairs can also be represented as an AVR vs Cumulative Frequency (Percentile Rank) plot. Outliers in the duplicate pairs can be visually identified as points that fall to the right of the inflection point, where the slope of the line steepens greatly. Ideally, less than 10% of the pairs should occur to the right of this point and the shape of the curve prior to the inflection point should be relatively shallow/flat. In addition, failures should not exceed 10%, i.e., 90% of the pairs should ideally have an AVR <0.3 for FDUPs, <0.2 for CDUPs or <0.1 for PDUPs (Long, S., AMEC International, 2007).

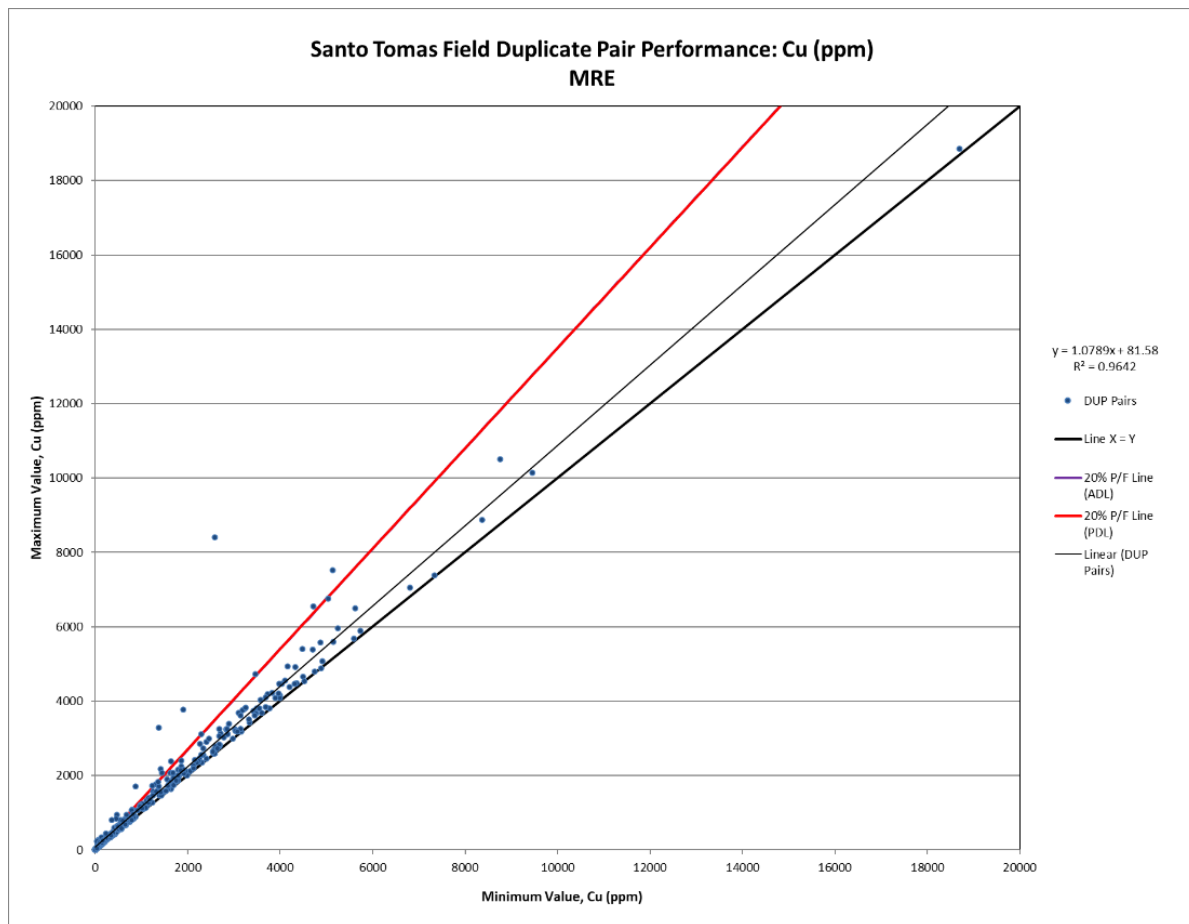
11.9.3 Field Duplicates

For the Max/Min analysis, the Au and Ag pairs meet the above stated criteria of at least 90% passing but Cu and Mo pairs are only ~80% passing. Although this failure rate is higher than recommended, increased variability is expected in field duplicate pairs due to the inequitable spread of mineralization across the two core halves, especially in areas of veined mineralization. The Au pairs exhibit a low R value; most of the returned Au results are very low-grade with little difference observed between the paired values, however, a few (relatively) higher-grade Au samples exhibit a much larger difference between the paired results, indicating a clumpy nature or nugget effect. A summary table and an example Min/Max plot for FDUPs can be seen below (Table 11-10) and plotted in Figure 11-9.

Table 11-10: Summary of Min/Max Plot Analysis for FDUP Pairs

Duplicate Type	Element	Total Pairs	Analytical Detection Limit			Practical Detection Limit			R2	R
			Value	Failures	% Passing	Value	Failures	% Passing		
FDUP	Cu ppm	374	1	74	80.2	1.5	73	80.5	0.9642	0.9819
	Au ppm	374	0.005	10	97.3	0.005	10	97.3	0.5695	0.7547
	Ag ppm	374	0.5	8	97.9	0.5	8	97.9	0.9459	0.9726
	Mo ppm	374	1	84	77.5	1.5	79	78.9	0.8723	0.9340

Figure 11-9: FDUP Min Cu vs. Max Cu Plot



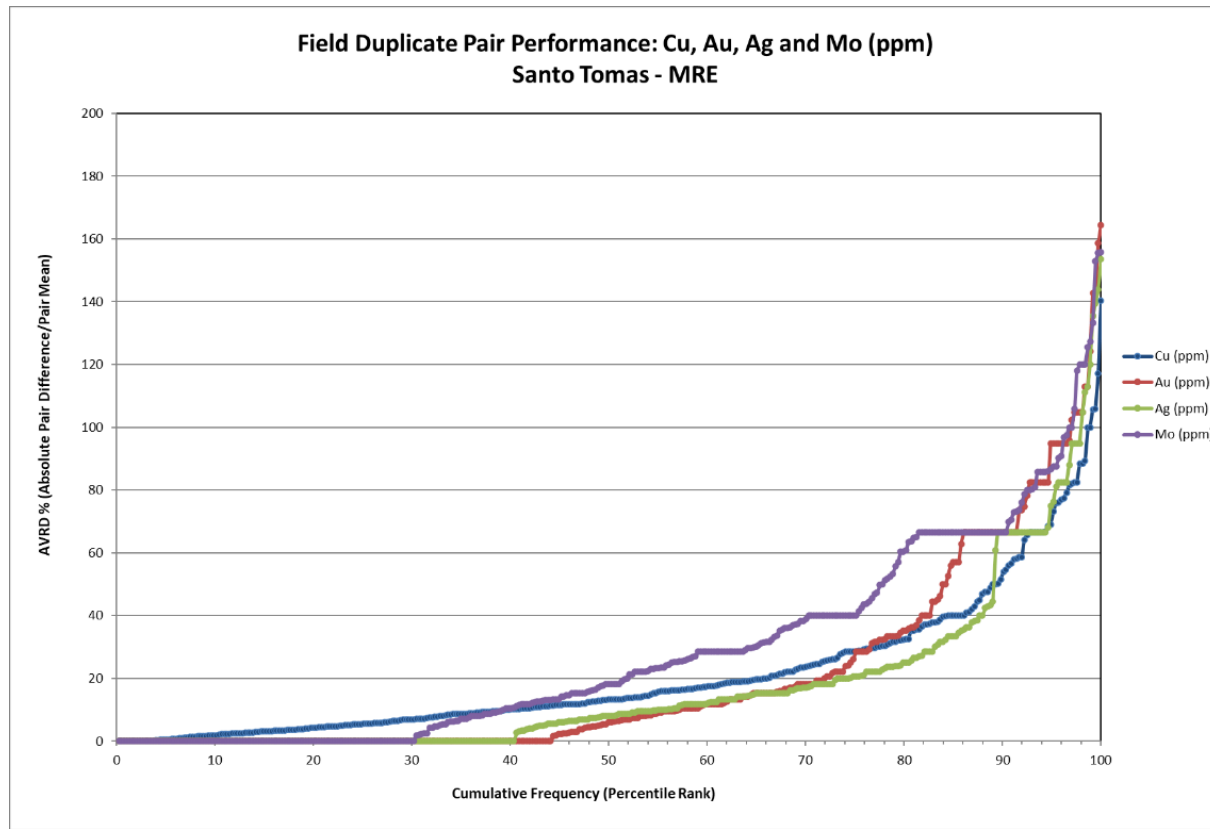
Source: Oroco, 2023.

Evaluating the FDUPs using the AVR method, the pairs fall below the desired 90% passing (see Table 11-11). The plot (Figure 11-10) also displays steeper curves prior to the inflection point than desired. As stated above, although this failure rate is higher than recommended, it is understandable due to the nature of FDUP pairs and the inequitable spread of mineralization across the core halves.

Table 11-11: Summary Table of AVRDR Analysis for FDUP Pairs

Element	FDUP Pairs w AVRDR<0.3
Cu	77.1
Au	76.5
Ag	82.9
Mo	64.7

Figure 11-10: FDUP Cumulative Frequency vs. AVRDR Plot for Cu, Au, Ag, and Mo



Source: Oroco, 2023.

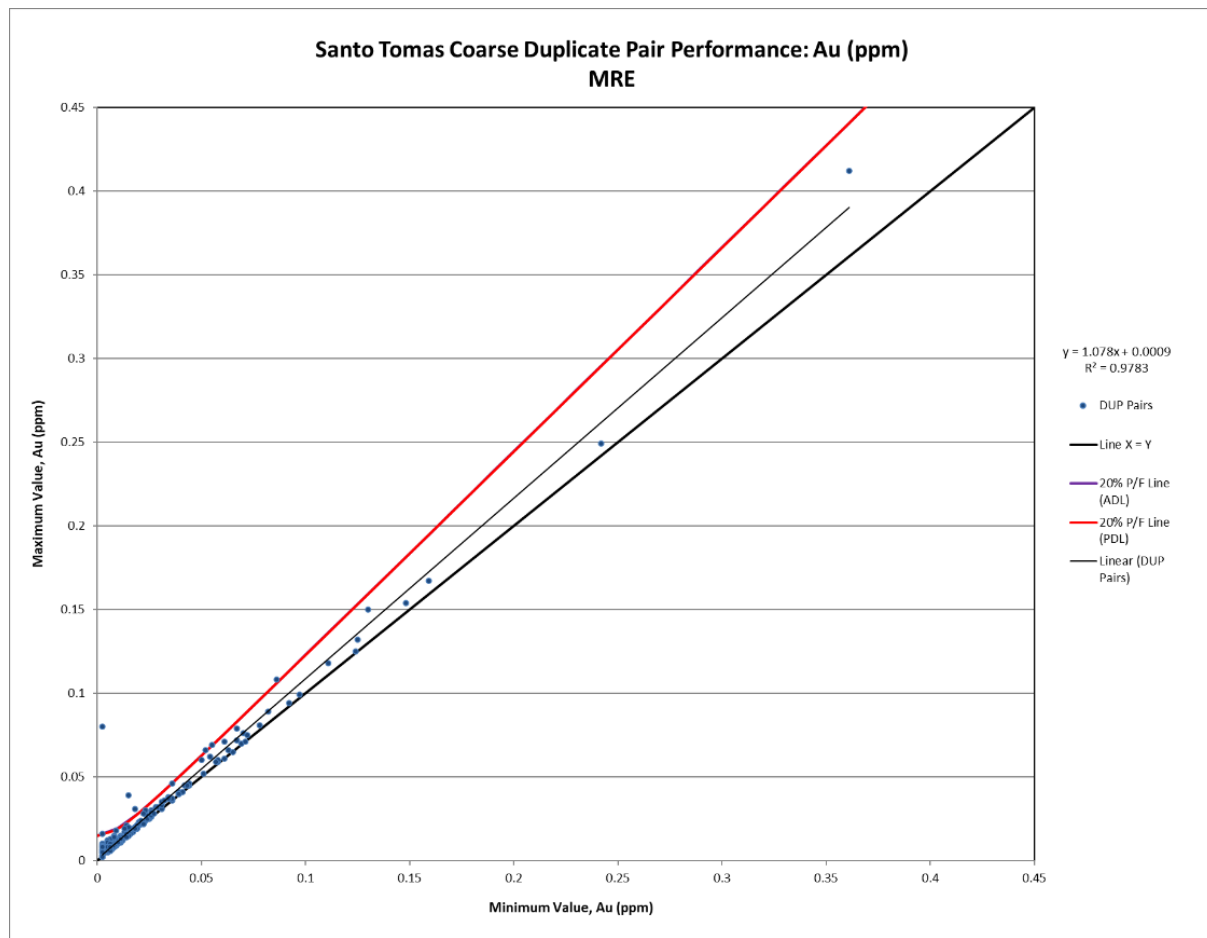
11.9.4 Coarse Duplicates

For the Max/Min analysis, Cu, Au, Ag and Mo pairs meet the above stated criteria of at least 90% passing. A summary table (Table 11-12) and an example Min/Max plot (Figure 11-11) for CDUPs can be seen below.

Table 11-12: Summary of Min/Max Plot Analysis for CDUP Pairs

Duplicate Type	Element	Total Pairs	Analytical Detection Limit			Practical Detection Limit			R2	R
			Value	Failures	% Passing	Value	Failures	% Passing		
CDUP	Cu ppm	376	1	6	98.4	1.5	5	98.7	0.9994	0.9997
	Au ppm	376	0.005	7	98.1	0.005	7	98.1	0.9783	0.9891
	Ag ppm	376	0.5	5	98.7	0.5	5	98.7	0.9818	0.9909
	Mo ppm	376	1	17	95.5	1.5	11	97.1	0.9958	0.9979

Figure 11-11: Course Duplicate Min Au vs. Max Cu Plot



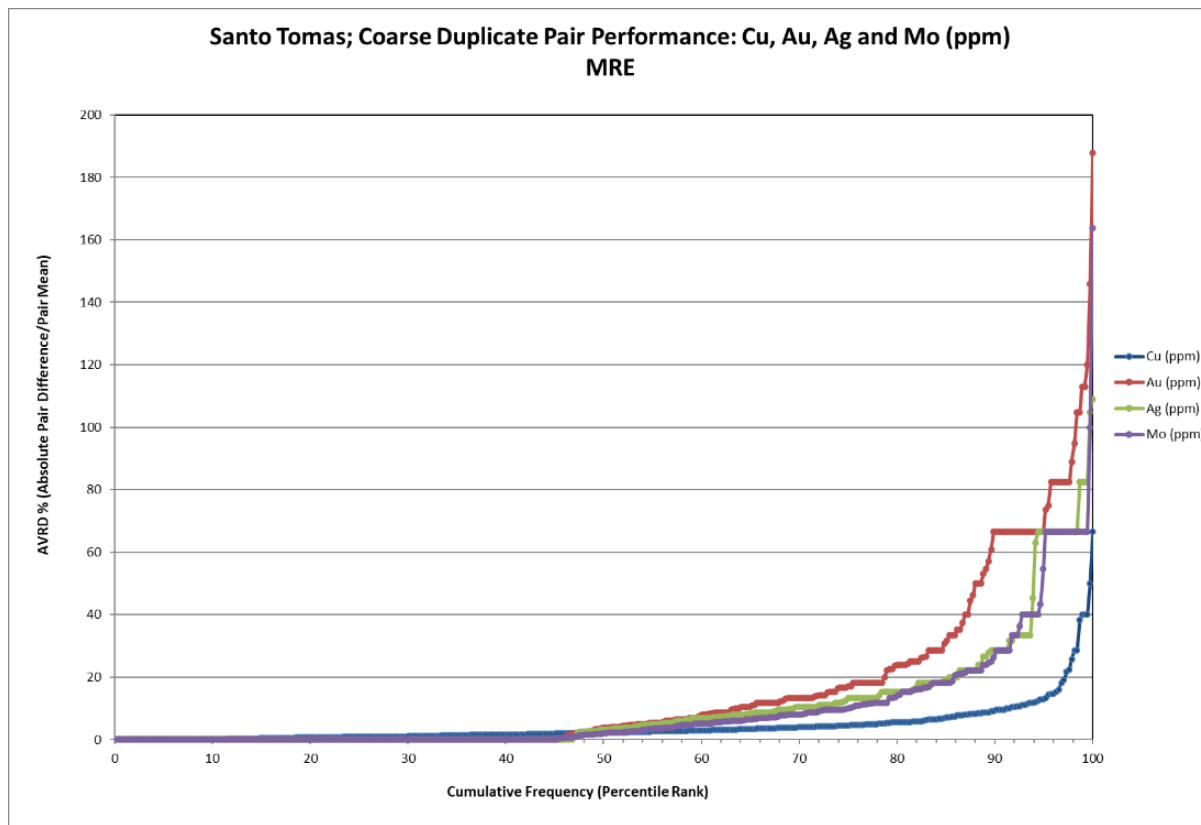
Source: Oroco, 2023.

Using the AVRDR method, the CDUPs achieve the desired 90% passing for Cu (see Table 11-13) but fall ~10% short for Au and ~5% short for Ag and Mo. Visually, the AVRDR plot in Figure 11-12 shows better shaped curves, although the inflection point occurs early for Au, Ag and Mo.

Table 11-13: Summary Table of AVRD Analysis for CDUP Pairs

Element	CDUP Pairs w AVRD<0.2
Cu	97.1
Au	78.5
Ag	85.1
Mo	85.6

Figure 11-12: CD Cumulative Frequency vs. AVRD Plot



Source: Oroco, 2023.

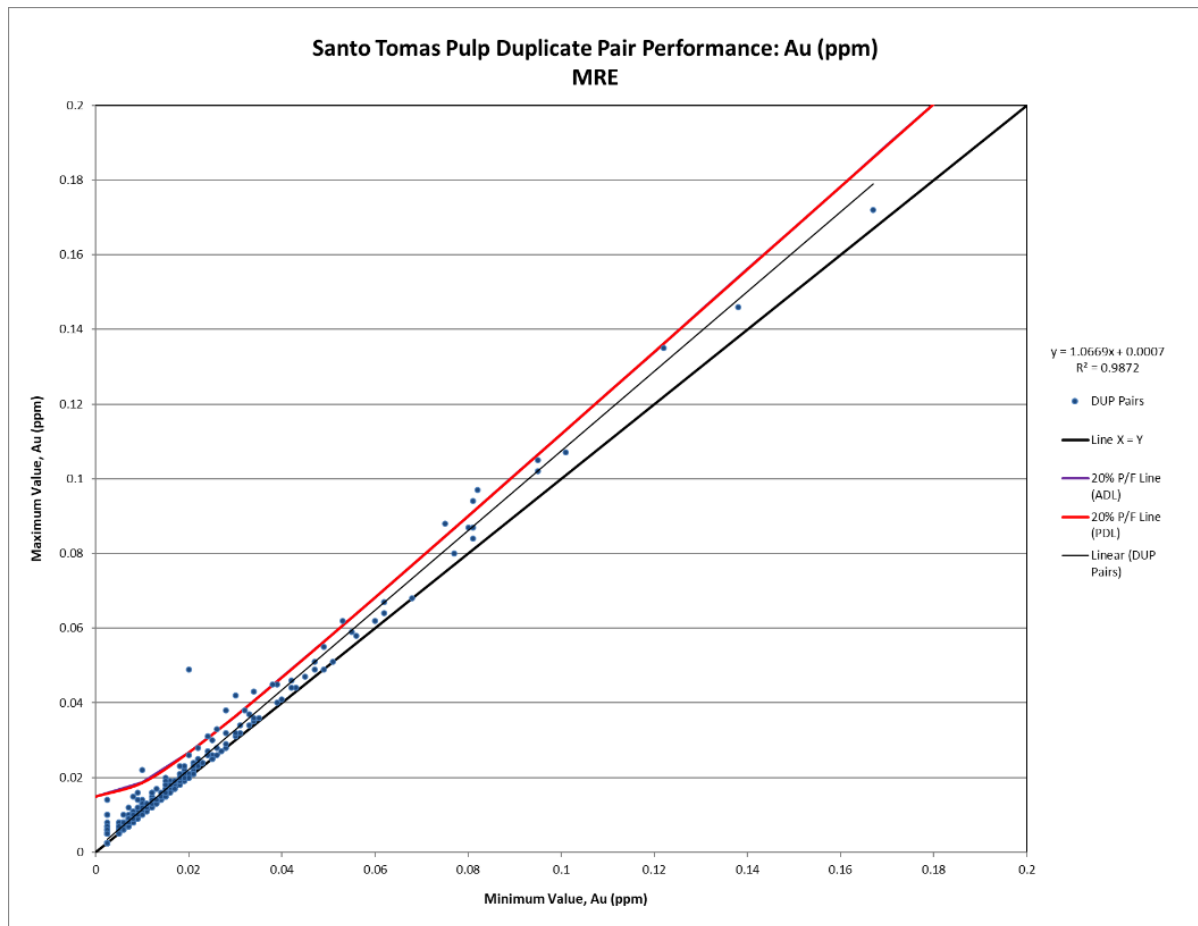
11.9.4.1 Pulp Duplicates

For the Max/Min analysis, Cu, Au, Ag and Mo pairs meet the above stated criteria of at least 90% passing. A summary table (Table 11-14) and an example Min/Max plot shown in Figure 11-13 for PDUPs can be seen below.

Table 11-14: Summary of Min/Max Plot Analysis for PDUP Pairs

Duplicate Type	Element	Total Pairs	Analytical Detection Limit			Practical Detection Limit			R2	R
			Value	Failures	% Passing	Value	Failures	% Passing		
PDUP	Cu ppm	451	1	11	97.5	1.5	7	98.5	0.9997	0.9998
	Au ppm	451	0.005	12	97.3	0.005	12	97.3	0.9872	0.9936
	Ag ppm	451	0.5	2	99.6	0.5	2	99.6	0.9855	0.9927
	Mo ppm	451	1	18	96	1.5	18	96	0.9994	0.9997

Figure 11-13: Pulp Duplicate Min Au vs. Max Au Plot



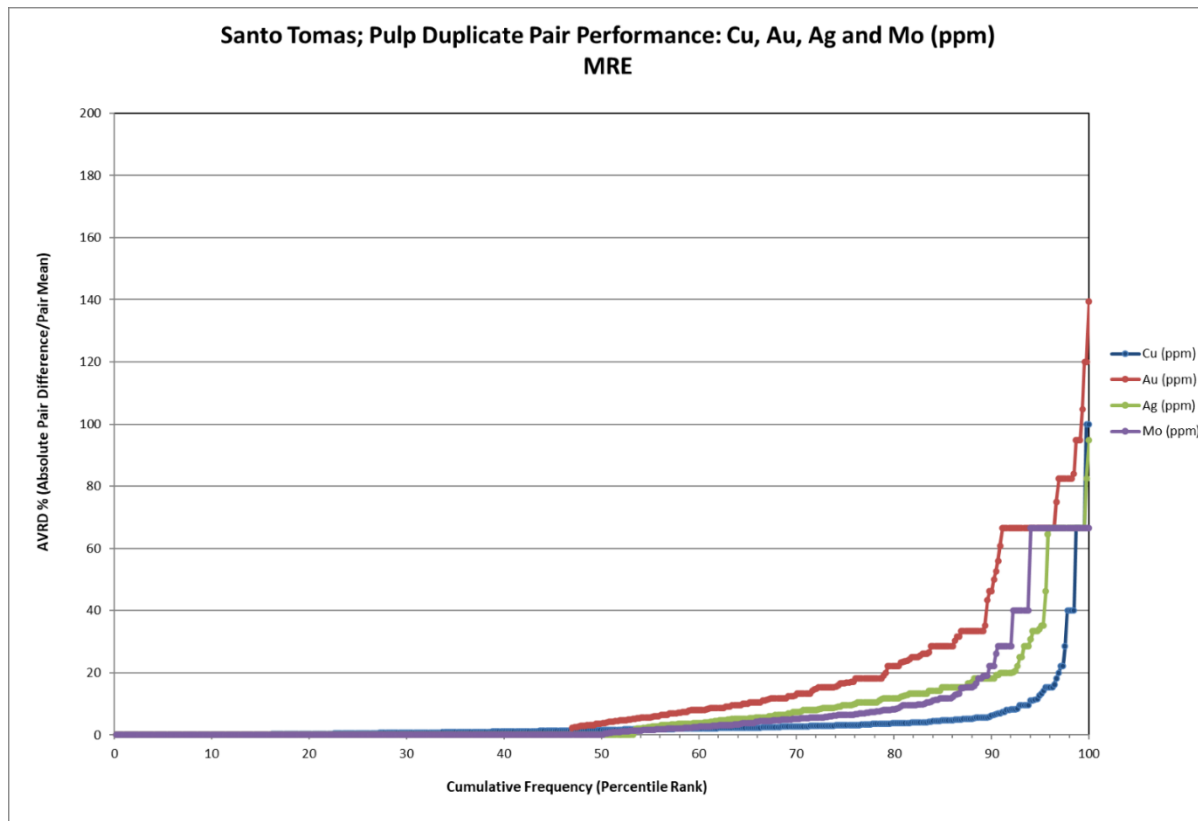
Source: Oroco, 2023.

Using the AVR method, the CDUPs achieve the desired 90% passing for Cu (see Table 11-15) but fall ~25% short for Au and ~10% short for Ag and Mo. Visually, the AVR plots in Figure 11-14 show better shaped curves, although the inflection point occurs earlier than desired for Au, Ag and Mo.

Table 11-15: Summary Table of AVRD Analysis for PDUP Pairs

Element	PDUP Pairs w AVRD<0.1
Cu	93.8
Au	64.3
Ag	75.8
Mo	83.2

Figure 11-14: CD Cumulative Frequency vs. AVRD Plot



Source: Oroco, 2023.

11.9.4.2 Blanks

Blanks were inserted in order to assess the laboratory sample preparation methods and determine if there was any cross-contamination between samples (mineralization that is smeared from one sample to the next). Two types of blanks were used at Santo Tomás: a certified pulp blank (OREAS 23b) and a site-generated coarse blank (CBLK2). At the beginning of the program, a landscaping rock (identified as CBLK1) was briefly used as the coarse blank material while CBLK2 was being prepared and analyzed. Blank performance was evaluated using an upper threshold limit (fail line) generated from the CV or mean plus a multiple of the PDL of the element of interest, as well as the mean of the returned results + 3SD. Neither material was truly “blank”, i.e., the expected value for the four elements of interest was not zero, which is why

failure lines were generated from the mean/CV, rather than from the origin. A certain amount of apparent carry-over from the preceding sample was also required in order for the sample to be sent for re-assay.

11.9.4.3 Pulp Blanks

A pulp blank was considered to be failing if it exceeded the Certified Value + 5 x the PDL (CV + 5PDL), as well as the Mean of the Returned Results + 3 Standard Deviations ($\mu + 3SD$). A failed pulp blank also had to exceed 0.2% apparent carry-over from the preceding sample in order to be sent for re-assay.

Table 11-16: Summary Table of Pulp Blank Performance

Blank Type	Element	Total Pairs	CV + 5PDL			$\mu + 3SD$		
			Value	Failures	% Failed	Value	Failures	% Failed
OREAS 23b (Pulp Blank)	Cu ppm	702	54.2	35	5	57.4	8	1.1
	Au ppm	702	0.028	2	0.28	0.0137	14	2
	Ag ppm	702	2.565	0	0	0.327	5	0.71
	Mo ppm	702	10.7	0	0	4.7	1	0.1

Ideally, blank results should fall below the determined cut-off 90% of the time. This was achieved for all elements of interest, as the pulp blanks fell below the CV + 5PDL 95% of the time or greater (Table 11-16 and Figure 11-15).

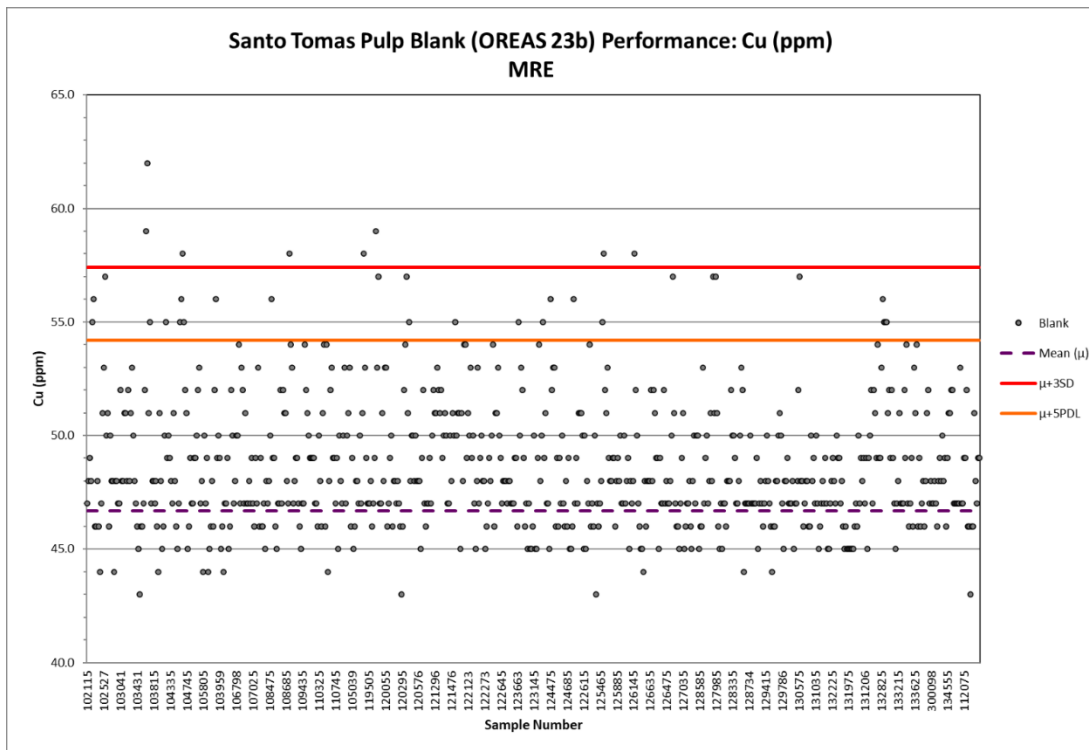
As OREAS 23b is a certified blank akin to a standard, a standard control chart can be used to evaluate the results in order to identify outliers that fall outside the $\mu \pm 3SD$ (Figure 11-16). Using this method of analysis, two percent or less of samples were identified as outliers or failures, for all elements of interest.

Smear charts or Blank Value vs. Proceeding Sample plots were also used to determine the amount of carry-over (if any) between samples (Figure 11-15). The smear charts show a small positive linear relationship for Cu, Ag and Mo. For example, the Cu Smear Chart produces the linear equation $y = 0.0009x + 47.278$, and therefore a potential proceeding sample of 10000ppm (or 1%) Cu, would induce a blank value of only 56 ppm Cu. Such a potential lift is inconsequential in terms of the average grade of this deposit.

Table 11-17: Pulp Blank Calculated Potential Carry-Over

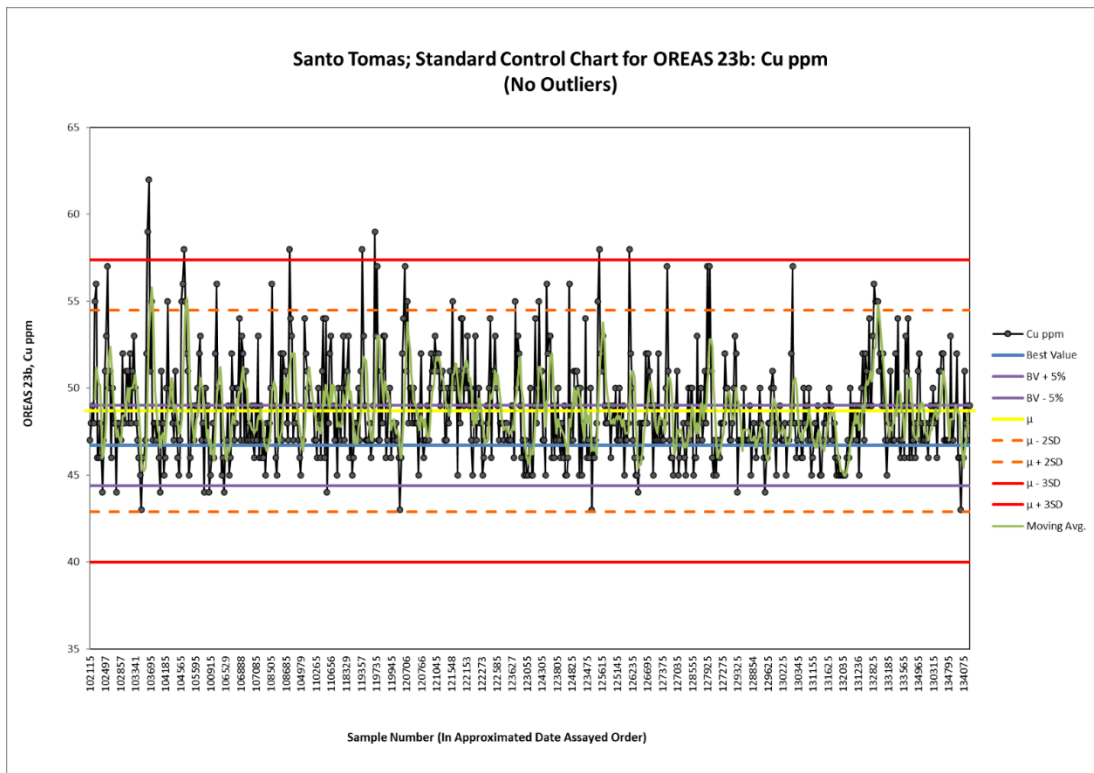
Amount of Potential Carry-Over (Pulp Blanks)			
Element	Smear Chart Linear Equation	Proceeding Sample Value (x) in PPM	Potential Carry-Over (y)
Cu	$y = 0.0009x + 47.278$	10000	56.28
Au	$y = -0.3794x + 0.0253$	1	-0.35
Ag	$y = 0.0003x + 0.2516$	1	0.25
Mo	$y = 0.0016x + 3.1196$	10	3.14

Figure 11-15: Pulp Blank Performance Chart Cu PPM



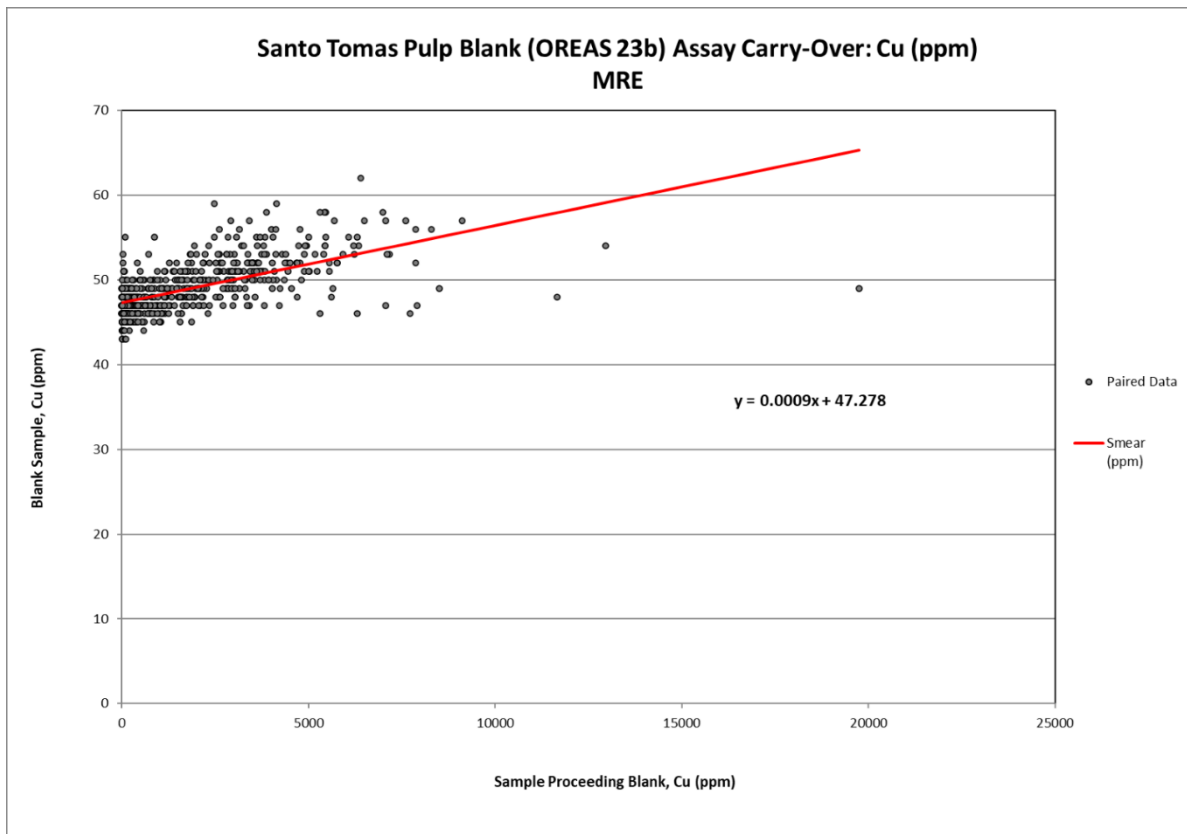
Source: Oroco, 2023.

Figure 11-16: Standard Performance Chart for OREAS 23b, Cu PPM



Source: Oroco, 2023.

Figure 11-17: Pulp Blank Potential Carry-Over or Smear, Cu PPM



Source: Oroco, 2023.

11.9.4.4 Coarse Blanks

A coarse blank (CBLK1/CBLK2) failed if it exceeded the Mean + 5 x the PDL ($\mu + 5PDL$), as well as the Mean of the Returned Results + 3 Standard Deviations ($\mu + 3SD$) as summarized in Table 11-18 and plotted in Figure 11-18. A failed coarse blank had to also exceed 1% apparent carry-over from the preceding sample in order to be sent for re-assay.

Table 11-18: Summary Table of Coarse Blank Performance

Blank Type	Element	Total Pairs	$\mu + 5PDL$			$\mu + 3SD$		
			Value	Failures	% Failed	Value	Failures	% Failed
CBLK1 (Coarse Blank)	Cu ppm	103	19.6	25	24.3	50.8	1	1
	Au ppm	103	0.028	0	0	0.0051	2	1.9
	Ag ppm	103	2.758	0	0	0.436	2	1.9
	Mo ppm	103	8.3	0	0	2.1	0	0
	Cu ppm	341	41	49	14.4	74.3	9	2.6
	Au ppm	341	0.028	0	0	0.0048	20	5.9

Blank Type	Element	Total Pairs	$\mu + 5PDL$			$\mu + 3SD$		
			Value	Failures	% Failed	Value	Failures	% Failed
CBLK2 (Coarse Blank)	Ag ppm	341	2.75	0	0	0.34	3	0.9
	Mo ppm	341	8.6	0	0	3.2	6	1.8

Ideally, blank results should fall below the determined cut-off 90% of the time. For both CBLK1 and CBLK2, Au, Ag and Mo passed 100% of the time. For Cu, the results fell below the CV + 5PDL only 75% of the time for CBLK1, and 85% of the time for CBLK2.

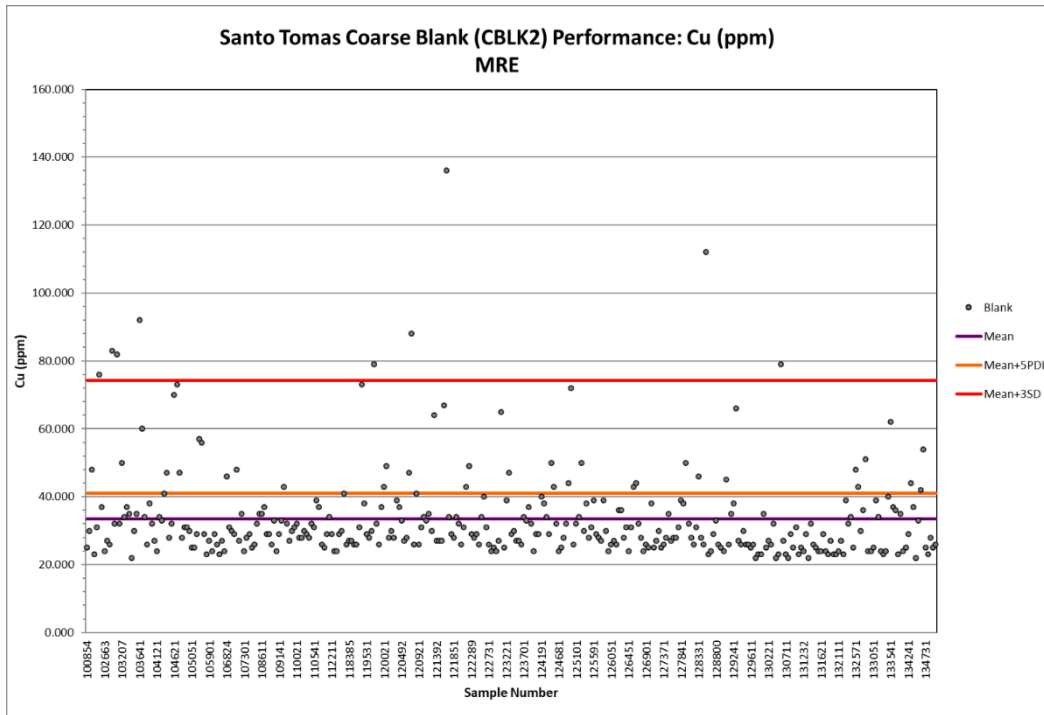
CBLK1 and CBLK2 are not certified blanks, but if a standard-type chart is used to evaluate the results based on the mean +/- 3SD to identify outliers, then >94% of coarse blanks pass for all elements of interest for both CBLK1 and CBLK2 (Figure 11-18).

Smear charts or Blank Value vs. Preceding Sample plots were also used to determine the amount of carry-over (if any) between samples (Table 11-19). CBLK1 shows a small positive linear relationship for Cu and Mo. The Cu Smear Chart produces the linear equation $y = 0.0051x + 2.8155$, and therefore a potential preceding sample of 10000ppm (or 1%) Cu, would induce a blank value of only 56 ppm Cu. For CBLK2, the smear chart (Figure 11-19) show a small positive linear relationship for all elements of interest. The Cu smear chart equation, $y = 0.0042x + 27.876$, would induce a blank value of only 70ppm Cu, with a preceding sample of 10000 ppm or 1% Cu. In both cases, such a potential Cu lift is inconsequential in terms of the average grade of this deposit.

Table 11-19: Pulp Blank Calculated Potential Carry-Over

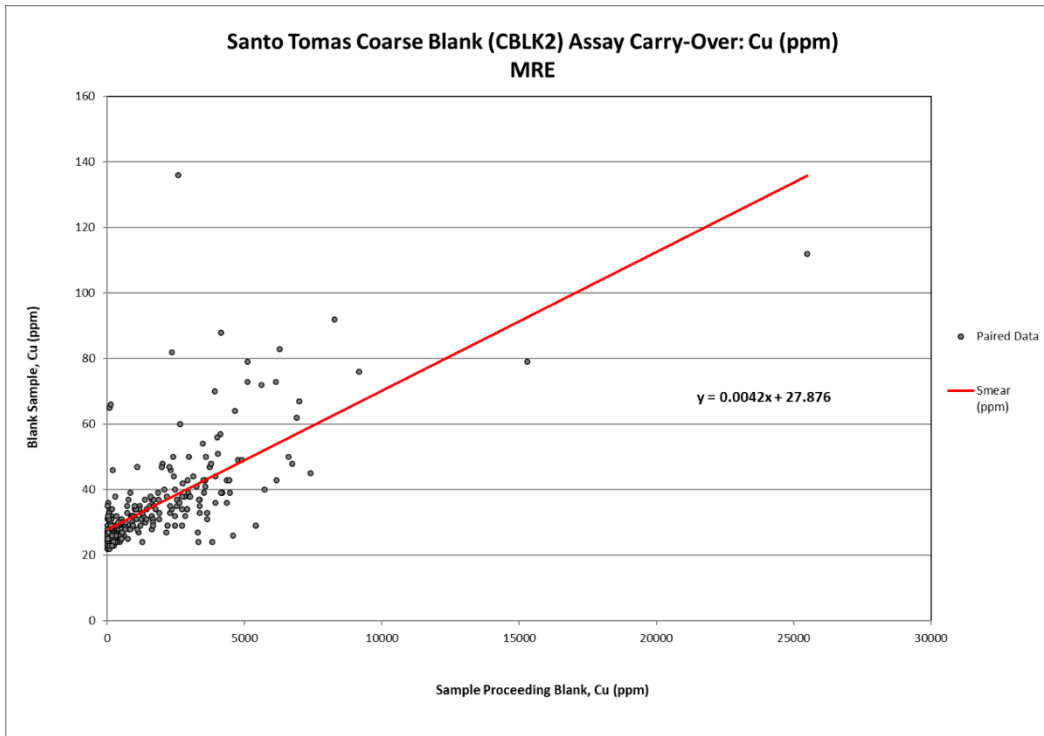
Blank No.	Amount of Potential Carry-Over (Coarse Blanks)			
	Element	Smear Chart Linear Equation	Preceding Sample Value (x) in PPM	Potential Carry-Over (y)
CBLK1	Cu	$y = 0.0051x + 2.8155$	10000	56.28
	Au	$y = -0.00002x + 0.0027$	1	-0.35
	Ag	$y = -0.0004x + 0.2586$	1	0.25
	Mo	$y = 0.0031x + 0.6618$	10	3.14
CBLK2	Cu	$y = 0.0042x + 27.876$	10000	69.88
	Au	$y = 0.0026x + 0.0026$	1	0.01
	Ag	$y = 0.0006x + 0.2502$	1	0.25
	Mo	$y = 0.0033x + 1.0303$	10	1.06

Figure 11-18: Coarse Blank Performance Chart for Cu



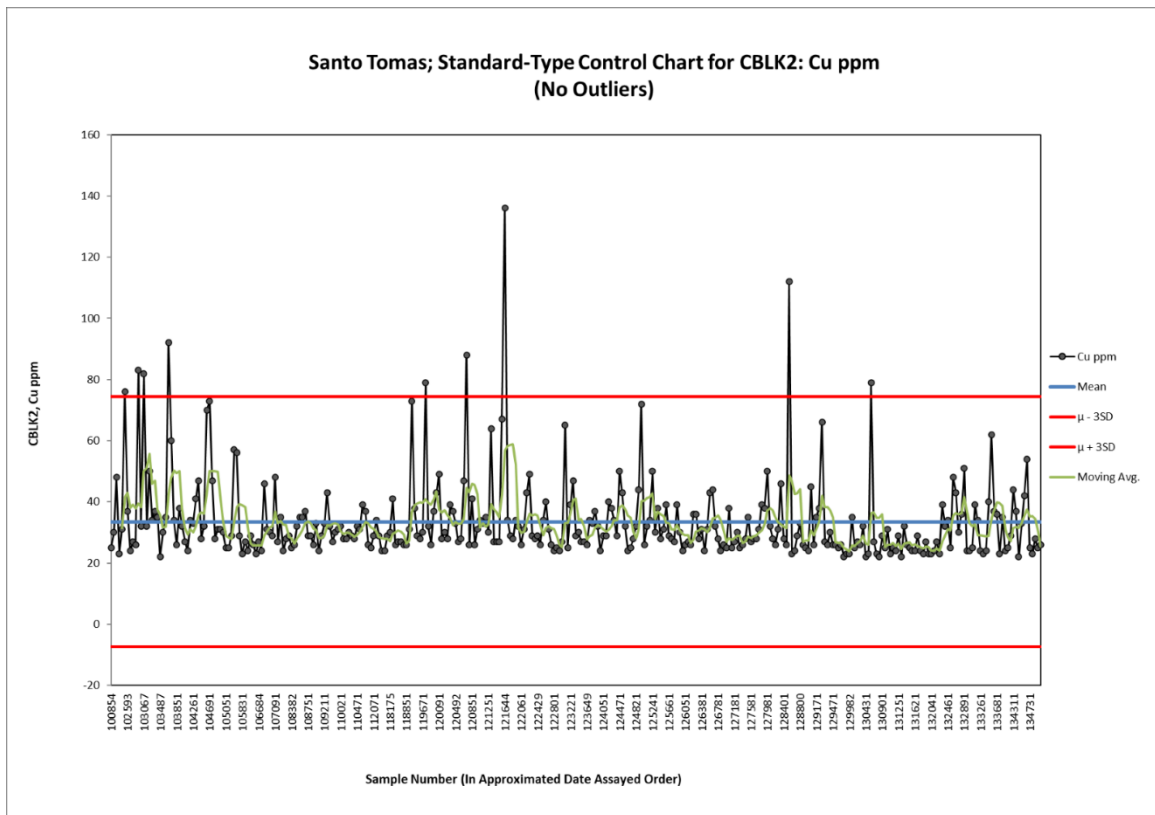
Source: Oroco, 2023.

Figure 11-19: Coarse Blank Performance Smear Chart for Cu



Source: Oroco, 2023.

Figure 11-20: Standard-Type Chart for CBLK2, Cu PPM



Source: Oroco, 2023.

11.9.5 Pulp Check Assays

Pulp check assays are sample pulps that are submitted to a second independent laboratory. Oroco is currently compiling a selection of 5% of the total samples to send for check assay analysis. These samples will likely be sent to Bureau Veritas. Once complete, pulp check assays will be evaluated by plotting the primary lab against secondary lab results and calculating the average, standard deviation, regression slope and R2 of the samples. Bias will be determined using the Reduction to the Major Axis (RMA) method and ideally, bias should be less than 5%. A bias of 5-10% is questionable and >10% is unacceptable (Simon, A., AMEC International, 2007).

11.9.5.1 QA/QC Analysis Conclusions

Standard performance for OREAS 151a, 151b, 505, 506 and 701 is good. Moving averages generally remain within plus or minus 5% of the Best Value and 95% of the samples assayed fall within two standard deviations of the mean, with a few exceptions that have been discussed previously and deemed reasonable. Thirteen samples exceed three times the standard deviation of the mean. The results of these samples have been reviewed and considered acceptable.

Coarse and Pulp Duplicate performance is good with >90% pairs passing and reasonable AVR curves. Field duplicate performance is slightly below target with Cu and Mo pairs only ~80% passing, but still meets expectations. The decreased precision is likely due to the difficulty in replicating results across twin samples due to veining or nugget effects.

Pulp blanks performed well with an overall failure rate of 2% or less for all elements of interest. Coarse blanks also performed well with an overall failure rate of 3% or less. Smear charts do not indicate any significant trends.

Overall, the performance of all types of inserted QA/QC sample types meets or exceed expectations.

11.10 Comments on Sample Preparation, Analyses and Security

The Authors are of the opinion that the sample preparation, QA/QC program and sample security measures undertaken by Oroco are appropriate for a high degree of confidence to be placed in the sample assays that form the basis for this MRE.

12 DATA VERIFICATION

12.1 Oroco Verification

Oroco has a well-documented series of Standard Operating Procedures (SOP) covering core handling, sampling QA/QC submission and geological data collection efforts. These go through periodic updates on an as-required basis as equipment or other data collection protocols are changed.

Data verification occurs prior to incorporation of data into final data bases. Oroco SOP's for various activities are listed below with last update date in Table 12-1. SOP's have been reviewed and improved through the use of consulting third-party subject matter experts.

Table 12-1: Oroco Core facility Standard Operating Procedure List

SOP Protocol	SOP Updated Date
Point Load Testing	Mar-22
Sample Preparation of Core + QA/QC	Mar-23
Specific Gravity Measurements	Apr-22
Core Logging Manual	May-23
K-Staining Analysis	Jun-22
Niton Sampling and Manual	Apr-23
Core Handling Flowsheet	Feb-22
Rig Alignment TN14 Gyrocompass	Apr-22
Oriented Core ACT III	Apr-22
EZ-Gamma tool	Apr-22
EZ-Gyro Tool	Apr-22
IQ Logger - Geotechnical	Apr-22
TerraSpec Manual/Procedure	Apr-23
Field Procedure for Core Collection and Transport	Apr-22

SRK has reviewed the SOP's and found them to be acceptable by industry standards. Oroco's technical staff will follow the procedures and document any changes in a systematic manner.

12.2 Assay Data and QA/QC Results Verification

Submission rates for commercial standards, blanks and duplicates is to industry standard, averaging one control sample submitted for every four core samples. Laboratory Assay failures are managed in a consistent manner. Pass/fail rates are detailed in Section 11 along with a more detailed review of QA/QC management. All Oroco assay work is performed at an independent third-party laboratory. Assay data is stored in DataShed™ which uses an SQL backend. In February 2023, Oroco sent assay certificates for all holes through to N043 to SRK. SRK verified assay data as discussed in Section 12.7.

12.3 Down Hole Survey Data Verification

SRK reviewed the down hole survey files. Three survey tool types were used in the program. An internal Oroco memo on downhole survey data outlines the procedure for capturing and incorporating survey data into a final database. Documentation of the data collection, verification and quality evaluation procedures were reviewed. The collection and management of down hole survey data is at acceptable industry standards.

Hole orientation verification is managed through the use of the IMDEX TN-14 rig orientation tool. Gyro tool data from the downhole survey is “adjusted” with the TN-14 tool collar reading to produce the actual collar dip and azimuth.

12.4 Point Load Testing and Specific Data Verification

Data checks performed on the Specific Gravity measurements include an on-going program of comparison of results for individual lithologies. In the event that an SG measurement was out of range, the SG measurement was repeated on the other half of the HQ core or in the case of NQ core the next 10-15 cm of core in the core box was repeated.

For point load testing, there were no repeated tests as the process is destructive.

Point Load Testing and SG data collection methodologies are documented and changes in procedures over the life of the drill program captured in site SOPs.

12.5 Core Orientation Verification of Continuity

Validation of measured RQD data is done by comparing final data bases with the photos of the whole core. Low or high values are checked and rectified as necessary. This functions as a check against data entry errors. When new staff are introduced to the project, the Lead Geotechnical logger logs in parallel with the new geologist for week. In addition to the training period, every two weeks the geological crew will run a spot check by logging the same section of core to ensure repeatability of measurements between the different geologists.

SOP's on the core orientation procedures and rig orientation procedures and equipment is documented and geologists are trained by the Geotechnical lead in data collection methods and data capture.

12.5.1 Geological Data Verification

Similarly, geological logging procedures and observational data recording is managed by the Geology lead and new employees are trained and supervised to ensure consistency in logging. At the end of the logging of a hole, the information is processed for each hole by the geologists using previously generated cross-sections.

When uncertainties in rock type and alteration assemblages arise, K-feldspar staining and TerraSpec data is used to resolve uncertainties. A systematic TerraSpec and Niton data collection program supports the interpretation of the geology. The use of lithogeochemistry data (by using ioGAS) also helps in the classification of intrusives. Kt-10 MagSus is used to correlate the amount of magnetite especially in the footwall in real-time. Cross-sections, updated daily, are used to correlate the lithology-alteration-mineralization along the strike of the deposit. Surface geological mapping is also used as a control to ensure geological continuity is maintained.

Evolution of the geological codes has resulted in the simplification of the geological codes at the end of 2022. A re-logging program was completed for all holes prior to November 2022. A third-party review (Cambria Geoscience Inc.) of all drill core logging, structural data and surface mapping is an on-going program and functions as check on data generated on-site at the El Ranchito core logging facility.

12.6 Field Surveying Data Verification

An internal Oroco memo on collar and point surveying was reviewed and found to meet industry standards. Processed field data using the control point has sub-decimeter accuracy in both the horizontal and vertical. A third-party surveying check on the Santo Tomás Control point should provide the same results as the closest geodetic control points used. This is a recommended action.

Summary data base statistics are tabulated in Table 12-2.

Table 12-2: Data Collection Summary on Oroco and Historical Drilling

Drill Hole Data summary	Count Values	Meters
STD holes drilled / meters	50	16,004
STE holes drilled / meters	40	5,071
Oroco holes drilled Included in MRE	65	40,979
Oroco holes drilled Excluded in MRE	11	7,502
Re-logged Historic Meterage	20	14,872
Historical Core Recovered from El Bienestar Ranch	50	10,396
Assays STD drill holes	4,707	-
Assays STE drill holes	2,537	-

Drill Hole Data summary	Count Values	Meters
Assays Oroco Included	19,135	-
Assays Oroco North Zone	13,632	-
Assays Oroco South Zone	5,503	-
QA/QC Samples inserted	3,861	-
Intervals with RQD data calculated	14,643	-
Vein characterization Data	4,253	-
Faults characterization Data	7,753	-
Fractures characterization Data	13,534	-
Point Load Tests	3,632	-
Specific Gravity Data points	1,918	-
Niton XRF data points	29,563	-
TerraSpec Data points – Specific	8,077	-
TerraSpec Data Points – Systematic	20,426	-
Re surveyed Historical hole Collars	49	-

12.7 Verification Performed by the QP

SRK reviewed Oroco’s internal quality control program for analytical data and drilling survey confidence. The current procedures and protocols in place for data collection and validation are considered acceptable for use in mineral resource estimation.

SRK performed an independent review and validation of a select number of analytical samples to check for congruence and accuracy with the provided drilling database on the Santo Tomás project. Approximately 5% of assay intervals were manually checked with original digital assay certificates from the laboratory. All checked assays were deemed acceptable and align with laboratory reported values.

SRK performed statistical analyses on the drilling database to check for potential erroneous data in the collar, downhole survey, geology/lithology, specific gravity, and assay tables. The review included calculation of descriptive statistics, multiple charts, and review of potential outlier and erroneous data. This validation check aimed to identify errors common amongst drilling databases including use of zero value, treatment of below detection limits, negative or non-numeric values, extreme outlier identification, and interpretation of the distribution of mineralization across the property.

It is the QP's opinion that the statistical review did not identify material errors not already identified in associated validation steps.

12.8 Site Inspection

During March 2023, Scott Burkett, SME-RM (#4229765) of SRK conducted a site visit and tour of the project site, core shed, drill pads, and ancillary facilities located on the property. Mr. Burkett reviewed and discussed with site personnel the site geology, structure, mineralization, drilling, core logging and sampling, density measurements, site security, core and sample storage, and procedures involved with data management. The site visit was hosted by a combination of Oroco management and site-based staff. Mr. Burkett was provided unfettered access to all aspects of the project and staff with all questions satisfactory addressed by the Company. Also in March 2023, Ron Uken of SRK Vancouver conducted a site visit and tour of the project. Mr Uken had previously undertaken a field visit in 2022.

It is the QP's opinion that Oroco manages the site data acquisition, sample storage, and management of all items in a disciplined and organized fashion, consistent with accepted industry practices. The QP notes a knowledgeable and capable workforce with protocols in place consistent with good practice.

12.9 Limitations on Data Verification

The following items are identified as known limitations on data verification and accounted for in mineral resource classification by the QP mineral resources:

- Use of historical drilling and analytical data in support of the mineral resources with limited documentation on collar, downhole survey, and logging.
- Lack of documented quality assurance and quality control (QA/QC) protocols on drilling completed prior to 2021 performed by the previous owners.
- The QP did not directly supervise or oversee data acquisition of any drilling, logging, or analytical data used in the determination of mineral resources. Instead, the QP reviewed summary data, technical reporting, and supporting documentation that summarize procedures and protocols and performed independent verification. All descriptions of procedures and methods used in the collection of data supporting mineral resources were provided by Oroco when available. Based on these documents and communications, it is the QP's opinion that drilling and analytical data used in support of resources were collected in a manner aligned with good industry practice sufficient for resource classification.
- The QP has not conducted a visit or inspection to the analytical laboratories which provided the baseline analytical data supporting resources. The laboratories used are considered reputable and independent laboratories suitable for the analyses performed.
- No independent duplicate samples were collected nor analyzed for verification purposes by the QP.
- The QP did not perform field verification of drillhole collar locations but relied on historical collar surveys as accurate in X, Y, and Z coordinates with data being validated against aerial imagery and high-resolution topographic data.

12.10 Opinion on Data Adequacy

It is the QP's opinion that the geological mapping, topographic, and drilling data utilized during geological interpretation and in the estimating mineral resources has been adequately reviewed and classified in-line with CIM guidelines. Items identified as potential project risks, low confidence data, or lack of historical multi-element assay data are accounted for in the mineral resource classification.

13 MINERAL PROCESSING AND METALLURGICAL TESTING

13.1 Introduction

Metallurgical testing of the Santo Tomás mineralized material and host rocks began in 1975 with the most recent metallurgical test work prior to now (2023) completed in 1994 by Mountain States Research and Development Inc (MSRDI). This historical testing is described in the Santo Tomás Prefeasibility Study prepared for Exall and published by Bateman in 1994. The mineralized drill samples selected for testing by Exall were selected from what was then characterized as the “North pit area.” Prior to that only a very limited amount of metallurgical testing was conducted on Santo Tomás materials but the locations of which are unknown and test reports are no longer available to validate the data. As such, the legacy test work reported herein is thought to be conceptual in nature and not suitable to support a modern technical study.

The project is expected to be a large-scale open pit operation that would utilize froth flotation to produce saleable copper and molybdenum concentrates. A metallurgical sample selection process was initiated with Oroco’s geological team in 2022 to obtain suitable metallurgical data to support current development studies. The selected drill core samples were shipped to ALS Metallurgy in Kamloops, British Columbia, Canada for subsequent testing. The following sections summarize the results of the test program.

13.2 Metallurgical Test Work

13.2.1 Sample Preparation

The metallurgical samples were selected to meet the following criteria:

- Spatial coverage across the deposit, and within the expected pit shell.
- Contain similar levels of copper, sulphur and molybdenum as the potential Life of Mine (LOM) grades.
- Include samples that would be expected to represent some variance in characteristics that would affect metallurgical performance.

The resulting 9 samples selected based on these criteria are summarized in Table 13-1.

Table 13-1: Selected Metallurgical Variability Samples

Sample	Description
South Quartile	Spatially across deposit Average grades of approx. 0.3% Cu and 1.0% S
Mid-South Quartile	
Mid-North Quartile	
North Quartile	
High Cu	target 0.40%
Low Cu	target 0.18%
High S:Cu Ratio	target 10:1 ratio

Sample	Description
High Moly	target 0.025% Mo
High Point Load	harder material based on point load data

A Master Composite was then assembled from portions of selected individual samples to reflect spatial coverage and a target feed grade.

13.2.2 Chemical and Mineralogical Characterization

Head assays on the composites are shown in Table 13-2 and mineral contents of significant abundance are summarized in Table 13-3.

Table 13-2: Head Assay Data

Sample ID	Assay - percent							Assay – g/t	
	Cu	Zn	Mo	Fe	S(t)	S(s)	SO4	Au	Ag
South Quartile	0.29	0.01	0.004	3.39	0.77	0.71	0.04	0.02	1.7
Mid-South Quartile	0.23	0.01	0.007	2.78	0.77	0.73	0.02	0.02	1.6
Mid-North Quartile	0.30	0.03	0.004	2.66	1.16	0.99	0.03	0.02	1.9
North Quartile	0.26	0.03	0.006	2.71	1.18	1.09	0.07	0.03	1.5
High Point Load	0.36	0.01	0.024	3.09	0.51	0.45	0.04	0.02	2.1
Low Copper	0.20	0.01	0.014	2.01	1.09	0.82	0.08	0.03	1.6
High Copper	0.39	0.01	0.013	1.83	1.34	1.37	0.04	0.05	1.9
High Moly	0.31	0.01	0.018	4.40	0.92	0.88	0.02	0.01	1.8
High S:Cu Ratio	0.18	0.02	0.003	5.10	2.38	2.27	0.03	0.02	1.4
Master Composite	0.34	0.06	0.011	2.84	1.02	0.99	0.03	0.02	2.3

Table 13-3: Mineral Composition Data

Sample ID	Mineral Composition - percent							
	Chalcopyrite	Pyrite	Quartz	Feldspars	Chlorite	Ca Carb.	Micas	Epidote
South Quartile	0.9	0.6	18.3	52.2	11.0	1.1	7.7	2.8
Mid-South Quartile	0.8	1.3	28.7	42.2	7.9	1.3	12.5	1.5
Mid-North Quartile	0.8	1.9	35.6	34.8	7.4	0.6	13.9	2.5
North Quartile	0.6	1.6	30.3	40.3	6.0	0.4	16.0	2.3
High Point Load	0.9	0.2	22.0	46.9	8.5	0.2	15.4	2.6
Low Copper	0.6	1.4	39.1	40.1	5.0	1.0	9.9	0.8
High Copper	1.0	1.6	43.9	34.8	3.6	0.8	9.8	2.4
High Moly	0.7	1.4	15.0	53.5	6.9	0.1	16.5	2.1
High S:Cu Ratio	0.4	4.1	13.6	55.9	9.0	0.1	10.8	1.7
Master Composite	0.9	1.3	27.4	41.4	8.1	0.8	14.3	2.3

In general, the ratio of sulphur to copper contents is moderate, averaging 4.4 across all 10 samples. This suggests that a moderate level of regrinding and lime addition would be required to depress pyrite in the cleaner circuit and produce a saleable copper concentrate. Molybdenum concentrations averaging 0.010% suggest that production of a molybdenum concentrate is likely feasible. Precious metal contents are quite low but may provide payable credits in the copper concentrate.

Mineral composition was measured using QEMSCAN techniques. Chalcopyrite accounted for approximately 98% of the copper observed in the samples. Molybdenite and sphalerite accounted for less than 0.1% of and pyrite accounted for 1.5% of the total mass.

The host mineral assemblage varies across the samples somewhat, which will likely contribute to variances in grinding energy requirements.

The mineralogical analyses included an estimate of liberation on the variability samples. A detailed PMA was conducted on the Master Composite to more accurately measure liberation characteristics and mineral contents. Liberation values for copper sulphides and pyrite are presented in Table 13-4 along with details of the size distributions of the samples and required lab grinding times.

Table 13-4: Sulphide Mineral Liberation Data

Sample ID	Size P80 µm	Lab mill grind time minutes	Liberation %	
			Chalcopyrite	Pyrite
South Quartile	152	16	37.3	53.5
Mid-South Quartile	162	17	41.1	54.7
Mid-North Quartile	145	19	38.2	63.7
North Quartile	155	18	40.5	54.3
High Point Load	140	21	34.1	64.6
Low Copper	158	19	43.6	55.4
High Copper	158	14	48.9	63.5
High Moly	140	22	39.9	72.9
High S:Cu Ratio	143	25	36.0	76.2
Master Composite	155	18	39.0	55.1

The chalcopyrite was 40% liberated at a primary grind sizing of 150µm, which by itself suggests that this primary grind sizing is likely at the coarser limit of what would be required for effective rougher circuit flotation. However, pyrite showed increased liberation levels at this sizing, averaging 61%.

The detailed mineralogy assessment on the Master Composite suggested that non-liberated chalcopyrite was primarily in binary form with gangue. The average chalcopyrite content of these binaries was 26%, which is of sufficient quality for recovery by froth flotation. This mitigates the somewhat lower liberation value in terms of expected rougher recovery performance at this sizing.

Approximately 9% of the chalcopyrite in the ground Master Composite was present in the >150µm fraction in grains that had less than 15% surface exposure of chalcopyrite. These grains are typically difficult to recovery by conventional flotation means, but a portion could likely be recovered by coarse particle flotation techniques.

Only 2.4% of the copper sulphides in the Master Composite were associated with pyrite in either binaries or in multiphase form. This suggests that regrinding requirements to depress pyrite would be moderate.

13.2.3 Comminution

Each of the variability samples was individually tested for comminution properties, returning the measurements shown in Table 13-5. Average Point Load Index values measured at the Santo Tomás site are shown for reference. In addition, a Rod Mill Work Index test was conducted on the Master Composite that returned a value of 18.4 kWh/tonne.

The 75th percentile values of the variability results were selected for design, an Axb value of 30 and ball mill work index of 18.3 kWh/tonne. HPGR crushing was considered to be more favorable than SAG milling for this project since a significant portion of the samples were hard with respect to impact breakage and the planned throughput for the operation is somewhat high.

Table 13-5: Comminution Test Data Summary

Sample	SMC Test Results			Bond ball mill Wi (kWh/t)	Bond Abrasion Index (g)	Site Point Load Index (MPa)
	DWi kWh/m ³	Mih kWh/t	A x b			
South Quartile	7.7	17.2	33.8	17.8	0.09	12.9
Mid-South Quartile	5.7	12.5	46.6	16.4	0.11	7.6
Mid-North Quartile	7.2	15.6	37.3	17.6	0.13	2.1
North Quartile	8.9	19.5	29.9	17.8	0.16	6.3
High Point Load	9.6	20.8	27.7	18.3	0.16	23.8
Low Copper	4.4	9.7	59.6	18.1	0.19	8.8
High Copper	4.8	10.6	54.8	15.4	0.16	1.7
High Moly	10.4	22.4	26.0	19.4	0.13	16.9
High S:Cu Ratio	7.9	17.5	33.1	20.0	0.15	22.5
Master Composite	7.3	16.1	36.1	17.0	0.14	-

There appears to be a relationship between the Point Load Index measurements collected at site on the drill core and the comminution results. This could prove to be a valuable measurement in estimating the hardness characteristics in the block model and assisting in the prediction of mill throughput.

13.2.4 Flotation Test work

In the following subsections, Ausenco presents a review of the flotation test work conducted in this program.

The flotation test program is summarized below:

- Flowsheet development testing on the Master Composite
 - Primary grind and rougher chemistry evaluation
 - Cleaner circuit and regrind requirements

- Confirmation of closed-circuit performance with locked cycle test
- Application of developed flowsheet to variability samples

Rougher flotation performance on the Master Composite is summarized in Figure 13-6. Kinetic results are displayed graphically in Figure 13-1 and Figure 13-2. Results suggest that a primary grind sizing of 155 μ m P80 is suitable to achieve 90% recovery of copper in the rougher circuit. Copper rougher recoveries around 89% can still be achieved at primary grind size as coarse as 200 μ m, however less selective pulp chemistry is required such as natural pH and PAX as a collector. Subsequent cleaner circuit testing indicated that less selective rougher chemistry compromised the ability to produce a concentrate of suitable copper grade.

The more selective chemistry conditions selected included addition of 300 g/t lime to achieve a pulp pH of 9.5 and 8 g/t of a phosphine-based collector, 3418A.

Molybdenum recoveries to the rougher concentrate of approximately 82% were achieved at the selected rougher conditions. Fuel oil was added to the primary grind at a dosage of 10 g/t to promote molybdenite recovery. Similar to copper, molybdenum recovery was somewhat insensitive to the range of applied primary grind sizes.

Rougher mass recoveries of approximately 8.5% were required to achieve the target copper recoveries under the applied conditions.

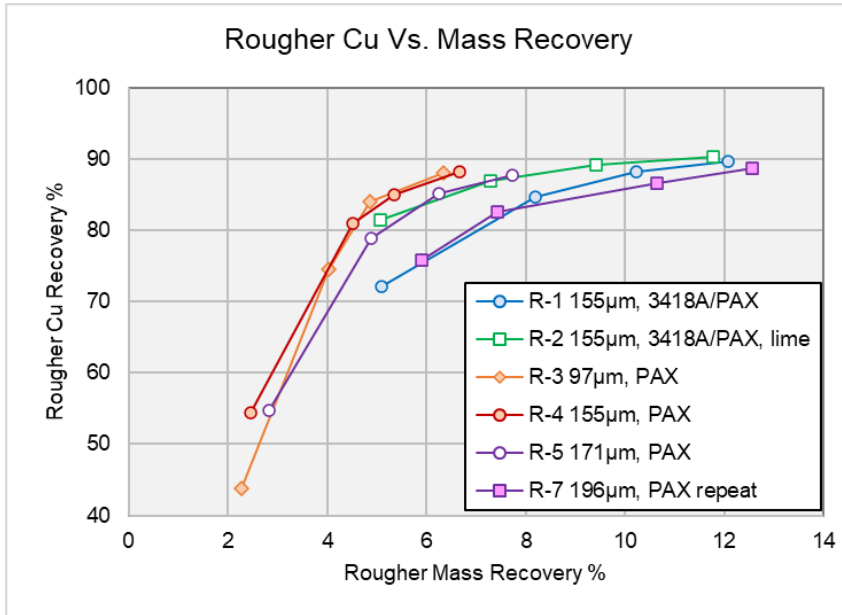
Table 13-6: Rougher Flotation Results – Effect of Grind and Chemistry – Master Composite

Test No.	Primary Grind		Lime	pH	Collector	Calculated Head			Rougher Tail			Recovery % to RoCon			
	minutes	P80				Cu %	Mo %	S %	Cu %	Mo %	S %	Mass	Cu	Mo	S
1 R	18	155	-	8.4	3418A/PAX	0.323	0.010	1.02	0.038	0.002	0.09	12.1	89.7	83.2	92.2
2 R	18	155	Y	9.2	3418A/PAX	0.336	0.011	1.04	0.037	0.002	0.08	11.8	90.3	84.1	93.2
3 R	22	97	-	8.5	PAX	0.306	0.011	1.05	0.039	0.002	0.09	6.4	88.1	82.9	92.0
4 R	18	155	-	8.4	PAX	0.326	0.011	1.02	0.041	0.002	0.09	6.7	88.3	82.9	91.8
5 R	16	171	-	8.4	PAX	0.337	0.011	1.05	0.045	0.003	0.09	7.7	87.7	75.3	92.1
7 R	16	196	-	8.5	PAX	0.325	0.011	1.09	0.042	0.002	0.10	12.6	88.7	84.4	92.0
8 Cl	18	155	-	8.7	3418A	0.325	0.011	1.05	0.040	0.002	0.11	11.4	89.1	84.1	90.7
9 Cl	18	155	Y	9.5	3418A	0.322	0.012	1.04	0.033	0.003	0.15	8.1	90.6	77.6	86.8
10 Cl	18	155	Y	9.5	3418A	0.334	0.011	1.05	0.034	0.002	0.13	8.3	90.7	83.6	88.6
11 Cl	15.5	222	Y	9.6	3418A	0.323	0.011	0.98	0.053	0.003	0.13	7.9	84.9	75.3	87.8
13 LC	18	155	Y	9.6	3418A	0.354	0.013	1.09	0.038	0.003	0.14	8.7	90.1	82.5	87.8

Table 13-7: Rougher Flotation Results – Variability Samples

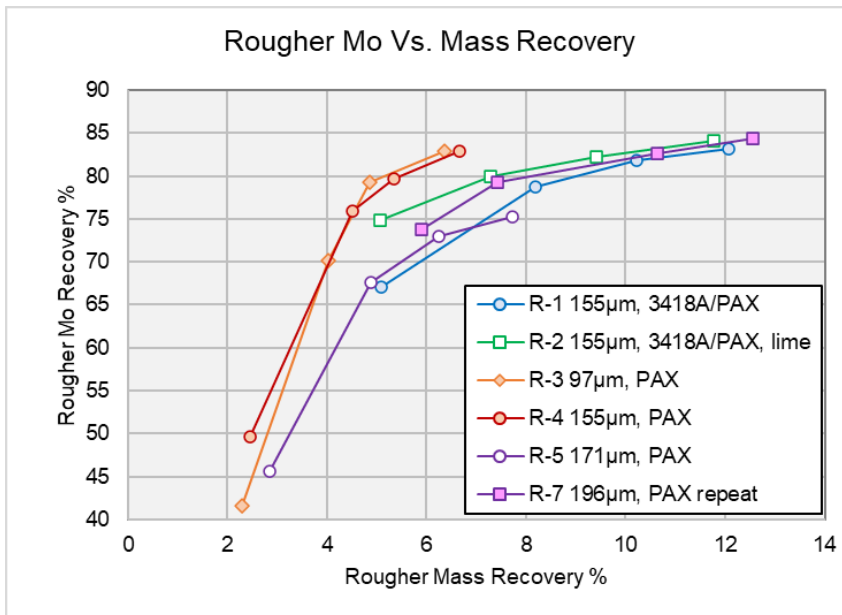
Sample	Test No.	Primary Grind		Lime g/t	pH	3418A g/t	Calculated Head			Rougher Tail			Recovery % to RoCon			
		minutes	P80				Cu %	Mo %	S %	Cu %	Mo %	S %	Mass	Cu	Mo	S
South Quartile	21 Cl	16	152	300	9.8	8	0.283	0.004	0.79	0.032	0.001	0.11	8.1	89.6	76.3	87.3
Mid-South Quartile	19 Cl	16	165	300	9.7	8	0.221	0.008	0.76	0.037	0.002	0.11	7.5	84.5	75.9	86.6
Mid-North Quartile	18 Cl	19	145	300	9.6	8	0.303	0.005	1.24	0.042	0.001	0.17	12.3	87.8	82.1	88.0
North Quartile	20 Cl	18	155	300	9.8	8	0.245	0.005	1.13	0.024	0.001	0.14	9.7	91.1	82.9	88.8
High Point Load	16 Cl	20	181	300	9.8	8	0.370	0.029	0.55	0.045	0.006	0.09	8.5	88.9	81.0	85.2
Low Copper	17 Cl	19	158	300	9.6	8	0.194	0.016	1.14	0.026	0.003	0.14	7.1	87.6	82.7	88.6
High Copper	14 Cl	14	158	300	9.5	8	0.402	0.012	1.39	0.027	0.002	0.09	7.7	93.8	84.5	94.0
High Moly	24 Cl	21	174	300	10.1	8	0.297	0.018	0.91	0.036	0.005	0.09	7.9	88.8	74.2	90.9
High S:Cu Ratio	12 R	23	213	300	9.8	8	0.166	0.005	2.35	0.026	0.004	0.08	14.7	86.6	36.6	97.1
High S:Cu Ratio	22 R	23	213	500	10.5	6	0.163	0.003	2.42	0.019	0.001	0.44	7.4	89.2	67.7	83.2
High S:Cu Ratio	23 Cl	23	213	500	10.5	6	0.172	0.003	2.43	0.019	0.001	0.27	9.0	90.0	66.7	89.9

Figure 13-1: Copper Rougher Kinetic Results – Master Composite



Source: Ausenco, 2023.

Figure 13-2: Molybdenum Rougher Kinetic Results – Master Composite



Source: Ausenco, 2023.

The developed rougher conditions were applied to the variability samples. Separate rougher kinetic tests were first conducted on the High S:Cu Ratio sample, otherwise open circuit cleaner tests were conducted on all other samples. Variability rougher results are summarized in Table 13-7.

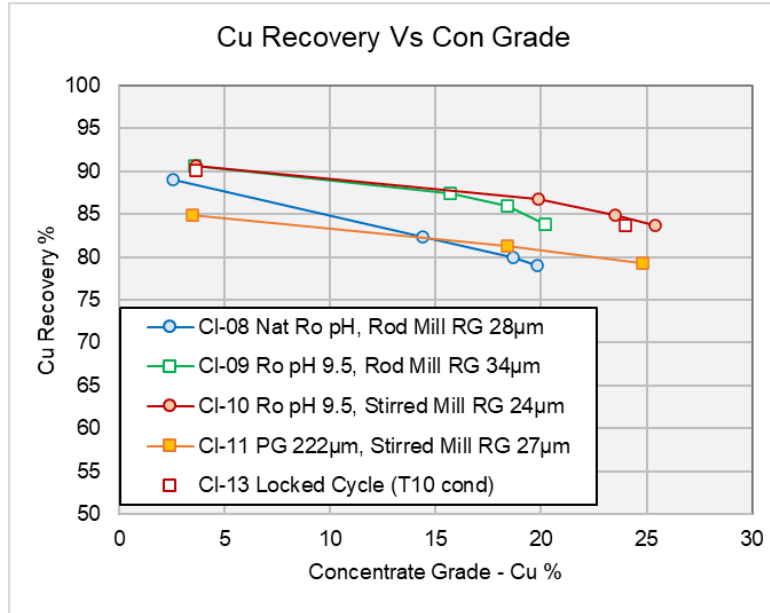
A primary grind size target of approximately 150µm P80 was selected for the variability samples, except in the case of 3 harder samples. For the High Point Load, High Moly and High S:Cu Ratio samples, the grinding times were limited to 20, 21 and 23 minutes respectively in order to minimize the variance from the expected average ball milling energy that would be applied in the process.

Variability rougher performance was generally in line with the Master Composite, however more selective conditions were required for the High S:Cu Ratio sample.

A series of open circuit cleaner tests were conducted on the Master Composite, results are presented graphically in Figure 3 3. It was determined the following conditions were required to achieve suitable cleaner circuit performance with respect to copper concentrate quality and recovery:

- More selective rougher conditions – pH 9.5, 3418A collector
- Regrinding to approximately 23µm P80
- pH 11.0 in the cleaner circuit, achieved by 200 g/t lime addition to the regrind mill
- 3 stages of dilution cleaning

Figure 13-3: Copper Cleaner Performance – Master Composite



Source: Ausenco, 2023.

The developed conditions were applied to the Master Composite in a locked cycle test protocol to demonstrate closed-circuit cleaner performance. The locked cycle test results indicate bulk concentrate recoveries of 82.6% and 61.8% for

copper and moly, respectively, to a concentrate grading 24.7% Cu and 0.68% Mo. The concentrate contained 1.1 ppm gold and 114 ppm silver. A simplified metallurgical balance is presented in Table 13-8.

Table 13-8: Metallurgical Balance – Master Composite Locked Cycle Test

Flotation Stream	Mass %	Assay %			Assay ppm		Distribution %				
		Cu	Mo	S	Au	Ag	Cu	Mo	S	Au	Ag
Rougher Feed	100	0.33	0.012	1.09	0.02	2.30	100	100	100	100	100
Rougher Tail	91.4	0.04	0.003	0.14	-	-	10.6	18.6	12.2	-	-
Rougher Con	8.6	3.46	0.116	11.0	-	-	89.4	81.4	87.8	-	-
1st Cleaner Tail	7.5	0.30	0.032	7.50	-	-	6.8	19.5	51.6	-	-
3rd Cleaner Con	1.11	24.7	0.680	32.1	1.08	114	82.6	61.8	36.3	66.6	61.1
Final Tail	98.9	0.06	0.005	0.70	-	-	17.4	38.2	63.7	33.4	38.9

The developed conditions were subsequently applied to the variability samples in open circuit cleaner tests. Results are summarized in Table 13-9.

Table 13-9: Variability Cleaner Flotation Test Results

Sample	Test No.	Calculated Feed			Head ppm		S:Cu Ratio	Concentrate Grade % or ppm				Recovery to Concentrate %			
		Cu %	Mo %	S %	Au	Ag		Cu	Mo	Au	Ag	Cu	Mo	Au	Ag
South Quartile	21 Cl	0.28	0.004	0.79	0.020	1.650	2.81	25.2	0.27	1.19	112	85.2	66.7	56.9	64.9
Mid-South Quartile	19 Cl	0.22	0.008	0.76	0.020	1.600	3.45	24.6	0.70	1.41	120	77.0	63.0	48.8	51.9
Mid-North Quartile	18 Cl	0.30	0.005	1.24	0.020	1.900	4.09	22.0	0.28	0.90	116	80.1	62.9	49.6	67.3
North Quartile	20 Cl	0.24	0.005	1.13	0.030	1.500	4.63	21.5	0.39	2.00	82	85.0	71.6	64.5	52.9
High Point Load	16 Cl	0.37	0.029	0.55	0.020	2.050	1.50	25.2	1.66	0.86	114	83.0	70.1	52.4	67.7
Low Copper	17 Cl	0.19	0.016	1.14	0.025	1.600	5.88	21.5	1.46	0.89	106	80.2	65.7	25.8	48.0
High Copper	14 Cl	0.40	0.012	1.39	0.050	1.900	3.47	25.6	0.57	2.45	72	86.7	65.3	66.7	51.6
High Moly	24 Cl	0.30	0.018	0.91	0.010	1.750	3.08	23.8	1.09	0.61	86	81.8	62.3	62.3	50.2
High S:Cu Ratio	23 Cl	0.17	0.003	2.43	0.020	1.400	14.1	21.0	0.17	0.56	102	74.3	38.0	17.1	44.4

The variability results suggest that the developed process is suitable for treating material represented by these variability samples. The data suggests that samples with higher ratios of sulphur to copper present a greater challenge to upgrading in the cleaner circuit, which is typical of copper porphyry deposits.

The test program did not include copper-molybdenum separation, however, there do not appear to be any issues identified in the lab testing that would suggest that typical copper-moly separation techniques using NaHS would not be effective. Generally, a molybdenum content in the bulk concentrate of at least 0.5% is sufficient to justify the inclusion of a copper-moly separation circuit. A more thorough review of copper and molybdenum levels across the resource would be required to estimate the viability of producing a molybdenum concentrate over the mine life.

13.2.5 Concentrate Quality

Final concentrate produced from the Master Composite locked cycle test was analyzed for minor elements. Deleterious element levels measured in the concentrate are presented in Table 13-10, along with typical penalty limits. Most minor elements of specific interest were below levels that would be expected to trigger penalties from smelters. Mercury was just above the typical penalty limit at 7 ppm. Smelter penalty terms specific to this concentrate should be confirmed with a concentrate marketing specialist.

It is uncertain why the Master Composite contained a somewhat higher level of zinc than expected, resulting in a level in the concentrate that is near penalty limits see Table 13-10. Based on copper and zinc recoveries measured in the test program, a Cu:Zn ratio of 8:1 or lower in the feed would be required to approach zinc penalties levels in the concentrate. The drill hole assay data suggests that the average grades of intervals above 0.1% copper are 0.335% copper and 261 ppm zinc. This equates to an average Cu:Zn ratio of approximately 13:1, suggesting that that Cu:Zn ratio in the Master Composite was not representative of the average resource.

Table 13-10: Master Composite Concentrate – Minor Elements

Element	Units	Assay	Typical Penalty Limit
Arsenic	%	0.14	0.2
Antimony	ppm	347	500
Bismuth	ppm	46.4	200
Cadmium	ppm	134	300
Cobalt	ppm	45	-
Fluorine	ppm	230	300
Lead	%	0.18	1
Mercury	ppm	7	5
Nickel	ppm	42	-
Nickel + Cobalt	%	0.009	0.5
Selenium	ppm	130	300
Zinc	%	2.51	3

13.2.6 Tailings Acid-Base Measurements

Sub-samples of the rougher flotation tails and total flotation tails (rougher plus cleaner tails) generated in the Master Composite locked cycle test were submitted for acid-base accounting (ABA) analyses.

The results indicate that the Net Neutralization Potential (NNP) of the total flotation tails was -4 tCaCO₃/kt, which is considered potentially acid generating. The NNP of the rougher tails however measured 14 tCaCO₃/kt. This suggests that the pyrite rich cleaner tails has more acid generation potential than the neutralization potential of the total tails.

These results suggest that some additional level of tailings management might be required to ensure that the tailings impoundment does not generate acid. One strategy might be to deposit the cleaner tails separately in a specific area of the impoundment and ensure that this material remains sub-aqueous. Note that the cleaner tails are quite fine and would mostly report to the overflow of the proposed tailings sand cyclone system. The implications of these results should be reviewed with a specialist in environmental monitoring related to tailings impoundments.

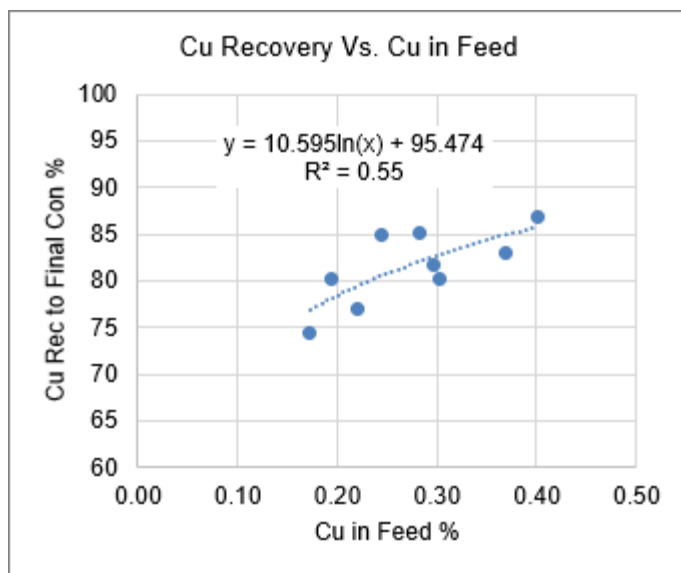
13.3 Recovery Estimates

Ausenco consolidated test work results with head grades within the range of the MRE and presents the following forecasts of copper, molybdenum and silver, zinc recoveries for the Santo Tomás Project as a function of oxidation and head grade.

13.3.1 Copper (Cu)

Figure 13-4 shows the copper recovery versus copper feed grade based on the results presented in Table 13-9.

Figure 13-4: Copper Recovery vs. Head Grade



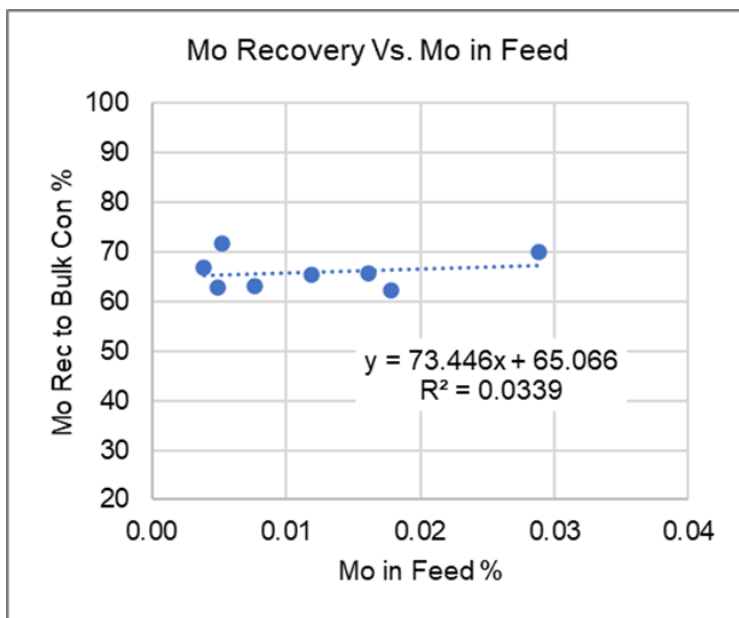
Source: Ausenco, 2023.

13.3.2 Molybdenum (Mo)

Figure 13-5 shows the molybdenum recovery versus molybdenum feed grade based on the results presented in Table 13-9. The result on the High S:Cu Ratio sample is excluded, as the low copper and high sulphur contents of this sample may be compromising the molybdenum recovery, and it may not be representative of the performance of material with lower molybdenum feed grades.

There is not a clear relationship between molybdenum feed grade and recovery obtained from this data set, results suggest a relatively consistent recovery to bulk concentrate of approximately 65%. Molybdenum recovery is likely more sensitive to primary grind size and levels of pyrite rejection in the cleaner circuit than copper recovery. Developing a more accurate prediction of molybdenum will require more variability testing that covers a wider range of feed sample characteristics.

Figure 13-5: Molybdenum Recovery vs. Head Grade



Source: Ausenco, 2023.

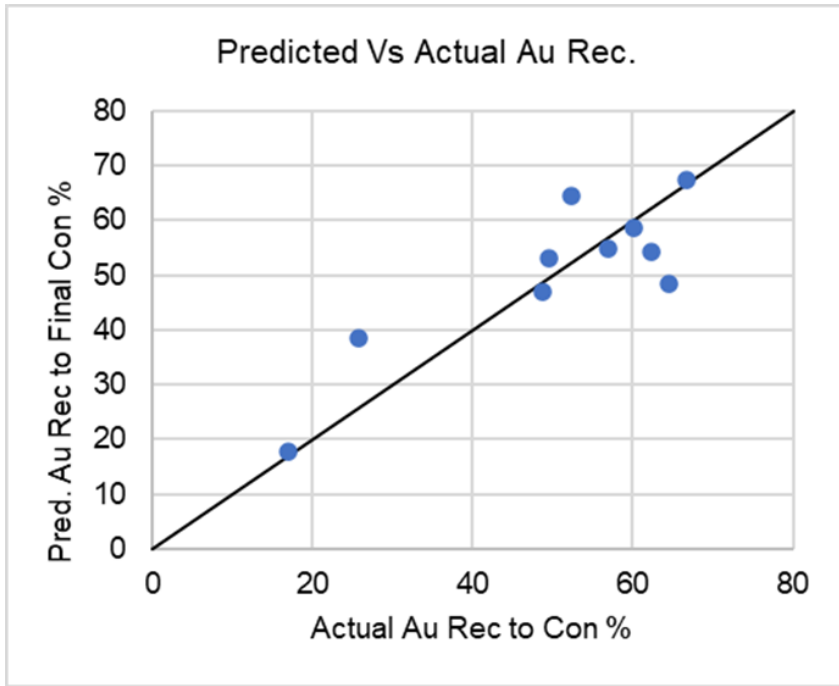
13.3.3 Gold (Au)

Gold recovery to the final bulk concentrate was estimated from variability results using a multi-variable relationship as follows:

$$\text{Au Rec} = 28.42 + 104*(\text{Cu}\%) + 129*(\text{Au ppm}) - 2.42*(\text{S/Cu})$$

A comparison of predicted vs actual gold recoveries is presented in Figure 13-6. The R2 value of this multi-variable relationship was 0.736.

Figure 13-6: Predicted vs Actual Gold Recoveries



Source: Auenco, 2023.

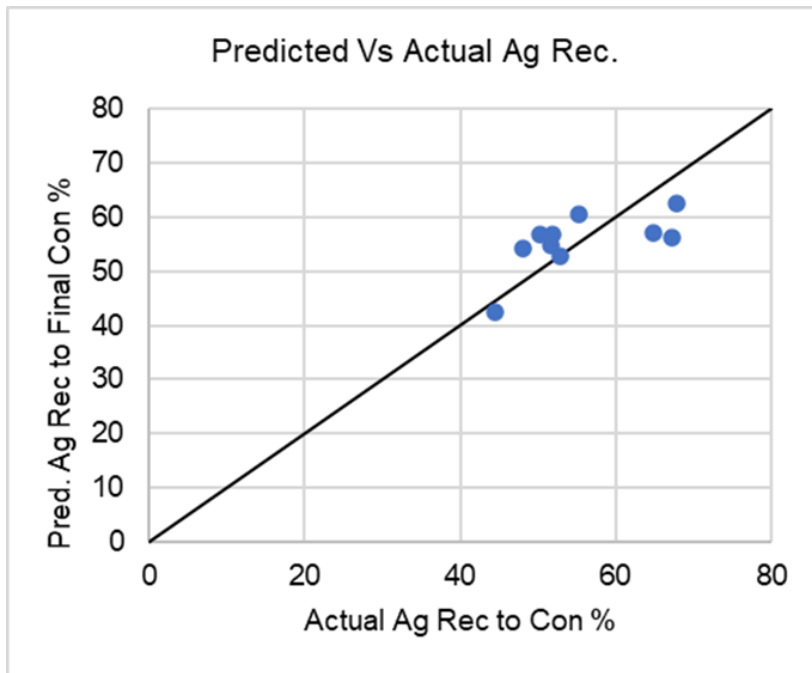
4.4 Silver (Ag)

Silver recovery to the final bulk concentrate was estimated from variability results using a multi-variable relationship as follows:

$$\text{Ag Rec} = 49 + 8.3 \cdot (\text{Ag ppm}) - 7.77 \cdot (\text{S}\%)$$

A comparison of predicted vs actual silver recoveries is presented in Figure 13-7. The R2 value of this multi-variable relationship was 0.495.

Figure 13-7: Predicted vs Actual Silver Recoveries



Source: Ausenco, 2023.

13.4 Conclusions

The Santo Tomás metallurgical performance represented by these samples appears to be typical of copper porphyry deposits.

The host rock is somewhat hard with respect to both impact breakage and ball mill grinding, therefore finding an economical balance between a coarse primary grind size and recovery will be a key focus of the project. It appears that a primary grind size in the 150 to 175 μ m range is suitable for effective rougher flotation.

The mineralization appears to be quite clean with respect to flotation processing, that is:

- Copper is primarily present in chalcopyrite, only trace levels of secondary copper sulphide forms were measured.
- The flotation kinetics are relatively fast and require low dosages of collector.
- Pyrite rejection can be achieved with moderate levels of lime and regrinding, along with the use of a selective copper collector.
- There do not appear to be any problematic gangue minerals reporting to the concentrate or interfering with the flotation process.

-
- Final concentrate produced from the Master Composite locked cycle test was analyzed for deleterious elements with zinc (Zn) and mercury (Hg) being elevated to levels which may trigger penalties at smelter. These elements have been identified as associated with the skarn materials which have been flagged for exclusion from the mine plan moving forward. Penalty limits for these elements should be confirmed with a concentrate marketing specialist.

Molybdenite is reasonably well recovered through the flotation process, although cleaner circuit losses may be somewhat elevated due to the high pH in this circuit.

14 MINERAL RESOURCE ESTIMATES

14.1 Introduction

SRK performed the MRE in support of the Santo Tomás Mineral Resource Estimate Technical Report with an effective date of 21 April 2023. Mineral resource work was performed or supervised by Mr. Scott Burkett, SME-RM (#4229765), Principal Consultant with SRK acting as Qualified Person (QP) for mineral resources.

All supporting drilling and geological data were provided by Oroco or their consultants and reviewed by the QP. SRK, in collaboration with Oroco staff, constructed the geological model, block model, performed grade shelling of mineralization, interpolation of key quality variables (Cu, Mo, Au, Ag, S, and bulk density), assigning resource classification based on CIM guidelines, and calculating the mineral resource statement as presented in this chapter.

14.2 Drillhole Database

14.1 Drillhole Database

The drillhole database (DHDB) supporting the mineral resources contains 156 drillholes for 62,678 m on the property between the North Zone and South Zone mineralized areas. Drilling on the property is performed by diamond drill core (DDH) drill methods, with 67% of total meters drilled performed by Oroco since 2021. The 33% of drilling meters on the property were completed by previous owners and provide valuable information on continuity of Cu mineralization along with geological data. The historical data lack QA/QC documentation, have identified uncertainty associated with some collar elevation, and lack multi-element assay. The identified limitations of historical data are acknowledged and considered during mineral resource classification of the Santo Tomás mineral resources. The QP notes that historical drilling has been infilled and surrounded by more recent drilling by Oroco which corroborates historical data.

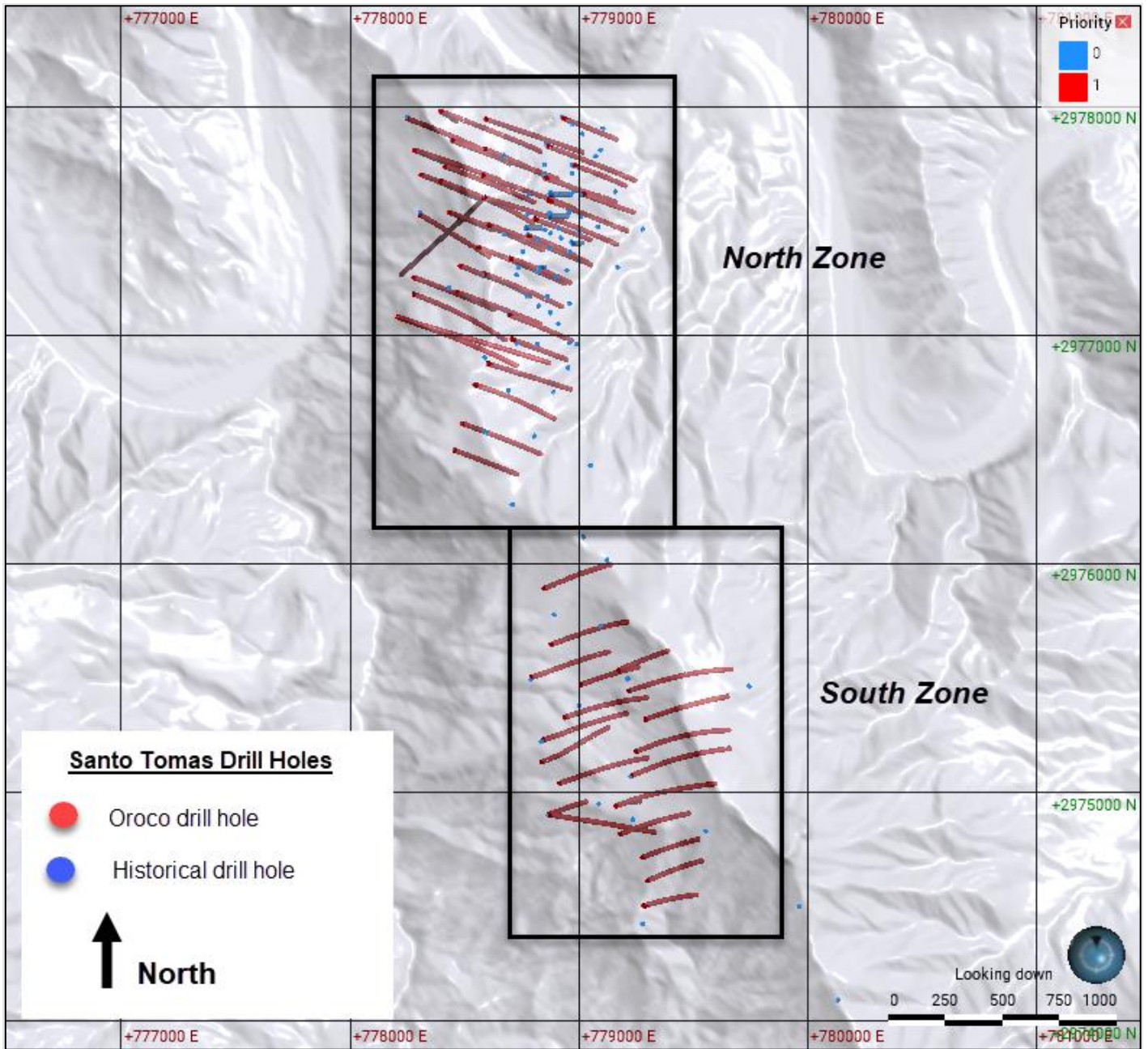
Property drilling is focused on evaluation of the two main mineralization zones and shown in Figure 14-1. In addition to the North and South Zones, drilling has provided broader geological and geotechnical information on the property. A breakdown of drilling vintage, number of holes, and total meterage by zone is presented in Table 14-1.

Table 14-1: Drilling Summary on the Santo Tomás Property

Zone	Owner	Total m	%
North Zone	Historical	17,044.3	27%
	Oroco	29,448.7	47%
North Zone Total			74%
South Zone	Historical	4,030.8	6%
	Oroco	12,154.1	19%
South Zone Total			26%
Total Drilling		62,678	

Source: SRK, 2023.

Figure 14-1: Drill Hole Locations on the Santo Tomás Property (scale in meters)



Source: SRK, 2023.

14.2.1 Assay

The property drilling database contains 26,669 sample intervals within the drilling database used in support of mineral resources. Sampling represents a combination of historical and Oroco-completed drill holes with sampling generally completed on the entire drill hole with limited exceptions in some historical holes. The QP notes that historical drilling performed prior to 2021 by previous owners, focused on Cu assays while the more recent Oroco samples include multi-element analyses. This results in the following sample data counts by key economic element:

- 25,622 samples analyzed for copper (Cu)
- 19,475 samples analyzed for molybdenum (Mo)
- 19,535 samples analyzed for gold (Au)
- 19,665 samples analyzed for silver (Ag)
- 19,135 samples analyzed for sulphur (S).

The mean sampling interval length is 2.13 m with interval length ranges down to 0.1 m based on lithology and observed mineralization in the core.

The QP notes that all analyses were completed at independent laboratories using ICP (as further described in Section 11). These values represent a total digest analytical value and does not break down oxide versus sulphide mineral species. The analyses and mineral resources at the Santo Tomás property are focused on sulphide mineralization at this stage of the study with plans by Oroco to further investigate oxide potential with more advanced property studies.

During database validation and review exercises by SRK, several non-sampled intervals were identified along with the lack of multi-element data in historical drill holes. As such, SRK performed the modification of select intervals for the purposes of exploratory data analyses and handing for mineral resource estimation. For this special handling, all non-sampled intervals are assumed to be deliberately selected for no sampling based on decisions made by logging geologists due to observing a lack of mineralization. In the case of historical intervals which only contain analyses for Cu but lack other elements, values for Mo, Au, Ag, and S are treated as null values. Table 14-2 provides a summary of special handling and modification of missing intervals or elements.

Table 14-2: Modification of Missing Data

Element	Unit	Unsampled	Untested
		Missing interval	Missing value
Cu	ppm	0.01	omit
Ag	ppm	0.01	omit
As	ppm	0.01	omit
Au	ppm	0.001	omit
Ca	%	omit	omit
Fe	%	omit	omit
K	%	omit	omit
Mo	ppm	0.01	omit
Pb	ppm	0.01	omit

Element	Unit	Unsampled	Untested
		Missing interval	Missing value
S	%	omit	omit
Zn	ppm	0.01	omit
SG	n/a	omit	omit

Source: SRK, 2023.

14.2.2 Survey

Collection of collar and downhole survey data are further described in Chapter 10. During DHDB validation, SRK identified several historical drill hole collars located above the current high-resolution topography. These holes were individually reviewed and confirmed based solely on aerial imagery of constructed drill pads. Once the X and Y coordinates were confirmed, SRK modified the elevation (Z) value to lie directly on the LiDAR topography.

Historical drilling was completed vertically with a lack of downhole survey documentation. This lack of downhole survey control is considered a low risk due to the vertical nature of drilling and has thus been accounted for in overall drilling data confidence. Volumes in the mineral resources which are largely supported by the historical drilling have been identified and accounted for in the resource classification.

14.2.3 Specific Gravity

Specific gravity (SG) data from diamond drill core was provide to SRK for incorporation into the resource block model. SG is collected and measured on-site with procedures further described in Chapter 11. SG sample interval mean is 0.14 m. SRK notes that SG varies slightly across the various property lithologies with Tertiary volcanics showing the lowest density with a mean SG at 2.48 and the highest density materials being in the carbonate skarn with a mean at 3.04.

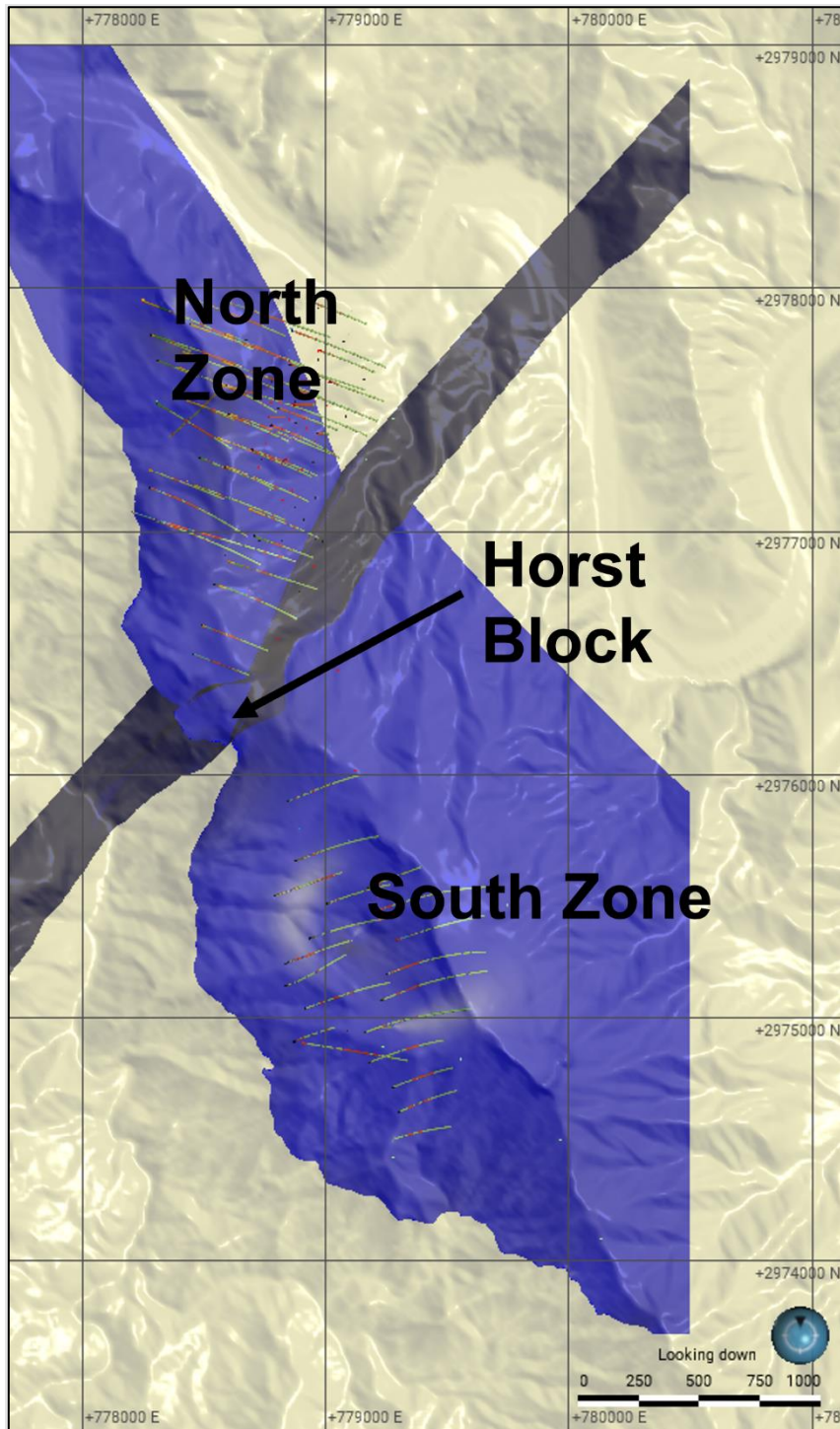
14.3 Geological Model

SRK constructed a geologic model using Leapfrog Geo™ software. A combination of geologic mapping, cross-sections and downhole lithologic logging were used to model six primary structures and five primary lithologic units observed at the Project (Sierra Madre Tuff, Upper Andesite, Paleozoic Sediments, Lower Andesite, Granodiorite and the Quartz Monzonite Porphyry).

14.3.1 Structural Geologic Model

Six primary structures were modeled and activated to generate the structural model for the Project. Each structure has been observed in the drilling and field mapping. The Project is structurally complex and consist of hundreds of smaller structures however only the primary structures were captured in the geologic model. These primary features are important because they limit the extents of mineralization and are treated as hard boundaries. Most notably is a horst block that separated the deposit into two domains (North Zone and the South Zone). Figure 14-2 is a plan view of the horst block that divides the North and South Zone.

Figure 14-2: Plan View of the Modeled Horst Block



Source: SRK, 2023.

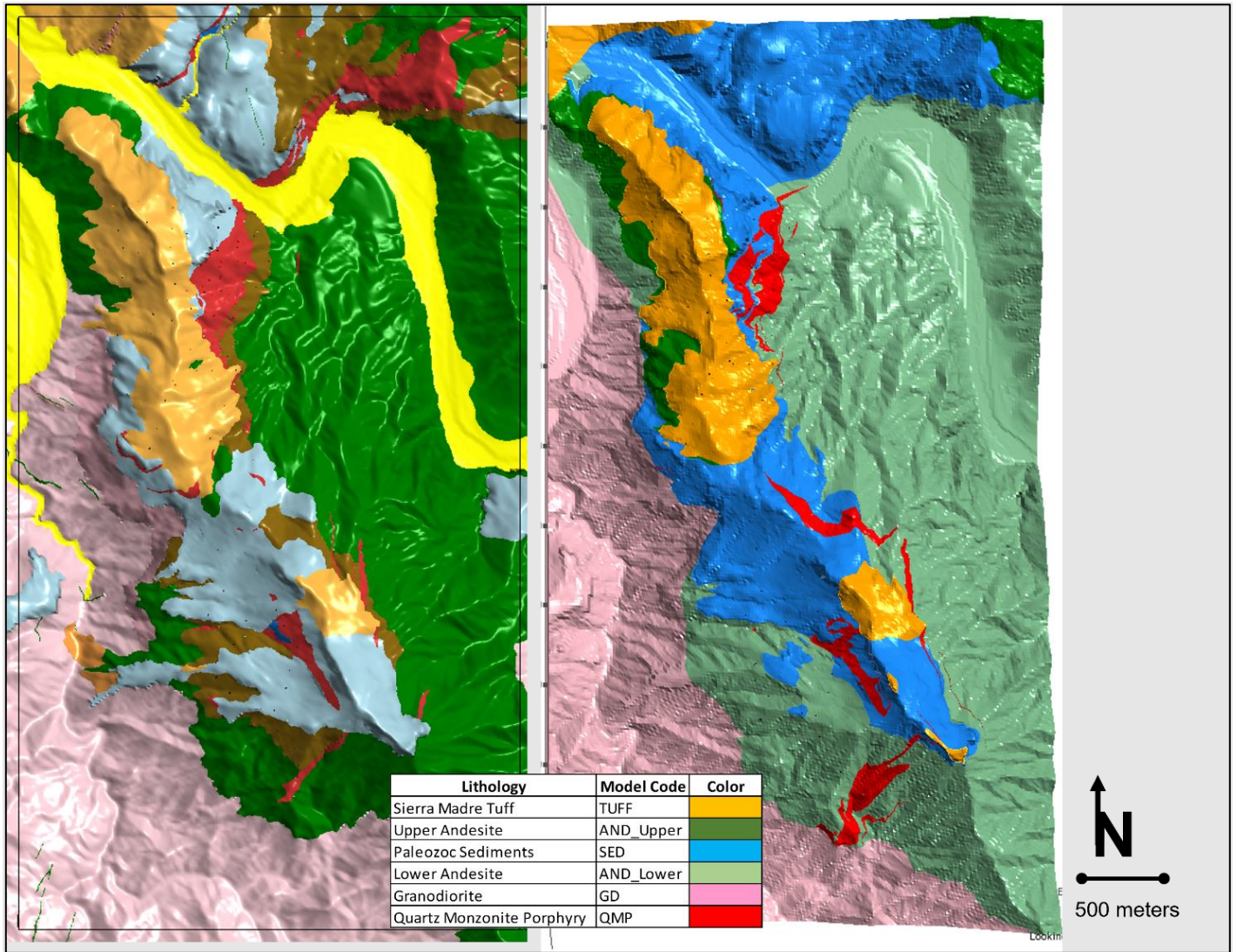
14.3.1.1 Lithological Model

Lithologic modeling used a combination of surface mapping, downhole logging and manually drawn interpreted cross-sections by site geologist. Five primary lithologic units were modeled (Sierra Madre Tuff, Upper Andesite, Paleozoic Sediments, Lower Andesite, Granodiorite and the Quartz Monzonite Porphyry (QMP)) and were utilized in the resource domaining process. The model was created using control points digitized on the Project surface geology map and downhole lithologic contacts. Stratigraphic relationships were established in Leapfrog resulting in a dynamic data driven model that can be updated easily as new information is added.

A more interpretive modeling approach was used to capture the QMP intrusive, which appears to be emplaced as a series of sheeted sills. Lateral and down-dip continuity is observed in the field and in the drilling and is best reflected in the model as a series of “veins”. The interval selection and vein modeling tools were utilized to best reflect the QMP geometry and cross-cutting relationships.

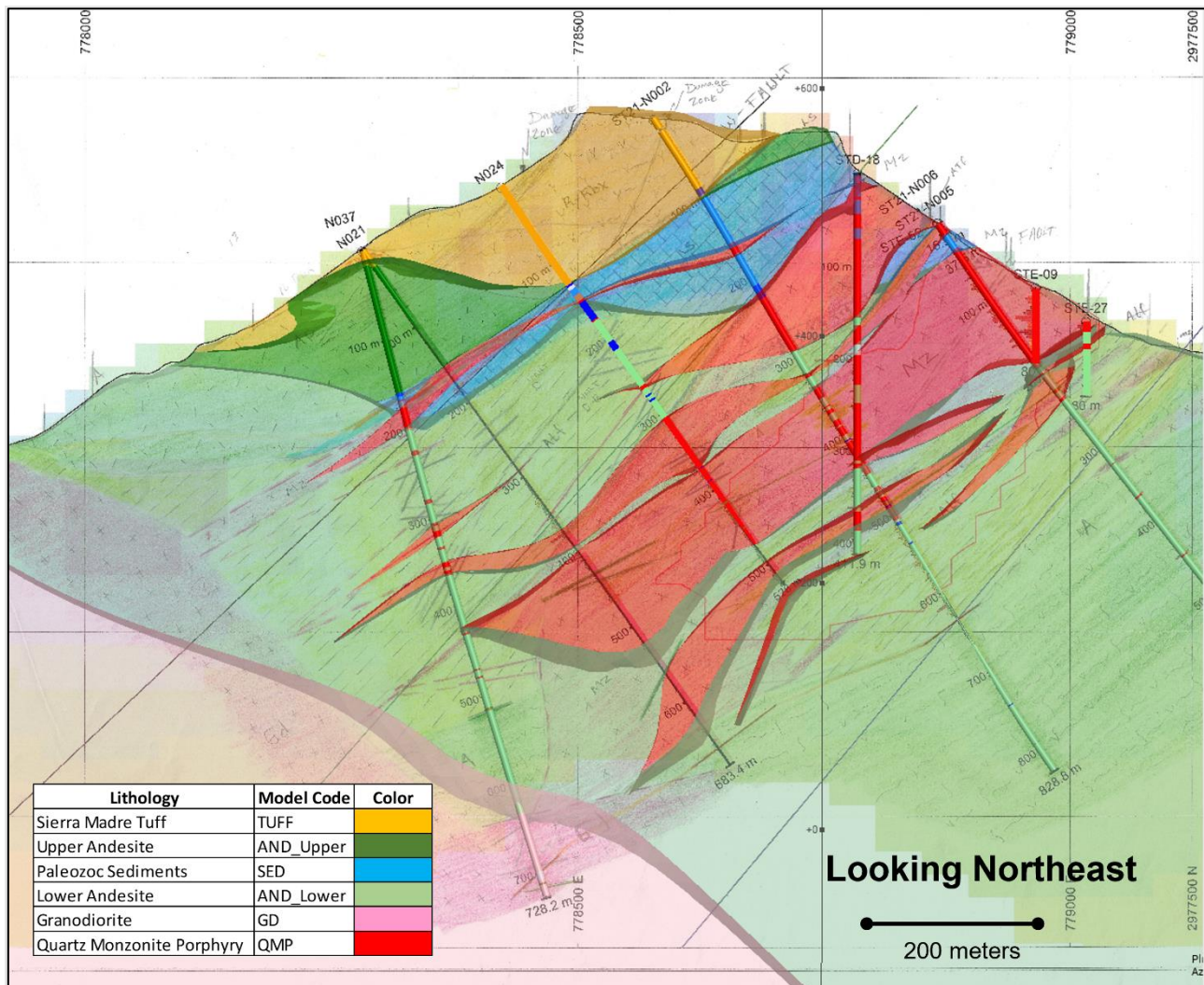
Three of the modeled lithologies are barren and do not host mineralization (Sierra Madre Tuff, Upper Andesite and Granodiorite). These three units are treated as hard boundaries and limit the extents of the mineralization at the Project. Figure 14-3 shows a comparison of the geologic mapping (left) and geologic model (right). Figure 14-4 shows a comparison of the geologic model and cross-sectional interpretation which is representative of the North Zone geology.

Figure 14-3: Geologic Mapping (Left) and Geology Model (Right) Comparison



Source: SRK, 2023.

Figure 14-4: Comparison of Cross-Sectional Interpretation and Geologic Model (Looking Northeast)



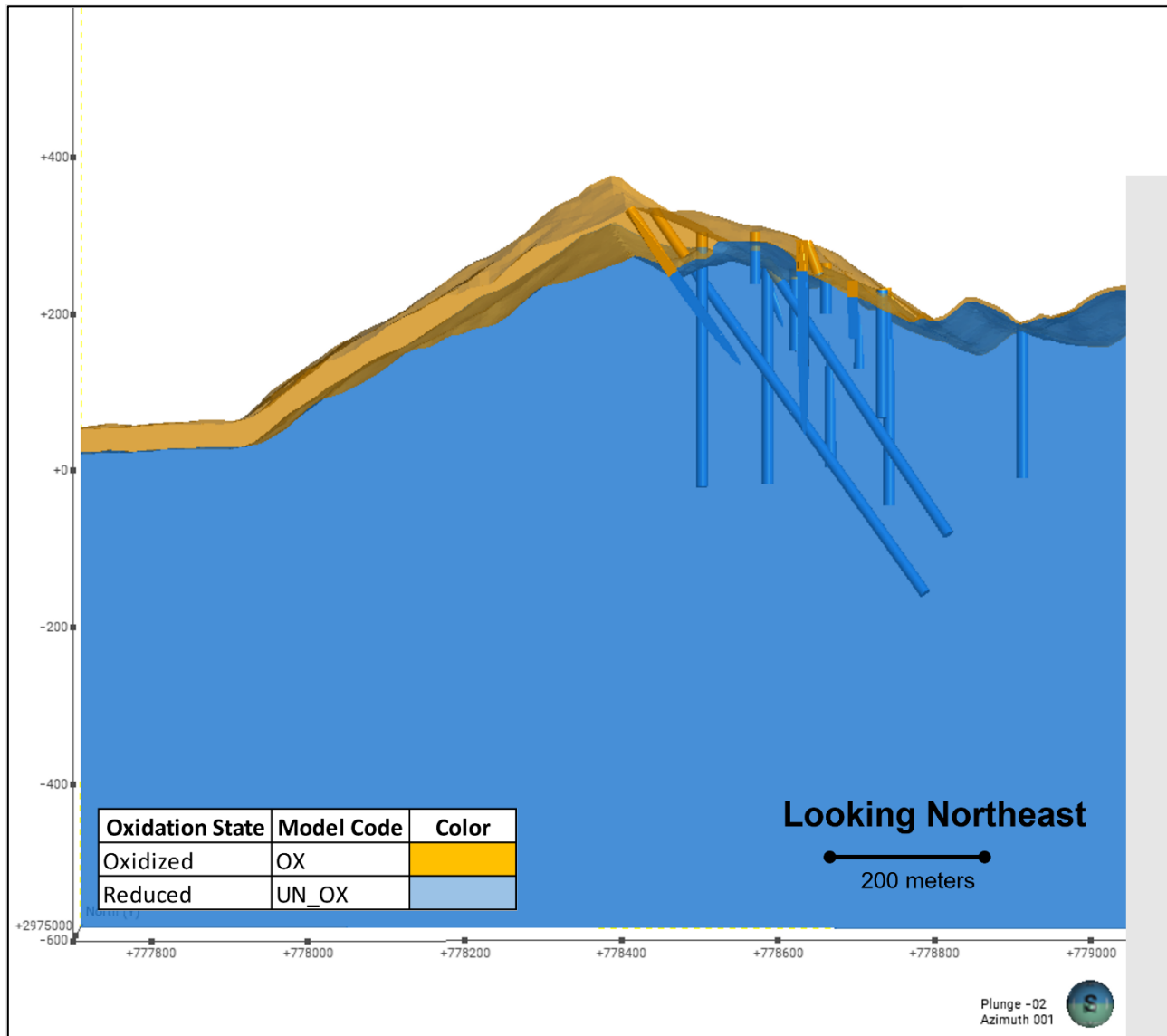
Source: SRK/Oroco, 2023.

14.3.2 Oxidation Model

Oxidation is limited to the upper 80 m of material below the surface with an average depth of 30 m. In areas where mineralization is present, pervasive supergene enrichment is not observed however Oroco has not collected any metallurgical samples in the oxidized horizon and metal recoveries are unknown at this time. Due to this uncertainty, an oxidation model was constructed to code the block model and excluded oxidized material from the resource statement. SRK applied an offset to the topographic surface and utilized drillhole oxidation logging to create the oxide model. This resulted in a dynamic, data driven oxidation model that covers the extents of the model.

Figure 14-5 is a cross-section showing the oxide domain.

Figure 14-5: Cross-section of Oxidation Model (Looking Northeast)



Source: SRK, 2023.

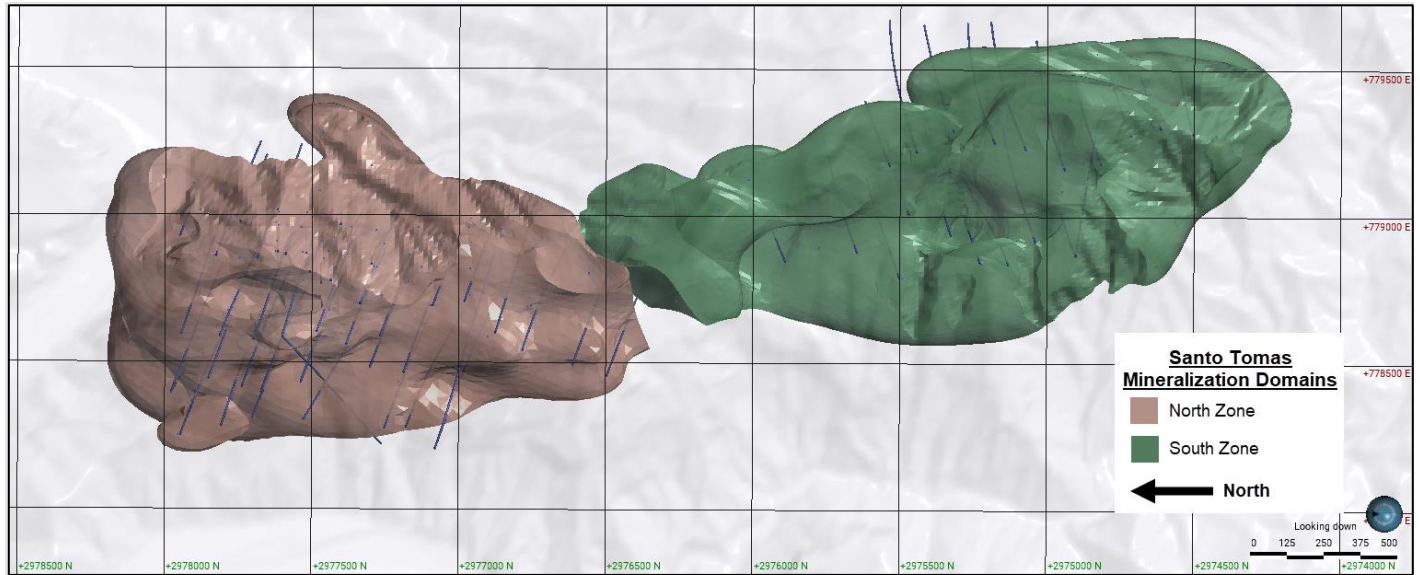
14.3.3 Mineralization Grade Shells

As the primary metal mineralization is not restricted to any one lithology and lithologic domain analyses demonstrate similar grade department in both the andesite and monzonite rock types, a modified grade shell approach was selected for establishing estimation domains. Indicator grade shells were constructed in Leapfrog Geo software in both the North Zone and South Zone based on the general Cu mineralization trend and a threshold of 750 ppm Cu. The 750 ppm Cu threshold was selected based on statistical analyses and communication with Oroco staff to generally align with site logging determination of mineralized versus unmineralized material. Using an ISO-value of 0.4 and 0.35 in the North and

South Zones respectively, grade shell volumes were calculated. These volumes were then truncated by bordering post-mineralization faults and confined to lithologic units with observable mineralization. The resultant volumes represent discrete mineralization volume by zone (Figure 14-6).

SRK generated similar litho-structural grade domains for Mo, Au, Ag, and S, noting the similar spatial continuity and volume for each element. Ultimately, it was decided to utilize the Cu mineralization.

Figure 14-6: Plan View of Mineralized Domains



Source: SRK, 2023.

Summary statistical analyses for the North Zone and South Zone indicator shells are provided in Table 14-3 and Table 14-5, respectively.

Table 14-3: Indicator Grade Shell Summary - Cu in North Zone

North Zone - Cu @ 750 ppm Threshold		
Indicator statistics		
Total number of samples	17,833	-
Cut-off value	750	-
-	≥ cut-off	< cut-off
Number of points	11,501	6,332
Percentage	64.5%	35.5%
Mean value	3308.05	238.9
Minimum value	750	0.01
Maximum value	25,500	749
Standard deviation	2364	227.6
Coefficient of variance	0.7	0.95
Variance	5,588,380	51795
Output volume statistics		
Resolution	40	-
Iso-value	0.4	-
-	Inside	Outside
≥ cut-off	-	-
Number of samples	11,027	474
Percentage	61.8%	2.7%
< cut-off		
Number of samples	1,257	5,075
Percentage	7.1%	28.5%
All points		
Mean value	3080.4	309.8
Minimum value	0.01	0.01
Maximum value	25,500	8,370
Standard deviation	2419.5	571.8
Coefficient of variance	0.7	1.8
Variance	5,853,940	326,941
Volume	397,990,102	903,650,078
Number of parts	2	4

Source: SRK, 2023.

Table 14-4: Indicator Grade Shell Summary - Cu in South Zone

South Zone - Cu @ 750 ppm Threshold		
Indicator statistics		
Total number of samples	7,697	-
Cut-off value	750	-
	≥ cut-off	< cut-off
Number of points	3,412	4,285
Percentage	44.33%	55.67%
Mean value	2766.15	166.29
Minimum value	750	0.01
Maximum value	11,100	749.5
Standard deviation	1805.93	208.27
Coefficient of variance	0.652868	1.25245
Variance	3,261,390	43376.5
Output volume statistics		
Resolution	40	-
Iso-value	0.35	-
-	Inside	Outside
≥ cut-off		
Number of samples	3,294	118
Percentage	42.80%	1.53%
< cut-off	-	-
Number of samples	530	3,755
Percentage	6.89%	48.79%
All points		
Mean value	2491.21	161.187
Minimum value	0.01	0.01
Maximum value	11,100	7,510
Standard deviation	1868.16	305.201
Coefficient of variance	0.749901	1.89346
Variance	3,490,030	93147.4
Volume	320,679,042	4,332,687,253
Number of parts	1	3

Source: SRK, 2023.

14.4 Exploratory Data Analysis

Exploratory data analysis (EDA) was performed on the key economic variables (Cu, Mo, Au, Ag, S, and SG) in the drilling database as provided by Oroco. EDA included a statistical analysis, an assessment of raw sample lengths, composite length analysis (CLA), high-end outlier capping analysis, and domain assessment within the mineralized grade shells of the North and South Zones.

14.4.1 Statistical Analyses

SRK performed a statistical analysis of all assay and SG data based on the drilling database obtained from Oroco. Broadly defined North Zone and South Zone areas were used to investigate statistical differences in the spatially discrete zones. SRK notes that EDA presented below represent a non-mineralized domained statistics as thresholds (grade shells) are not applied for this exercise.

Key economic variables (KEV) were analyzed which include Cu, Mo, Au, Ag and S for the MRE. Additional variables were reviewed from a high level but not further investigated at this stage of the project study. Only KEV are used in the reporting of mineral resources while the secondary variables are utilized in determining lithology, alteration, and recovery considerations. Analyses include calculation of descriptive statistics Table 14-5, histograms of raw data by domain per KEV (Figures Figure 14-7 through Figure 14-9).

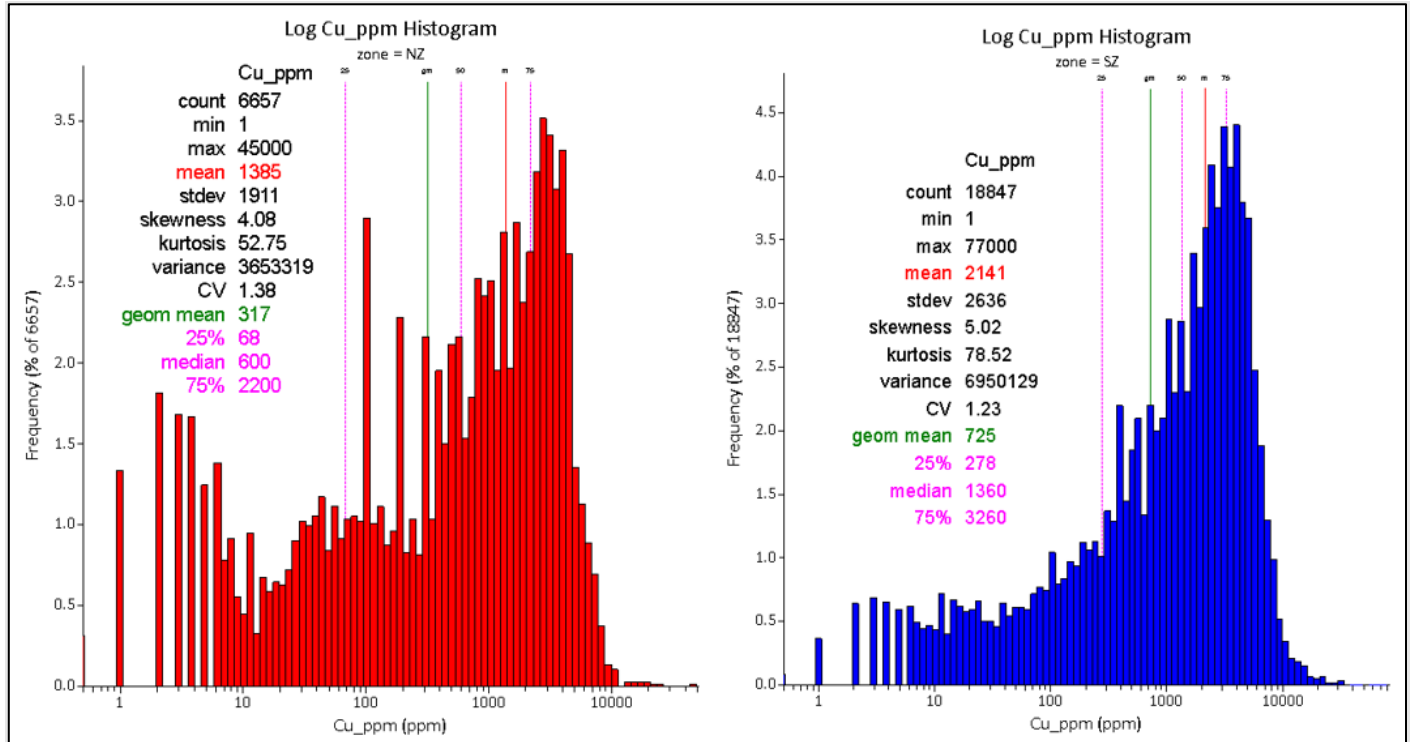
Interpretation and conclusions of the statistical analyses show material differences in KEV between the North Zone and the South Zone which, in addition to differences in spatial trends of mineralization, warrants separation into estimation domains. Additionally, most elements demonstrate a variable log-normal distribution suggesting a mix of populations due to the complexity of mineralizing fluids' interaction with various lithologies and showing the potential for multiple mineralizing events.

Table 14-5: Summary Descriptive Statistics for Raw Sample Intervals (2m Composites)

Zone	Elements (ppm & capped value)	Count	Length	Mean	Minimum	Maximum	Median	StDev	CV	Variance	Lower quartile	Upper quartile
North Zone Indicator	Ag_ppm	7,267	14,530	1.90	0.01	21.7	1.70	1.40	0.7	2.10	1.00	2.60
	Au_ppm	7,251	14,498	0.00	0.00	1.10	0.00	0.00	1.4	0.00	0.00	0.00
	Cu_ppm	12,284	24,555	3,090	0.01	77,000	2,620	2,568	0.8	6,594,366	1,376	4,160
	Mo_ppm	7,183	14,363	66.8	0.01	2,280	35.8	98.8	1.5	9,763	11.0	86.0
	Ag_cap	7,267	14,530	1.90	0.01	17.5	1.70	1.40	0.7	2.10	1.00	2.60
	Au_cap	7,251	14,498	0.00	0.00	0.30	0.00	0.00	1.3	0.00	0.00	0.00
	Cu_cap	12,284	24,555	3,081	0.01	25,500	2,620	2,420	0.8	5,856,863	1,376	4,160
	Mo_cap	7,183	14,363	66.6	0.01	1,500	35.8	96.7	1.5	9,357	11.0	86.0
South Zone Indicator	Ag_ppm	2,688	5,376	2.00	0.01	141	1.50	4.10	2.1	16.80	0.90	2.20
	Au_ppm	2,638	5,276	0.00	0.00	1.10	0.00	0.00	1.7	0.00	0.00	0.00
	Cu_ppm	3,824	7,646	2,512	0.01	25,500	2,100	2,016	0.8	4,064,130	1,056	3,465
	Mo_ppm	2,683	5,366	68.1	0.01	1,015	32.0	99.4	1.5	9,872	13.50	79.0
	Ag_cap	2,688	5,376	1.80	0.01	17.5	1.50	1.60	0.9	2.70	0.90	2.20
	Au_cap	2,638	5,276	0.00	0.00	0.30	0.00	0.00	1.3	0.00	0.00	0.00
	Cu_cap	3,824	7,646	2,491	0.01	11,100	2,100	1,869	0.8	3,492,615	1,056	3,465
	Mo_cap	2,683	5,366	68.1	0.01	1,015	32.0	99.4	1.5	9,872	13.5	79.0
Outside of North and South Zone Indicators	Ag_ppm	11187	22,336	0.51	0.01	96.60	0.40	1.61	3.2	2.58	0.01	0.48
	Au_ppm	11123	22,208	0.01	0.00	2.72	0.00	0.04	6.5	0.00	0.00	0.01
	Cu_ppm	12210	24,380	207.6	0.01	10,900	47.00	462.86	2.2	214,238	2.00	256
	Mo_ppm	11086	22,134	4.23	0.01	1,625	1.00	24.55	5.8	602.8	0.01	3.00
	Ag_cap	11187	22,336	0.49	0.01	17.5	0.25	1.16	2.4	1.35	0.01	0.48
	Au_cap	11123	22,208	0.01	0.00	0.33	0.00	0.02	2.9	0.00	0.00	0.01
	Cu_cap	12210	24,380	207.6	0.01	10,900	47.00	462.86	2.2	214,238	2.00	256
	Mo_cap	11086	22,134	4.22	0.01	1,500	1.00	23.82	5.7	568	0.01	3.00

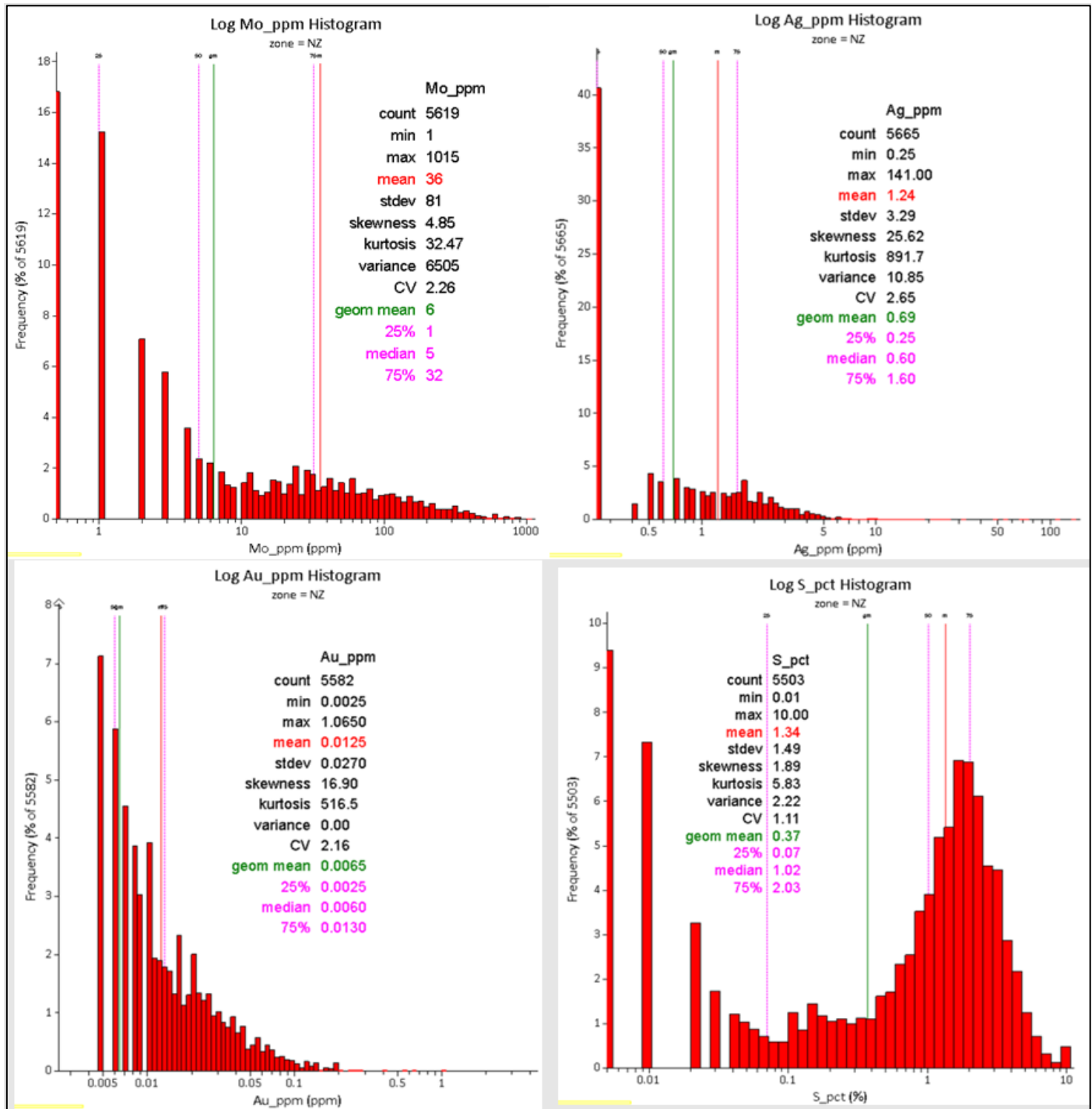
Source: SRK, 2023.

Figure 14-7: Log Histograms of Cu (ppm) Distribution in the North Zone (left) and South Zone (right)



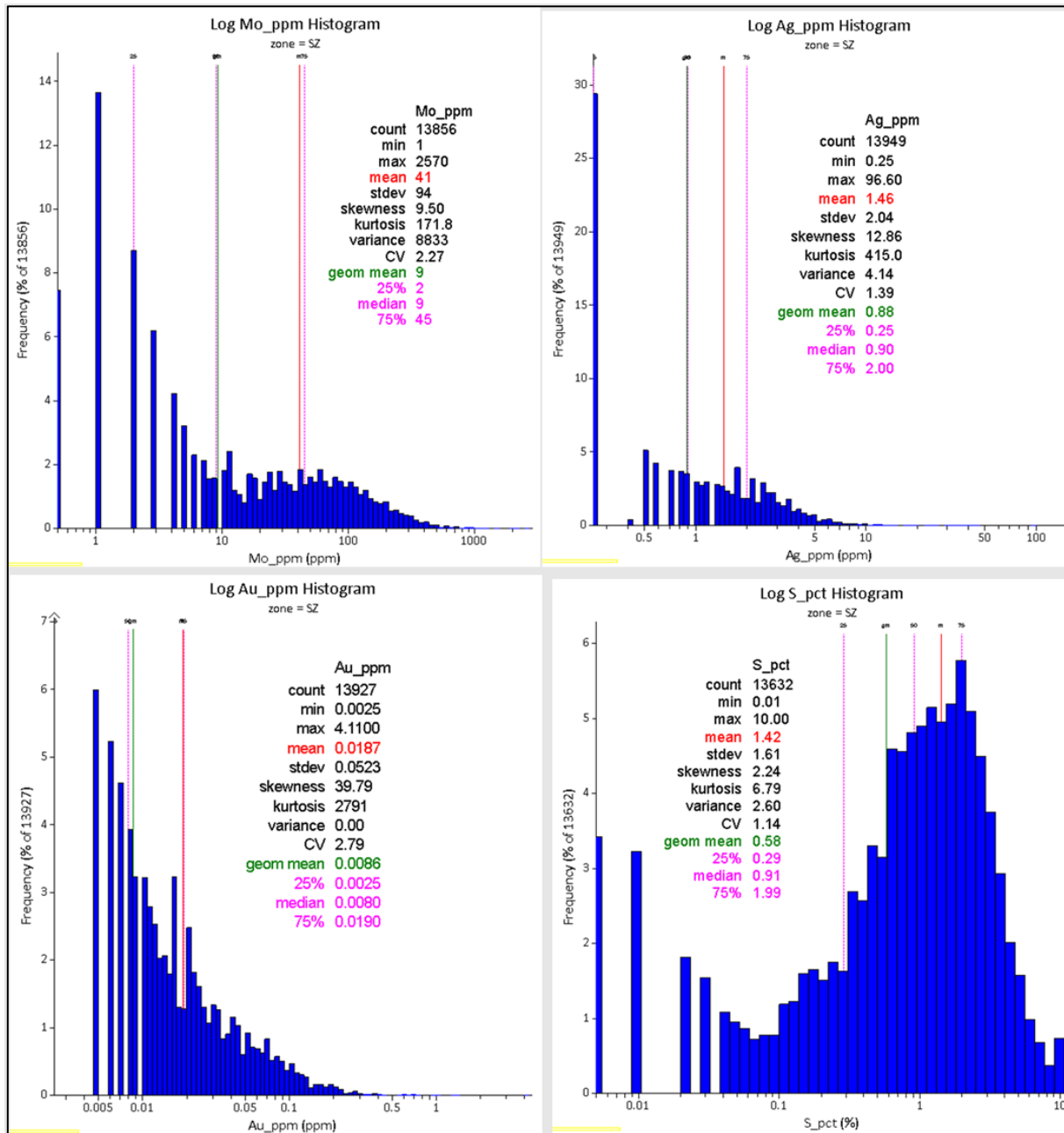
Source: SRK, 2023.

Figure 14-8: Raw Sample Log Histograms for Mo, Ag, Au, and S in the North Zone



Source: SRK, 2023.

Figure 14-9: Raw Sample Log Histograms for Mo, Ag, Au, and S in the South Zone



Source: SRK, 2023.

SG data was flagged by lithology and summarized in Table 14-6. SRK notes only minor differences in measured SG values across the various lithologies with the exception of the Tertiary volcanics, which display a materially lower mean SG value.

Table 14-6: Summary Descriptive Statistics for Specific Gravity (SG) Measurements by Lithology

Parameter	Lithology	Count	Mean	Min	Max	Median	Variance	StDev	CV
SG	ALL	1872	2.65	1.65	3.93	2.65	0.02	0.14	0.05
SG	AND_Lower	1033	2.69	2.18	3.48	2.69	0.01	0.1	0.04
SG	AND_Upper	35	2.69	2.56	2.84	2.68	0	0.07	0.03
SG	Felsic Dyke	12	2.36	2.16	2.63	2.31	0.02	0.15	0.06
SG	Granodiorite	53	2.63	2.43	2.78	2.63	0.01	0.07	0.03
SG	Inter. Dyke	16	2.57	2.26	2.76	2.59	0.01	0.11	0.04
SG	Monzonite	423	2.61	2.09	3.67	2.6	0.01	0.1	0.04
SG	Sediments	91	2.67	2.4	3.19	2.65	0.01	0.09	0.03
SG	Skarn	28	3.04	2.63	3.93	2.97	0.11	0.33	0.11
SG	Tertiary Volcanics	121	2.48	1.65	2.77	2.59	0.05	0.23	0.09

Source: SRK/Oroco, 2023.

SRK calculated bivariate statistics to investigate potential correlations between elements in the North Zone and South Zone areas. X-Y scatterplots and correlation coefficients as shown in Table 14-7, were generated for all major elements. SRK notes that there are no strong direct or indirect correlations in mineralization magnitude based on Pearson correlations but a spatial review of concentrations show a distinct mineralization zone in both the North Zone and South Zone areas. The primary metals of Cu, Mo, Au, and Ag show moderate correlations which may be skewed due to a lack of historical drilling containing multi-element analyses. Additionally, there is a clear indirect relationship between K enrichment and Ca depletion. The strongest correlations are Cu-Mo, Cu-Ag, Cu-Au, S-Fe, S-Cu, Ag-Au, and Ag-Pb-Zn.

Table 14-7: Correlation Coefficients of Primary Elements – All Domains

Element	Ag_ppm	As_ppm	Au_ppm	Ca_pct	Cu_ppm	Fe_pct	K_pct	Mo_ppm	Pb_ppm	S_pct	Zn_ppm
Ag_ppm	1	-	-	-	-	-	-	-	-	-	-
As_ppm	0.04	1	-	-	-	-	-	-	-	-	-
Au_ppm	0.32	0.05	1	-	-	-	-	-	-	-	-
Ca_pct	0.02	0.13	-0.02	1	-	-	-	-	-	-	-
Cu_ppm	0.54	-0.03	0.44	-0.22	1	-	-	-	-	-	-
Fe_pct	0.06	-0.05	-0.03	-0.2	-0.13	1	-	-	-	-	-
K_pct	0.04	-0.06	0.07	-0.56	0.26	-0.18	1	-	-	-	-
Mo_ppm	0.19	-0.02	0.08	-0.14	0.41	-0.12	0.2	1	-	-	-
Pb_ppm	0.43	0.07	0.11	0.22	0.04	0	-0.11	-0.01	1	-	-
S_pct	0.2	-0.06	0.09	-0.2	0.24	0.38	0.17	0.11	0.06	1	-
Zn_ppm	0.22	0.04	0.1	0.16	0.04	0.13	-0.11	-0.01	0.45	0.13	1

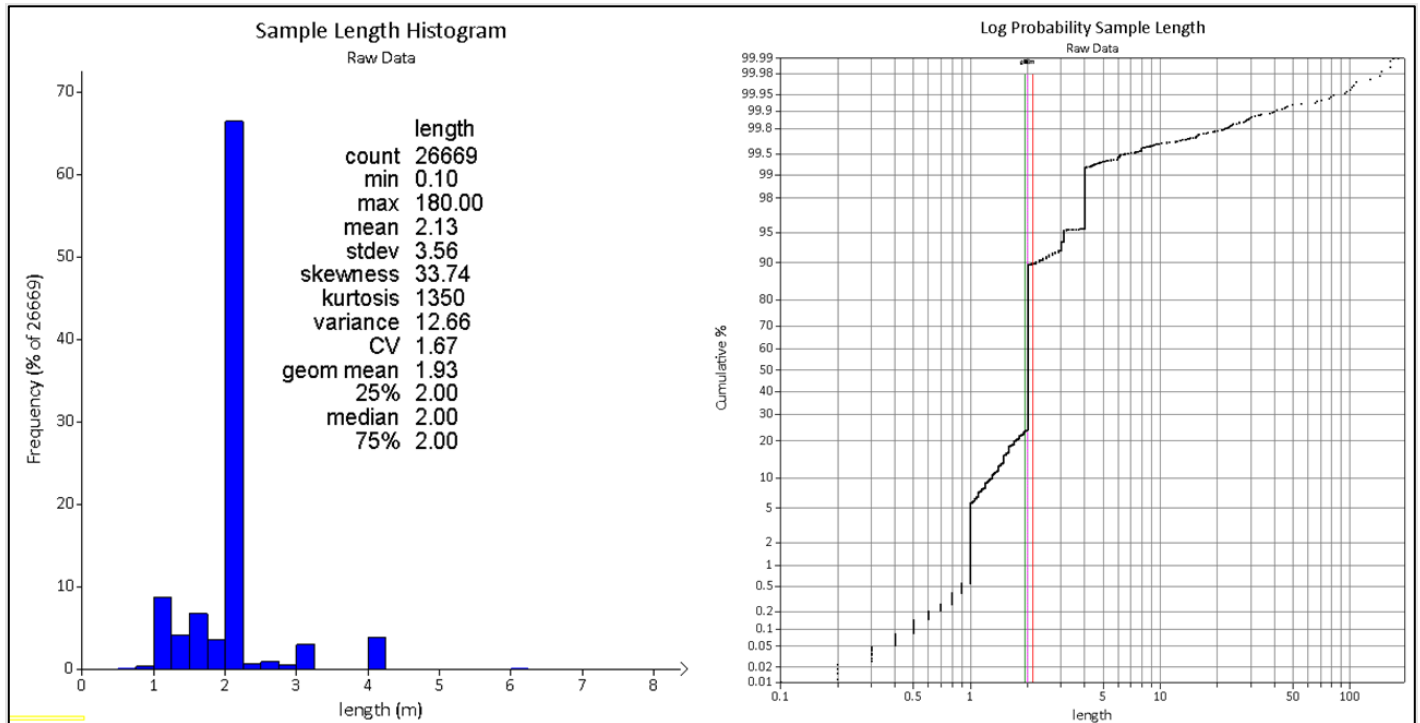
Source: SRK, 2023. Note: Colored boxes reflect commentary of correlation coefficients mentioned above.

14.4.2 Composite Length Analysis

Prior to performing sample compositing, a CLA was performed to assess the effects of compositing on diluting or modifying the underlying raw sample statistics. For estimation to have equal weighting of all analytical variables, the sample support (equal volume represented) must be consistent. Therefore, composites aid in establishing consistent sample support and diluting extreme outlier data that are considered unrepresentative of the broader data population.

Raw sample lengths were investigated to determine descriptive statistics and population characteristics via histogram and log-probability charts (Figure 14-10). The majority of sample interval lengths are at 2 m across the property with a majority of non-2 m intervals smaller than 2 m in length. SRK noted that many of the larger intervals as represented in the statistics are non-sampled intervals outside mineralization boundaries. Final compositing methodology was selected as a full hole, run length 2 m composite. Small intervals of less than 0.5 m at the end of holes were merged with the previous interval.

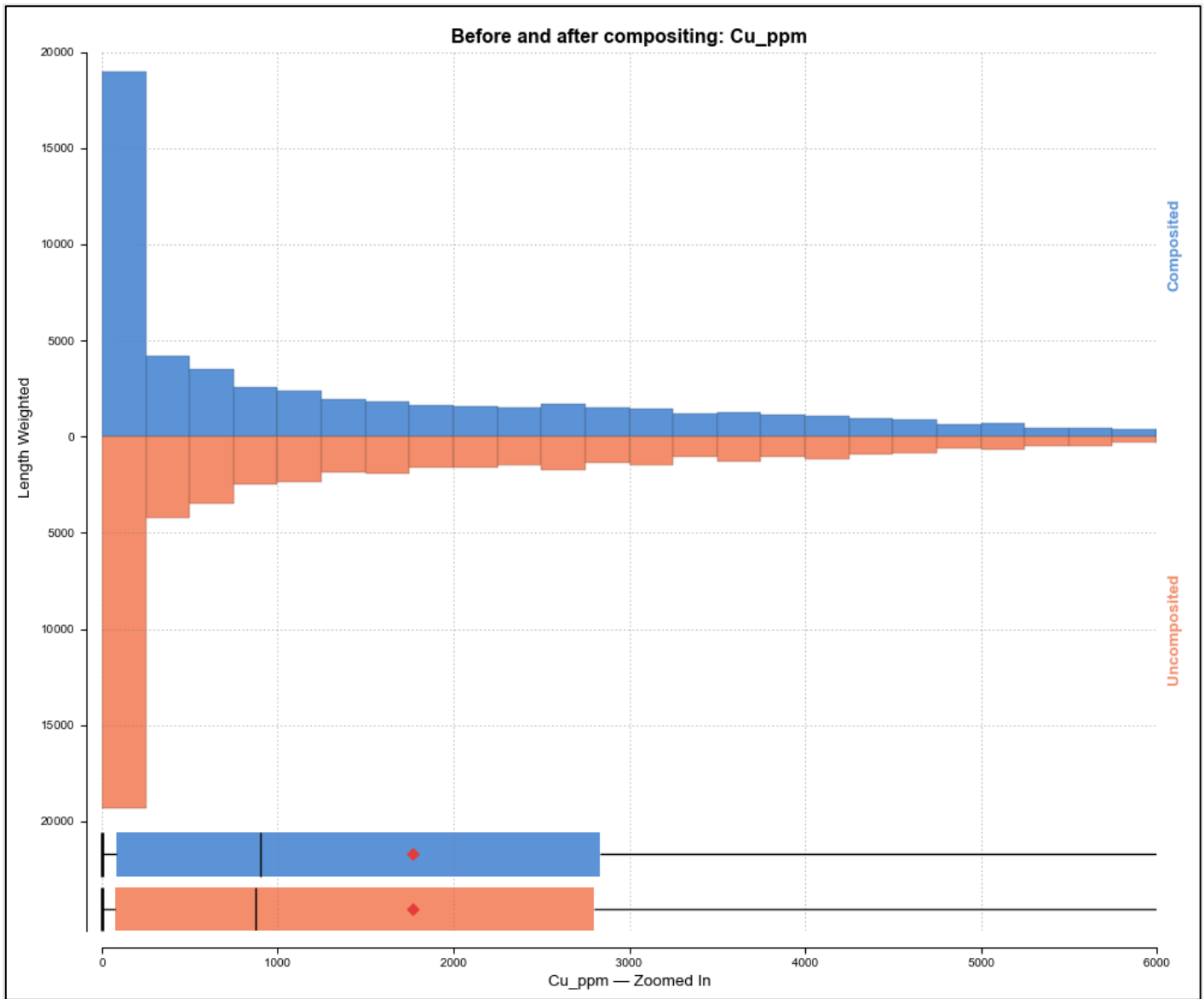
Figure 14-10: Raw Sample Interval Histogram (left) and Log-Probability (right)



Source: SRK, 2023

Comparing KEV grade statistics and population distribution show minimal change between raw samples and 2 m composite grade statistics. Figure 14-11 show Cu grade distribution is nearly identical with minor dilution of extreme outlier data based on non-representative small intervals of extreme high grade.

Figure 14-11: Distribution of Cu Grade in Raw and 2 m Composites



Source: SRK, 2023

Table 14-8: Summary Descriptive Statistics for 2m Composite Samples

Element	Domain	Count	Mean	Min	Max	Median	Variance	StDev	CV	IQR	Outlier
Cu_ppm	ALL	28318	1769	0	77000	900	5383888	2320	1.31	2745	6947.5
Cu_ppm	NZ	20496	1958	0	77000	1125	6047312	2459	1.26	2968	7552
Cu_ppm	SZ	7704	1288	0	25500	464	3341526	1828	1.42	2010	5055
Mo_ppm	ALL	20952	34	0	2280	5	5914	77	2.27	32	81
Mo_ppm	NZ	14746	35	0	2280	5	6143	78	2.23	36	91
Mo_ppm	SZ	6206	31	0	1015	3	5357	73	2.38	26	66
Au_ppm	ALL	21012	0.0144	0.001	2.723	0.0055	0	0.0384	2.67	0.0117	0.03175
Au_ppm	NZ	14817	0.0158	0.001	2.723	0.006	0	0.0428	2.7	0.0135	0.03625
Au_ppm	SZ	6169	0.0109	0.001	1.065	0.0045	0	0.0248	2.26	0.0085	0.02375
Ag_ppm	ALL	21142	1.19	0.01	141	0.65	4.73	2.18	1.83	1.45	3.875
Ag_ppm	NZ	14839	1.23	0.01	96.6	0.73	3.03	1.74	1.41	1.55	4.125
Ag_ppm	SZ	6252	1.08	0.01	141	0.48	8.78	2.96	2.75	1.15	3.125

Source: SRK, 2023.

For SG samples, the majority of data was collected on 0.17 m intervals. These data were utilized directly for estimation purposes as SG data do not represent continuous samples, but merely representative samples collected with the various lithologies.

14.4.3 Capping Analysis

A comparative upper capping analysis was performed to review the presence of upper outliers and assess the potential estimation impact. Upper outliers were identified within the composited data and subsequently capped with limits shown in Table 14-8. The capping process does not eliminate the sample but re-assigned the upper cap limit to the outlier. Figure 14-12 through Figure 14-15 illustrate the log-probability charts and associated tabulated (Table 14-9 through Table 14-13) impact used to assess the upper capping composited population statistics.

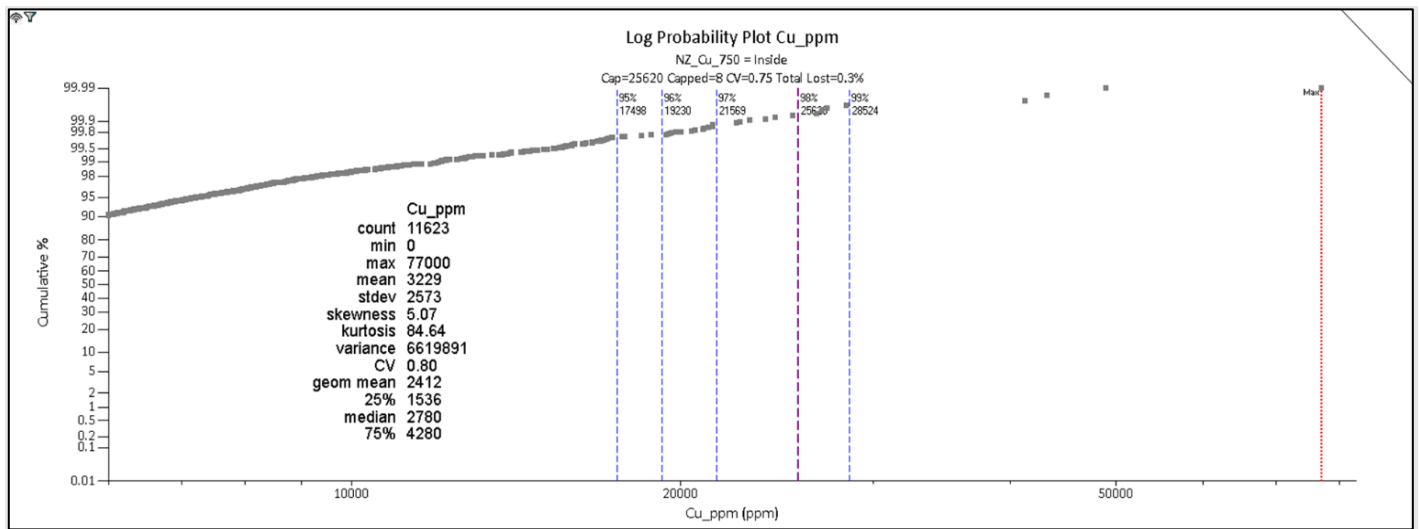
SRK selected upper-end capping limits for Cu based on the mineralized domain with Mo, Au, and Ag caps selected for the entire property. No capping was deemed necessary for S.

Table 14-9: Summary Upper Capping Applied for Santo Tomás

Element	Zone	Upper Cap	Unit
Cu	North Zone	25,500	ppm
Cu	South Zone	11,000	ppm
Mo	Both	1,500	ppm
Au	Both	0.33	ppm
Ag	Both	17.5	ppm

Source: SRK, 2023.

Figure 14-12: Log-Probability Chart on North Zone Cu for Capping Analysis



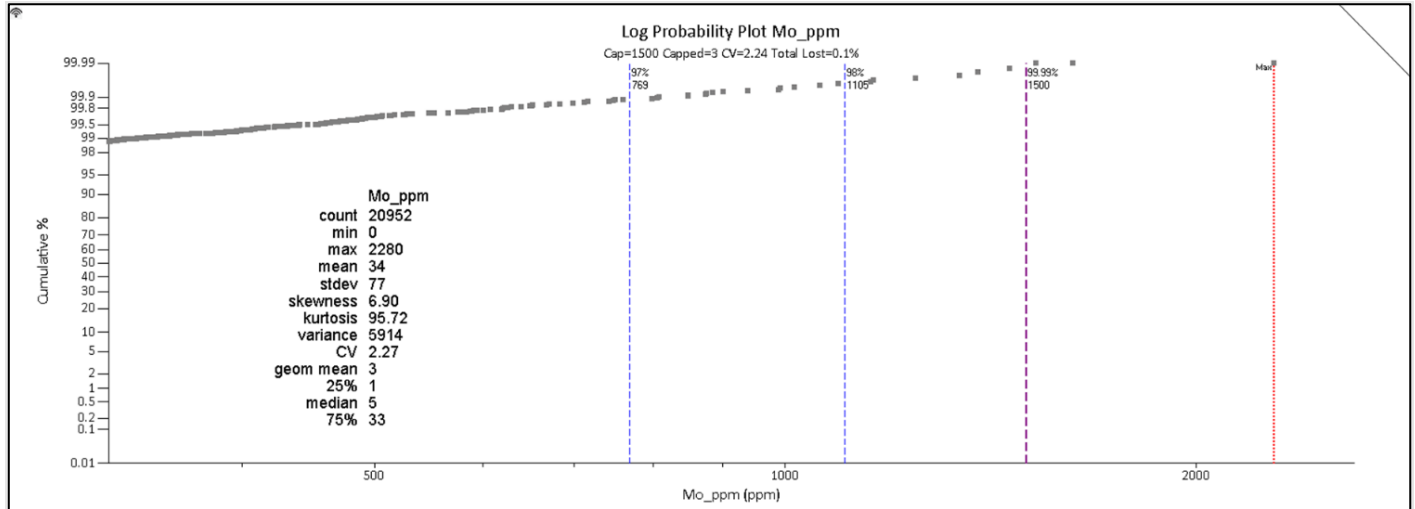
Source: SRK, 2023.

Table 14-10: Tabulated Capping Options for North Zone Copper

Element	Capping Option	Capped ppm	Capped	Percentile	Capped%	Lost Total %	Lost CV %	Count	Min	Max	Mean	Variance	CV
Cu_ppm	NZ_Cu_750 = Inside	-	-	-	-	-	-	11623	0	77000	3229	6619891	0.8
Cu_ppm	NZ_Cu_750 = Inside	28524	4	99%	0.03%	0.30%	5.10%	11623	0	28524	3221	5929766	0.76
Cu_ppm	NZ_Cu_750 = Inside	25500	8	98%	0.10%	0.30%	5.70%	11623	0	25500	3219	5852120	0.75
Cu_ppm	NZ_Cu_750 = Inside	21569	14	97%	0.10%	0.40%	6.80%	11623	0	21569	3215	5700085	0.74
Cu_ppm	NZ_Cu_750 = Inside - Cu_ppm > 25500	-	-	-	-	-	-	8	26600	77000	39933	301762807	0.44
Cu_ppm	NZ_Cu_750 = Inside - Cu_ppm <= 25500	-	-	-	-	-	-	11615	0	25320	3204	5513959	0.73

Source: SRK, 2023.

Figure 14-13: Log-Probability Chart on Mo (Both Zones) for Capping Analysis



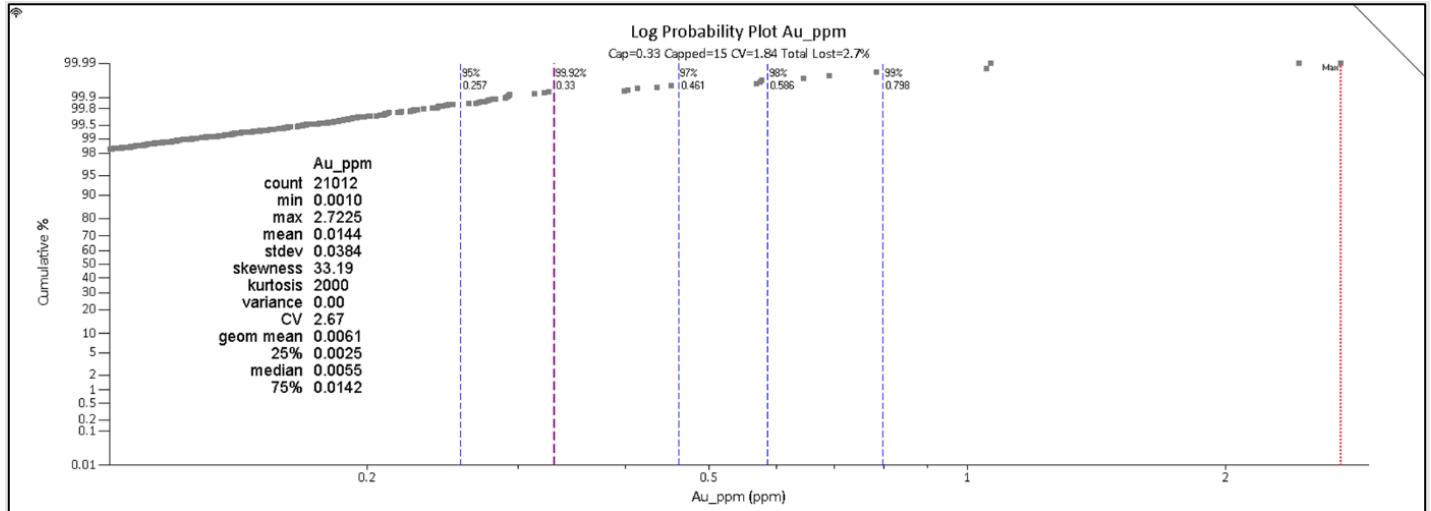
Source: SRK, 2023.

Table 14-11: Tabulated Capping Options for Molybdenum (Both Zones)

Column	Capping Option	Capped ppm	Capped	Percentile	Capped%	Lost Total %	Lost CV%	Count	Min	Max	Mean	Total	Variance	CV
Mo_ppm	-	-	-	-	-	-	-	20952	0	2280	34	709034	5914	2.27
Mo_ppm	-	1500	3	99%	0.01%	0.10%	1.20%	20952	0	1500	34	708104	5754	2.24
Mo_ppm	-	1105	9	98%	0.04%	0.50%	3.30%	20952	0	1105	34	705803	5483	2.2
Mo_ppm	-	769	24	97%	0.10%	1.20%	6.50%	20952	0	769	33	700585	5047	2.12
Mo_ppm	Mo_ppm > 1500	-	-	-	-	-	-	3	1525	2280	1810	5430	168196	0.23
Mo_ppm	Mo_ppm <= 1500	-	-	-	-	-	-	20949	0	1460	34	703604	5447	2.2

Source: SRK, 2023.

Figure 14-14: Log-Probability Chart on Au (Both Zones) for Capping Analysis



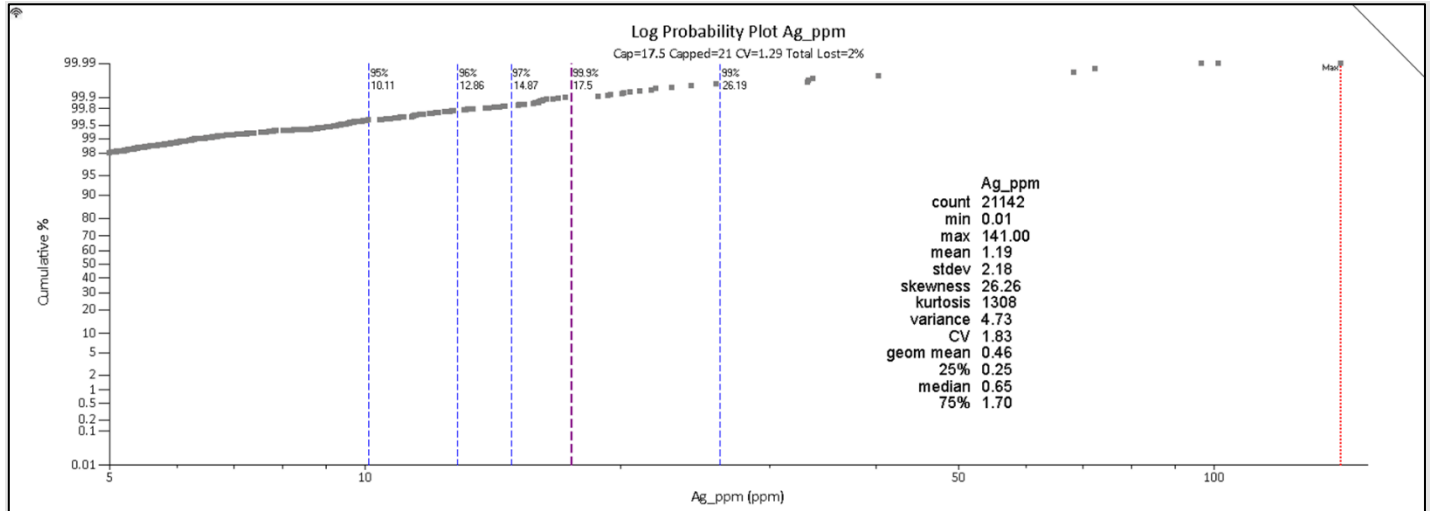
Source: SRK, 2023.

Table 14-12: Tabulated Capping Options for Gold (Both Zones)

Element	Capping Option	Capped ppm	Capped	Percentile	Capped%	Lost Total%	Lost CV%	Count	Min	Max	Mean	Variance	CV
Au_ppm	-	-	-	-	-	-	-	21012	0.001	2.723	0.0144	0	2.67
Au_ppm	-	0.798	4	99%	0.02%	1.30%	23%	21012	0.001	0.798	0.0142	0	2.07
Au_ppm	-	0.586	7	98%	0.03%	1.70%	26%	21012	0.001	0.586	0.0141	0	1.98
Au_ppm	-	0.461	10	97%	0.05%	2.10%	28%	21012	0.001	0.461	0.0141	0	1.91
Au_ppm	-	0.33	15	96%	0.10%	2.70%	31%	21012	0.001	0.33	0.014	0	1.84
Au_ppm	-	0.257	32	95%	0.20%	3.30%	33%	21012	0.001	0.257	0.0139	0	1.79
Au_ppm	Au_ppm > 0.33	-	-	-	-	-	-	15	0.398	2.723	0.881	0.52	0.82
Au_ppm	Au_ppm <= 0.33	-	-	-	-	-	-	20997	0.001	0.326	0.0138	0	1.77

Source: SRK, 2023.

Figure 14-15: Log-Probability Chart on Ag (Both Zones) for Capping Analysis



Source: SRK, 2023.

Table 14-13: Tabulated Capping Options for Silver (Both Zones)

Element	Capping Option	Capped ppm	Capped	Percentile	Capped%	Lost Total%	Lost CV%	Count	Min	Max	Mean	Variance	CV
Ag_ppm	-	-	-	-	-	-	-	21142	0.01	141	1.19	4.73	1.83
Ag_ppm	-	26.19	9	99%	0.04%	1.50%	26%	21142	0.01	26.19	1.17	2.5	1.35
Ag_ppm	-	17.5	21	98%	0.10%	2%	29%	21142	0.01	17.5	1.16	2.26	1.29
Ag_ppm	-	14.87	36	97%	0.20%	2.30%	31%	21142	0.01	14.87	1.16	2.16	1.27
Ag_ppm	-	12.86	47	96%	0.20%	2.60%	32%	21142	0.01	12.86	1.15	2.06	1.24
Ag_ppm	-	10.11	80	95%	0.40%	3.30%	35%	21142	0.01	10.11	1.15	1.9	1.2
Ag_ppm	Ag_ppm > 17.5	-	-	-	-	-	-	21	18.8	141	41.71	1163	0.82
Ag_ppm	Ag_ppm <= 17.5	-	-	-	-	-	-	21121	0.01	17.2	1.15	2	1.23

Source: SRK, 2023.

14.5 Spatial Continuity

The spatial continuity of KEV grades by mineralization zone was assessed through variogram maps, experimental, and modeled semi-variograms calculated using Leapfrog Geo software. Composited and capped data was used to determine spatial continuity constrained by the North Zone and South Zone domains. Variogram maps and visualization of mineralization trends were analyzed to determine dominant directionality with downhole and directional experimental semi-variograms calculated and ultimately modeled. The nugget effect was determined based on the downhole semi-variogram.

Summary findings from the variography analyses includes:

- The North Zone and South Zone Cu mineralization domains were used to constrain all key economic variables for variography.
- Grade population distributions show log-normal characteristics; therefore, Cu, Mo, Au, and Ag was transformed to Gaussian space using normal score transforms for variography modeling.
- A well-structured experimental variogram could not be calculated for S in the South Zone. S in the North Zone did not require a normal score transform for modeling due to the composited data distribution being Gaussian.
- Variogram major directions are aligned with the mineralization trends observed in drilling and grade shell modeling.
- In general, the nugget effect is considered low with values ranging between 15 and 30% of the sill.
- Most variables are modeled using nested nugget plus two spherical structures.
- Ranges are considered relatively long with ranges between 350 m and 500 m in the major direction (along trend). The minor direction typically shows ranges less than 200 m which is expected given the tabular geometry of identified mineralization in both the North Zone and South Zone.
- Spatial continuity is considered robust with relatively low nugget effect, long ranges, and robust structure of variography. Given the deposit type and observed continuity of mineralization in drilling and mapping of this porphyry copper deposit, the final modeled variograms are considered applicable for use in estimation.

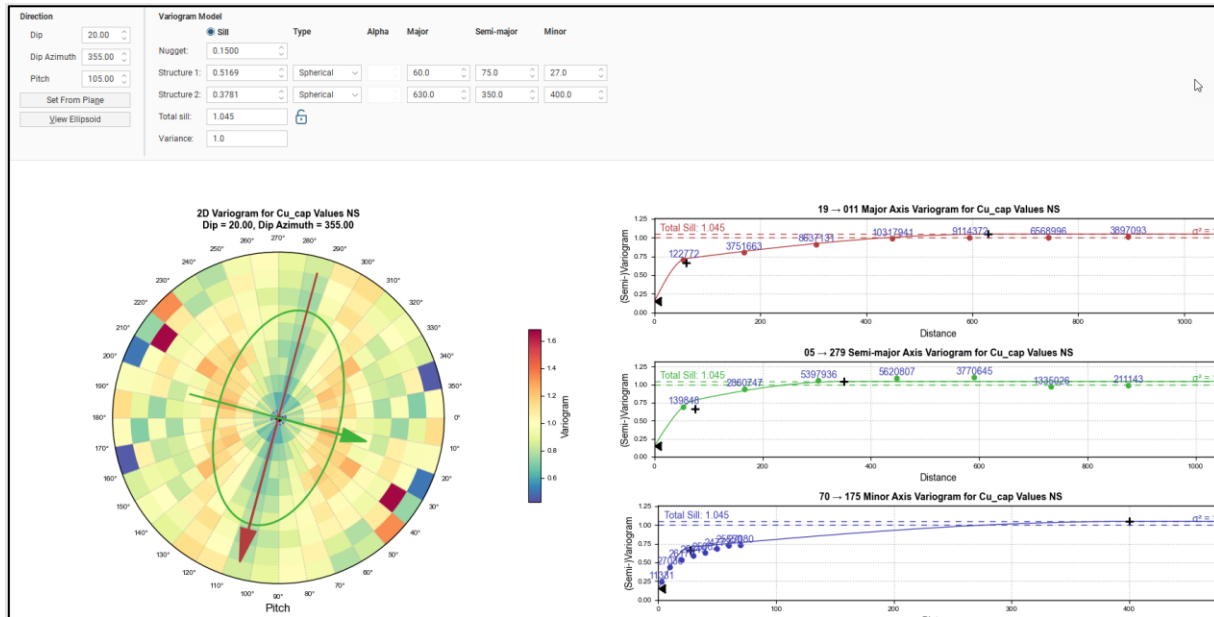
Modeled variograms are shown below for select elements. All variography parameters by domain and element are presented in Table 14-14. Variography was modeled with similar parameters in the major and semi-major direction with some variables showing isotropic continuity in X and Y directions. In general, the major directional anisotropy is aligned with the mineralized estimation domains. Overall, the KEV exhibit relatively low nugget values with long ranges in the major and semi-major direction. SRK notes that it was common to observe a reduced sill in the minor direction resulting in modeling requiring a long second structure to maintain “best fit” model in this direction. SRK cautions to not interpret minor direction ranges based on final modeled semi-variograms distance parameters in the minor direction. Instead, it is recommended to interpret minor direction range from the graphic semi-variogram models as shown in Figure 14-16 through Figure 14-24.

Table 14-14: Variography Parameters for Key Economic Variables

Zone	Variable	Model space	Direction						Structure 1					Structure 2						
			Dip	Dip Azimuth	Pitch	Variance	Nugget	Normalized Nugget	Sill	Normalized sill	Structure	Major	Semi-major	Minor	Sill	Normalized Nugget	Structure	Major	Semi-major	Minor
NZ	Ag	Normal score	20	355	105	1	0.21	-	0.44	-	Spherical	70	60	40	0.39	-	Spherical	420	230	130
NZ	Ag	Data	20	355	105	2.1	0.52	0.25	0.93	0.45	Spherical	70	60	40	0.67	0.32	Spherical	420	230	130
NZ	Au	Data	20	355	105	0	0	0.15	0	0.39	Spherical	45	45	32	0.0005	0.47	Spherical	425	425	225
NZ	Au	Normal score	20	355	105	1	0.11	-	0.31	-	Spherical	45	45	32	0.6	-	Spherical	425	425	225
NZ	Cu	Normal score	20	355	105	1	0.15	-	0.52	-	Spherical	60	75	27	0.38	-	Spherical	630	350	400
NZ	Cu	Data	20	355	105	5,832,588	1,054,532	0.18	3,101,187	0.53	Spherical	60	75	27	1,891,508	0.32	Spherical	630	350	400
NZ	Mo	Data	20	355	105	9,356	2,173	0.23	4,784	0.51	Spherical	80	80	23	2,899	0.31	Spherical	430	350	160
NZ	Mo	Normal score	20	355	105	1	0.16	-	0.46	-	Spherical	80	80	23	0.47	-	Spherical	430	350	160
NZ	Mo	Normal score	30	260	155	1	0.16	-	0.33	-	Spherical	225	310	17.66	0.41	-	Spherical	590	310	150
NZ	Mo	Data	30	260	155	9,836	2,144	0.22	3,998	0.41	Spherical	225	310	17.66	3,050	0.31	Spherical	590	310	150
NZ	S	Data	20	355	80	2.3	0.7	0.3	1.02	0.44	Spherical	140	135	30	0.74	0.32	Spherical	600	540	80
SZ	Ag	Normal score	20	260	30.4	1	0.2	-	0.38	-	Spherical	100	250	20	0.45	-	Spherical	500	600	200
SZ	Ag	Data	20	260	30.4	2.7	0.76	0.28	1.1	0.41	Spherical	100	250	20	0.87	0.33	Spherical	500	600	200
SZ	Au	Normal score	23	260	170	1	0.15	-	0.57	-	Spherical	185.7	180	24	0.4033	-	Spherical	525	472	400
SZ	Au	Data	23	260	170	0	0	0.23	0	0.61	Spherical	185.7	180	24	0	0.23	Spherical	525	472	400
SZ	Cu	Normal score	25	260	170	1	0.15	-	0.43	-	Spherical	60	62	20	0.38	-	Spherical	365	280	150
SZ	Cu	Data	25	260	170	3,395,385	563,294	0.17	1,509,249	0.44	Spherical	60	62	20	1,205,701	0.36	Spherical	365	280	150
SZ	Mo	Normal score	30	260	155	1	0.16	-	0	-	Spherical	225	310	17.66	0	-	Spherical	590	310	150
SZ	Mo	Data	30	260	155	9,836	2,144	0.22	3,998	0.41	Spherical	225	310	17.66	3,050	0.31	Spherical	590	310	150

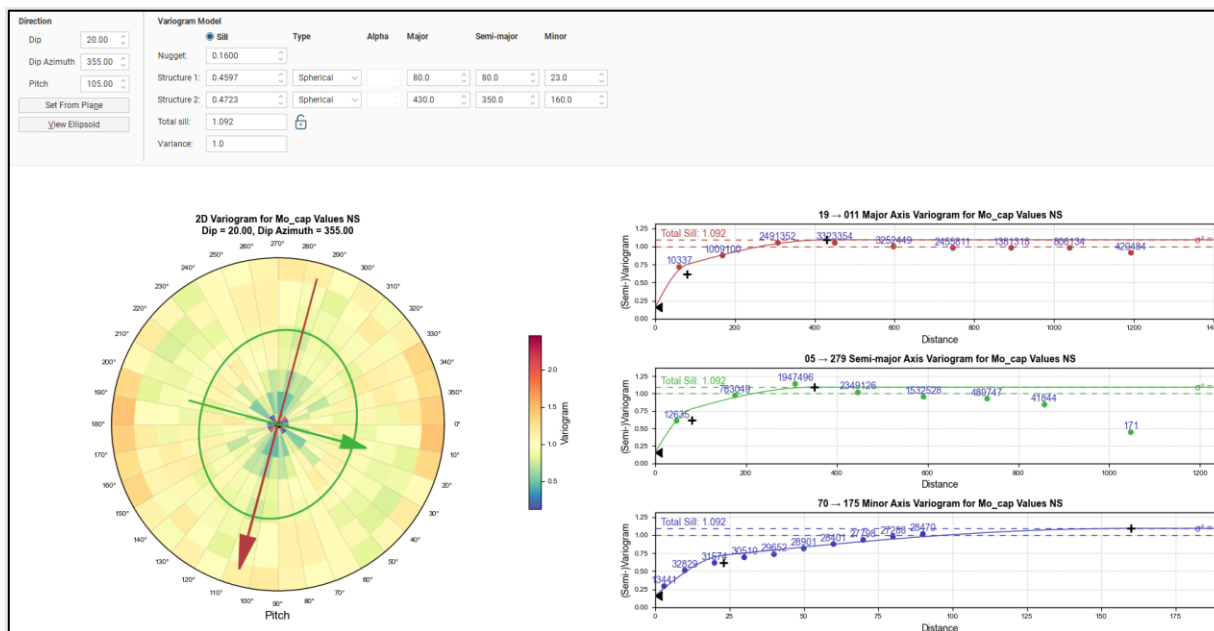
Source: SRK, 2023.

Figure 14-16: Normal Score Transformed Modelled Semi-Variogram for Cu in North Zone



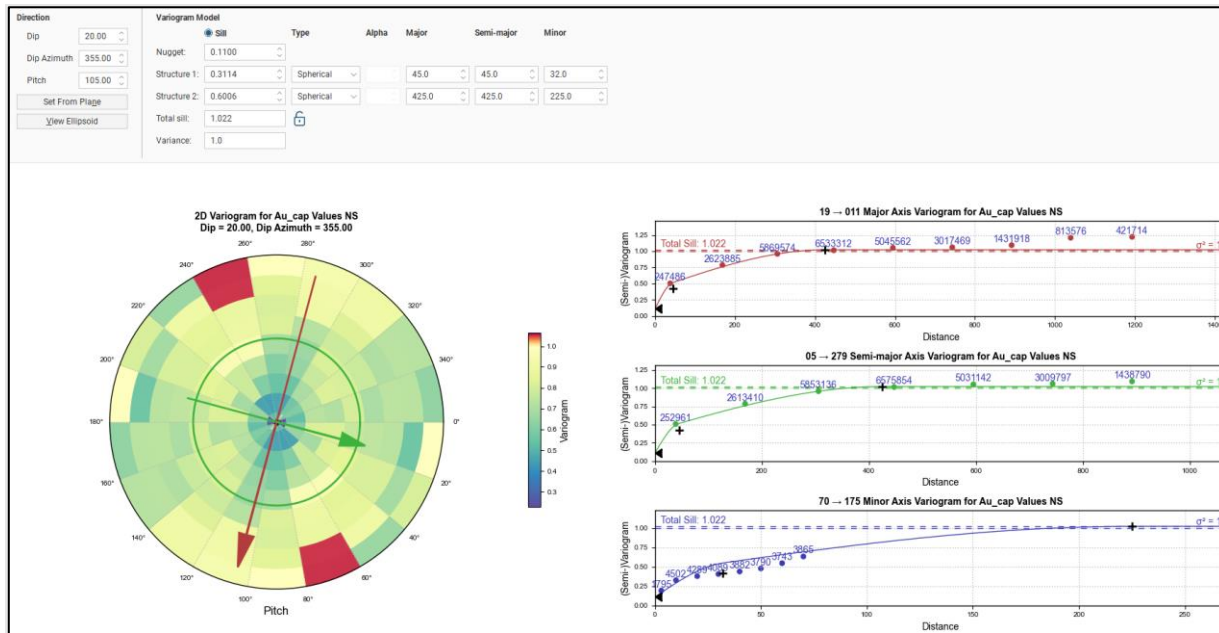
Source: SRK, 2023.

Figure 14-17: Normal Score Transformed Modelled Semi-Variogram for Mo in North Zone



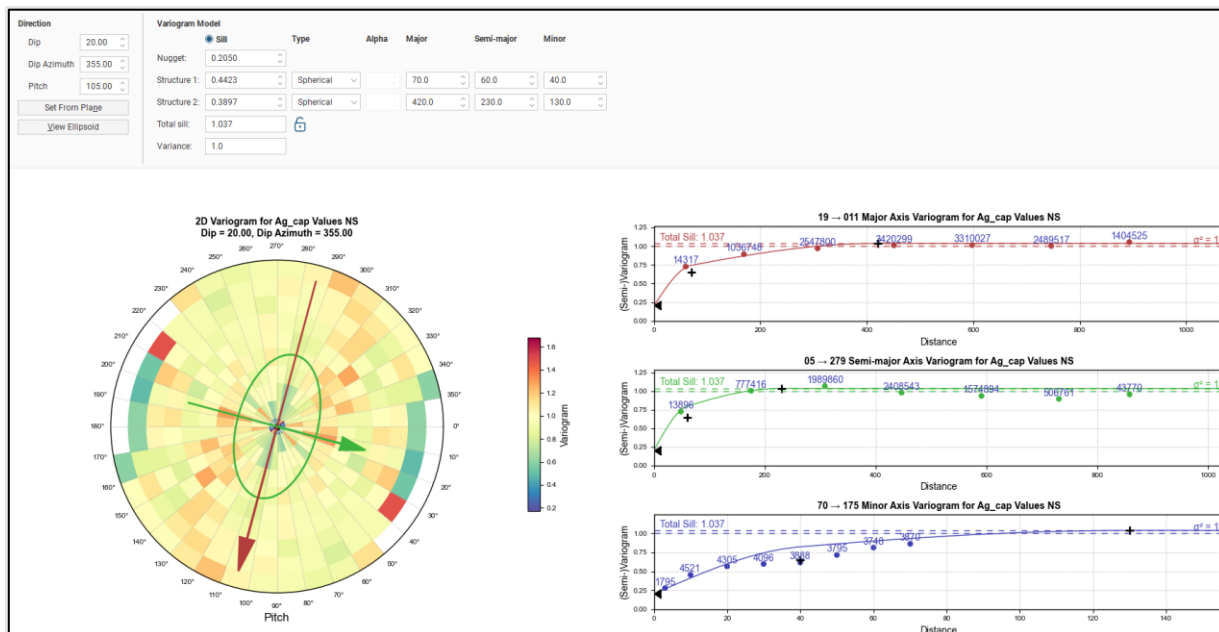
Source: SRK, 2023.

Figure 14-18: Normal Score Transformed Modelled Semi-Variogram for Au in North Zone



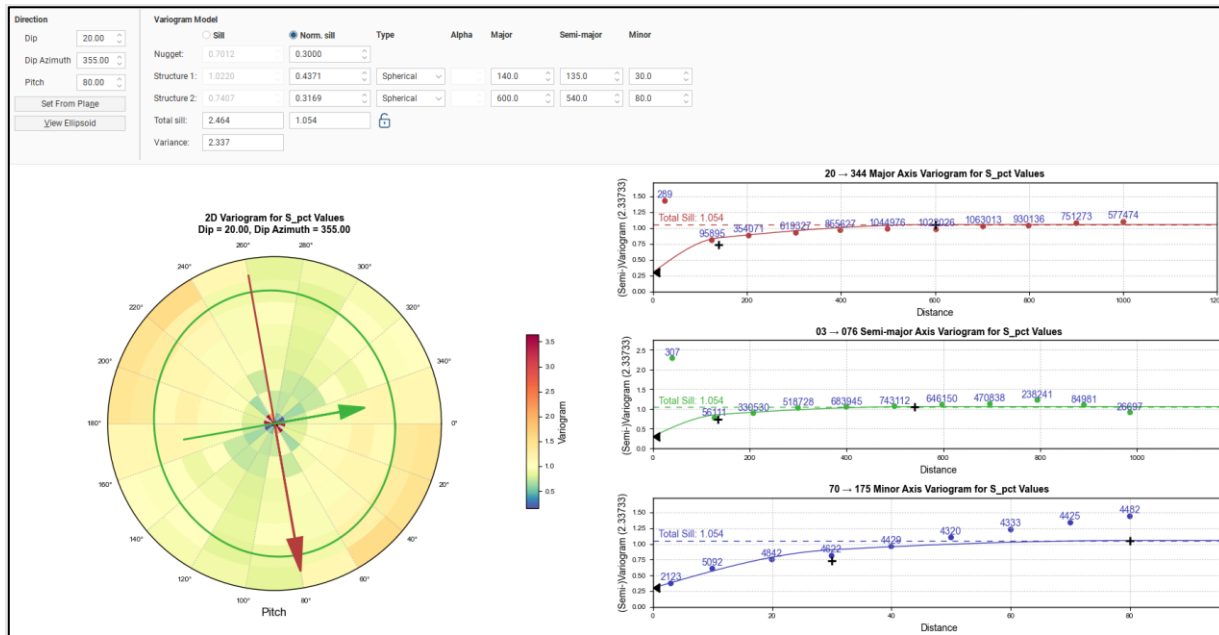
Source: SRK, 2023.

Figure 14-19: Normal Score Transformed Modelled Semi-Variogram for Ag in North Zone



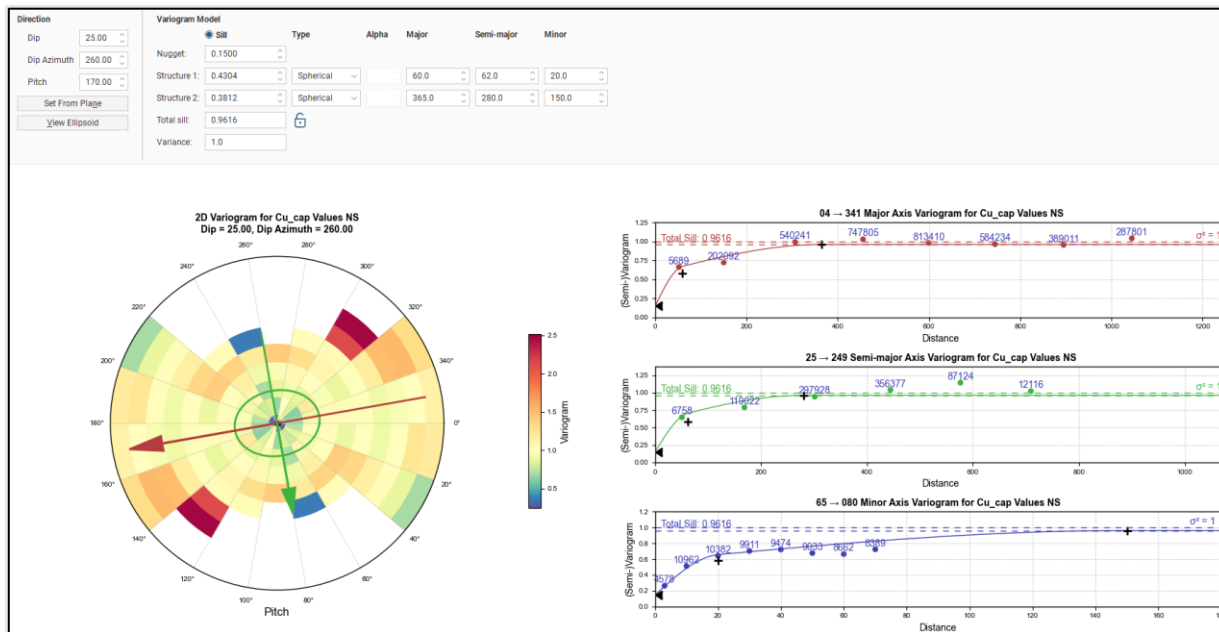
Source: SRK, 2023.

Figure 14-20: Modelled Semi-Variogram for S in North Zone



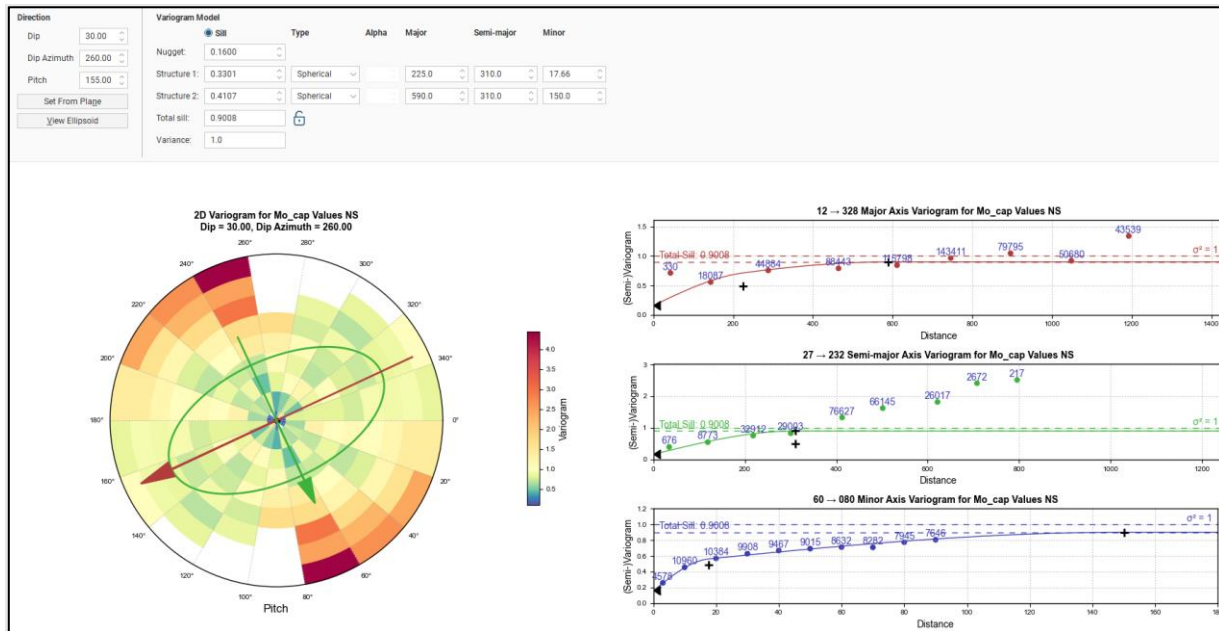
Source: SRK, 2023.

Figure 14-21: Normal Score Transformed Modelled Semi-Variogram for Cu in South Zone



Source: SRK, 2023.

Figure 14-22: Normal Score Transformed Modelled Semi-Variogram for Mo in South Zone



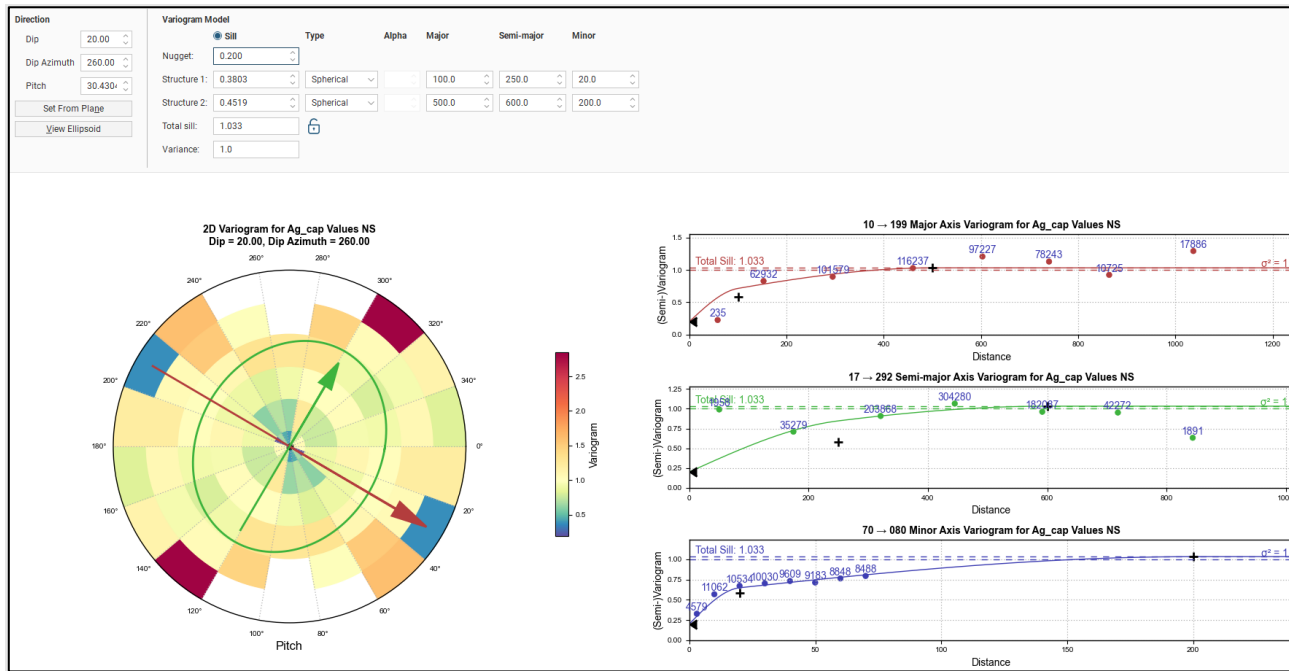
Source: SRK, 2023.

Figure 14-23: Normal Score Transformed Modelled Semi-Variogram for Au in South Zone



Source: SRK, 2023.

Figure 14-24: Normal Score Transformed Modelled Semi-Variogram for Ag in South Zone



Source: SRK, 2023.

14.6 Block Model

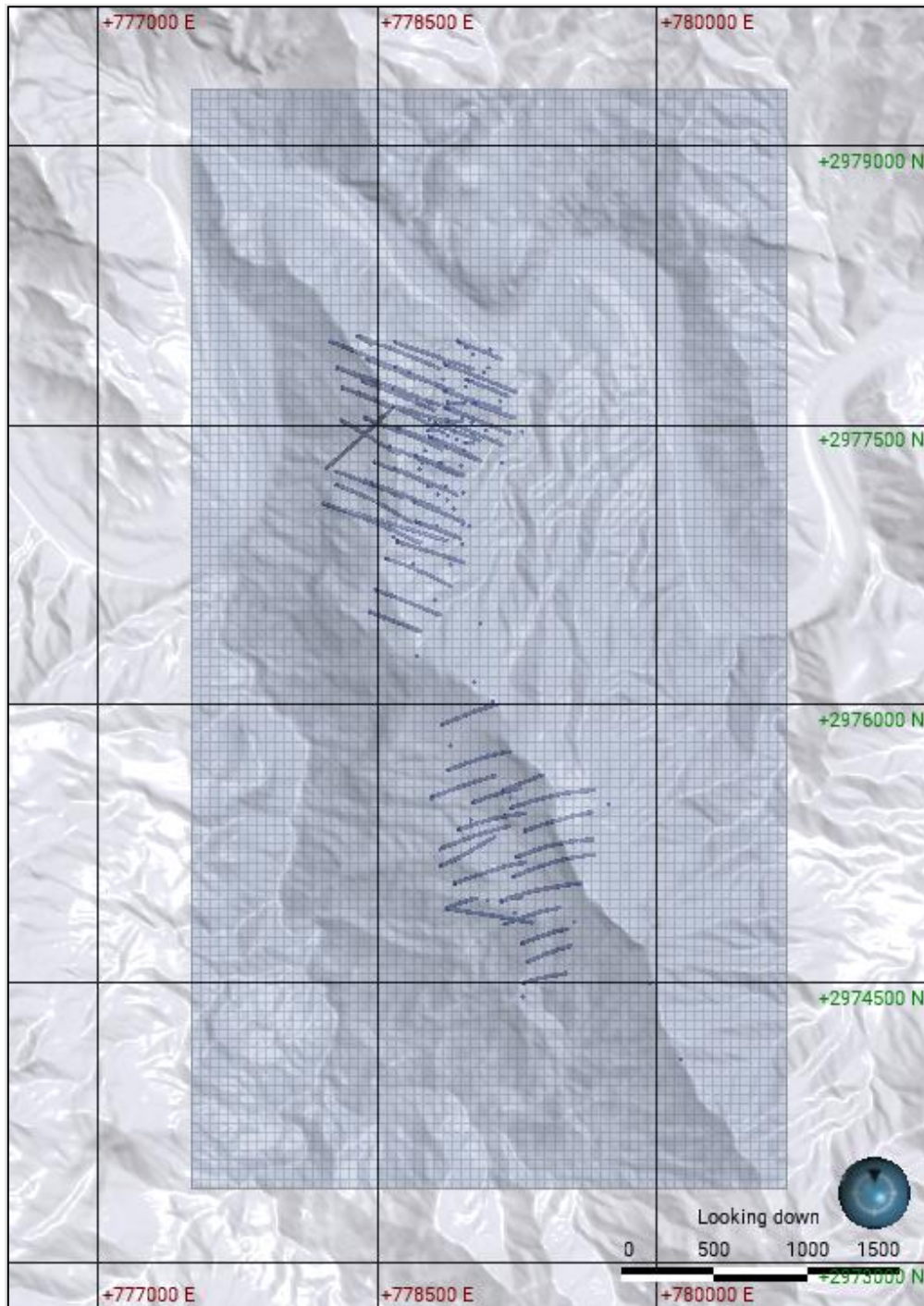
SRK created a digital 3D resource block model using Leapfrog Geo software. The model extents and block size were influenced by the property and drilling extents, geometry of mineralization, anticipated open pit mining method, expected selective mining unit (SMU), and mean data spacing across the deposit which is nominally 150 m. The 2023 MRE block model construction parameters and extents are shown in Table 14-15 with Figure 14-25 illustrating the plan view extents of the block model. The block model is a regularized model with no rotation and block size at 50 m (X) by 50 m (Y) by 10 m (Z).

Table 14-15: Santo Tomás 2023 MRE Block Model Parameters

Parameters (m)	X	Y	Z
Origin	777,500	2,973,400	1,400
Offset	3,200	5,900	2,000
Block Size	50	50	10
Rotation	None		

Source: SRK, 2023.

Figure 14-25: Aerial Extents of the Santo Tomás 2023 MRE Block Model



Source: SRK, 2023.

Variables in the 2023 MRE block model include:

- Mineralization zone based on 750 ppm Cu grade shell, lithology, and structure.
- Oxidation model domain: oxidized or reduced (sulphide) from the oxidation model.
- Primary lithology (protolith) from the geological model.
- Estimated block Cu (%), Mo (%), Au (ppm), Ag (ppm) and S (%).
- Calculated copper equivalent (CuEQ)(%).
- Estimated block bulk density (g/cm³) based on core SG measurements.
- CONAGUA high water reservoir boundary.
- Mineral resource classification, constrained by the economic pit shell.

The QP notes that the model may be improved and refined based on recommendations as summarized in Chapter 26 of this report.

14.7 Estimation Methodology

The Santo Tomás 2023 MRE block model was estimated using a variety of estimation methods tailored to each variable based on findings from the EDA and spatial continuity analyses. Composited and capped values were utilized for estimating block variables. For the key economic grade variables, a combination of Ordinary Kriging (OK) and inverse distance weighted cubed (IDW3) methodologies constrained within the mineralized domains for North Zone and South Zone. For block bulk density, a combination of Simple Kriging (SK) and inverse distance weighting squared (IDW2) domained by modeled lithology from the geological model described in Section 14.3.

Search neighborhoods were designed per variable by domain and refined based on model validation techniques. Summary search parameters are presented in Table 14-16 and Table 14-17.

Table 14-16: Summary Estimation Parameters for Grade Variables

Zone	Element / Pass	Domain	Numeric Values	Estimation Method	Ellipsoid Ranges			Ellipsoid Directions			Number of Samples		Drillhole Limit
					Maximum	Intermediate	Minimum	Dip	Dip Azimuth	Pitch	Minimum	Maximum	Max Samples per Hole
North Zone	Cu Pass1	NZ_Cu_cap Ind 750.0 ISO_0.4: Inside	Cu_cap	OK	630	400	150	20	355	105	4	6	3
	Cu Pass2	NZ_Cu_cap Ind 750.0 ISO_0.4: Inside	Cu_cap	IDW3	800	600	250	20	355	105	3	6	2
	Mo Pass1	NZ_Cu_cap Ind 750.0 ISO_0.4: Inside	Mo_cap	OK	500	400	150	20	355	105	4	6	3
	Mo Pass2	NZ_Cu_cap Ind 750.0 ISO_0.4: Inside	Mo_cap	IDW3	700	500	200	20	355	105	3	5	2
	Au Pass1	NZ_Cu_cap Ind 750.0 ISO_0.4: Inside	Au_cap	OK	630	400	150	20	345	90	4	6	3
	Au Pass2	NZ_Cu_cap Ind 750.0 ISO_0.4: Inside	Au_cap	IDW3	750	600	200	20	345	90	3	6	n/a
	Ag Pass1	NZ_Cu_cap Ind 750.0 ISO_0.4: Inside	Ag_cap	OK	630	400	150	20	345	90	4	6	3
	Ag Pass2	NZ_Cu_cap Ind 750.0 ISO_0.4: Inside	Ag_cap	IDW3	800	600	200	20	345	90	3	6	n/a
	S	NZ_S_pct Ind 0.8: Inside	S_pct	OK	600	540	125	20	355	105	4	8	3
South Zone	Cu Pass1	SZ_Cu_cap Ind 750.0 ISO_0.35: Inside	Cu_cap	OK	500	400	150	27	260	175	4	6	3
	Cu Pass2	SZ_Cu_cap Ind 750.0 ISO_0.35: Inside	Cu_cap	IDW3	1000	750	200	27	260	175	3	5	2
	Mo Pass1	SZ_Cu_cap Ind 750.0 ISO_0.35: Inside	Mo_cap	OK	375	250	100	28.5	260	170	4	6	3
	Mo Pass2	SZ_Cu_cap Ind 750.0 ISO_0.35: Inside	Mo_cap	IDW3	1000	750	200	25	260	175	3	6	2
	Au Pass1	SZ_Cu_cap Ind 750.0 ISO_0.35: Inside	Au_cap	OK	500	400	150	20	260	170	4	6	3
	Au Pass2	SZ_Cu_cap Ind 750.0 ISO_0.35: Inside	Au_cap	IDW3	750	600	200	25	260	170	3	5	2
	Ag Pass1	SZ_Cu_cap Ind 750.0 ISO_0.35: Inside	Ag_cap	OK	400	500	150	20	260	85	4	6	3
	Ag Pass2	SZ_Cu_cap Ind 750.0 ISO_0.35: Inside	Ag_cap	IDW3	600	750	250	20	260	85	3	7	2
	S	SZ_S_pct Ind 0.8 ISO_0.4: Inside	S_pct	IDW2	750	600	200	27	260	175	4	9	3

Source: SRK, 2023.

Table 14-17: Summary Estimation Parameters for Geological Domains

Lithology	Domain	Numeric Values	Estimation Method	Ellipsoid Ranges			Ellipsoid Directions			Number of Samples		Drillhole Limit
				Maximum	Intermediate	Minimum	Dip	Dip Azimuth	Pitch	Minimum	Maximum	Max Samples per Hole
Lower Andesite	01_SRK_GeologyModel_20230402: AND_Lower	SG	SK	300	250	100	10	355	30	4	10	None
Upper Andesite	01_SRK_GeologyModel_20230402: AND_Upper	SG	IDW2	600	600	200	10	355	30	3	7	None
Granodiorite	01_SRK_GeologyModel_20230402: GD	SG	IDW2	400	300	150	10	355	80	4	10	None
Monzonite	01_SRK_GeologyModel_20230402: QMP	SG	IDW2	500	500	200	10	355	75	4	10	None
Monzonite	01_SRK_GeologyModel_20230402: QMP	SG	SK	500	500	200	10	355	75	4	10	None
Sediments and Skarn	01_SRK_GeologyModel_20230402: SED	SG	IDW2	400	300	150	10	355	80	4	10	None
Volcanics	01_SRK_GeologyModel_20230402: VOLC	SG	IDW2	400	300	150	10	355	80	4	10	None

Source: SRK, 2023.

It is QP's opinion that the Santo Tomás 2023 MRE block model resources represents a satisfactory evaluation of the quantity and quality of material as it pertains to known mineralization style and deposit. The model is considered acceptable for use in the reporting of mineral resources under CIM Standards and Definitions (2014) and CIM Best Practice Guidelines for Mineral Resources and Mineral Reserves (2019).

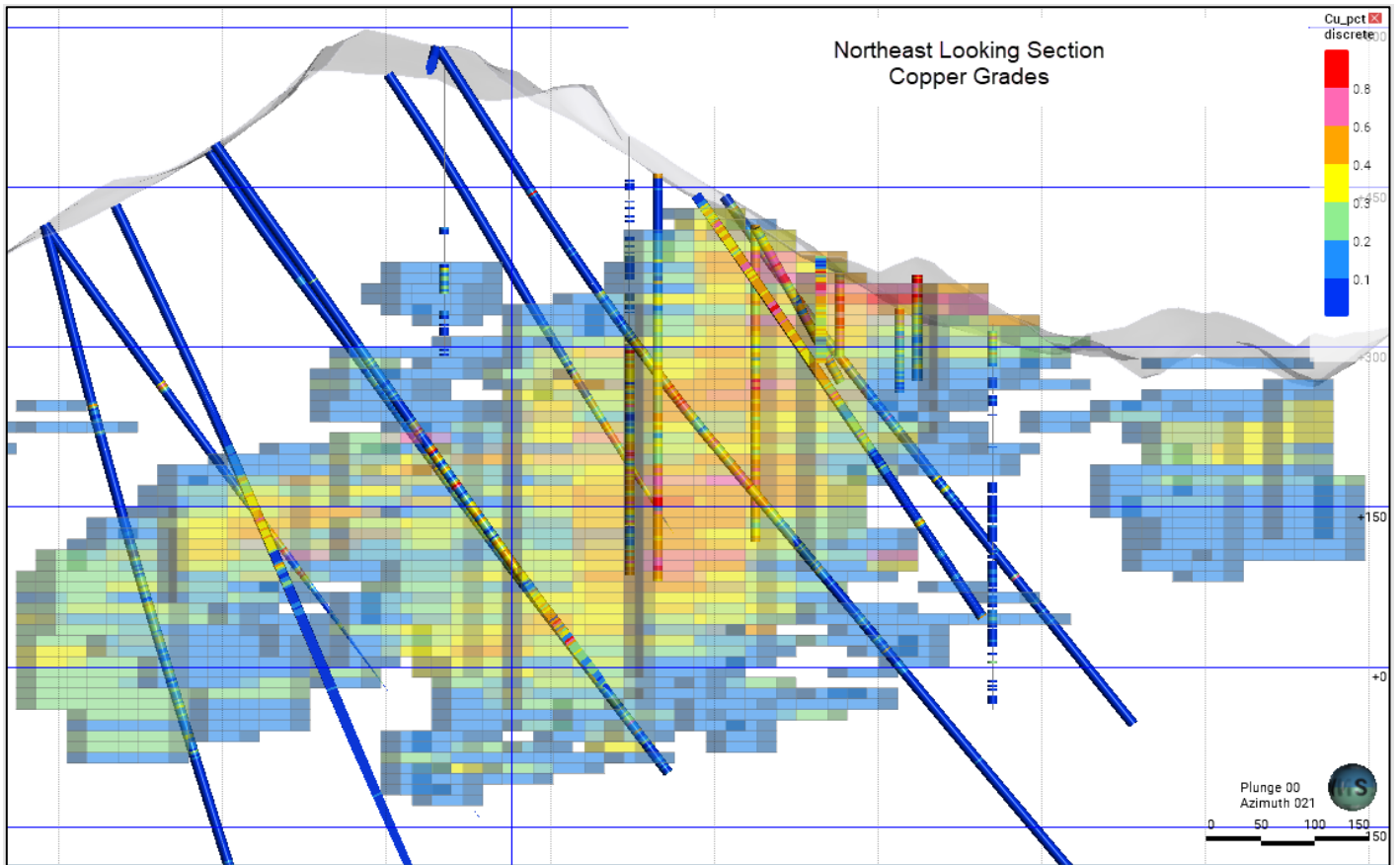
14.8 Block Model Validation

The 2023 MRE block model was validated by SRK using a combination of visual and statistical comparisons to original sampling, capped composites, block height capped composites (10 m composite) and alternative estimation methods. Validation was performed using a combination of Leapfrog Geo and X-10 Geo software. It is the QP's opinion that the 2023 MRE block model is satisfactory for use in the prediction of quantity and quality of material for mine planning, economics, and associated studies as well as for the application of mineral resource classification and reporting.

14.8.1 Visual Comparison

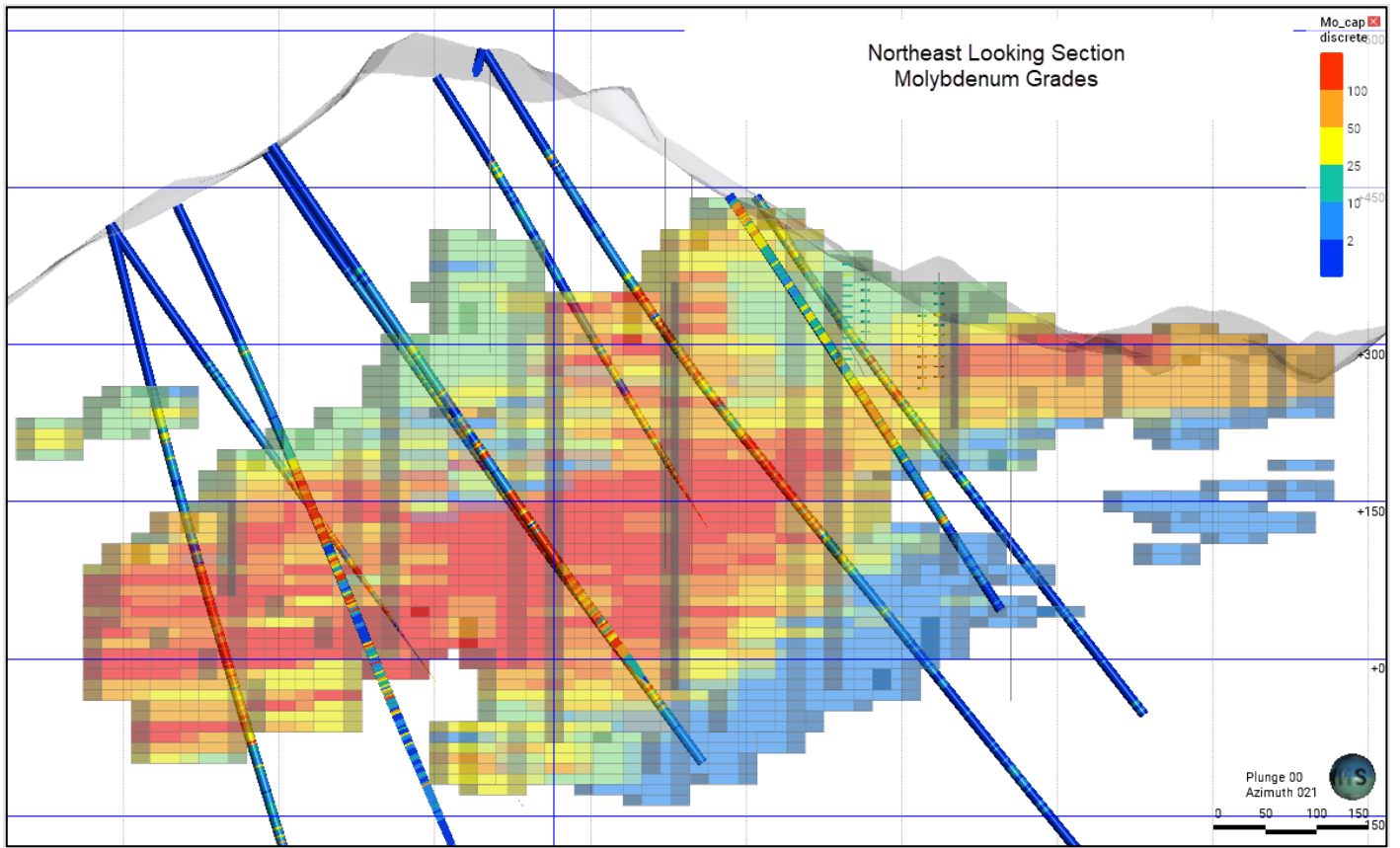
The estimated block grades, capped composites, and original drilling intervals were compared visually along cross-sections on the property. The QP notes challenges in visual block validation due to the high nugget effect, block geometry, and low continuity of Au grades across the deposit but also notes that detailed visual inspection appears satisfactory for block volume estimates considering drill sample variance. Example cross-sections used in the visual validation are presented in Figure 14-26 through Figure 14-33.

Figure 14-26: Cross-Section Used in Visual Comparison - North Zone Cu Values



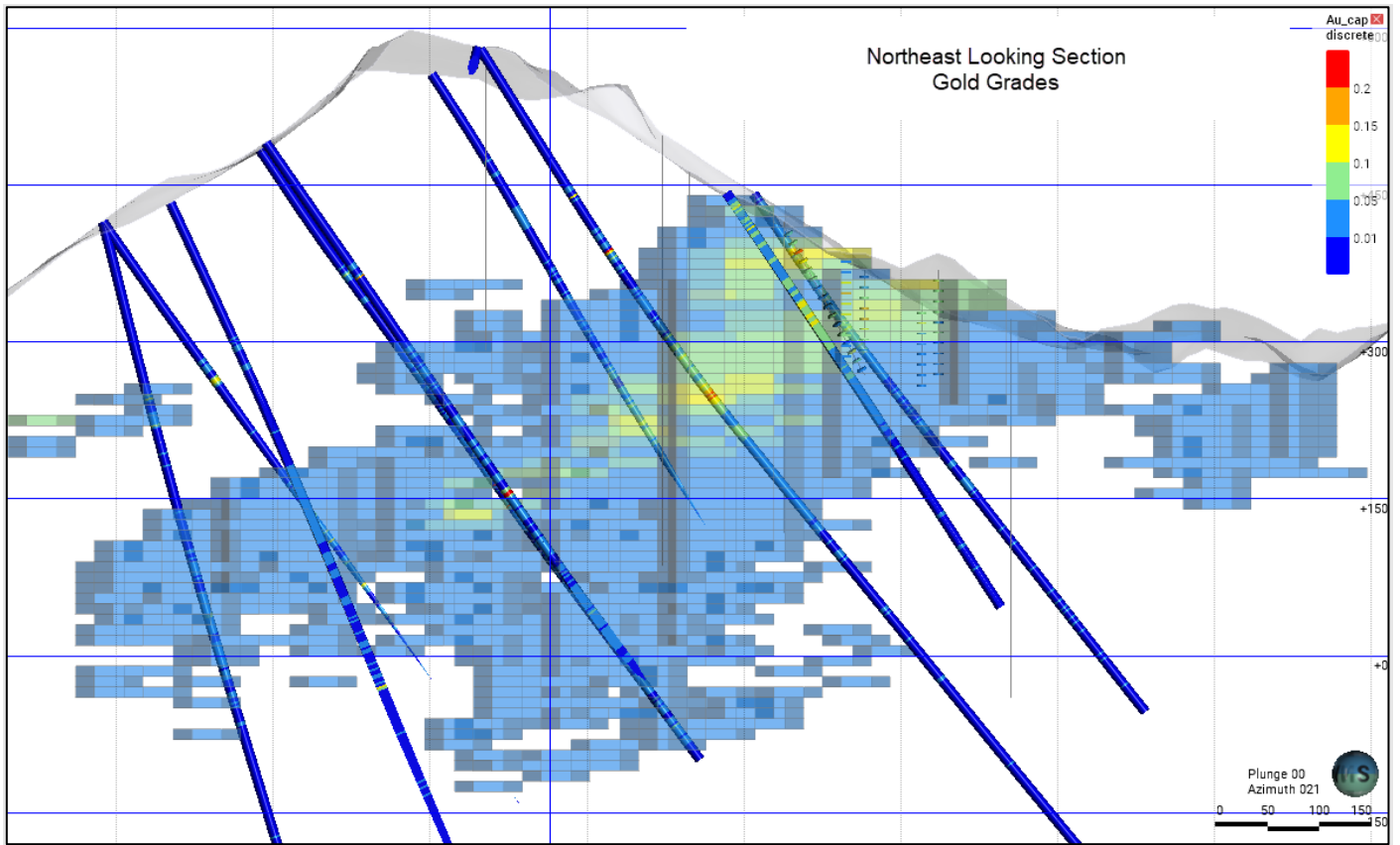
Source: SRK, 2023.

Figure 14-27: Cross-Section Used in Visual Comparison - North Zone Mo Values



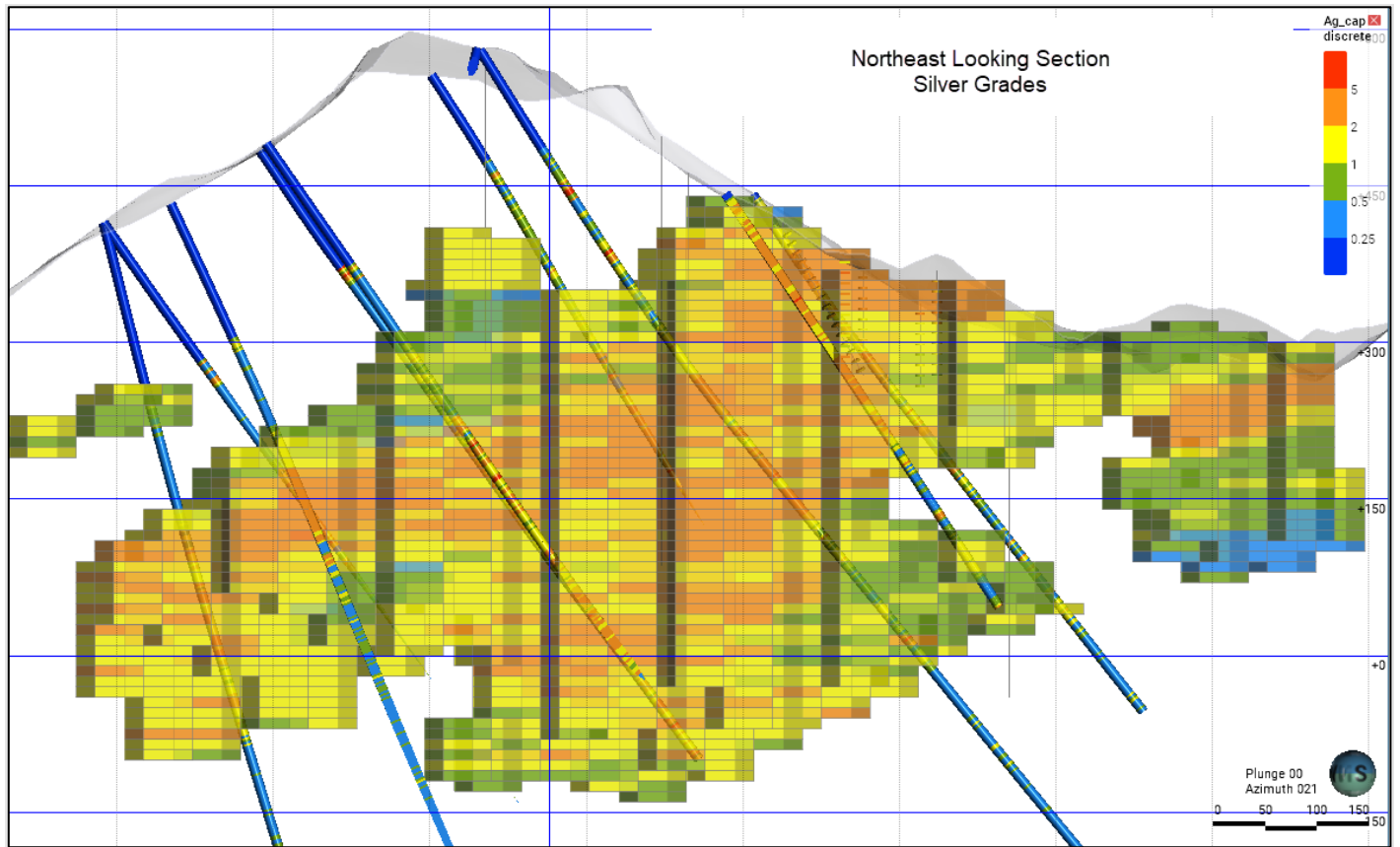
Source: SRK, 2023.

Figure 14-28: Cross-Section Used in Visual Comparison - North Zone Au Values



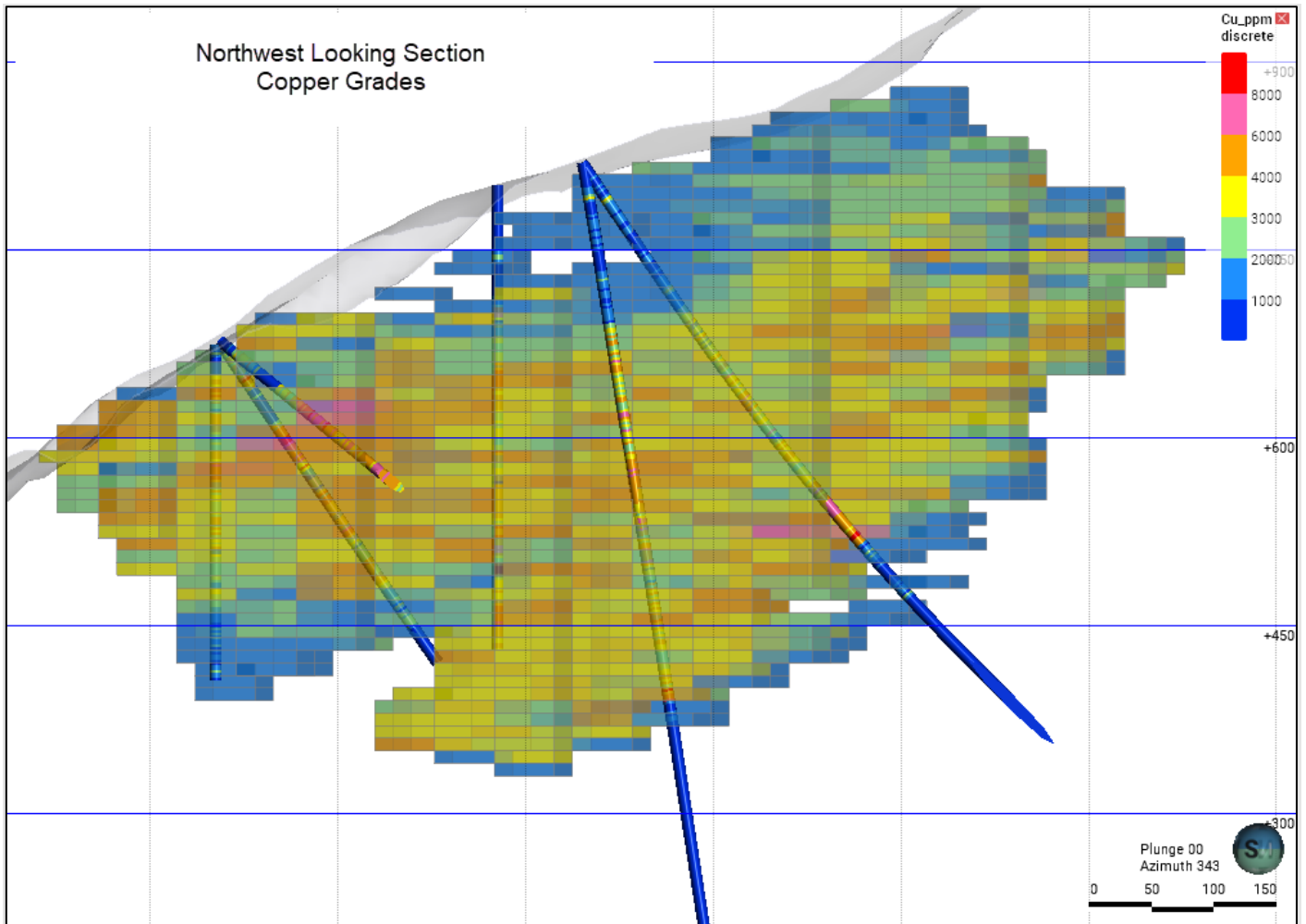
Source: SRK, 2023.

Figure 14-29: Cross-Section Used in Visual Comparison - North Zone Ag Values



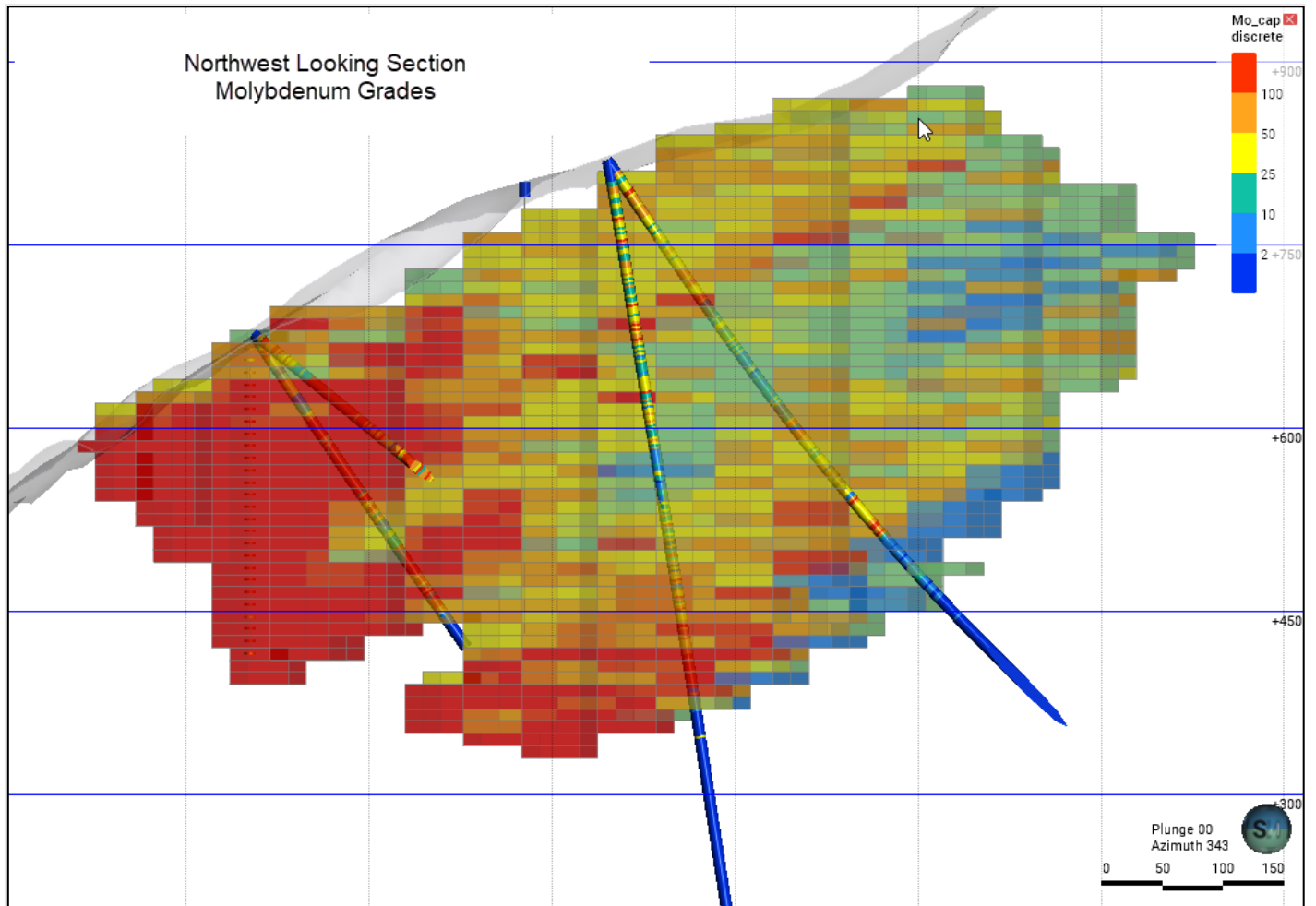
Source: SRK, 2023.

Figure 14-30: Cross-Section Used in Visual Comparison - South Zone Cu



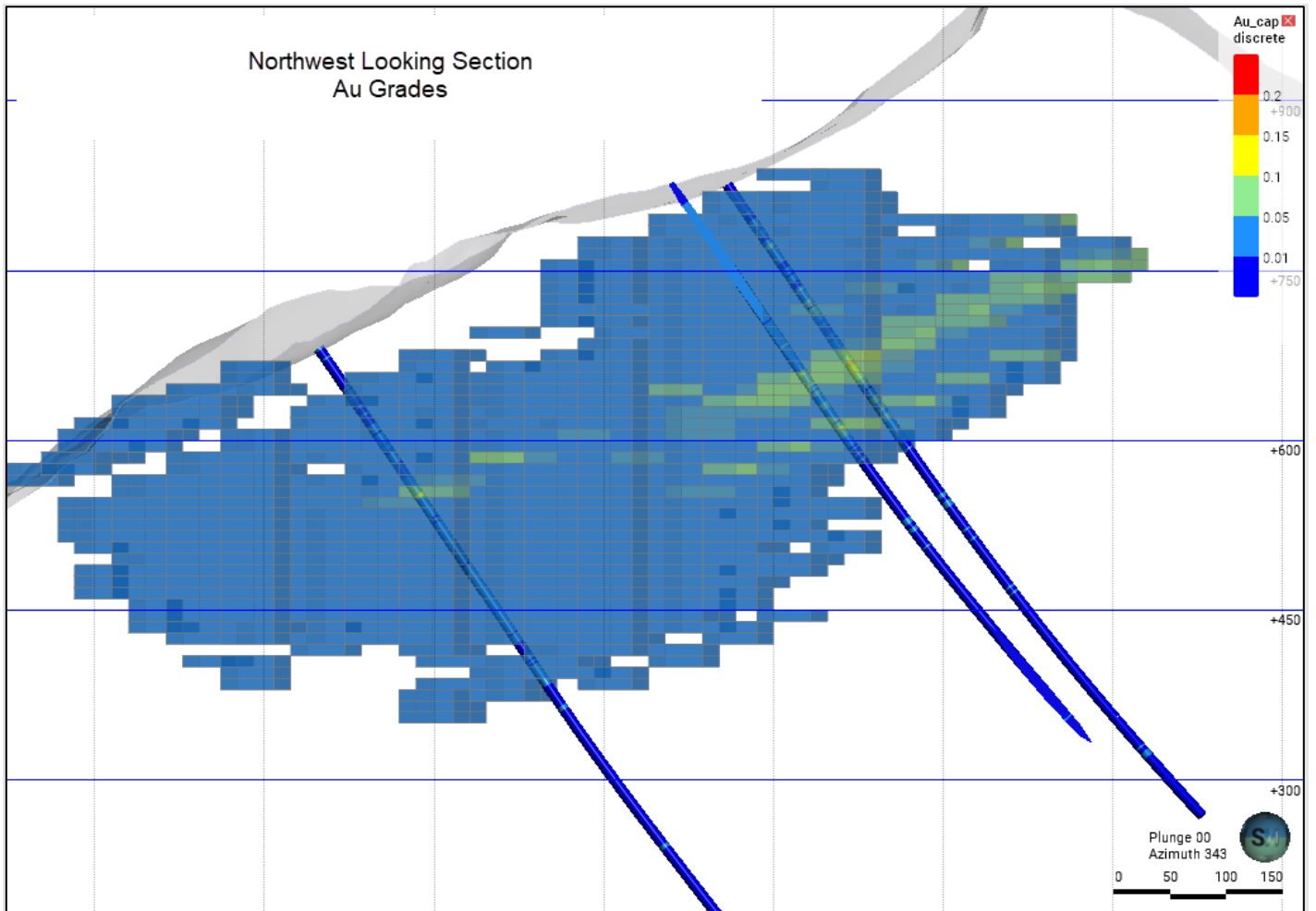
Source: SRK, 2023.

Figure 14-31: Cross-Section Used in Visual Comparison - South Zone Mo



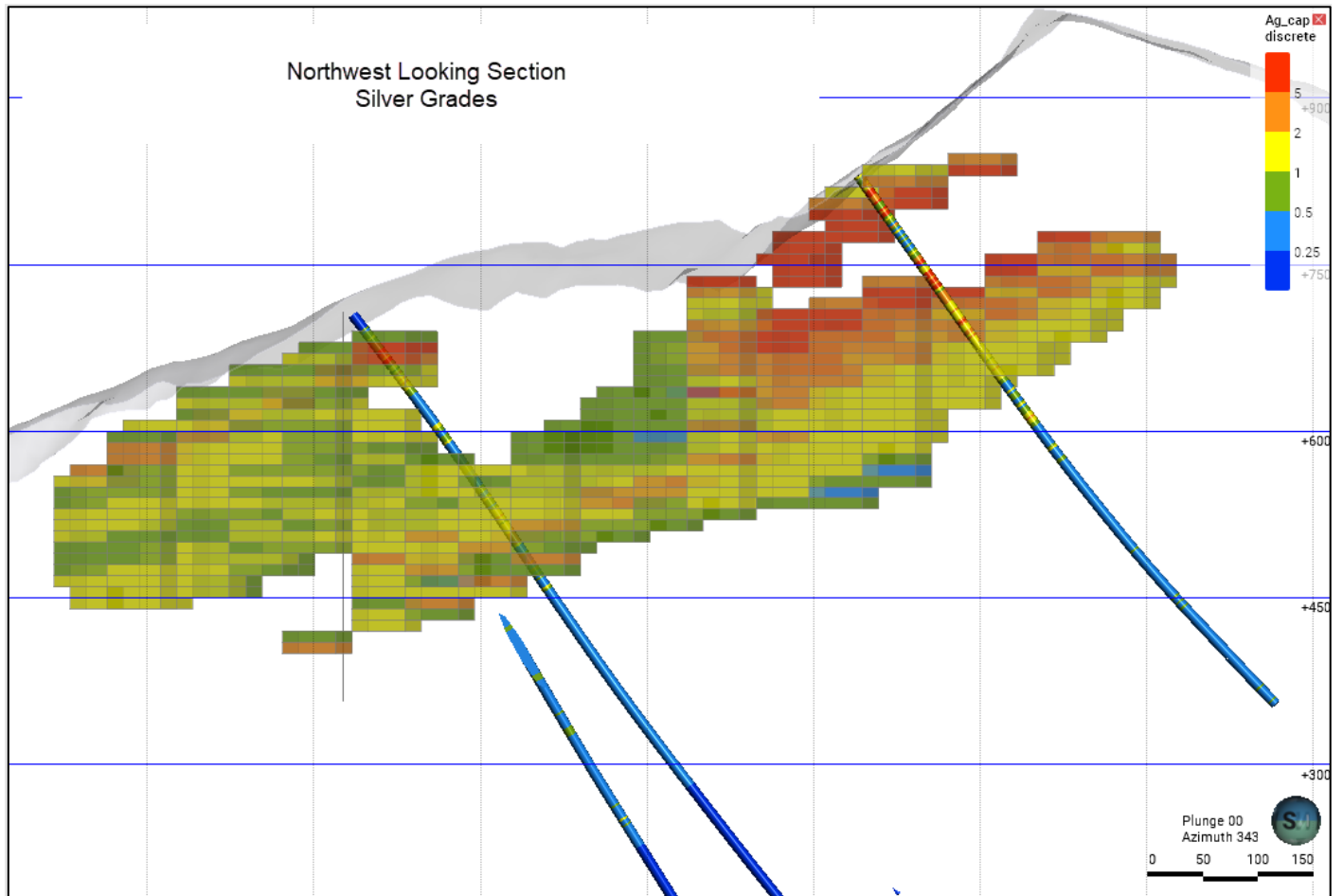
Source: SRK, 2023.

Figure 14-32: Cross-Section Used in Visual Comparison - South Zone Au



Source: SRK, 2023.

Figure 14-33: Cross-Section Used in Visual Comparison - South Zone Ag



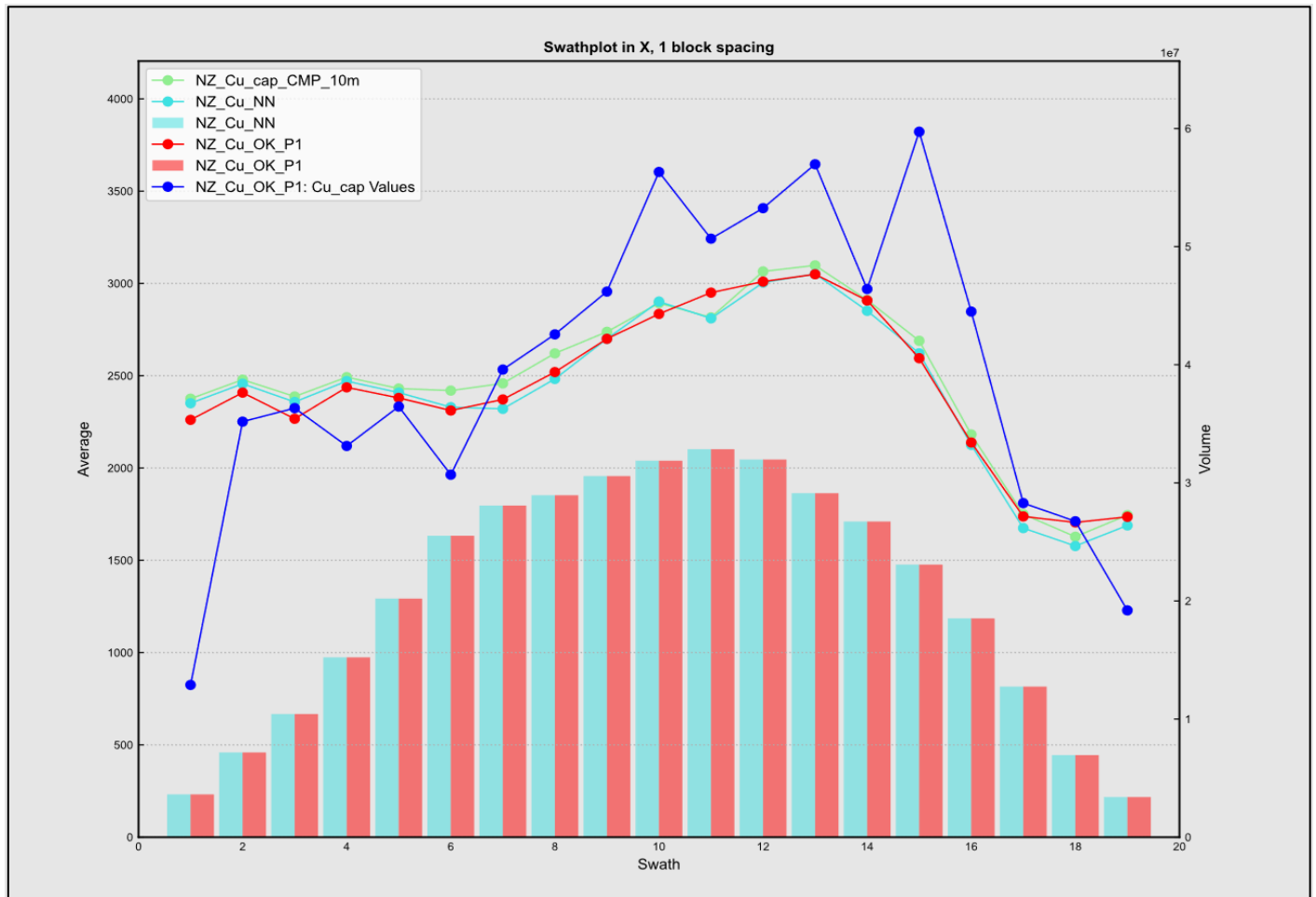
Source: SRK, 2023.

14.8.2 Comparative Statistics

The 2023 MRE block model was validated using a variety of statistical comparisons and analyses. These include general descriptive statistics comparing composite grades and estimated block grades along with swath plots for mean spatial comparisons of data. It is the QP's opinion that the 2023 MRE block model provides acceptable validation and correlation with spatially de-clustered composite grades to support confidence in resource estimation. Differences in observed grades between raw, composited, spatially de-clustered composites (represented as the nearest neighbor [NN] estimate), and block grades are explained by a combination of volume-variance differences, locally clustered drilling data, and the orientation of swath plots compared to oblique drilling data.

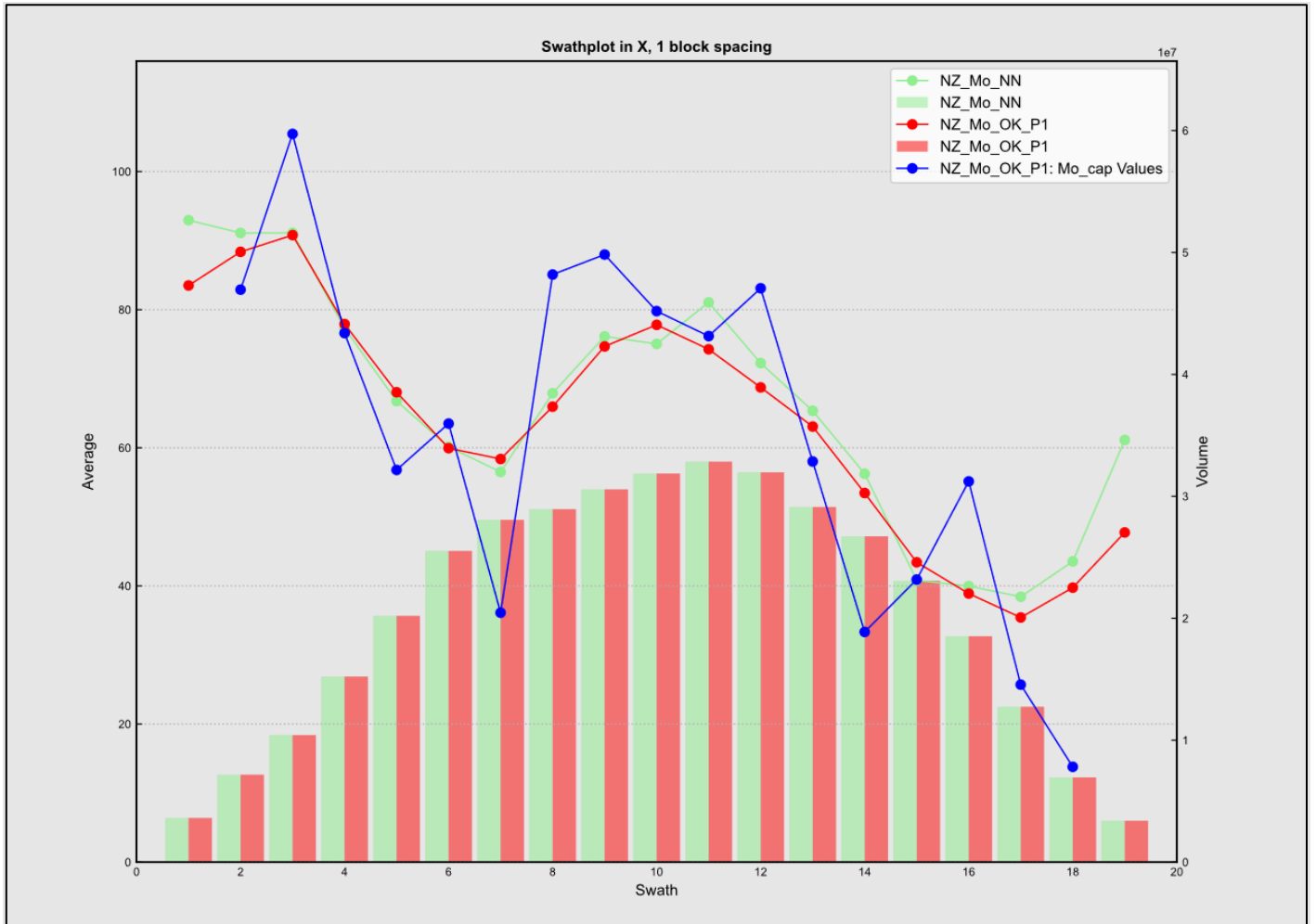
A swath plot analysis was performed to assess conditional bias or smoothing and demonstrates that when comparing the estimated block grades via OK to the NN estimate, the mean values show strong correlation (Figure 14-34 through Figure 14-41). Given that NN represents spatially de-clustered composites, this suggests only minor clustering of data, evident in the historical pit area.

Figure 14-34: Swath plot in X direction - North Zone Cu



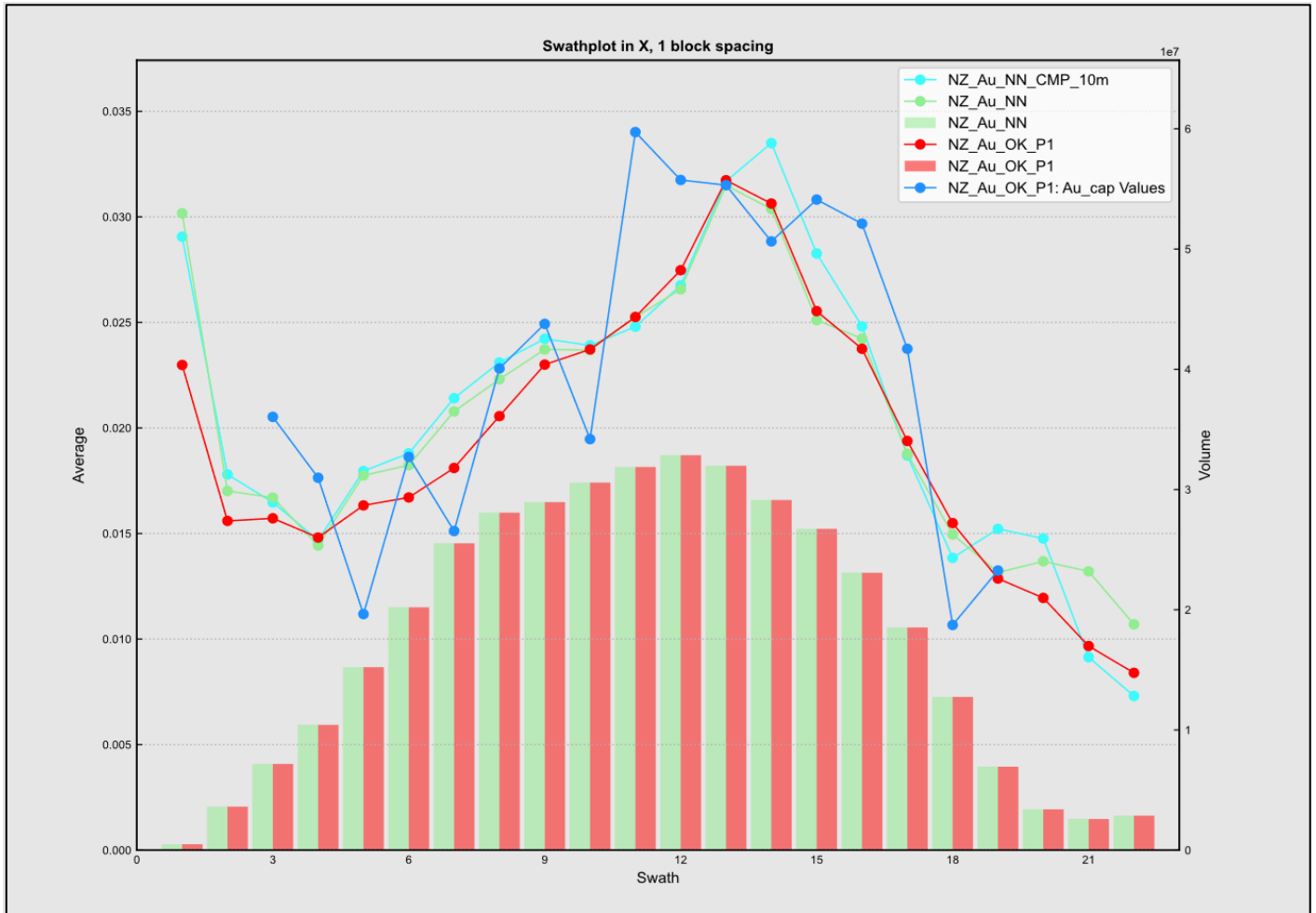
Source: SRK, 2023.

Figure 14-35: Swath plot in X direction - North Zone Mo



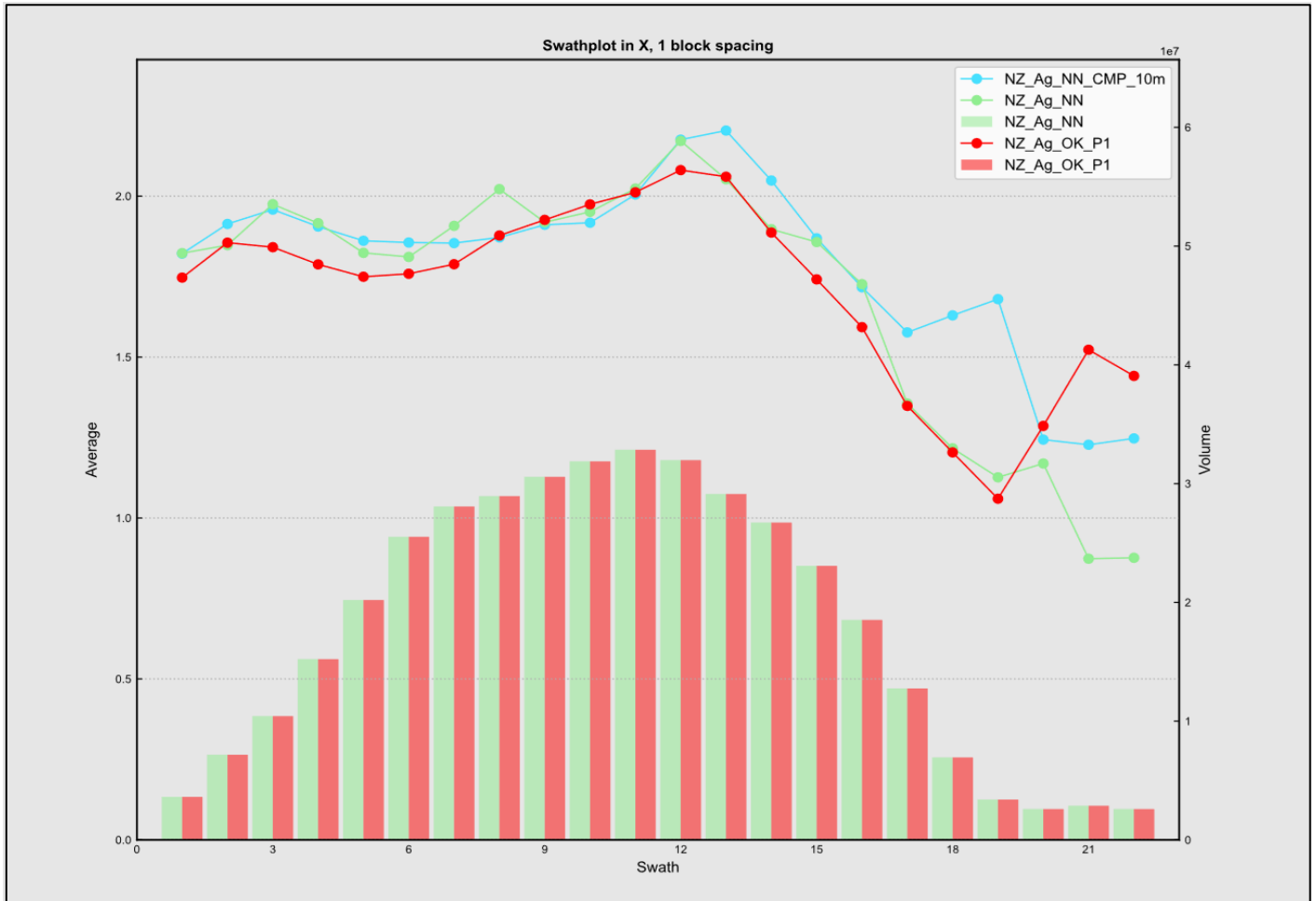
Source: SRK, 2023.

Figure 14-36: Swath plot in X direction - North Zone Au



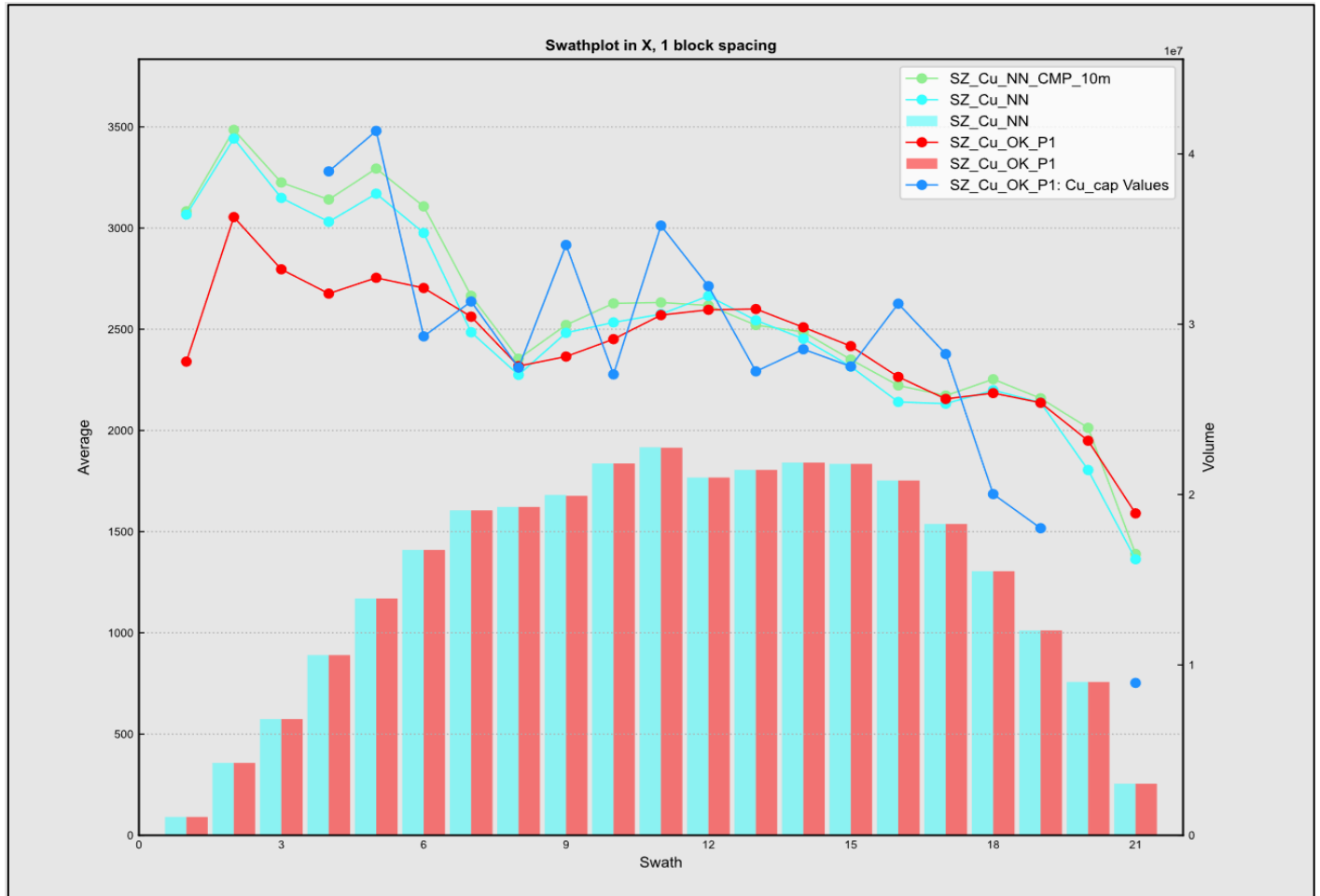
Source: SRK, 2023.

Figure 14-37: Swath plot in X direction - North Zone Ag



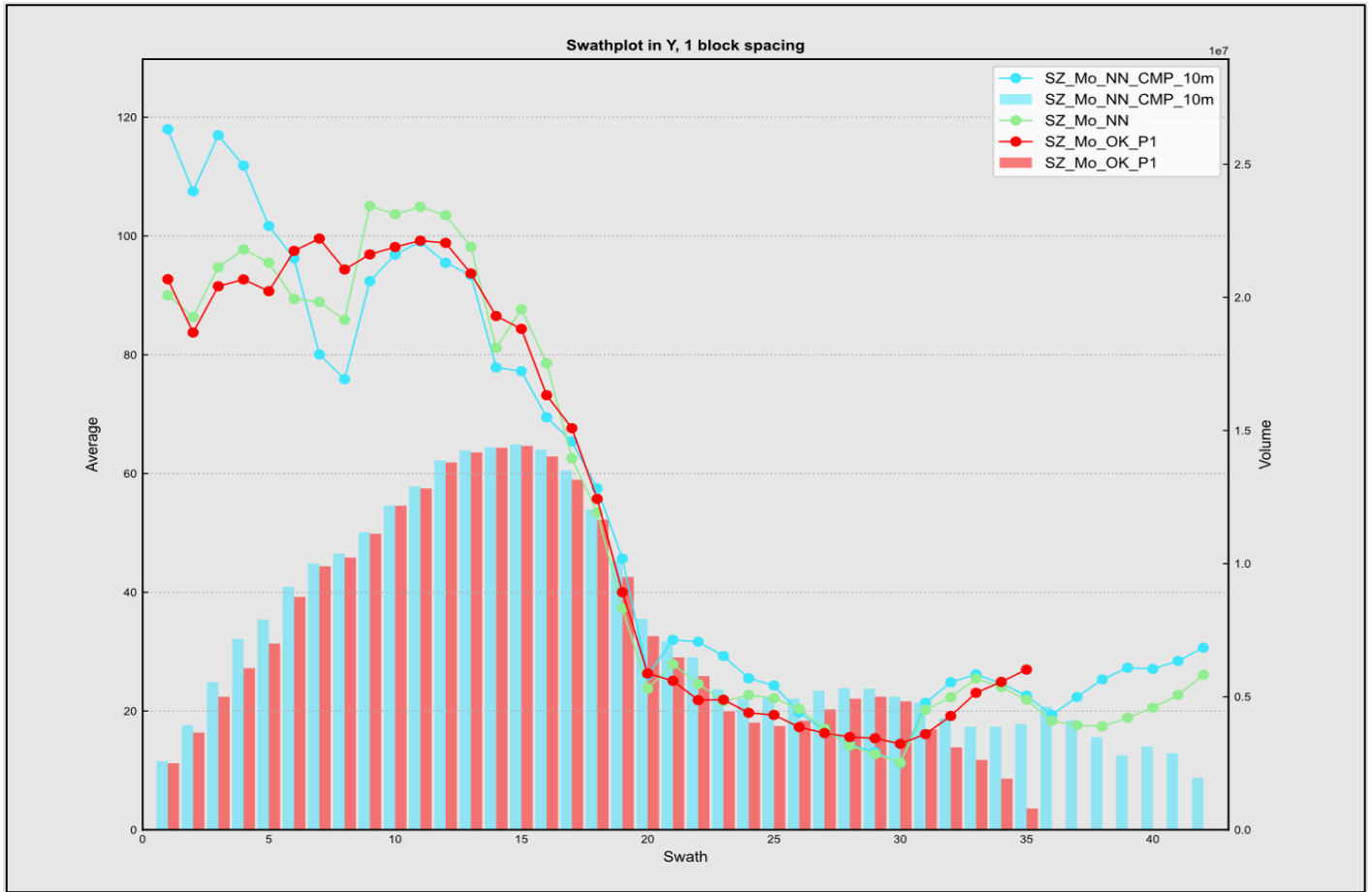
Source: SRK, 2023.

Figure 14-38: Swath plot in X direction - South Zone Cu



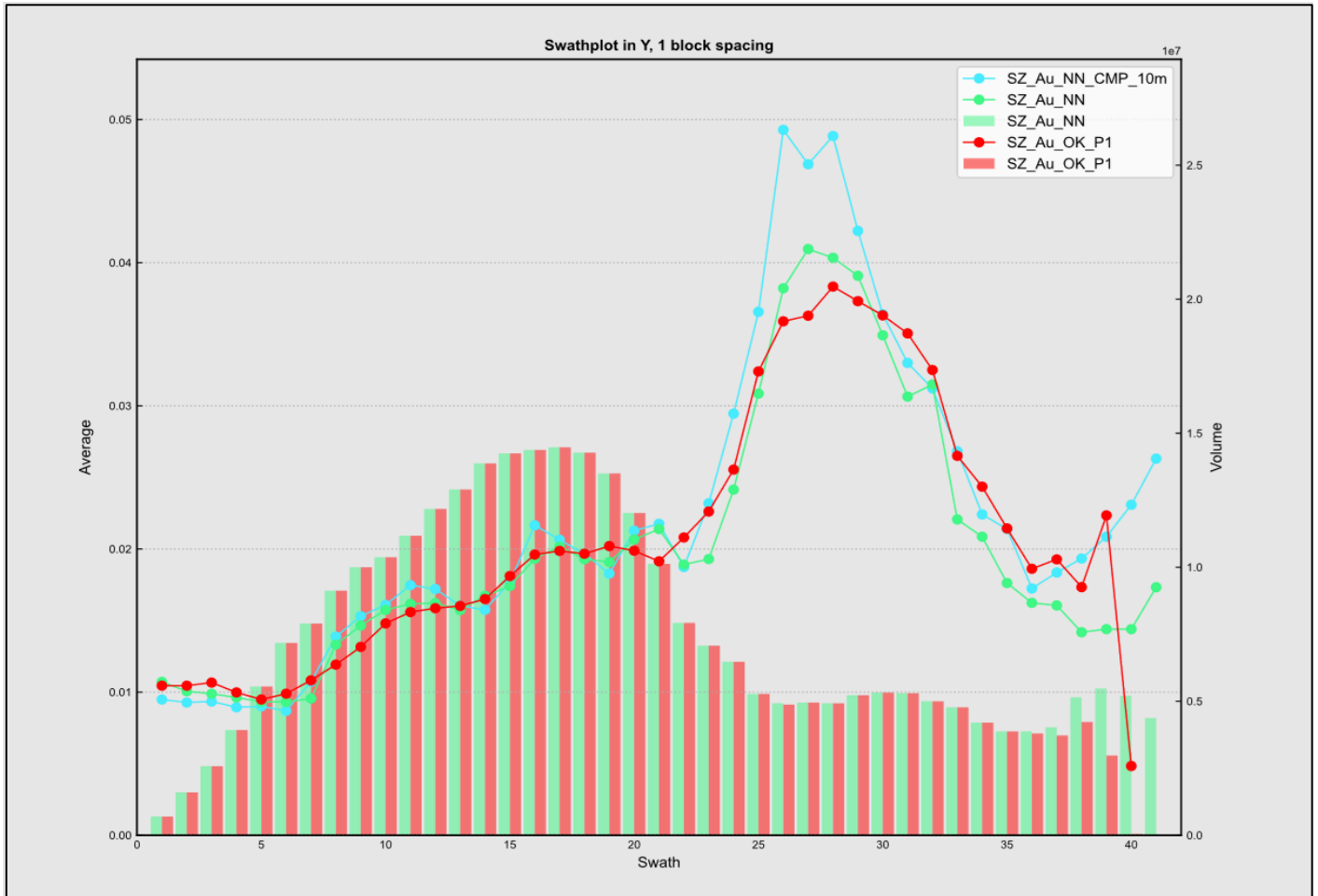
Source: SRK, 2023.

Figure 14-39: Swath plot in Y direction - South Zone Mo



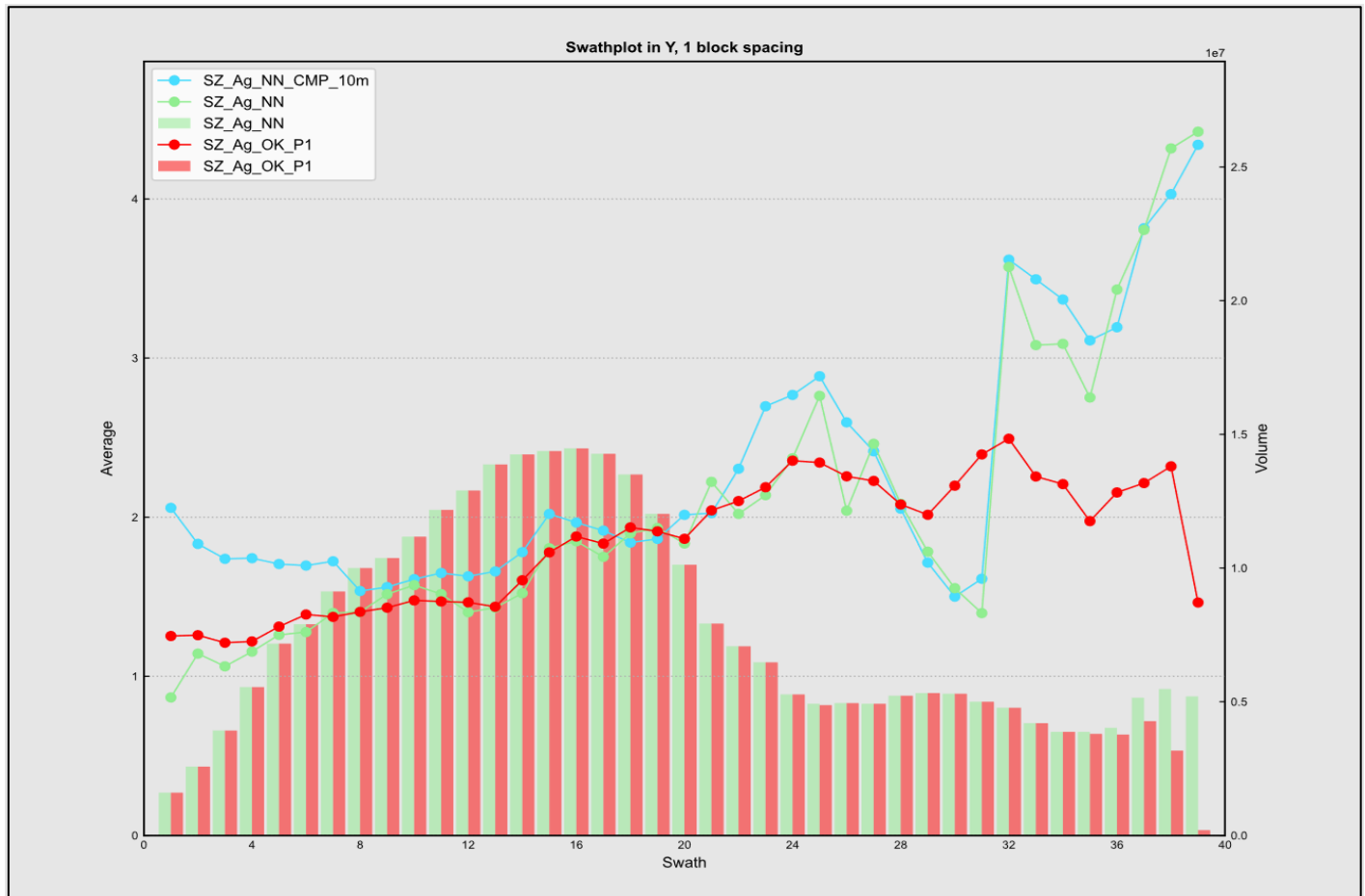
Source: SRK, 2023.

Figure 14-40: Swath plot in Y direction - South Zone Au



Source: SRK, 2023.

Figure 14-41: Swath plot in Y direction - South Zone Ag



Source: SRK 2023.

14.9 Resource Classification

Mineral resources are classified in accordance with NI 43-101 and CIM Standard Definitions (CIM, 2014) into Indicated and Inferred categories based on confidence, current understanding, and identified uncertainty. Resource classification is shown by blocks in Figure 14-42. Blocks are assigned a classification based on the following criteria:

Measured resources – The Santo Tomás project currently does not contain measured mineral resources at this time due to uncertainties related to use of historical drilling to inform geology and Cu grades, lack of multi-element analyses to support Mo, Au, Ag, and S estimates, preliminary metallurgical work establishing recoverability of all elements, and no geometallurgical characterization of mineral species (oxide v. sulphide) with associated deleterious materials.

Indicated resources – The Santo Tomás project contains indicated mineral resources based on the following criteria:

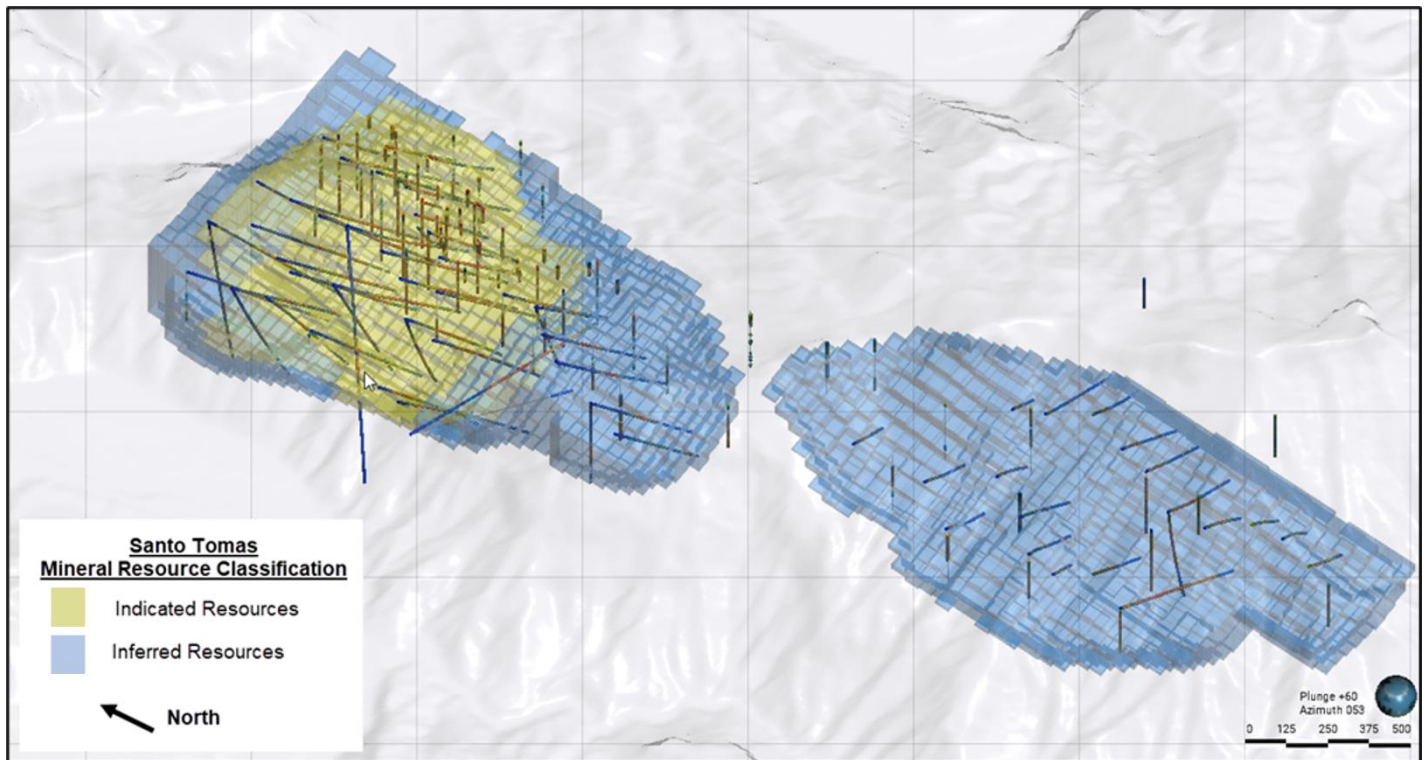
-
- Geological understanding based on surface mapping, structural modeling, geophysical surveys, and drilling across the mineralization zones.
 - Review of QA/QC of drilling completed by Oroco (2021 to date).
 - Robust estimation and established spatial continuity of grades.
 - Mean drill spacing less than or equal to approximately 150 m.
 - SG measurements across multiple lithology with robust spatial distribution on the property.
 - Blocks within the economic pit shell.

Indicated mineral resources are concentrated in the higher density drilling area of the North Zone. This area shows robust spatial continuity of geology and grades with significant support from the combined recent and historical drilling data. Data spacing in this area of identified Indicated mineral resources is below 150 m distance with historical holes highly focused on the high-grade zone with spacing commonly less than 100 m.

Inferred resources – The Santo Tomás project contains inferred mineral resources based on the following criteria:

- Geological understanding based on surface mapping, structural modeling, geophysical surveys, and drilling across the mineralization zones.
- Review of QA/QC of drilling completed by Oroco (2021 to date) with consideration of areas primarily informed by historical data with established uncertainties.
- Mean drill spacing greater than approximately 150 m.
- Quantity of SG measurements support volume.
- Blocks within the economic pit shell.

Figure 14-42: Oblique View of Block Model Colored by Resource Classification.



Source: SRK, 2023.

14.10 Reasonable Prospects for Eventual Economic Extraction

In order to establish reasonable prospects for eventual economic extraction (RPEEE) as per CIM Definitions and Standards (2014) of mineral resources, SRK applied an economic Cu CoG to blocks constrained within an economic pit shell on the property. The economic assumptions for establishing the resource CoG were provided by Oroco and their consultant and shown in Table 14-18. Cost and pricing assumptions are considered long-term in nature for establishing mineral resources at this level of study of the project. The QP has reviewed and accepted all assumptions used in establishing RPEEE for mineral resources at Santo Tomás (Table 14-18).

The input assumption parameters used to determine the economic CoG for Cu was sourced from Oroco, SRK, and Ausenco for all metallurgical recoveries and processing costs. The economic CoG is 0.13% Cu. Oroco has decided to use an effective CoG of 0.15% Cu to align with historical estimates on the property. For mineral resources, this effective CoG at 0.15% Cu was applied.

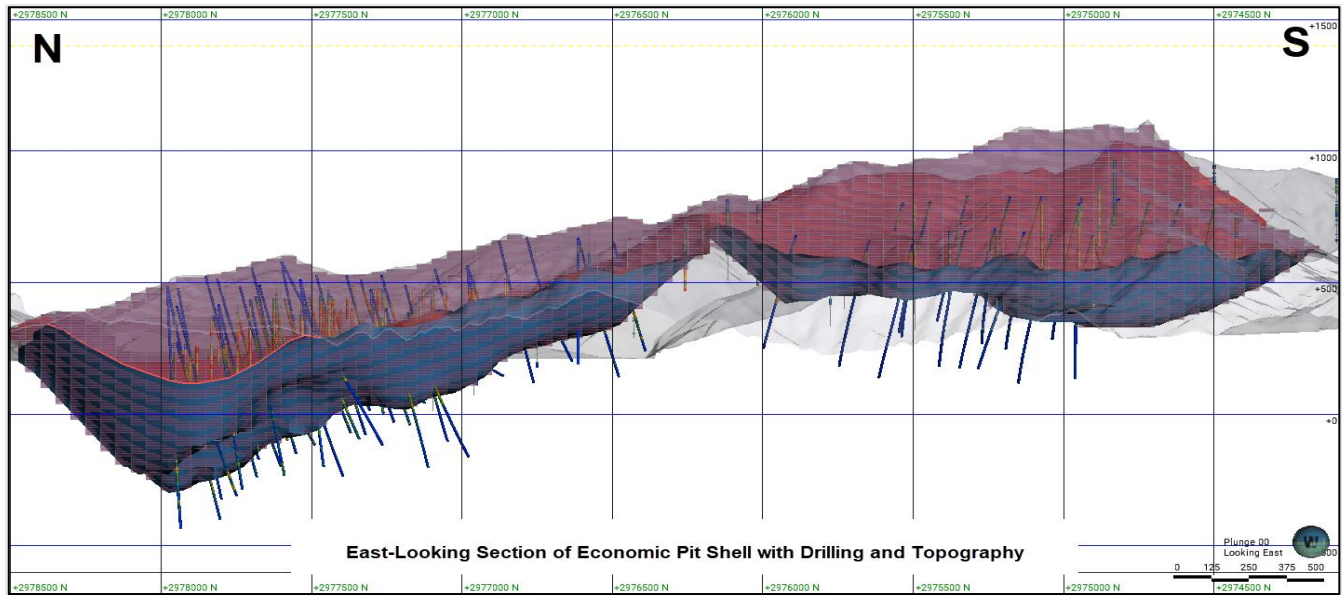
Table 14-18: Input Parameters for Economic Cut-Off Grade

Economic Cut-off Grade Calculation (Cu%)			
Parameter	Unit of Measurement	Value	Source
Mining Cost	US\$/t	2.25	SRK
Processing Cost	US\$/t	5.00	Ausenco
G&A Costs	US\$/t	1.00	Oroco
Sales costs	US\$/t	1.00	Oroco
Royalty	dec %	1.5	Oroco
Mine recovery	%	99	SRK
Mill Recovery - Cu	%	84.3	Ausenco
Copper Price	US\$/t	8,378	SRK

Source: Oroco, SRK, and Ausenco, 2023.

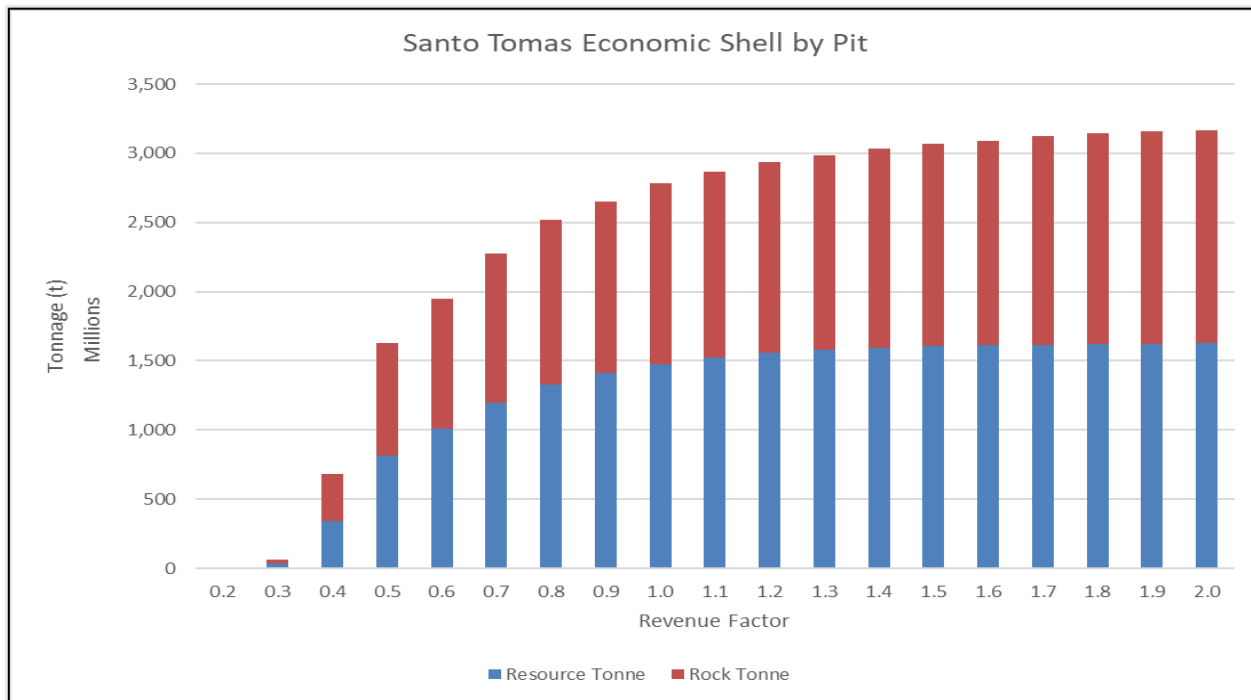
Based on the assumed mining method being open pit, SRK has generated an economic pit shell using Geovia's Whittle software. The economic inputs for the pit shell were held consistent with those presented in Table 14-18 for the CoG in addition to applying slope angles of 50 degrees below 360 m elevation and 45 degrees above 360 m elevation. The high water boundary on the Huites Reservoir was ignored for the purposes of spatial economic constraints considering additional work is required to establish feasibility of mining in this area during future project studies. The economic pit shell is shown in Figure 14-43. A graph of resource and rock tonnage is shown in Figure 14-44. Table 14-19 lists the revenue factors of whittle economic pit shell scenarios.

Figure 14-43: East Looking Section of Economic Pit Shell



Source: SRK, 2023.

Figure 14-44: Graph of Resource and Rock Tonnage by Economic Pit Shell Scenario



Source: SRK, 2023.

Table 14-19: Revenue Factors of Whittle Economic Pit Shell Scenarios

Pit	Revenue Factor	Total Tonnes (Mt)	Resources Tonnes (Mt)	Rock Tonnes (Mt)	Strip Ratio	Cu Metal (Mlb)	Cu Grade (%)	Mo Metal (Mlb)	Mo Grade (%)	Au Metal (Koz)	Au Grade (ppm)	Ag Metal (Koz)	Ag Grade (ppm)
1	0.2	5	3	2	0.9	50	0.83	0	0.002	7	0.08	254	2.9
2	0.3	63	35	28	0.79	391	0.51	3	0.004	65	0.058	2,708	2.4
3	0.4	679	343	337	0.98	2,912	0.39	62	0.008	427	0.039	25,440	2.3
4	0.5	1,629	815	815	1	6,089	0.34	149	0.008	754	0.029	55,006	2.1
5	0.6	1,948	1,009	939	0.93	7,025	0.32	178	0.008	854	0.026	65,534	2
6	0.7	2,278	1,199	1,078	0.9	7,811	0.3	198	0.008	956	0.025	75,915	2
7	0.8	2,522	1,327	1,195	0.9	8,293	0.28	212	0.007	1,012	0.024	82,481	1.9
8	0.9	2,648	1,409	1,239	0.88	8,541	0.28	219	0.007	1,041	0.023	86,075	1.9
9	1	2,780	1,477	1,303	0.88	8,743	0.27	224	0.007	1,062	0.022	89,093	1.9
10	1.1	2,868	1,526	1,342	0.88	8,871	0.26	227	0.007	1,077	0.022	91,173	1.9
11	1.2	2,937	1,558	1,379	0.89	8,953	0.26	229	0.007	1,087	0.022	92,460	1.8
12	1.3	2,985	1,579	1,407	0.89	9,004	0.26	230	0.007	1,092	0.022	93,236	1.8
13	1.4	3,034	1,595	1,439	0.9	9,046	0.26	230	0.007	1,097	0.021	93,901	1.8
14	1.5	3,067	1,605	1,462	0.91	9,071	0.26	231	0.007	1,100	0.021	94,261	1.8
15	1.6	3,087	1,611	1,475	0.92	9,086	0.26	231	0.007	1,101	0.021	94,508	1.8
16	1.7	3,127	1,617	1,510	0.93	9,108	0.26	231	0.006	1,103	0.021	94,732	1.8
17	1.8	3,146	1,622	1,525	0.94	9,119	0.26	232	0.006	1,104	0.021	94,884	1.8
18	1.9	3,157	1,624	1,533	0.94	9,125	0.26	232	0.006	1,105	0.021	94,972	1.8
19	2	3,164	1,626	1,538	0.95	9,129	0.26	232	0.006	1,105	0.021	95,038	1.8

Source: SRK, 2023.

14.11 Copper Equivalent Calculation

In order to provide a general copper equivalent value which incorporates all credit metals, SRK applied the following equation on a block volume basis. Input block grades are used with all recovery and pricing assumptions set as constants for CuEQ determination.

Equation 1: Block Volume Basis

$$CuEQ = \frac{(Cu \text{ grade} \times Cu \text{ recovery}_1 \times Cu \text{ price}_2) + (Mo \text{ grade} \times Mo \text{ recovery}_3 \times Mo \text{ price}_4) + (Au \text{ grade} \times Au \text{ recovery}_5 \times Au \text{ price}_6) + (Ag \text{ grade} \times Ag \text{ recovery}_7 \times Ag \text{ price}_8)}{(Cu \text{ recovery}_1 \times Cu \text{ price}_2)}$$

Notes:

1. Copper recovery is assumed a constant 83.4% based on preliminary recovery test work.
2. Long-term copper pricing used is US\$3.80 per pound (lb).
3. Molybdenum recovery is assumed a constant recovery of 66.0% based on preliminary recovery test work.
4. Long-term molybdenum pricing used is US\$12.00/lb.
5. Gold recovery is assumed a constant recovery of 57.0.0% based on preliminary recovery test work.
6. Long-term gold pricing used is US\$1,650 per troy ounce (oz).
7. Silver recovery is assumed a constant recovery of 54.0.0% based on preliminary recovery test work.
8. Long-term silver pricing used is US\$22.00/lb.

14.12 Mineral Resource Statement

The mineral resource statement is presented in Table 14-20 with an effective date of April 21, 2023. The resource estimate and classification were performed by SRK.

Table 14-20: Mineral Resource Statement, Effective April 21, 2023 - SRK Consulting (US), Inc.

Category	Zone	Tonnes Mt	Average Grade					Contained Metal ³				
			CuEq ¹⁰	Cu	Mo	Au	Ag	CuEq ¹⁰	Cu ¹¹	Mo ¹¹	Au ¹¹	Ag ¹¹
			%	%	%	ppm	ppm	Mlb	Mlb	Mlb	Koz	Koz
Indicated	North Zone	487.3	0.36	0.32	0.009	0.03	2.1	3,864	3,400	91.9	392.8	32,719
	Total Indicated	487.3	0.36	0.32	0.009	0.03	2.1	3,864	3,400	91.9	392.8	32,719
Inferred	North Zone	197.1	0.36	0.32	0.005	0.03	2.1	1,570	1,400	23.6	214.4	13,375
	South Zone	402.8	0.35	0.31	0.008	0.02	1.9	3,127	2,772	72.0	286.2	25,083
	Total Inferred	599.9	0.36	0.32	0.007	0.03	2.0	4,697	4,171	95.6	500.6	38,458

Notes:

1. Mineral resources are not mineral reserves and do not have demonstrated economic viability.
2. The Mineral Resources are reported at an in-situ cut-off grade of 0.15% Cu.
3. All figures are rounded to reflect the relative accuracy of the estimates. Totals in Table 1 may not sum or recalculate from related values in the table due to rounding of values in the table, reflecting fewer significant digits than were carried in the original calculations.
4. The MRE excludes identified oxide material due to a lack of confidence in recovery assumptions of oxidized tonnages at this stage of the project.
5. Metal assays are capped where appropriate. At this stage of the project, it is the Company's opinion that all the elements included in the metal equivalents calculation have a reasonable potential to be recovered and sold.
6. All dollar amounts are presented in US dollars.
7. Bulk density is estimated on a block basis using specific gravity data collected on diamond drill core.
8. Economic pit constrained resource with reasonable prospects of eventual economic extraction ("RPEEE") were based on a copper price of \$3.80/lb, molybdenum price of \$12.00/lb, a gold price of \$1,650/oz, and a silver price of \$22.00/oz. Metal recovery factors of 84.3% for copper, 66% for molybdenum, 57% for gold and 54% for silver have been applied. Average slope angles of 50 degrees are applied (45 degrees for over 360 m elevation and 50 degrees below 360 m elevation) and is based on geotechnical data collected to date.
9. The in-situ economic copper (Cog) was calculated resulting in a 0.13% Cu CoG. To align with previously published mineral resources, Oroco has selected to use an effective CoG at 0.15% Cu. CoG assumptions include: a copper price of \$3.80/lb, molybdenum price of \$12.00/lb, gold price of \$1,650/oz, and silver price of \$22.00/oz. Suitable benchmarked technical and economic parameters for open pit mining, including a 99% mining recovery and costs of mining at \$2.25/t, processing at \$5.00/t, G&A at \$1.00/t, and selling costs at \$1.00/t, with Private Royalties at 1.5%, have been applied in consideration of the RPEEE. Recoveries are applied as listed in Note 8.
10. Equivalent Copper (CuEQ) percent is calculated with the formula $CuEq\% = ((Cu\ grade * Cu\ recovery\ [84.3\%] * Cu\ price) + (Mo\ grade * Mo\ recovery\ [66\%] * Mo\ price) + (Au\ grade * Au\ recovery\ [57\%] * Au\ price) + (Ag\ grade * Ag\ recovery\ [54\%] * Ag\ price)) / (Cu\ price * Cu\ recovery\ [84.3\%])$. It assumed that the Santo Tomás Project will produce a conventional (flotation) copper concentrate product based on metal recoveries at 84.3% Cu, 66% Mo, 57% Au, and 54% Ag based on initial preliminary metallurgical test work.
11. Reported contained individual metals in Table 1 represent in-situ metal, calculated on a 100% recovery basis, except for CuEq% (see Note 10).

14.13 Mineral Resource Sensitivity

The sensitivity of mineral resources to changes in the economic CoG are presented below through the grade-tonnage table presented in Table 14-21. For the purposes of the MRE study, the effective CoG is 0.15% Cu. The QP notes that any material changes to project economic or technical assumptions may materially affect the mineral resource tonnage and average grades. The degree of change to tonnage and mean grades are presented below. Although the base case CoG is 0.15% Cu all sensitivities presented meet reasonable prospects for eventual economic extraction.

Table 14-21: Grade-Tonnage Sensitivity to Cut-Off Grade

Cu CoG (percent)	Tonnes ≥ cut-off (Mt)	Average Cu grade ≥ cut-off (percent)	Average CuEQ grade ≥ cut-off (percent)	Average Mo grade ≥ cut-off (percent)	Average Au grade ≥ cut-off (ppm)	Average Ag grade ≥ cut-off (ppm)
0.10	1,304.5	0.28	0.32	0.007	0.02	1.9
0.11	1,270.3	0.29	0.33	0.007	0.02	1.9
0.12	1,225.9	0.30	0.34	0.007	0.02	2.0
0.13	1,180.0	0.30	0.34	0.008	0.03	2.0
0.14	1,132.7	0.31	0.35	0.008	0.03	2.0
0.15	1,087.2	0.32	0.36	0.008	0.03	2.0
0.16	1,045.2	0.32	0.36	0.008	0.03	2.1
0.17	1,006.2	0.33	0.37	0.008	0.03	2.1
0.18	962.3	0.34	0.38	0.008	0.03	2.1
0.19	921.7	0.34	0.39	0.008	0.03	2.1
0.20	879.9	0.35	0.39	0.008	0.03	2.2
0.21	840.4	0.36	0.40	0.008	0.03	2.2
0.22	798.3	0.36	0.41	0.008	0.03	2.2
0.23	760.1	0.37	0.42	0.008	0.03	2.2
0.24	722.8	0.38	0.42	0.009	0.03	2.2
0.25	685.4	0.38	0.43	0.009	0.03	2.3
0.26	650.2	0.39	0.44	0.009	0.03	2.3
0.27	615.4	0.40	0.45	0.009	0.03	2.3
0.28	583.7	0.41	0.45	0.009	0.03	2.3
0.29	550.8	0.41	0.46	0.009	0.03	2.3
0.30	516.7	0.42	0.47	0.009	0.03	2.4
0.31	485.7	0.43	0.48	0.009	0.03	2.4
0.32	454.0	0.44	0.48	0.009	0.03	2.4
0.33	422.6	0.44	0.49	0.009	0.03	2.4
0.34	394.3	0.45	0.50	0.009	0.04	2.5
0.35	365.9	0.46	0.51	0.009	0.04	2.5
0.36	339.1	0.47	0.52	0.009	0.04	2.5
0.37	310.9	0.48	0.53	0.009	0.04	2.5
0.38	285.6	0.49	0.54	0.008	0.04	2.6
0.39	262.0	0.50	0.55	0.008	0.04	2.6
0.40	240.4	0.50	0.56	0.008	0.04	2.6

Source: SRK, 2023.

14.14 Relevant Factors

Factors that may affect the mineral resource statement on the Santo Tomás property include:

- Ability to recover all stated metals at the assumed recovery factors.
- Changes to metal price assumptions in long-term outlook.
- Changes to the input economic assumptions on the economic CoG and pit shell including mining, process, capital, and G&A costs, recovery assumptions and mining dilution.
- Changes to the geotechnical slope angle used in the economic pit shell.
- Future identification and assessment of potentially deleterious materials or elements that may materially affect the ability to mine or recovery gold to the baseline assumptions.
- The ability to demonstrate a feasible path to mining in the Huites Reservoir area with appropriate offset or allotment that may be required based on further studies.
- Additional land or infrastructure constraints that may be identified during future studies on the property.
- Changes to the input values for the CuEq grade used to constrain the estimate.
- Variations in geotechnical, hydrogeological and mining assumptions.
- Changes as to assumptions as to ability to continue with existing agreements, or renew or renegotiate those agreements.
- Changes to environmental, permitting, and social license assumptions.

14.15 Opinion on Mineral Resource Estimates

In the opinion of the QP, the Company has completed detailed and thorough geologic work programs to support the construction of a robust geologic model and fundamentally sound structural domain model. The models adequately reflect the geologic setting that both controls and limits mineralization in the North and South Zones. The oxidation model is rudimentary however delineates oxidized material from reduced material that can be isolated in the block model properly. Mineralization domains are utilized to constrain the MRE and limiting geologic features are used when tabulating the mineral resource statement. The MRE and statement for the Santo Tomás project conforms to satisfactory industry practices and satisfies the requirements of the CIM Definition Standards required for disclosure under NI 43-101.

Principal Amendments affecting existing concessions are: (1) the reduction of the term of renewal to a one-time period of 25 years, with the right to bid for the concession thereafter if the concessionaire matches 90% of the highest bid in a public bidding process; (2) the requirement of government approval for the transfer of mineral concessions; (3) the addition of grounds for cancellation, including: (i) failure to pay mining fees for two consecutive years; (ii) failure to submit verification reports for works for two consecutive years or five non-consecutive years; (iii) failure to initially commence work within one year; (iv) failure to carry out work for a period of two consecutive years; (v) failure to submit a mine closure plan within the time required; and (vi) lack of a valid water concession; and (4) the elimination of mining's preferential nature and the related right to expropriate land when required.

15 MINERAL RESERVE ESTIMATES

This section is not applicable to an MRE Technical Report.

16 MINING METHODS

This section is not applicable to an MRE Technical Report.

17 RECOVERY METHODS

This section is not applicable to an MRE Technical Report.

18 PROJECT INFRASTRUCTURE

This section is not applicable to an MRE Technical Report.

19 MARKET STUDIES AND CONTRACTS

This section is not applicable to an MRE Technical Report.

20 ENVIRONMENTAL STUDIES, PERMITTING AND SOCIAL AND COMMUNITY IMPACT

This section is not applicable to an MRE Technical Report.

21 CAPITAL AND OPERATING COST

This section is not applicable to an MRE Technical Report.

22 ECONOMIC ANALYSIS

This section is not applicable to an MRE Technical Report.

23 ADJACENT PROPERTIES

Several mineral deposits are documented adjacent to the Santo Tomás Property. The qualified person has been unable to verify the following information and that the information is not necessarily indicative of the mineralization on the property that is the subject of this technical report.

23.1 La Reforma Mine

La Reforma mine, located approximately 7.5 km north of Santo Tomás, was operated by Compañía Minera la Campaña S.A., a former subsidiary of Industria Peñoles S.A. de C.V. from 1968 to 1980.

The La Reforma deposit contains Zn-Pb-Cu-Ag mineralization in replacement zones in Cretaceous limestones, intruded by a Laramide-age granodiorite and a granite porphyry with biotite K-Ar ages of 59.9 ± 1.3 and 59.2 ± 1.3 Ma, respectively (Damon et al., 1983; Clark et al., 1978).

23.2 El Tempisque Deposit

El Tempisque (formerly El Creston), an iron skarn deposit, is located 4.5 km west of the Santo Tomás deposit. The host to the mineralization is an altered and metamorphosed sequence of interbedded sediments and limestone contained in what appears to be a roof pendant in granodiorite. Skarn development occurs near the contact with the surrounding granodiorite and is accompanied by selective metasomatic replacement by magnetite of limestone and calcareous units in the metasedimentary rocks. The magnetite-rich units are massive and generally occur as discrete tabular bodies or as discontinuous pods and lenses. They are characteristically hard, massive, and generally homogenous with thicknesses ranging from 5 to 15 m. (Verzosa, 2011).

23.3 Bahuerachi

The Bahuerachi Project, explored by Tyler Resources Inc., is located 2 km northeast of the boundary of the Santo Tomás property. The main porphyry complex at Bahuerachi is exposed over 4 km of strike length, with widths varying from lenses of tens of meters to an interpreted true thickness of approximately 400 m.

23.4 El Sauzal Mine

The reclaimed El Sauzal Mine is located some 31 km to the northeast from the Santo Tomás Project. El Sauzal operated for 12 years, between 2004 and 2012, producing 1.8 Moz of gold. Mining operations ceased in August 2014, but the mill continued to operate up to year-end.

24 OTHER RELEVANT DATA AND INFORMATION

There are no other data and information relevant to the MRE. All relevant information has been included in the report.

25 INTERPRETATION AND CONCLUSIONS

25.1 Introduction

The QPs note the following interpretations and conclusions in their respective areas of expertise, based on their review of data available for this Report.

25.2 Mineral Tenure, Surface Rights, Water Rights, Royalties and Agreements

Oroco controls sufficient mineral rights and additional agreements to obtain additional fractional ownership in mineral rights over the resource as currently defined. Oroco has in place surface access and agreements to acquire surface rights to support an open pit operation with ancillary infrastructure in the immediate area of the mineral resource as currently defined.

25.3 Geology and Mineralization

The geology of the deposit is well understood and the controls on mineralization are better defined with the completion of the Phase I drilling program. A much better understanding of structural controls and structure bounding limits on mineralization has been captured in the updated 3D geology, alteration and structural model and applied to the MRE presented in this report. Additional drilling will be required in the southwest sector of the South Zone to better understand the limits on the mineralization and alteration observed and mapped at surface.

25.4 Exploration, Drilling and Analytical Data Collection in Support of Mineral Resource Estimation

Additional surface mapping and exploration has been incorporated with the drilling-supported 3D models. Surface mapping and exploration should be continued in an effort to more precisely the western footwall fault and resource internal faulting defined through drilling. Analytical data collection in support of the Mineral Resource Estimation should continue with focus on historical drill re-logging and check sampling for comparison of historical results. This will confirm some of the historical reporting on the repeatability of target economic elements. Additional drilling in resource defined as Inferred will increase confidence in the resource estimate, especially in the South Zone that is currently all classified as Inferred.

An on-going review of the gross sulphide bearing veins and their orientations will help better refine additional drilling program design in regards to the dips and azimuth of drill holes.

25.5 Metallurgical Test Work

Ausenco reviewed the results from the recent metallurgical test work program undertaken this year (2023) conducted by ALS as well as past test work results reported by Bateman (1994) that were presented in the 1994 Prefeasibility Study for the Santo Tomás Project. Mineralogical studies indicated that copper sulphide minerals (primarily chalcopyrite) were sufficiently liberated for recovery by froth flotation at a grind size of approximately 150 µm P80. Elevated Zn & Hg levels

were measured for some of the concentrates produced during flotation testing. Both elements have been identified as being associated with the skarn materials which have been flagged for exclusion from the mine plan moving forward. Drop weight index values measured for some of the samples are characterized as very hard (A*b values of 28-30) suggesting HPGR crushing should be considered over SAG milling for this project. Locked cycle cleaner flotation test achieved a Cu concentrate grade of 24.7% at a Cu recovery of 82.6%. Moly recovery measured 61.8%. The bulk concentrate from the locked cycle test contained 1.1 ppm gold and 114 ppm silver. Cu-Mo separation test work was not conducted.

From the variability test work results, Ausenco forecasts the following recoveries to be used in the MRE:

- Cu Recovery – 84.3%
- Mo Recovery – 66%
- Au Recovery – 57%
- Ag Recovery – 54%

The samples provided for recent metallurgical testing are considered sufficient for a preliminary metallurgical assessment but are by no means exhaustive and may not capture the variability of metallurgical performance that could be present in the deposit. Further metallurgical studies with a greater number of samples are required to assess the variances with respect to rock hardness and metallurgical performance.

25.6 Mineral Resources Estimates

In the opinion of the QP, the Company has completed detailed and thorough geologic work programs to support the construction of a robust geologic model and fundamentally sound structural domain model. The models adequately reflect the geologic setting that both controls and limits mineralization in the North and South Zones. The oxidation model is rudimentary however delineates oxidized material from reduced material that can be isolated in the block model properly. A better constrained oxide resource may represent an opportunity in future resource estimates. Mineralization domains are utilized to constrain the MRE and limiting geologic features are used when tabulating the mineral resource statement. The MRE and statement for the Santo Tomás project conforms to satisfactory industry practices and satisfies the requirements of the CIM Definition Standards required for disclosure under NI 43-101.

25.7 Risks and Opportunities

On April 29, 2023 (effective May 9, 2023), the Mexican Congress approved a decree amending the Mining Law and other national laws regarding mining and water concessions (the “Amendments”). The Amendments focus principally, but not exclusively, on the process of granting of new concessions and their associated rights and obligations, which are not seen as being applicable to Oroco given that the Project is comprised of existing concessions. The amendment reducing the initial term of mineral concessions from 50 years to 30 years does not affect the term of current concessions.

Principal Amendments affecting existing concessions are: (1) reduction of the term of renewal to a one-time period of 25 years, with the right to bid for the concession thereafter if the concessionaire matches 90% of the highest bid in a public bidding process; (2) the requirement of government approval for the transfer of mineral concessions; (3) the addition of grounds for cancellation, including: (i) failure to pay mining fees for two consecutive years; (ii) failure to submit verification reports for works for two consecutive years or five non-consecutive years; (iii) failure to commence work within one year;

(iv) failure to carry out work for a period of two consecutive years; (v) failure to submit a mine closure plan within the time required; and (vi) lack of a valid water concession; (4) the elimination of mining's preferential nature and the related right to expropriate land when required.

Legal challenges to the mining reform legislation have been initiated by several Canadian mining and exploration companies.

Additional drilling and metallurgical test work will reduce uncertainty on forecast metal recoveries and resource estimation. Additional variability samples for metallurgical test work will help resolve the apparent deleterious Zn & Hg levels in the concentrates. The inclusion of zinc-rich skarn samples influenced the preliminary metallurgy results. Drilling is required to upgrade mineral resource classifications. Currently, the South Zone is classified as inferred resources but with additional drilling there is potential to upgrade this classification and delineate more mineralized materials.

Further logging and (re)sampling of historical drill cores should be undertaken to increase confidence in the geologic interpretation and resource estimation.

26 RECOMMENDATIONS

26.1 Overview

The QPs recommend a future PEA study and supporting data acquisition be conducted on the Project.

The following subsections summarize the key recommendations identified for future stages of study for the Santo Tomás Project. Table 26-1 presents a budget for each recommended item described in the subsections that follow:

Table 26-1: Proposed Budget Summary

Description	Cost in US Dollars
PEA Report	700,000
Exploration Geology and Mineral Resources	1,250,000
Mineral Processing	200,000
Total	2,150,000

26.2 Exploration and Drilling and Recommended PEA Study

Engineering deliverables towards a PEA study would include the following:

- Process flows diagrams (comminution, recovery processes, tails) and equipment list(s).
- Detailed material and water balance.
- Detailed process design criteria.
- GA and Elevation drawings (for crushing/overland conveying, comminution, recovery, reagents, tailings).
- Power study on cost and consumption.
- High-level architectural, steel and concrete estimates.
- Capital cost estimate.
- Operating cost estimate.
- An updated mineral resource estimate.
- Environmental permitting review and recommendations.
- Off-site infrastructure studies.
- Site access evaluation.

- Risks and opportunities review.
- Logistics and marketing studies.
- Mine plan and schedule development.
- Labor cost investigation.

The estimated cost for the PEA Study is \$700K.

The QP has the following recommendations to implement on the Santo Tomás project to further improve the deposit understanding to reduce uncertainty and risk associated with geology and mineral resources.

- Perform validation checks on historical drilling collars and downhole survey. The collars should be available to re-survey with high precision instruments and if drill holes are open at depth, a gyroscopic survey should be conducted to confirm downhole deviation.
- Re-assay retained drill core and/or sample pulps for all historical data. The QP recommends re-assay to confirm historical Cu values and analyzes for multi-elements to ensure consistent data coverage on all key metals and potentially deleterious materials.
- Perform re-logging or check logging of drilling data with an emphasis on zones of oxidation, transition, and reduction mineralogy. Once drilling data has been deemed acceptable, update the 3D oxidation model for use in resource modeling.
- Expand the existing knowledge of the various alteration zones related to the porphyry mineralization at Santo Tomás. This may include collecting of additional mineralogical, geochemical, or other data with 3D modeling of grouped alteration zonation to align with metallurgical recovery, deleterious materials, and understanding of deposit genesis.
- Additional resource definition drilling targeting zones of inferred mineralization along with expanding the known mineralization envelope to the north and south. Additionally drilling across the South Zone and in areas of inferred mineral resources in the North Zone will aid in reducing uncertainties in these areas as part of future studies.

The cost estimate to complete the exploration geology and mineral resources drilling for the next phase of the study is \$1.25M.

26.3 Metallurgical Test Work

The samples provided for recent metallurgical testing are considered sufficient for a preliminary metallurgical assessment but are by no means exhaustive and may not capture the variability of metallurgical performance that could be present in the deposit. Further metallurgical studies with a greater number of samples are required to assess the variances with respect to mineral hardness and metallurgical performance.

Ausenco recommends the following additional metallurgical tests be conducted for the next phase of study:

- Mineralogy

All future variability testing should include similar mineral composition measurements as were collected in the recent test work program. This study. Furthermore, the development of a relationship between SEM measurements and hyperspectral results would enhance future geometallurgical modeling of the deposit.

- **Comminution**

Due to the variance demonstrated for the measured mineralized material hardness properties from the variability samples, it is recommended additional comminution test work be conducted on a greater number of samples representing better spatial coverage throughout the deposit. Piston press testing should be completed on variability samples to better estimate HPGR parameters. Crushing Work Index tests should be completed on whole core samples. A regrind specific energy test on a suitable mass of rougher concentrate using vendor specific test protocols, such as an IsaMill Signature Plot test, is also recommended.

- **Flotation**

Additional variability samples should be tested using the developed process. Master composites assembled from a greater coverage of the deposit could be used to further optimize the metallurgical performance. Coarse Particle Flotation (CPF) should also be investigated as this project would likely benefit from its inclusion in a scavenging application. Additional bulk flotation testing should be completed in order to generate concentrate for Cu-Mo separation testing which is also recommended.

- **Solid-liquid Separation**

Concentrate dewatering requirements will need to be confirmed through testing in a later study. Tailings thickening tests should also be conducted.

- **Oxide Materials**

A full evaluation of the oxide materials should be characterized including leach bottle roll tests and column studies.

The cost estimate to complete the next phase of metallurgical testing is \$200K.

27 REFERENCES

- Aguirre-Díaz, G.J., McDowell, F.W. (1991). The volcanic section at Nazas, Durango, Mexico, and the possibility of widespread Eocene volcanism within the Sierra Madre Occidental. *J. Geophys. Res.*, 96, 13-373–13-388.
- Aguirre-Díaz, G.J., McDowell, F.W. (1993). Nature and timing of faulting and syn-extensional magmatism in the southern basin and range, central-eastern Durango, Mexico. *Bull. Geol. Soc.Am.*, 105, 1435–1444.
- Anderson, T.H., Silver, L.T. (1969). Mesozoic magmatic events of the northern Sonora coastal region, Mexico (abstract): *Geological Society of America Abstracts with Programs*, 3-4.
- Bridge, D., (2019). *Geology, Mineralization, and Exploration of the Santos Tomás Cu-(Mo-Au-Ag) Porphyry Deposit, Sinaloa, Mexico: NI 43-101 Technical Report prepared by Dane A. Bridge Consulting Inc., for Oroco Resource Corp. and Altamura Copper Corp.*
- Bridge, D., (2020). *Geology, Mineralization, and Exploration of the Santos Tomás Cu-(Mo-Au-Ag) Porphyry Deposit, Sinaloa, Mexico: NI 43-101 Technical Report prepared by Dane A. Bridge Consulting Inc., for Oroco Resource Corp. and Altamura Copper Corp.*
- Bridge, D. (2020). *Technical Report prepared for Oroco Resource Corp. Geology, Mineralization, and Exploration of the Santo Tomás Cu-(Mo-Au-Ag) Porphyry Deposit Sinaloa, Mexico, 145 pp.*
- Campa, M.F., and Coney, P.J. (1983). Tectono-stratigraphic terranes and mineral resource distributions in Mexico: *Canadian Journal of Earth Sciences*, v. 20, p. 1040–1051.
- Centeno-García, E., Guerrero-Suástegui, M., and Talvera-Mendonza, O. (2008). The Guerrero composite terrane of western Mexico: Collision and subsequent rifting in a suprasubduction zone, in Draut, A.E., Clift, P.D., and Scholl, D.W., eds., *Formation and Application of the Sedimentary Record in Arc Collision Zones: Geological Society of America Special Paper 436*, p. 279–308, doi: 10.1130/2008.2436(13).
- Centeno-García, E., Ruíz, J., Coney, P., Patchett, J.P., and Ortega, G.F. (1993). Guerrero Terrane of Mexico: Its role in the Southern Cordillera from new geochemical data: *Geology*, v. 21, p. 419–422.
- Coney, P.J., and Campa, M.F., 1987. Lithotectonic terrane map of Mexico (west of the 91st meridian): U.S. Geological Survey Miscellaneous Field Studies Map MF-1874-D, 1 plate, 1:2,500,000 scale.
- Cueva, A;C., Boris, E., Hernandez, I.P., 1996. Carta geologico-minera Tasajeras G12-B59, Sinaloa y Chihuahua: Servicio Geológico Mexicano map G12-B59, 1 plate, 1:50,000 scale.
- Dias Geophysical Limited, May 2021. Santo Tomás Project, Sinaloa/Chihuahua, Mexico. 3D DC Resistivity and Induced Polarization Logistical Report, for Minera Xochipala, S.A. De C.V, Work Period: September 1, 2020 – March 16, 2021, UTM Zone 12N WGS84., 31p
- Dickinson, W.R., and Lawton, T.F. (2001). Carboniferous to Cretaceous assembly and fragmentation of Mexico: *Geological Society of America Bulletin*, v. 113, p. 1142–1160, doi: 10.1130/0016-7606(2001)113<1142:CTCAAF>2.0.CO;2.

Eagle Mapping, 2021 Santo Tomás Property Report – EM#: 21-011., 4p

Gastil, R.G., Krummenacher, D., Jensky, W.E. (1979). Reconnaissance geology of west-central Nayarit, Mexico. Geological Society of America, Text to accompany Map and Chart Series Map MC-24, 8 p.

Hammarstrom, J.M., Robinson, G.R., Jr., Ludington, S., Gray, F., Drenth, B.J., Cendejas-Cruz, F., Espinosa, E., Perez-Segura, E., Valencia-Moreno, M., Rodríguez -Castaneda, J.L., Vasquez-Mendoza, R., Zurcher, L., 2010. Global mineral resource assessment—porphyry copper assessment of Mexico: U.S. Geological Survey Scientific Investigations Report 2010-5090-A, 176 p.

Henry, C.D., Fredrikson, G. (1987). Geology of part of southern Sinaloa, Mexico adjacent to the Gulf of California. Geological Society of America Map and Chart Series MCH063, 14 p.

Keppie, D.J. (2004). Terranes of México revisited: A 1.3 billion year odyssey: International Geology Review, v. 46, p. 765–794, doi: 10.2747/0020- 6814.46.9.765. Campa and Coney, 1983,

McDowell, F.W., Clabaugh, S.E. (1979). Ignimbrites of the Sierra Madre Occidental and their relation to the tectonic history of western Mexico. In: Chapin, C.E. and Elston, W.E. (Eds), Ash-Flow Tuffs, Geological Society of America Special Paper, 180, pp. 113–124.

Mira Geoscience, 2022. Integrated Interpretation and Geophysical Modelling, Santo Tomás Project, Mexico. For Xochipala Gold, S.A. de C.V., Project Number: 5023, July 29, 2022. 57 p.

Moul, F., 2021. Magnetic susceptibility smooth model inversion of heliborne mag. data at the Oroco Resource Corp., Santo Tomás project, Sinaloa, Mexico. Condor North Consulting ULC, Memorandum of Oct. 4, 2021

Oroco Resource Corp., June (2021). Technical information, Santo Tomás, 3D DCIP geophysical survey, Field work: September 1, 2020 to March 16, 2021: Oroco Resource Corp Technical Disclosure, 35 p.

Oroco Resource Corp., April (2023). Environment, Social and Governance Site Manual, Rev. C.: Oroco Resource Corp. revised April 24, 2023.

Ortega-Gutiérrez, F., Elías-Herrera, M., Reyes-Salas, M., Ortega-Gutiérrez, F., Prieto-Vélez, R., Zúñiga, Y., and Flores, S. (1979). Una secuencia volcanoplutónica-sedimentaria cretácica en el norte de Sinaloa; ¿un complejo ofiolítico?: Universidad Nacional Autónoma de México, Instituto de Geología: Revista Mexicana de Ciencias Geológicas, v. 3, p. 1–8.

Ramos-Velázquez, E., T. Calmus, V. Valencia, A. Iriondo, M. Valencia-Moreno, and H. Bellon. (2008). U-Pb and $40\text{Ar}/39\text{Ar}$ geochronology of the coastal Sonora batholith: New insights on Laramide continental arc magmatism. Revista Mexicana de Ciencias Geológicas 25(2): 314–333.

Roldán-Quintana, J., Gonzalez-Leon, C.M., and Amaya-Martínez, R. (1993). Geologic constraints on the northern limit of the Guerrero Terrane in northwestern Mexico, in Ortega Gutiérrez, F., et al., eds., First Circum-Pacific and Circum-Atlantic Terrane Conference: Guanajuato, México, Proceedings, p. 124–127.

Valencia-Moreno, M., Ruiz, J., Ochoa-Landín, L., Martínez-Serrano, R., Vargas-Navarro, P. (2003). Geochemistry of the Coastal Sonora Batholith, Northwestern México: Canadian Journal of Earth Sciences, 40(6), 819-831.

Wark, D.A., Kempter, K.A., McDowell, F.W. (1990). Evolution of waning subduction related magmatism, northern Sierra Madre Occidental, Mexico. *Geol. Soc. Am. Bull.*, 102, 1555–1564.